

Xanthenes from the Stem Bark of *Garcinia nigrolineata*

Thunwadee Ritthiwigrom

Master of Science Thesis in Organic Chemistry

Prince of Songkla University

2002

เลขที่	RD405	T48	2002	C.2
Bib Key	225817			
	- 4 W.R. 2547			

Thesis Title Xanthenes from the Stem Bark of *Garcinia nigrolineata*
Author Miss Thunwadee Ritthiwigrom
Major Program Organic Chemistry
Academic Year 2001

Advisory committee

.....*V. Rukachaisirikul*.....Chairman
(Assoc.Prof.Dr.Vatcharin Rukachaisirikul)

.....*K. Panthong*.....Committee
(Dr.Kanda Panthong)

Examining committee

.....*V. Rukachaisirikul*.....Chairman
(Assoc.Prof.Dr.Vatcharin Rukachaisirikul)

.....*K. Panthong*.....Committee
(Dr.Kanda Panthong)

.....*C. Karalai*.....Committee
(Asst.Prof.Dr.Chatchanok Karalai)

.....*Anuchit Plubrukarn*.....Committee
(Dr.Anuchit Plubrukarn)

The Graduate School, Prince of Songkla University, has approved this thesis as partail fulfillment of the requirment for the Master of Science degree in Organic Chemistry.

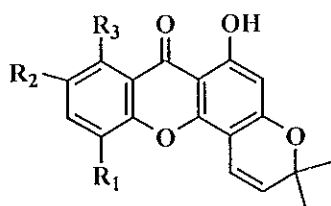
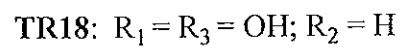
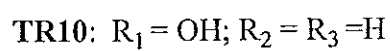
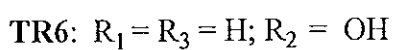
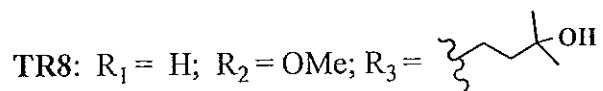
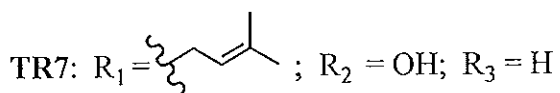
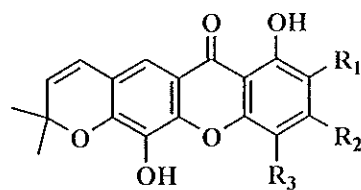
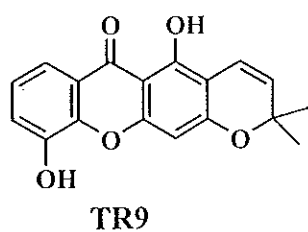
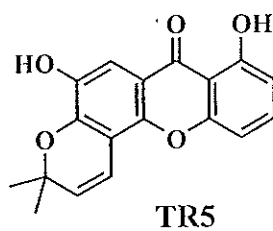
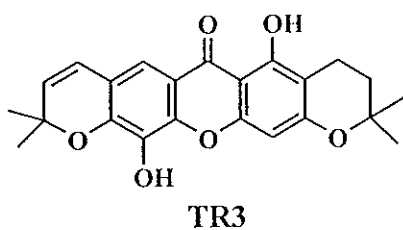
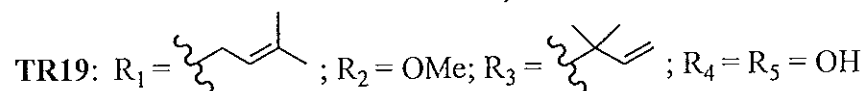
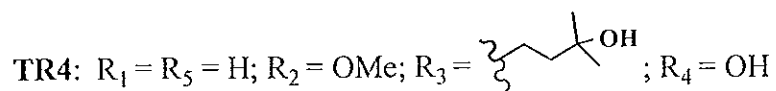
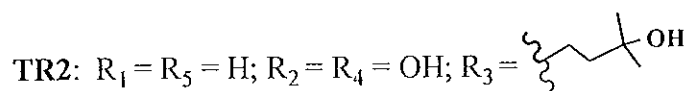
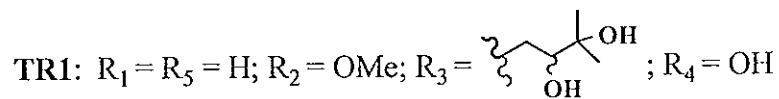
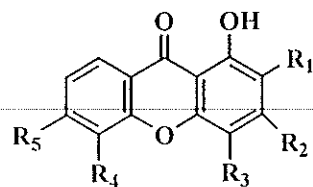
P. Trisdikoon

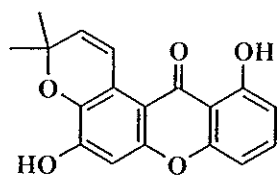
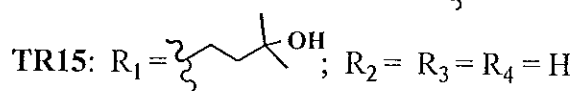
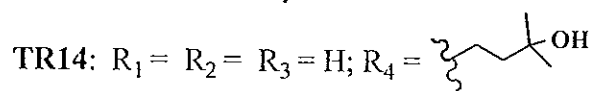
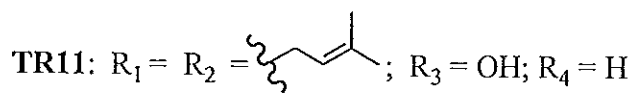
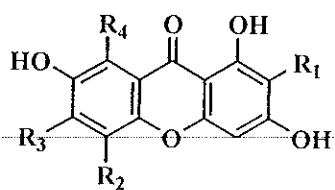
.....
(Piti Trisdikoon, Ph.D.)
Associate Professor and Dean
Graduate School

Thesis Title	Xanthones from the Stem Bark of <i>Garcinia nigrolineata</i>
Author	Miss Thunwadee Ritthiwigrom
Major Program	Organic Chemistry
Academic Year	2001

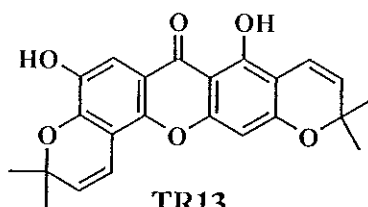
ABSTRACT

The crude methanol extract from the stem bark of *Garcinia nigrolineata*, upon chromatographic separation, yielded eleven new compounds: ten xanthones (**TR1**, **TR3**, **TR4**, **TR5**, **TR6**, **TR8**, **TR11**, **TR13**, **TR14** and **TR19**) and one dibenzofuran derivative (**TR20**) together with nine known xanthones: 1,3,5-trihydroxy-4-(3-hydroxy-3-methylbutyl)xanthone (**TR2**), latisxanthone D (**TR7**), 6-deoxyjacareubin (**TR9**), 6-deoxyisojacareubin (**TR10**), tovoxanthone (**TR12**), 1,3,7-trihydroxy-2-(3-hydroxy-3-methylbutyl)xanthone (**TR15**), brasilixanthone A (**TR16**), rheedixanthone A (**TR17**) and morusignin C (**TR18**). However, two of the new xanthones (**TR3** and **TR6**) were previously reported as synthetic xanthones. All structures were elucidated using 1D and 2D NMR spectroscopic data. The ^{13}C NMR signals were assigned from DEPT, HMQC and HMBC spectra. For known xanthones, their ^1H and/or ^{13}C spectral data, were compared with those reported in the literature.

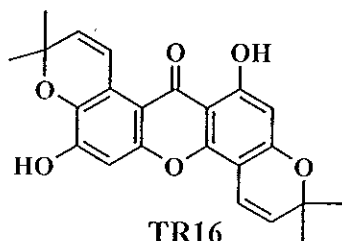




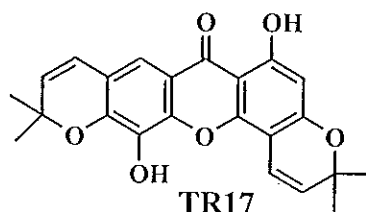
TR12



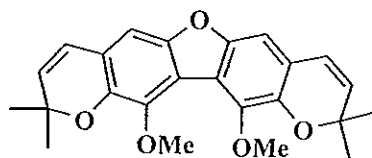
TR13



TR16



TR17

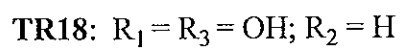
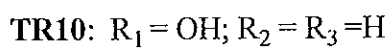
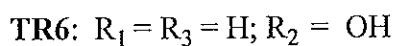
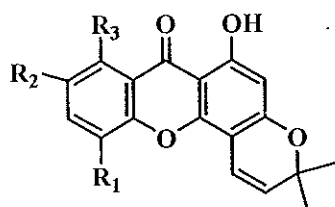
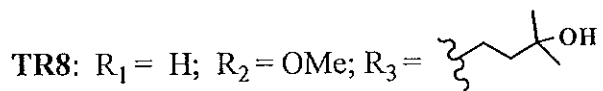
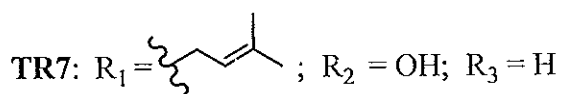
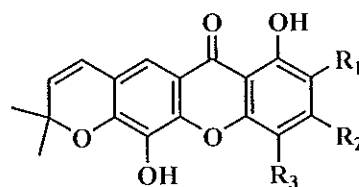
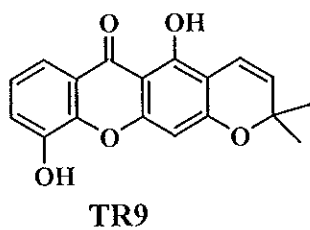
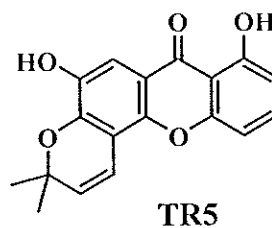
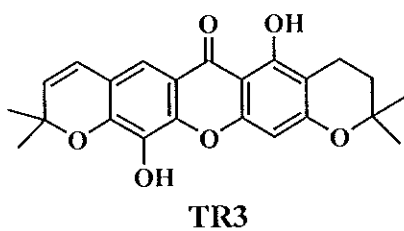
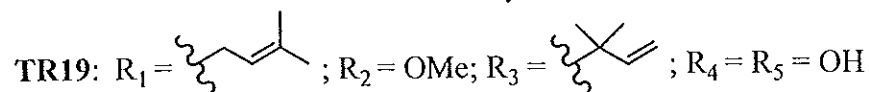
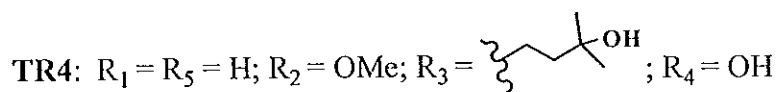
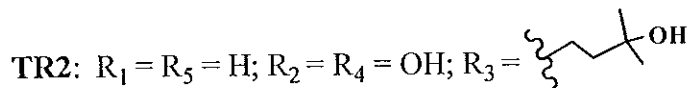
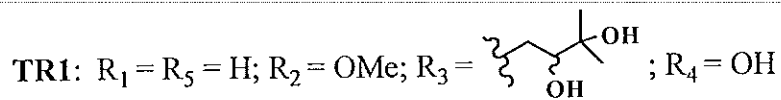
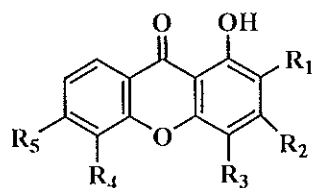


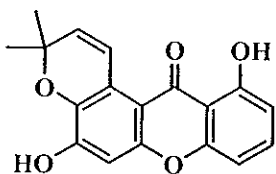
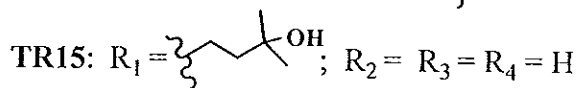
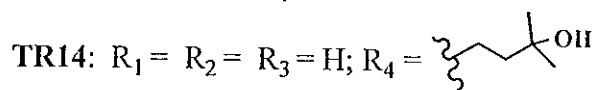
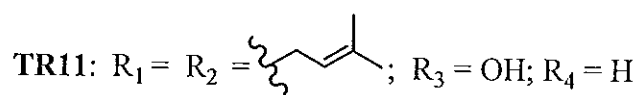
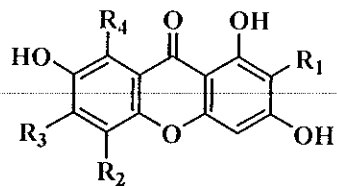
TR20

ชื่อวิทยานิพนธ์	เซนโตนจากเปลือกต้นชะมวง (<i>Garcinia nigrolineata</i>)
ผู้เขียน	นางสาวรัชฎวดี ฤทธิวิกรม
สาขาวิชา	เคมีอินทรีย์
ปีการศึกษา	2544

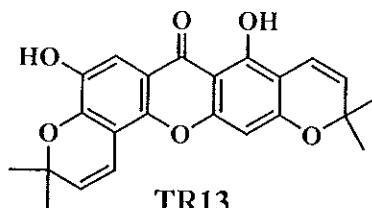
บทคัดย่อ

ส่วนสกัดหยาบเมธานอลของเปลือกต้นชะมวง เมื่อนำมาแยกและทำให้บริสุทธิ์ด้วยวิธีทางโครมาโทกราฟี สามารถแยกสารใหม่ได้จำนวน 11 สาร ซึ่งเป็นสารประเภท xanthone จำนวน 10 สาร (TR1, TR3, TR4, TR5, TR6, TR8, TR11, TR13, TR14 และ TR19) และอนุพันธ์ dibenzofuran จำนวน 1 สาร (TR20) โดย TR3 และ TR6 เป็นสารที่ได้มีการรายงานโครงสร้างด้วยวิธีการสังเคราะห์มาแล้ว นอกจากนี้ยังแยกสารประเภท xanthone ที่ทราบโครงสร้างแล้วจำนวน 9 สาร [1,3,5-trihydroxy-4-(3-hydroxy-3-methylbutyl)xanthone (TR2), latisxanthone D (TR7), 6-deoxyjacareubin (TR9), 6-deoxyisojacareubin (TR10), tovoxanthone (TR12), 1,3,7-trihydroxy-2-(3-hydroxy-3-methylbutyl) xanthone (TR15), brasilixanthone A (TR16), rheedixanthone A (TR17) และ morusignin C (TR18)] โครงสร้างทั้งหมดวิเคราะห์โดยใช้ข้อมูลทางสเปกโทรสโกปี โดยเฉพาะ 1D และ 2D NMR สเปกโทรสโกปี ส่วนสัญญาณของ ^{13}C สามารถวิเคราะห์โดยอาศัยข้อมูลจาก DEPT, HMQC และ HMBC สเปกตรัม สำหรับสารที่มีการรายงานโครงสร้างแล้ว ได้เปรียบเทียบกับข้อมูล ^1H และ/หรือ ^{13}C NMR สเปกตรัมกับข้อมูลที่ได้รายงานไว้

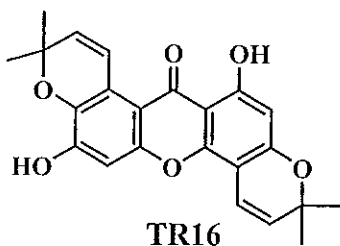




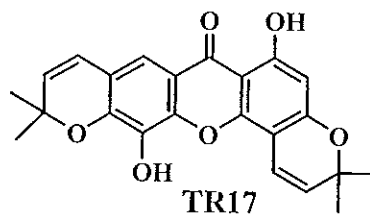
TR12



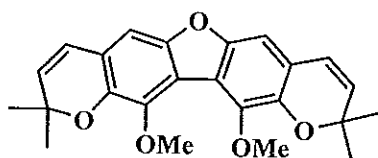
TR13



TR16



TR17



TR20

ACKNOWLEDGEMENTS

I wish to express my deepest and sincere gratitude to my supervisor, Associate Professor Dr. Vatcharin Rukachaisirikul, for her valuable instruction, expert guidance and excellent suggestion. I would also like to express my appreciation to her for correction of my thesis. Everything will be always kept in my mind.

My sincere thanks are expressed to Dr. Kanda Panthong, my co-advisor, for her kindness and valuable advice. Special thanks are addressed to Professor Dr. Walter C. Taylor, Department of Organic Chemistry, the University of Sydney, Australia for providing mass spectral data.

I would like to extend my appreciation to the staff of the Department of Chemistry, Faculty of Science, Prince of Songkla University, including the officers for making this thesis possible and to Ms. Dusanee Langjae, the Scientific Equipment Center, Prince of Songkla University, for recording 500 MHz NMR spectra.

This work was made possible by a scholarship from Higher Education Development Project : Postgraduate Education and Research Program in Chemistry, funded by The Royal Thai Government. Additionally, I would also like to thank the Graduate School, Prince of Songkla University, for the material support.

Finally, none of this would have been possible without love and encouragement of my family, Miss Yaowapa Sukpondma, Miss Morakot Kaewpet and friends. I thank them all for their understanding during all of the times when I could not be with them. Their steady love, indeed, supported me.

Thunwadee Ritthiwigrom

CONTENTS

	Page
Abstract (in English)	(3)
Abstract (in Thai)	(6)
Acknowledgements	(9)
Contents	(10)
List of Tables	(12)
List of Illustrations	(18)
Abbreviations and Symbols	(25)
Chapter	
1 Introduction	1
1.1 Introduction	1
1.2 Review of Literatures	2
Chemical constituents from the genus <i>Garcinia</i>	2
Trioxxygenated and tetraoxxygenated xanthenes from the genus <i>Garcinia</i>	5
1.3 The Objective	27
2 Experimental	28
2.1 Chemicals and Instruments	28
2.2 Plant material	29
2.3 Isolation and extraction	29
2.4 Chemical investigation of the crude methanol extract of the stem bark	29
The First Investigation	30
The Second Investigation	56
3 Results and Discussion	101
3.1 Compound TR4	101
	(10)

CONTENTS (Continued)

	Page
3.2 Compound TR2	104
3.3 Compound TR8	106
3.4 Compound TR1	108
3.5 Compound TR14	110
3.6 Compound TR15	112
3.7 Compound TR19	114
3.8 Compound TR10	116
3.9 Compound TR6	118
3.10 Compound TR18	120
3.11 Compound TR17	122
3.12 Compound TR16	124
3.13 Compound TR12	127
3.14 CompoundTR7	128
3.15 CompoundTR11	131
3.16 CompoundTR3	133
3.17 CompoundTR9	136
3.18 CompoundTR5	138
3.19 CompoundTR13	140
3.20 CompoundTR20	142
Bibliography	273
Vitae	282

LIST OF TABLES

Table	Page
1 Compounds from Plants of the genus <i>Garcinia</i>	3
2 Trioxygenated xanthones from the genus <i>Garcinia</i>	6
3 Tetraoxygenated xanthones from the genus <i>Garcinia</i>	8
4 Solubility of the crude extract in various solvents at room temperature	30
5 Fractions obtained from the EtOAc soluble fraction by column chromatography over reverse phase silica gel	31
6 Fractions obtained from the fraction 2 by column chromatography over silica gel	32
7 Fractions obtained from the fraction 3 by column chromatography over silica gel	35
8 Fractions obtained from the fraction 5 by column chromatography over silica gel	36
9 Fractions obtained from the fraction 5.2 by flash column chromatography over silica gel	37
10 Fractions obtained from the fraction 6 by column chromatography over silica gel	40
11 Fractions obtained from the fraction 7 by column chromatography over silica gel	42
12 Fractions obtained from the fraction 7.2 by flash column chromatography over silica gel	43
13 Fractions obtained from the fraction B2 by flash column chromatography over silica gel	44

LIST OF TABLES (Continued)

Table	Page
14 Fractions obtained from the subfraction B2.2 by flash column chromatography over silica gel	45
15 Fractions obtained from the fraction 8 by column chromatography over silica gel	46
16 Fractions obtained from the fraction 9 by column chromatography over silica gel	47
17 Fractions obtained from the combined fraction of fractions 9.1 and 8.1 by flash column chromatography over silica gel	48
18 Fractions obtained from the fraction 10 by column chromatography over silica gel	50
19 Fractions obtained from the fraction 10.2 by flash column chromatography over silica gel	51
20 Fractions obtained from the fraction D3 by flash column chromatography over silica gel	52
21 Fractions obtained from the fraction 11 by column chromatography over reverse phase silica gel	54
22 Fractions obtained from the fraction 12 by column chromatography over silica gel	55
23 Fractions obtained from the crude extract by column chromatography over reverse phase silica gel	57
24 Fractions obtained from the fraction 2' by column chromatography over silica gel	58

LIST OF TABLES (Continued)

Table	Page
25 Fractions obtained from the fraction 2'.1 by flash column chromatography over silica gel	59
26 Fractions obtained from the fraction A'2 by flash column chromatography over silica gel	59
27 Fractions obtained from the subfraction A'2.3 by flash column chromatography over silica gel	62
28 Fractions obtained from the fraction A'3 by flash column chromatography over silica gel	64
29 Fractions obtained from the fraction 3' by column chromatography over silica gel	66
30 Fractions obtained from the fraction 3'.1 by flash column chromatography over silica gel	66
31 Fractions obtained from the fraction B'6 by flash column chromatography over silica gel	70
32 Fractions obtained from the subfraction B'6.1 by flash column chromatography over silica gel	70
33 Fractions obtained from the subfraction B'6.3 by flash column chromatography over reverse phase silica gel	71
34 Fractions obtained from the fraction 3'.3 by flash column chromatography over silica gel	73
35 Fractions obtained from the fraction C'2 by flash column chromatography over silica gel	74

LIST OF TABLES (Continued)

Table	Page
36 Fractions obtained from the fraction 4' by column chromatography over silica gel	76
37 Fractions obtained from the fraction 4'.4 by flash column chromatography over silica gel	78
38 Fractions obtained from the combined fraction of fraction 4'.5 and band 2.2 of the fraction D'2 by column chromatography over reverse phase silica gel	80
39 Fractions obtained from the fraction 4'.7 by flash column chromatography over silica gel	83
40 Fractions obtained from the fraction F'1 by flash column chromatography over silica gel	84
41 Fractions obtained from the fraction 5' by column chromatography over silica gel	86
42 Fractions obtained from the fraction 5'.3 by flash column chromatography over silica gel	87
43 Fractions obtained from the fraction G'3 by flash column chromatography over silica gel	88
44 Fractions obtained from the fraction G'5 by flash column chromatography over silica gel	90
45 Fractions obtained from the fraction 5'.5S by column chromatography over reverse phase silica gel	91
46 Fractions obtained from the fraction 5'.5L by flash column chromatography over silica gel	93

LIST OF TABLES (Continued)

Table	Page
47 Fractions obtained from the fraction 5L2 by flash column chromatography over silica gel	94
48 Fractions obtained from the fraction H'2 by flash column chromatography over silica gel	94
49 Fractions obtained from the subfraction H'2.2 by flash column chromatography over silica gel	95
50 Fractions obtained from the subfraction H'2.3 by flash column chromatography over silica gel	96
51 Fractions obtained from the fraction 6' by column chromatography over silica gel	98
52 Fractions obtained from the fraction 6'.3 by flash column chromatography over silica gel	99
53 The NMR data of compound TR4	103
54 The NMR data of compound TR2	105
55 The NMR data of compound TR8	107
56 The NMR data of compound TR1	109
57 The NMR data of compound TR14	111
58 The NMR data of compound TR15	113
59 The NMR data of compound TR19	115
60 The NMR data of compound TR10	117
61 The NMR data of compound TR6	119
62 The NMR data of compound TR18	121

LIST OF TABLES (Continued)

Table	Page
63 The NMR data of compound TR17	123
64 The NMR data of compound TR16	125
65 The NMR data of compound TR12	128
66 The NMR data of compound TR7	130
67 The NMR data of compound TR11	132
68 The NMR data of compound TR3	135
69 The NMR data of compound TR9	137
70 The NMR data of compound TR5	139
71 The NMR data of compound TR13	141
72 The NMR data of compound TR20	143

LIST OF ILLUSTRATIONS

Figure	Page
3.1 UV (MeOH) spectrum of TR4	144
3.2 FT-IR (neat) spectrum of TR4	144
3.3 ¹ H NMR (500 MHz)(CDCl ₃) spectrum of TR4	145
3.4 ¹³ C NMR (125 MHz)(CDCl ₃) spectrum of TR4	146
3.5 DEPT spectrum of TR4	147
3.6 NOEDIFF spectrum of TR4 after irradiation at δ_{H} 6.39	148
3.7 2D HMQC spectrum of TR4	149
3.8 2D HMBC spectrum of TR4	150
3.9 UV (MeOH) spectrum of TR2	151
3.10 FT-IR (neat) spectrum of TR2	151
3.11 ¹ H NMR (500 MHz)(CDCl ₃ +CD ₃ OD) spectrum of TR2	152
3.12 ¹³ C NMR (125 MHz)(CDCl ₃ +CD ₃ OD) spectrum of TR2	153
3.13 DEPT spectrum of TR2	154
3.14 2D HMQC spectrum of TR2	155
3.15 2D HMBC spectrum of TR2	156
3.16 UV (MeOH) spectrum of TR8	157
3.17 FT-IR (neat) spectrum of TR8	157
3.18 ¹ H NMR (500 MHz)(CDCl ₃) spectrum of TR8	158
3.19 ¹³ C NMR (125 MHz)(CDCl ₃) spectrum of TR8	159
3.20 DEPT spectrum of TR8	160
3.21 NOEDIFF spectrum of TR8 after irradiation at δ_{H} 7.45	161
3.22 NOEDIFF spectrum of TR8 after irradiation at δ_{H} 6.37	162

LIST OF ILLUSTRATIONS (Continued)

Figure	Page
3.23 2D HMQC spectrum of TR8	163
3.24 2D HMBC spectrum of TR8	164
3.25 UV (MeOH) spectrum of TR1	165
3.26 FT-IR (neat) spectrum of TR1	165
3.27 ¹ H NMR (500 MHz)(CDCl ₃) spectrum of TR1	166
3.28 ¹³ C NMR (125 MHz)(CDCl ₃) spectrum of TR1	167
3.29 DEPT spectrum of TR1	168
3.30 NOEDIFF of TR1 after irradiation at δ _H 6.43	169
3.31 2D HMQC spectrum of TR1	170
3.32 2D HMBC spectrum of TR1	171
3.33 UV (MeOH) spectrum of TR14	172
3.34 FT-IR (neat) spectrum of TR14	172
3.35 ¹ H NMR (500 MHz)(CDCl ₃ + CD ₃ OD) spectrum of TR14	173
3.36 ¹³ C NMR (125 MHz)(CDCl ₃ + CD ₃ OD) spectrum of TR14	174
3.37 DEPT spectrum of TR14	175
3.38 2D HMQC spectrum of TR14	176
3.39 2D HMBC spectrum of TR14	177
3.40 UV (MeOH) spectrum of TR15	178
3.41 FT-IR (neat) spectrum of TR15	178
3.42 ¹ H NMR (500 MHz)(Acetone- <i>d</i> ₆) spectrum of TR15	179
3.43 ¹³ C NMR (125 MHz)(Acetone- <i>d</i> ₆) spectrum of TR15	180
3.44 DEPT spectrum of TR15	181

LIST OF ILLUSTRATIONS (Continued)

Figure	Page
3.45 2D HMQC spectrum of TR15	182
3.46 2D HMBC spectrum of TR15	183
3.47 UV (MeOH) spectrum of TR19	184
3.48 FT-IR (neat) spectrum of TR19	184
3.49 ^1H NMR (500 MHz)(CDCl_3) spectrum of TR19	185
3.50 ^{13}C NMR (125 MHz)(CDCl_3) spectrum of TR19	186
3.51 DEPT spectrum of TR19	187
3.52 NOEDIFF of TR19 after irradiation at δ_{H} 5.30	188
3.53 2D HMQC spectrum of TR19	189
3.54 2D HMBC spectrum of TR19	190
3.55 Mass spectrum of TR19	191
3.56 UV (MeOH) spectrum of TR10	192
3.57 FT-IR (neat) spectrum of TR10	192
3.58 ^1H NMR (500 MHz)(CDCl_3) spectrum of TR10	193
3.59 ^{13}C NMR (125 MHz)(CDCl_3) spectrum of TR10	194
3.60 DEPT spectrum of TR10	195
3.61 2D HMQC spectrum of TR10	196
3.62 2D HMBC spectrum of TR10	197
3.63 UV (MeOH) spectrum of TR6	198
3.64 FT-IR (neat) spectrum of TR6	198
3.65 ^1H NMR (500 MHz)(CDCl_3) spectrum of TR6	199
3.66 ^{13}C NMR (125 MHz)(CDCl_3) spectrum of TR6	200

LIST OF ILLUSTRATIONS (Continued)

Figure	Page
3.67 DEPT spectrum of TR6	201
3.68 2D HMQC spectrum of TR6	202
3.69 2D HMBC spectrum of TR6	203
3.70 UV (MeOH) spectrum of TR18	204
3.71 FT-IR (neat) spectrum of TR18	204
3.72 ¹ H NMR (500 MHz)(CDCl ₃) spectrum of TR18	205
3.73 ¹³ C NMR (125 MHz)(CDCl ₃) spectrum of TR18	206
3.74 DEPT spectrum of TR18	207
3.75 2D HMQC spectrum of TR18	208
3.76 2D HMBC spectrum of TR18	209
3.77 UV (MeOH) spectrum of TR17	210
3.78 FT-IR (neat) spectrum of TR17	210
3.79 ¹ H NMR (500 MHz)(CDCl ₃) spectrum of TR17	211
3.80 ¹³ C NMR (125 MHz)(CDCl ₃) spectrum of TR17	212
3.81 DEPT spectrum of TR17	213
3.82 2D HMQC spectrum of TR17	214
3.83 2D HMBC spectrum of TR17	215
3.84 UV (MeOH) spectrum of TR16	216
3.85 FT-IR (neat) spectrum of TR16	216
3.86 ¹ H NMR (500 MHz)(CDCl ₃) spectrum of TR16	217
3.87 ¹³ C NMR (125 MHz)(CDCl ₃) spectrum of TR16	218
3.88 DEPT spectrum of TR16	219

LIST OF ILLUSTRATIONS (Continued)

Figure	Page
3.89 2D HMQC spectrum of TR16	220
3.90 2D HMBC spectrum of TR16	221
3.91 UV (MeOH) spectrum of TR12	222
3.92 FT-IR (neat) spectrum of TR12	222
3.93 ¹ H NMR (500 MHz)(CDCl ₃) spectrum of TR12	223
3.94 ¹³ C NMR (125 MHz)(CDCl ₃) spectrum of TR12	224
3.95 DEPT spectrum of TR12	225
3.96 2D HMQC spectrum of TR12	226
3.97 2D HMBC spectrum of TR12	227
3.98 UV (MeOH) spectrum of TR7	228
3.99 FT-IR (neat) spectrum of TR7	228
3.100 ¹ H NMR (500 MHz)(CDCl ₃) spectrum of TR7	229
3.101 ¹³ C NMR (125 MHz)(CDCl ₃) spectrum of TR7	230
3.102 DEPT spectrum of TR7	231
3.103 NOEDIFF of TR7 after irradiation at δ_{H} 5.31	232
3.104 2D HMQC spectrum of TR7	233
3.105 2D HMBC spectrum of TR7	234
3.106 UV (MeOH) spectrum of TR11	235
3.107 FT-IR (neat) spectrum of TR11	235
3.108 ¹ H NMR (500 MHz)(Acetone- <i>d</i> ₆) spectrum of TR11	236
3.109 ¹³ C NMR (125 MHz)(Acetone- <i>d</i> ₆) spectrum of TR11	237
3.110 DEPT spectrum of TR11	238

LIST OF ILLUSTRATIONS (Continued)

Figure	Page
3.111 NOEDIFF of TR11 after irradiation at δ_{H} 5.30	239
3.112 2D HMQC spectrum of TR11	240
3.113 2D HMBC spectrum of TR11	241
3.114 UV (MeOH) spectrum of TR3	242
3.115 FT-IR (neat) spectrum of TR3	242
3.116 ^1H NMR (500 MHz)(CDCl_3) spectrum of TR3	243
3.117 ^{13}C NMR (125 MHz)(CDCl_3) spectrum of TR3	244
3.118 DEPT spectrum of TR3	245
3.119 2D HMQC spectrum of TR3	246
3.120 2D HMBC spectrum of TR3	247
3.121 UV (MeOH) spectrum of TR9	248
3.122 FT-IR (neat) spectrum of TR9	248
3.123 ^1H NMR (500 MHz)(CDCl_3) spectrum of TR9	249
3.124 ^{13}C NMR (125 MHz)(CDCl_3) spectrum of TR9	250
3.125 DEPT spectrum of TR9	251
3.126 2D HMQC spectrum of TR9	252
3.127 2D HMBC spectrum of TR9	253
3.128 UV (MeOH) spectrum of TR5	254
3.129 FT-IR (neat) spectrum of TR5	255
3.130 ^1H NMR (500 MHz)(CDCl_3) spectrum of TR5	256
3.131 ^{13}C NMR (125 MHz)(CDCl_3) spectrum of TR5	257
3.132 DEPT spectrum of TR5	258

LIST OF ILLUSTRATIONS (Continued)

Figure	Page
3.133 NOEDIFF spectrum of TR5 after irradiation at δ_{H} 5.52	258
3.134 2D HMQC spectrum of TR5	259
3.135 2D HMBC spectrum of TR5	260
3.136 UV (MeOH) spectrum of TR13	261
3.137 FT-IR (neat) spectrum of TR13	261
3.138 ^1H NMR (500 MHz)(CDCl_3) spectrum of TR13	262
3.139 ^{13}C NMR (125 MHz)(CDCl_3) spectrum of TR13	263
3.140 DEPT spectrum of TR13	264
3.141 2D HMQC spectrum of TR13	265
3.142 2D HMBC spectrum of TR13	266
3.143 UV (MeOH) spectrum of TR20	267
3.144 FT-IR (neat) spectrum of TR20	267
3.145 ^1H NMR (500 MHz)(CDCl_3) spectrum of TR20	268
3.146 ^{13}C NMR (125 MHz)(CDCl_3) spectrum of TR20	269
3.147 DEPT spectrum of TR20	270
3.148 2D HMQC spectrum of TR20	271
3.149 2D HMBC spectrum of TR20	272

ABBREVIATIONS AND SYMBOLS

<i>s</i>	=	<i>singlet</i>
<i>d</i>	=	<i>doublet</i>
<i>t</i>	=	<i>triplet</i>
<i>m</i>	=	<i>multiplet</i>
<i>br</i>	=	<i>broad</i>
<i>brs</i>	=	<i>broad singlet</i>
<i>dd</i>	=	<i>doublet of doublet</i>
<i>qt</i>	=	<i>quartet of triplet</i>
<i>mt</i>	=	<i>multiple of triplet</i>
δ	=	chemical shift relative to TMS
<i>J</i>	=	coupling constant
<i>m/z</i>	=	a value of mass divided by charge
$^{\circ}\text{C}$	=	degree celcius
R_f	=	retention factor
<i>g</i>	=	gram
<i>mg</i>	=	miligram
<i>mL</i>	=	milliliter
cm^{-1}	=	reciprocal centimeter (wavenumber)
<i>nm</i>	=	nanometer
λ_{max}	=	maximum wavelength
ν	=	absorption frequencies
\mathcal{E}	=	Molar extinction coefficient
<i>Hz</i>	=	hertz
<i>MHz</i>	=	megahertz

ABBREVIATIONS AND SYMBOLS (Continued)

$[\alpha]_D$	=	specific rotation
c	=	concentration
H-n	=	position of protons
C-n	=	position of carbons
UV	=	Ultraviolet
IR	=	Infrared
NMR	=	Nuclear Magnetic Resonance
2D NMR	=	Two Dimensional Nuclear Magnetic Resonance
MS	=	Mass Spectroscopy
HMQC	=	Heteronuclear Multiple Quantum Coherence
HMBC	=	Heteronuclear Multiple Bond Correlation
DEPT	=	Distortionless Enhancement by Polarization transfer
NOE	=	Nuclear Overhauser Effect
NOEDIFF	=	Nuclear Overhauser Effect Difference Spectroscopy
TLC	=	Thin-Layer Chromatography
TMS	=	tetramethylsilane
DMSO	=	dimethylsulphoxide
MeOH	=	methanol
$CDCl_3$	=	deuteriochloroform
Acetone- d_6	=	hexadeuteroacetone
CD_3OD	=	tetradeuteromethanol
ASA	=	anisaldehyde-sulphuric acid in acetic acid solution

CHAPTER 1

INTRODUCTION

1.1 Introduction

Garcinia nigrolineata, a plant belonging to the Guttiferae family, was locally named “Cha Mwuang (ชะมวง)” (เต็ม, 2523) and found at Eastern peninsula, Malacca, Griffith and Maingay (Hooker, 1875). The family Guttiferae contains about 40 genera and over 1000 species. Only 6 genera and 60 species are found in Thailand; i.e., *Calophyllum*, *Cratoxylum*, *Garcinia*, *Mesua*, *Kayea* and *Orchrocarpus* (Panthong, 1999). *G. nigrolineata* is a small to medium tree or very rarely a shrub. Inner bark with scant, bright yellow latex (Whitemore, 1973), branches often knotted; bark dusky. Leaves lanceolate or ovate-lanceolate, 5-8 by 1.75-3 in., subcoriaceous, tapering to the base; veins many, delicate, 0.1-0.16 in. apart, inarching with an intramarginal one. Male flowers 3-9, fascicled on short axillary woody nodes; pedicels 0.25-0.5 in., slender, thickened above. Sepals 0.08 in., fleshy, orbicular. Petals a little longer and thinner, concave, reflexed above the middle. Stamens in a shortly pedicelled 4 cornered compressed mass; anthers 4-gonal, 4-celled. Female flowers solitary, axillary. Ovary ovoid (5-7-celled, Maingay); stigma 5-7 lobed, lobes lobulate, papillose. [“Fruits are subglobose, with a thick fleshy stipitate discoid apiculus, as large as a walnut, bright orange-yellow.”-Maingay.] (Hooker, 1875).

1.2 Review of Literatures

1.2.1 Chemical Constituents from the genus *Garcinia*

Plants in the genus *Garcinia* (Guttiferae) are well known to be rich in a variety of compounds: xanthenes (Huang, 2001; Ito, 2001; Xu, 2001; Gopalakrishnan, 2000; Nguyen, 2000; Okudaira, 2000), benzophenones (Cuesta Rudio, 2001; Huang, 2001; Ali, 2000; Iinuma, 1996e; Spino, 1995; Fukuyama, 1993; Gustafson, 1992; Nyemba, 1990), biflavonoids (Thoison, 2000; Spino, 1995; Fukuyama, 1993; Goh, 1992; Gunatilaka, 1983), benzophenone-xanthone dimers (Kosela, 2000, 1999; Iinuma, 1996b, c) and triterpenes (Nguyen, 2000; Rukachaisirikul, 2000b; Thoison, 2000). Some of these exhibit a wide range of biological and pharmacological activities, e.g., cytotoxic (Permana, 2001; Kosela, 2000; Thoison, 2000; Xu, 2000; Cao, 1998a, b), antiinflammatory (Peres, 2000; Chairungsrilerd, 1996a; Ilyas, 1994; Parveen, 1991), antimicrobial (Permana, 2001; Kosela, 2000; Peres, 2000; Iinuma, 1996d; Ilyas, 1994; Parveen, 1991), antifungal (Kosela, 2000; Peres, 2000; Gopalakrishnan, 1997), antiprotozoal (Parveen, 1991), antibacterial (Permana, 2001; Peres, 2000; Rukachaisirikul, 2000a; Ito, 1997; Iinuma, 1996b, e; Parveen, 1991), antiimmunosuppressive (Ilyas, 1994; Parveen, 1991), antitumor (Ito, 1998), antimalarial (Kosela, 2000; Likhitwitayawuid, 1998a, b), anti-HIV (Kosela, 2000; Lin, 1997; Gustafson, 1992) activities, antioxidant (Peres, 2001; Kosela, 2000; Iinuma, 1996d; Minami, 1996) and the sealing of skin infections and wounds (Ilyas, 1994).

Chemical constituents isolated from 62 species of the genus *Garcinia* were reported according to Information from NAPRALERT database developed by University of Illinois at Chicago and chemical abstracts in the year 2001. However, only additional chemical constituents from the genus *Garcinia* apart from those reported by Assdhawut Hiranrat (2001) are summarized in **Table 1**.

Table 1 Compounds from Plants of the genus *Garcinia*

Scientific name	Investigated part	Compound	Structure	Bibliography
<i>G. aristata</i>	fruits	aristophenone A	1a	Cuesta-Rudio, <i>et al.</i> , 2001
		aristophenone B	1b	
<i>G. atroviridis</i>	roots	atrovirinone	3a	Permana, <i>et al.</i> , 2001
		atrovirisidone	4a	
<i>G. mangostana</i>	fruit hulls	garcimangosone A	9.2rr	Huang, <i>et al.</i> , 2001
		garcimangosone B	9.2xx	
		garcimangosone C	9.2yy	
		garcimangosone D	1c	
		8-desoxygartanin	9.1q	
		gartanin	9.2u	
		α -mangostin	9.2aa	
		β -mangostin	9.2bb	
		γ -mangostin	9.2cc	
		1,5-di(OH)-2-isoprenyl-3-(OMe)xanthone	9.1j	
		5,9-di(OH)-8-(OMe)-2,2-di(Me)-7-(3-methylbut-2-enyl)-2H,6H-pyrano[3,2-b]-xanthone-6-one	9.2qq	
		garcinone B	9.2r	

Table 1 (Continued)

Scientific name	Investigated part	Compound	Structure	Bibliography
<i>G. mangostana</i>	fruit hulls	garcinone D	9.2s	Huang, <i>et al.</i> , 2001
		garcinone E	9.2t	
		1-isomangostin	9.2v	
		3-isomangostin	9.2w	
		mangostanol	9.2x	
		1,3,6,7-tetra(OH)-8-(3-methylbut-2-enyl)-xanthone	9.2g	
		1,7-di(OH)-2-isoprenyl-3-(OMe) xanthone	9.1k	
		(-)-epicatechin	5a	
		taxifolin-3-O- α -L-rhamnoside	6a	
		proanthocyanidin A ₁	7a	
		proanthocyanidin A ₂	7b	
		procyanidin B ₂	8a	
		procyanidin B ₅	8b	
		tovophyllin A	9.2y	
		tovophyllin B	9.2z	
<i>G. parvifolia</i>	bark	parvixanthone A	9.2zz	Xu, <i>et al.</i> , 2001
		parvixanthone B	9.2aaa	
		parvixanthone C	9.2bbb	

Table 1 (Continued)

Scientific name	Investigated part	Compound	Structure	Bibliography
<i>G. parvifolia</i>	bark	parvixanthone D	9.2ccc	Xu, <i>et al.</i> , 2001
		parvixanthone E	9.2ddd	
		parvixanthone F	9.2eee	
		parvixanthone G	9.2fff	
		parvixanthone H	9.2ggg	
		parvixanthone I	9.2hhh	

1.2.2 Trioxxygenated and tetraoxxygenated xanthonones from the genus *Garcinia*

The xanthonones isolated to date can be classified into five major groups: simple oxygenated xanthonones, xanthonone glycosides, prenylated and related xanthonones, xanthonolignoids and miscellaneous xanthonones. The simple oxygenated xanthonone can be subdivided into six groups according to the degree of oxygenation. Trioxxygenated xanthonones (Peres and Nagem, 1997) and tetraoxxygenated xanthonones (Peres, *et al.*, 2000) isolated from various sources were described. Additional trioxxygenated and tetraoxxygenated naturally occurring xanthonones isolated from the genus *Garcinia* were summarized in Table 2 and Table 3, respectively. We are interested in these oxygenated xanthonones since the new xanthonones from our investigation on the stem bark of *G. nigrolineata* were compounds of these types.

Table 2 Trioxxygenated xanthenes from the genus *Garcinia*

Scientific name	Investigated part	Compound	Structure	Bibliography
<i>G. assigu</i> Lantb.	stem bark	pancixanthone A	9.1m	Ito, <i>et al.</i> , 1997, 1998
		1,3,5-tri(OH)xanthone	9.1a	
<i>G. dioica</i>	bark	1,3,7-tri(OH)-2,4-diisoprenylxanthone	9.1p	linuma, <i>et al.</i> , 1996d
<i>G. dulcis</i>	roots	garciduol A	2a	linuma, <i>et al.</i> , 1996b,c
		garciduol B	2b	
		garciduol C	2c	
		2,5-di(OH)-1-(OMe)-xanthone	9.1d	
		1,4,5-tri(OH)xanthone	9.1c	
		(subelliptenone G)		
	roots	1,3,5-tri(OH)xanthone	9.1a	linuma, <i>et al.</i> , 1996a
		dulciol D	9.1o	
		dulciol E	9.1s	
		garciniaxanthone A	9.1t	
		garciniaxanthone B	9.1h	
	bark	garciniaxanthone D	9.1u	
		globuxanthone	9.1e	
		12b-hydroxy-des-D-garcigerrin A	9.1b	
stem bark	gentisein	9.1l	Ito, <i>et al.</i> , 1997, 1998	

Table 2 (Continued)

Scientific name	Investigated part	Compound	Structure	Bibliography
<i>G. dulcis</i>	stem bark	1,3,7-tri(OH)-2-(3-methyl-2-butenyl)-xanthone	9.1i	Ito, <i>et al.</i> , 1997, 1998
<i>G. kola</i>	stem	1,2,8-tri(OMe)xanthone	9.1g	Terashima, <i>et al.</i> , 1999
<i>G. mangostana</i>	fruit hulls	1,7-di(OH)-3-(OMe)-2-(γ,γ -dimethylallyl)-xanthone	9.1n	Chairungsri-lerd, <i>et al.</i> , 1996a
	fruit hulls	2,7-di(3-methylbut-2-enyl)-1,3,8-tri(OH)-4-(Me)xanthone	9.1r	Gopalakrishnan and Balaganesan, 2000
<i>G. puat</i> Guillaumin.	leaves	1,3,7-tri(OH)-2-(3-methyl-2-butenyl)-xanthone	9.1i	Ito, <i>et al.</i> , 2001
<i>G. subelliptica</i>	wood	garcinixanthone D	9.1u	Minami, <i>et al.</i> , 1996
		garcinixanthone F	9.1v	
		garcinixanthone G	9.1o	
<i>G. vilersiana</i>	bark	globuxanthone	9.1e	Nguyen, <i>et al.</i> , 2000
		12b-hydroxy-des-D-garcigerrin A	9.1b	

Table 2 (Continued)

Scientific name	Investigated part	Compound	Structure	Bibliography
<i>G. vilersiana</i>	bark	1- <i>O</i> -methylglobu-xanthone	9.1f	Nguyen, <i>et al.</i> , 2000

Table 3 Tetraoxygenated xanthenes from the genus *Garcinia*

Scientific name	Investigated part	Compound	Structure	Bibliography
<i>G. assigu</i> Lantb.	stem bark	assiguxanthone A	9.2h	Ito, <i>et al.</i> , 1997, 1998
		assiguxanthone B	9.2e	
		1,3,6,7-tetra(OH)-8-(3-methylbut-2-enyl)-xanthone	9.2g	
		toxyloxanthone B	9.2n	
<i>G. atroviridis</i>	stem bark	atroviridin	9.2o	Kosin, <i>et al.</i> , 1998
<i>G. cambogia</i>	root bark	garbogiol	9.2m	Iinuma, <i>et al.</i> , 1998
	bark	rheediaxanthone A	9.2kk	
<i>G. cowa</i>	bark	β -mangostin	9.2bb	Likhitwitaya-wuid, <i>et al.</i> , 1998
<i>G. dioica</i>	bark	rubraxanthone	9.2ss	Iinuma, <i>et al.</i> , 1996d

Table 3 (Continued)

Scientific name	Investigated part	Compound	Structure	Bibliography
<i>G. dioica</i>	bark	1,3,6-tri(OH)-8-(7-(OH)-3,7-di(Me)-2,5-octadienyl)-7-(OMe)-xanthone	9.2vv	Iinuma, <i>et al.</i> , 1996d
		1,3,6-tri(OH)-8-(6,7-epoxy-3,7-di(Me)-2-octenyl)-7-(OMe)-xanthone	9.2ww	
<i>G. dulcis</i>	roots	1, 3,6-tri(OH)-7-(OMe)-xanthone	9.2b	Iinuma, <i>et al.</i> , 1996b
		1,3,6-tri(OH)-5-(OMe)-xanthone	9.2d	
		1,3,6-tri(OH)- 8-isoprenyl-7-(OMe)-xanthone	9.2c	
	bark	toxyloxanthone B	9.2n	Iinuma, <i>et al.</i> , 1996a
	stem bark	dulxanthone A	9.2dd	Ito, <i>et al.</i> , 1997, 1998
		dulxanthone B	9.2ee	
		dulxanthone C	9.2ff	
dulxanthone D		9.2f		
isoprenylxanthone	9.2gg			

Table 3 (Continued)

Scientific name	Investigated part	Compound	Structure	Bibliography
<i>G. dulcis</i>	stem bark	jacareubin	9.2q	Ito, <i>et al.</i> , 1997, 1998
		ugaxanthone	9.2hh	
	bark	xanthone VI	9.2p	Likhitwitaya- wuid, <i>et al.</i> , 1998b
		1- <i>O</i> -(Me)- symphoxanthone	9.2j	
		symphoxanthone	9.2k	
<i>G. griffithii</i>	bark	griffipavixanthone	9.3a	Xu, <i>et al.</i> , 1998
<i>G. kola</i>	stem	1,3,5-tri(OH)-2-(OMe)- xanthone	9.2a	Terashima, <i>et al.</i> , 1999
<i>G. latissima</i>	stem bark	latisxanthone A	9.2mm	Ito, <i>et al.</i> , 1997, 1998
		latisxanthone B	9.2nn	
		latisxanthone C	9.2oo	
		latisxanthone D	9.2pp	
		pyranojacereubin	9.2ll	
<i>G. mangostana</i>	fruit hull	5,9-di(OH)-8-(OMe)- 2,2-di(Me)-7-(3- methylbut-2-enyl)- 2 <i>H</i> ,6 <i>H</i> -pyrano[3,2- <i>b</i>]- xanthon-6-one	9.2qq	Chairungsri- lerd, <i>et al.</i> , 1996a

Table 3 (Continued)

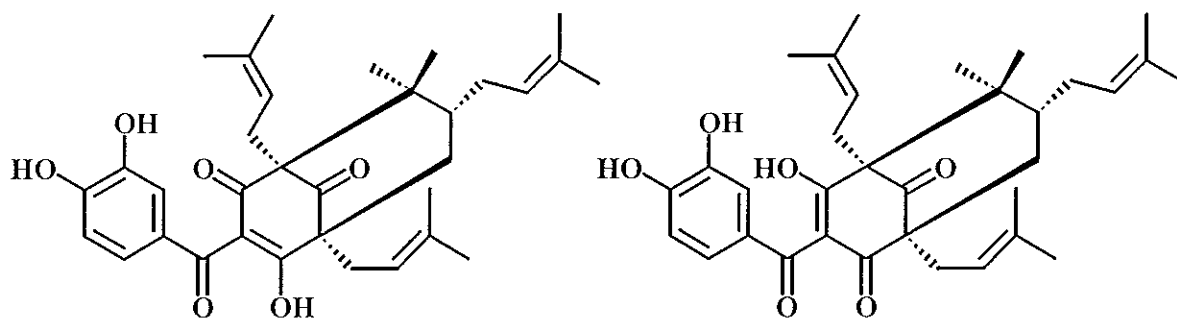
Scientific name	Investigated part	Compound	Structure	Bibliography
<i>G. mangostana</i>	fruit hulls	α -mangostin	9.2aa	Chairungsri- rd, <i>et al.</i> , 1996b
	fruit hulls	garcimangosone A	9.2rr	Huang, <i>et al.</i> , 2001
		garcimangosone B	9.2xx	
		garcimangosone C	9.2yy	
<i>G. parvifolia</i>	bark	griffipavixanthone	9.3a	Xu, <i>et al.</i> , 1998
		parvixanthone A	9.2zz	Xu, <i>et al.</i> , 2001
		parvixanthone B	9.2aaa	
		parvixanthone C	9.2bbb	
		parvixanthone D	9.2ccc	
		parvixanthone E	9.2ddd	
		parvixanthone F	9.2eee	
		parvixanthone G	9.2fff	
		parvixanthone H	9.2ggg	
parvixanthone I	9.2hhh			
<i>G. sessilis</i>	heartwood	5,9-di(OH)-8-(OMe)- 2,2-di(Me)-7-(3- methylbut-2-enyl)- 2 <i>H</i> ,6 <i>H</i> -pyrano[3,2- <i>b</i>]- xanthon-6-one	9.2qq	Ali, <i>et al.</i> , 1999

Table 3 (Continued)

Scientific name	Investigated part	Compound	Structure	Bibliography
<i>G. speciosa</i>	bark	α -mangostin cowanin cowanol	9.2aa 9.2tt 9.2uu	Okudaira, <i>et al.</i> , 2000
<i>G. subelliptica</i>	wood	garciniaxanthone H	9.2i	Minami <i>et al.</i> , 1996
	wood	1,6- <i>O</i> -di(Me)- symphoxanthone	9.2l	Minami <i>et al.</i> , 1998
<i>G. vilersiana</i>	bark	subelliptenone B subelliptenone H symphoxanthone	9.2ii 9.2jj 9.2k	Nguyen, <i>et al.</i> , 2000
<i>G. vitiensis</i>	heartwood	5,9-di(OH)-8-(OMe)- 2,2-di(Me)-7-(3- methylbut-2-enyl)- 2 <i>H</i> ,6 <i>H</i> -pyrano [3,2- <i>b</i>]- xanthon-6-one	9.2qq	Ali, <i>et al.</i> , 1999

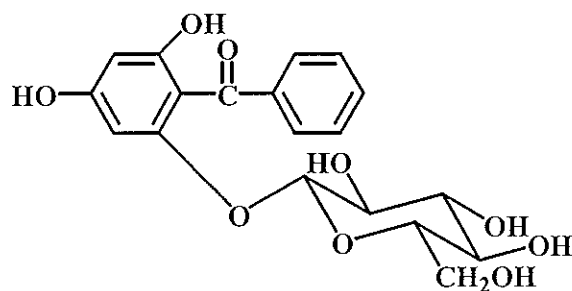
Structures of Compounds Isolated from Plants of the genus *Garcinia*

1. Benzophenones



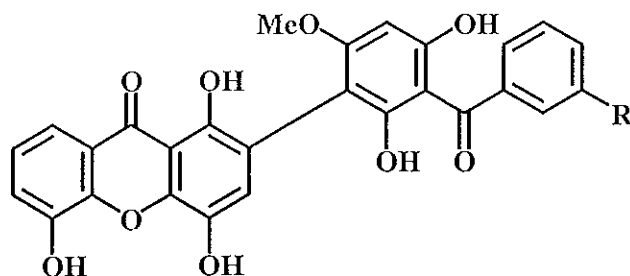
1a: aristophenone A

1b: aristophenone B



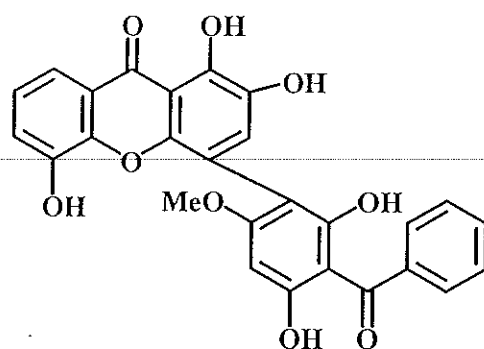
1c: garcimangosone D

2. Benzophenone-xanthone dimers



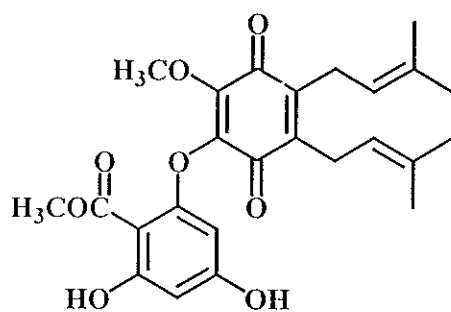
2a: R = H : garciduol A

2b: R = OH : garciduol B



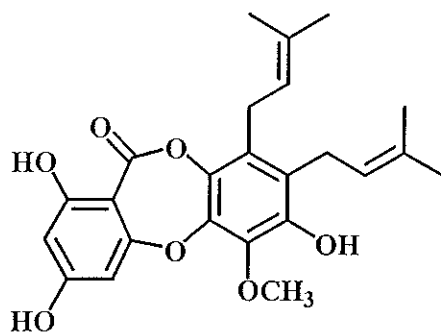
2c: garcidiol C

3. Benzoquinones



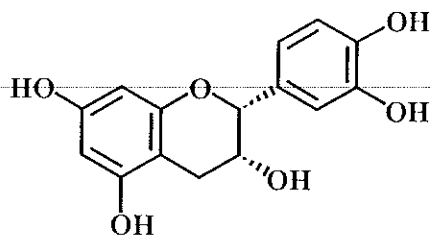
3a: atrovirine

4. Depsidones



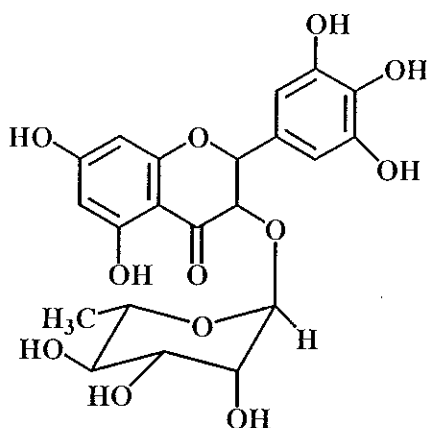
4a: atrovirisidone

5. Flavanes

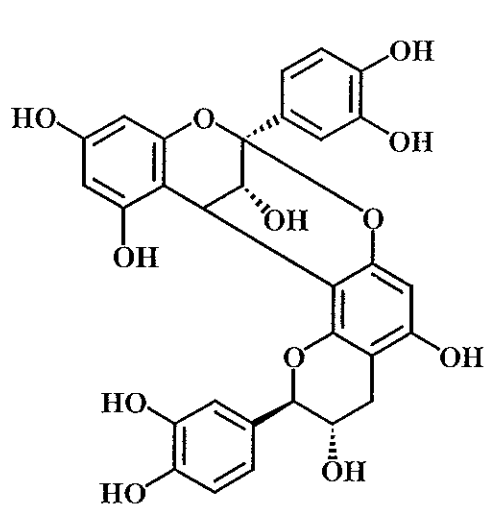
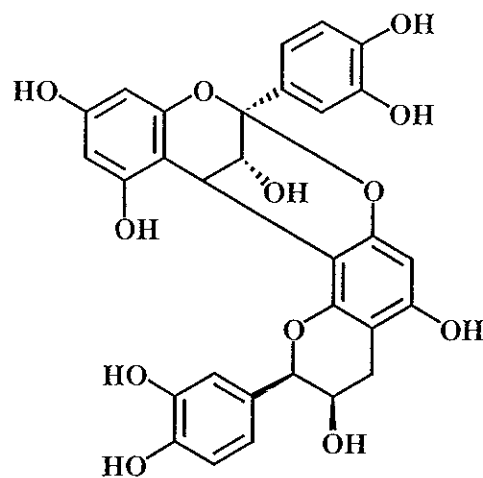


5a: (-)-epicatechin

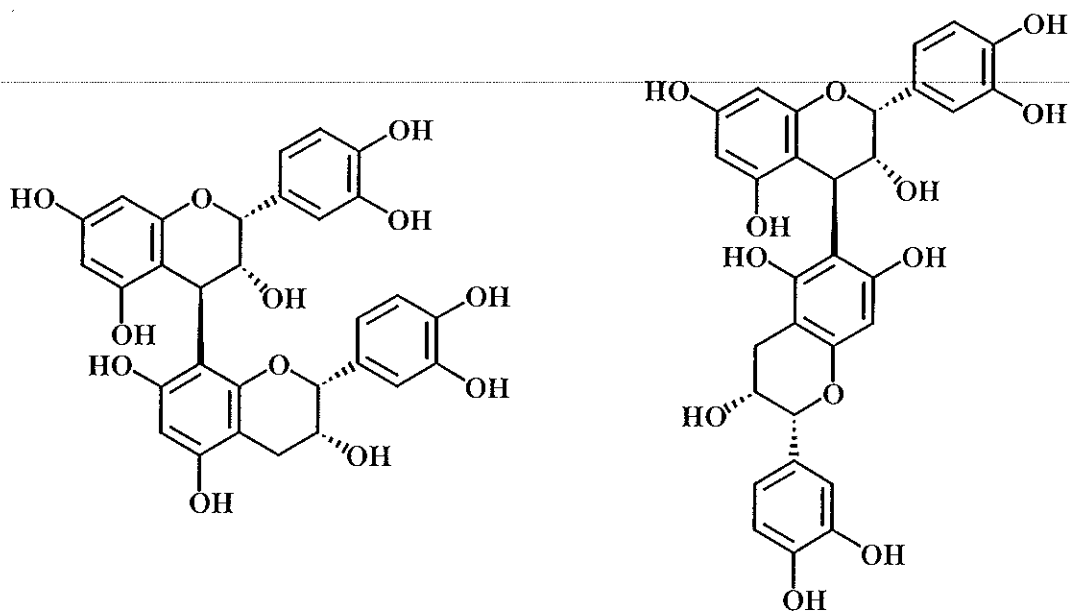
6. Flavanones

6a: taxifolin-3-O- α -L-rhamnoside

7. Proanthocyanidins

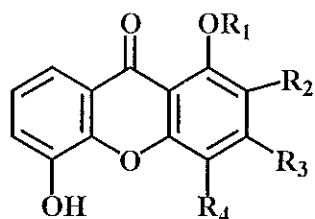
7a: proanthocyanidin A₁7b: proanthocyanidin A₂

8. Procyanidins

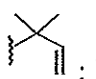
8a: procyanidin B₂8b: procyanidin B₅

9. Xanthenes

9.1 Trioxyxanthenes




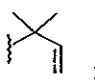
9.1a: R₁ = R₂ = R₄ = H ; R₃ = OH : 1,3,5-tri(OH)xanthone

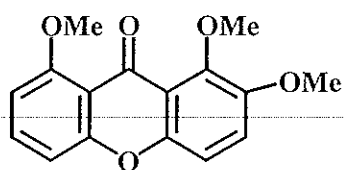
9.1b: R₁ = R₃ = H ; R₂ =  ; R₄ = OH : 12b-(OH)-des-D-garcigerin A

9.1c: R₁ = R₂ = R₃ = H ; R₄ = OH : 1,4,5-tri(OH)xanthone (subelliptenone G)

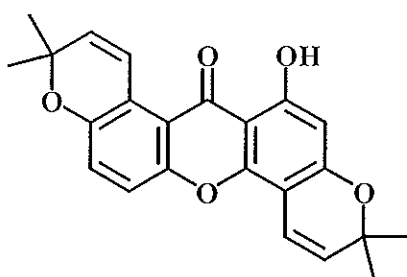
9.1d: R₁ = Me ; R₂ = OH ; R₃ = R₄ = H : 2,5-di(OH)-1-(OMe)xanthone

9.1e: R₁ = R₃ = H ; R₂ = OH ; R₄ =  : globuxanthone

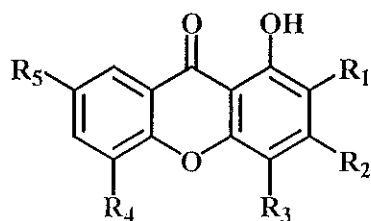
9.1f: R₁ = Me ; R₂ = OH ; R₃ = H ; R₄ =  : 1-O-methylglobuxanthone



9.1g: 1,2,8-tri(OMe)xanthone



9.1h: garciniaxanthone B



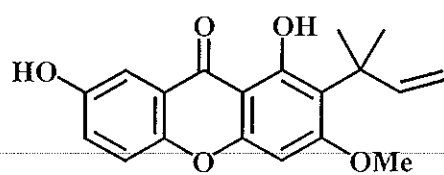
9.1i: $R_1 = \text{isoprenyl}$; $R_2 = R_5 = \text{OH}$; $R_3 = R_4 = \text{H}$; : 1,3,7-tri(OH)-2-(3-methyl-2-butenyl)xanthone

9.1j: $R_1 = \text{isoprenyl}$; $R_2 = \text{OMe}$; $R_3 = R_5 = \text{H}$; $R_4 = \text{OH}$: 1,5-di(OH)-2-isoprenyl-3-(OMe)xanthone

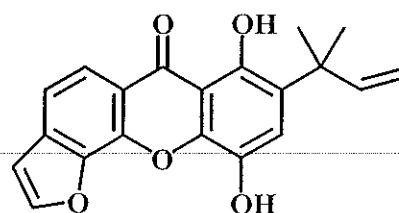
9.1k: $R_1 = \text{isoprenyl}$; $R_2 = \text{OMe}$; $R_3 = R_4 = \text{H}$; $R_5 = \text{OH}$: 1,7-di(OH)-2-isoprenyl-3-(OMe)xanthone

9.1l: $R_1 = R_3 = R_4 = \text{H}$; $R_2 = R_5 = \text{OH}$: gentisein

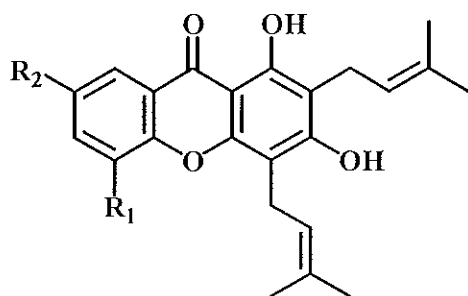
9.1m: $R_1 = R_5 = \text{H}$; $R_2 = R_4 = \text{OH}$; $R_3 = \text{isoprenyl}$: pancixanthone A



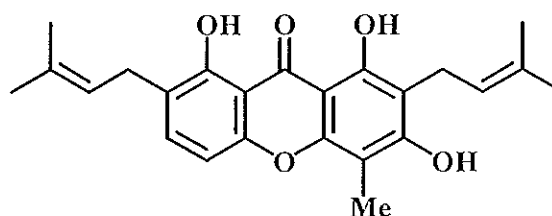
9.1n: 1,7-di(OH)-3-(OMe)-2-
(γ,γ -dimethylallyl)xanthone



9.1o: dulciol D (garciniaxanthone G)

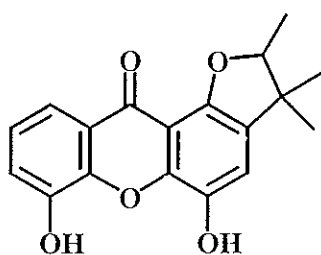


9.1p: $R_1 = H$; $R_2 = OH$: 1,3,7-tri(OH)-2,4-
diisoprenylxanthone

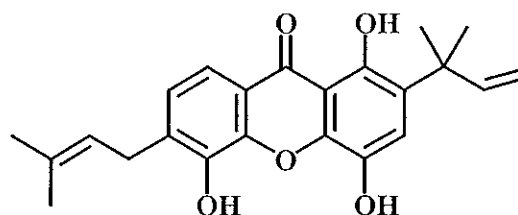


9.1r: 2,7-di(3-methylbut-2-enyl)-
1,3,8-tri(OH)-4-(Me)xanthone

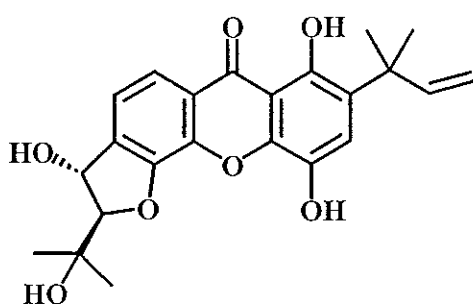
9.1q: $R_1 = OH$; $R_2 = H$: 8-desoxygartanin



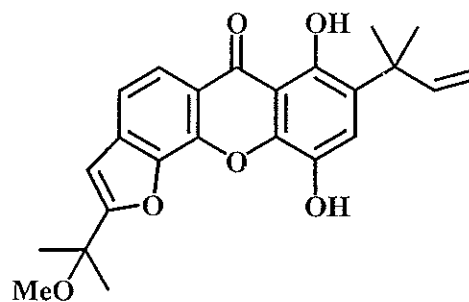
9.1s: dulciol E



9.1t: garciniaxanthone A

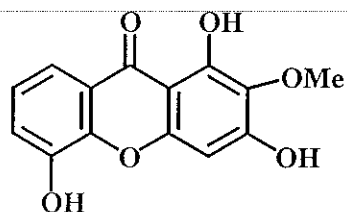


9.1u: gaciniaxanthone D

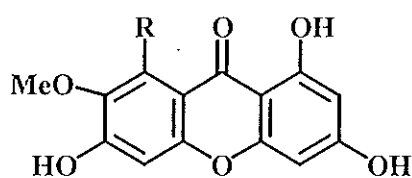
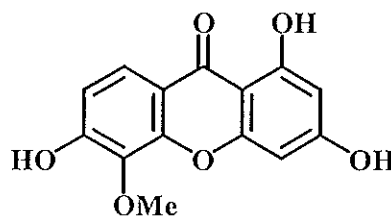


9.1v: garciniaxanthone F

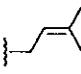
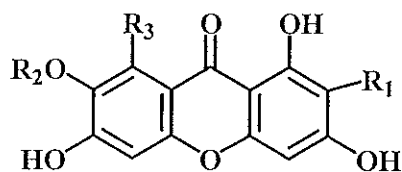
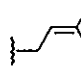
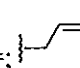
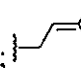
9.2 Tetraoxyxanthone

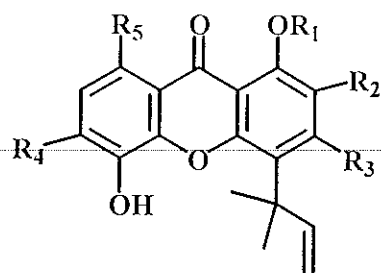


9.2a: 1,3,5-tri(OH)-2-(OMe)xanthone

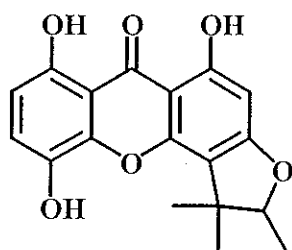
9.2b: R = H : 1,3,6-tri(OH)-7-(OMe)-
xanthone

9.2d: 1,3,6-tri(OH)-5-(OMe)xanthone

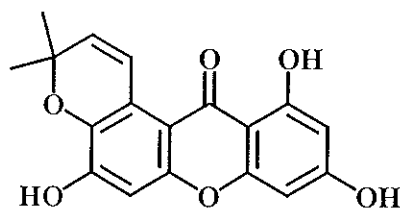
9.2c: R =  : 1,3,6-tri(OH)-8-isoprenyl-
7-(OMe)xanthone9.2e: R₁ = ; R₂ = R₃ = H : assiguxanthone B9.2f: R₁ = H; R₂ = Me; R₃ =  : dulxanthone D9.2g: R₁ = R₂ = H; R₃ =  : 1,3,6,7-tetra(OH)-8-(3-methylbut-2-enyl)xanthone



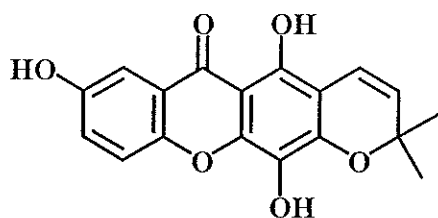
- 9.2h: $R_1 = R_2 = R_5 = H$; $R_3 = R_4 = OH$: assiguxanthone A
- 9.2i: $R_1 = Me$; $R_2 = R_5 = OH$; $R_3 = R_4 = H$: garciniaxanthone H
- 9.2j: $R_1 = Me$; $R_2 = R_4 = OH$; $R_3 = R_5 = H$: 1-*O*-methylsymphoxanthone
- 9.2k: $R_1 = R_3 = R_5 = H$; $R_2 = R_4 = OH$: symphoxanthone
- 9.2l: $R_1 = Me$; $R_2 = OH$; $R_3 = R_5 = H$; $R_4 = OMe$: 1,6-*O*-di(Me)symphoxanthone



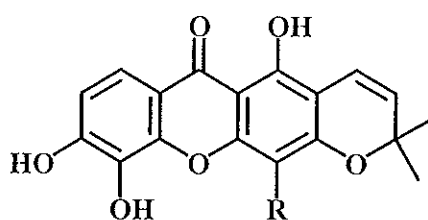
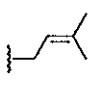
9.2m: garbogiol

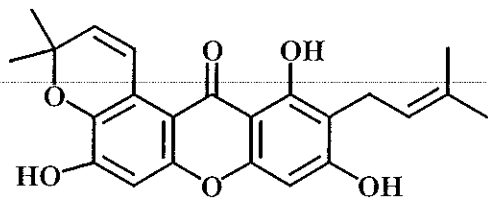


9.2n: toxyloxanthone B

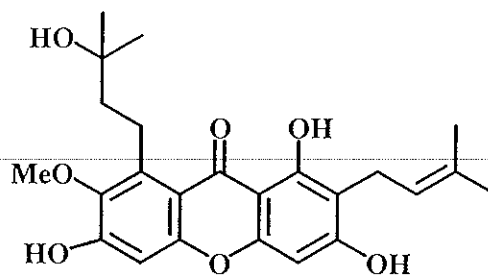


9.2o: atrioviridin

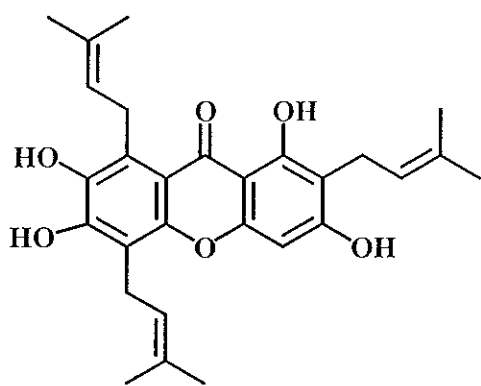
9.2p: $R =$  : xanthone VI9.2q: $R = H$: jacareubin



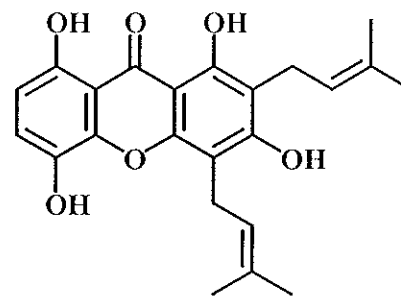
9.2r: garcinone B



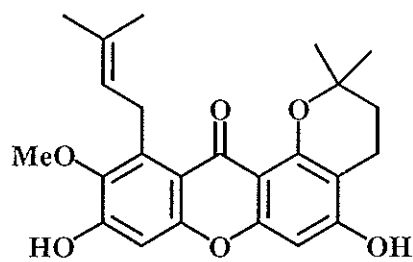
9.2s: garcinone D



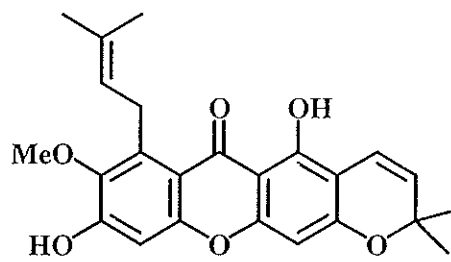
9.2t: garcinone E



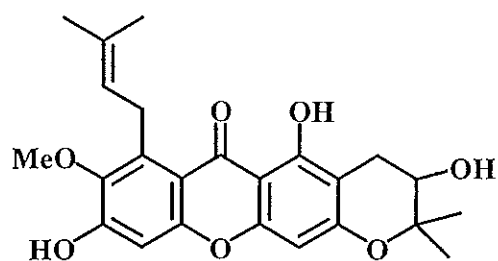
9.2u: gartanin



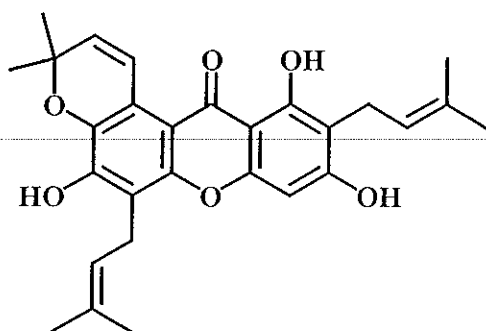
9.2v: 1-isomangostin



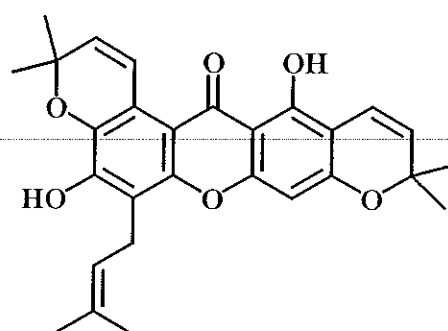
9.2w: 3-isomangostin



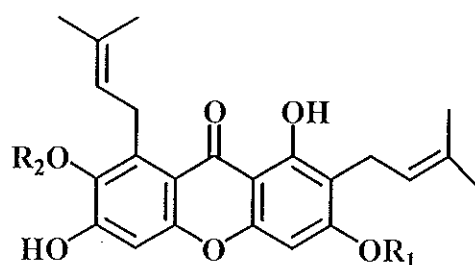
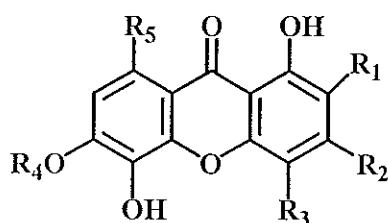
9.2x: mangostanol

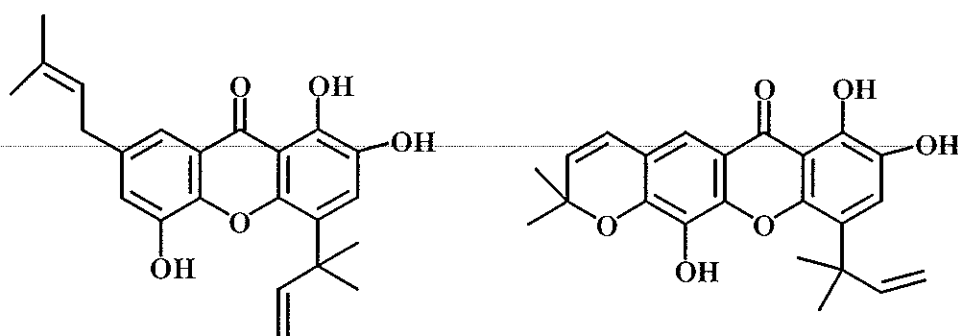


9.2y: tovophyllin A



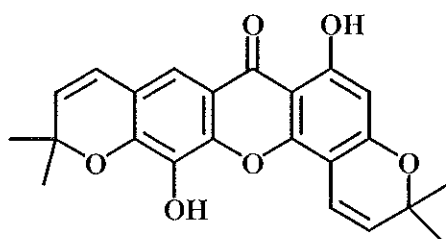
9.2z: tovophyllin B

9.2aa: $R_1 = H$; $R_2 = Me$: α -mangostin9.2bb: $R_1 = Me$; $R_2 = Me$: β -mangostin9.2cc: $R_1 = R_2 = H$: γ -mangostin9.2dd: $R_1 = R_4 = R_5 = H$; $R_2 = OMe$; $R_3 = \text{3-methylbut-1-en-1-yl}$: dulxanthone A9.2ee: $R_1 = R_3 = \text{3-methylbut-1-en-1-yl}$; $R_2 = OMe$; $R_4 = R_5 = H$: dulxanthone B9.2ff: $R_1 = H$; $R_2 = OMe$; $R_3 = R_5 = \text{3-methylbut-1-en-1-yl}$; $R_4 = Me$: dulxanthone C9.2gg: $R_1 = \text{3-methylbut-1-en-1-yl}$; $R_2 = OH$; $R_3 = R_4 = R_5 = H$: isoprenylxanthone9.2hh: $R_1 = R_4 = R_5 = H$; $R_2 = OH$; $R_3 = \text{3-methylbut-1-en-1-yl}$: ugaxanthone

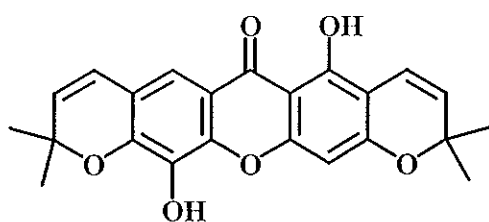


9.2ii: subelliptenone B

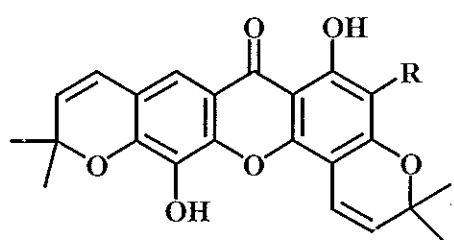
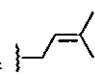
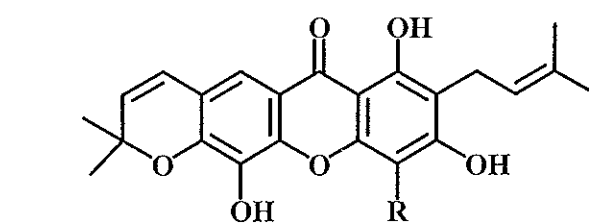
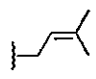
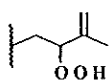
9.2jj: subelliptenone H



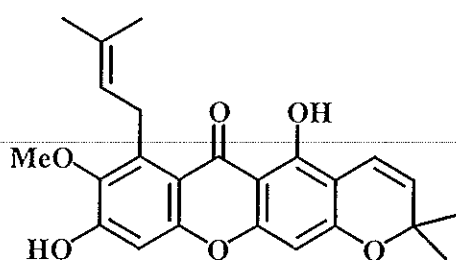
9.2kk: rheediaxanthone A



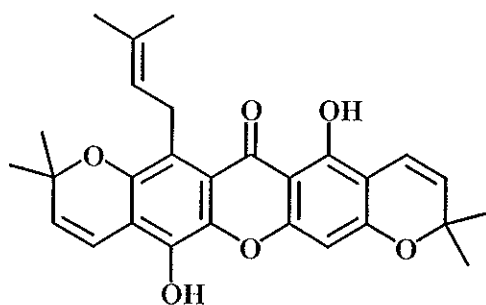
9.2ll: pyranojacareubin

9.2mm: R =  : latisxanthone A9.2oo: R =  : latisxanthone C9.2nn: R =  : latisxanthone B

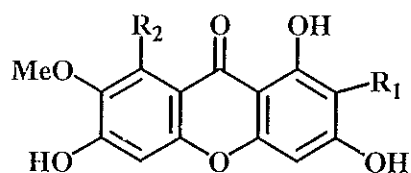
9.2pp: R = H : latisxanthone D

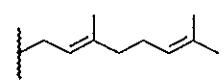


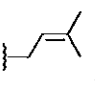
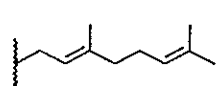
9.2qq: 5,9-di(OH)-8-(OMe)-2,2-di(Me)-7-(3-methylbut-2-enyl)-2H,6H-pyrano[3,2-*b*]xanthon-6-one

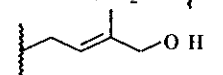
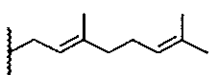


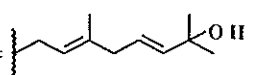
9.2rr: garcimagosone A

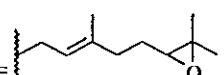


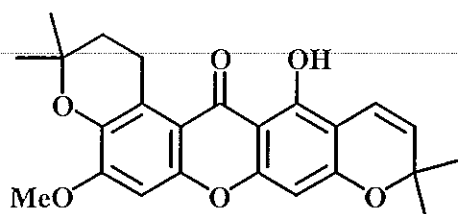
9.2ss: $R_1 = \text{H}$; $R_2 =$  : rubraxanthone

9.2tt: $R_1 =$  ; $R_2 =$  : cowanin

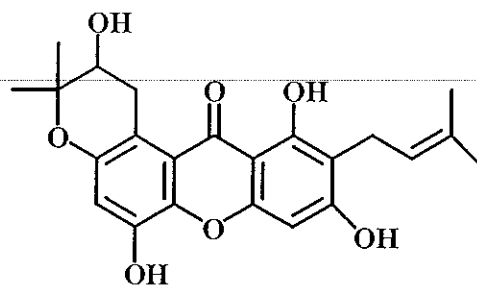
9.2uu: $R_1 =$  ; $R_2 =$  : cowanol

9.2vv: $R_1 = \text{H}$; $R_2 =$  : 1,3,6-tri(OH)-8-(7-(OH)-3,7-di(Me)-2,5-octadienyl)-7-(OMe)xanthone

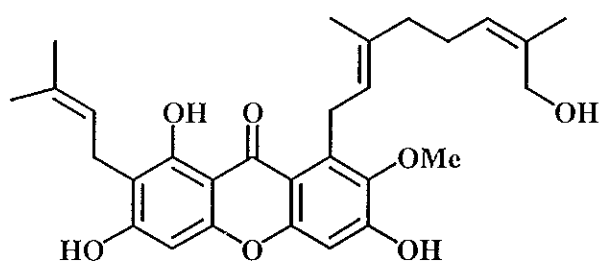
9.2ww: $R_1 = \text{H}$; $R_2 =$  : 1,3,6-tri(OH)-8-(6,7-epoxy-3,7-di(Me)-2-octaeenyl)-7-(OMe)xanthone



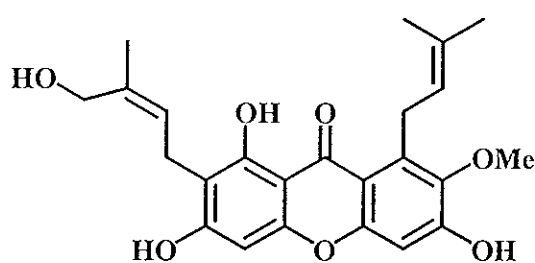
9.2xx: garcimagosone B



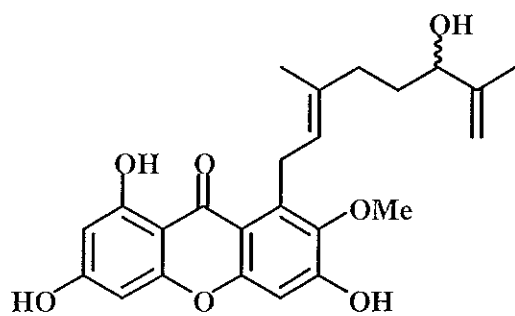
9.2yy: garcimagosone C



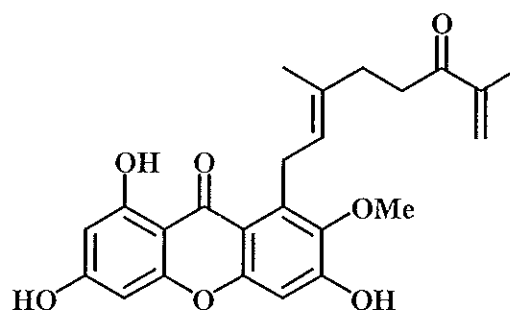
9.2zz: parvixanthone A



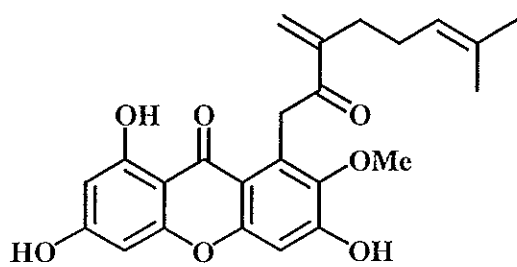
9.2aaa: parvixanthone B



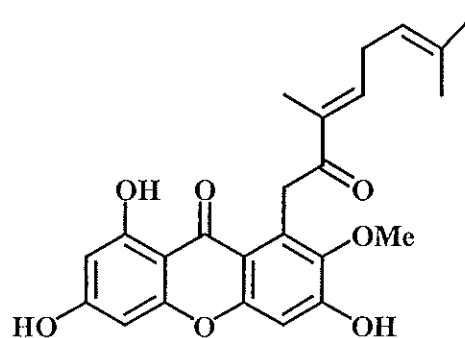
9.2bbb: parvixanthone C



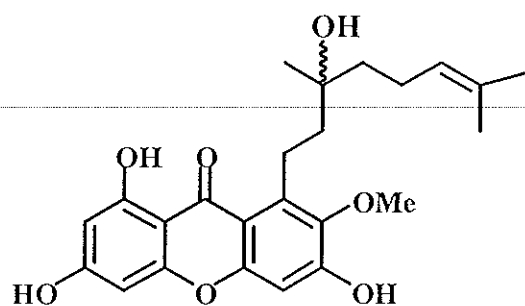
9.2ccc: parvixanthone D



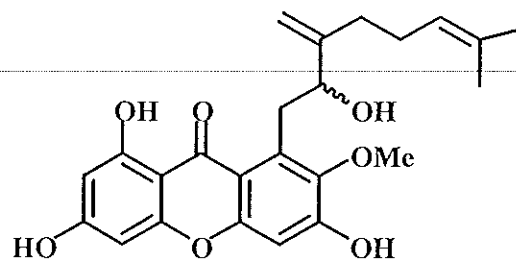
9.2ddd: parvixanthone E



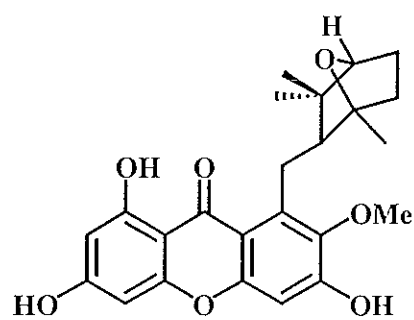
9.2eee: parvixanthone F



9.2fff: parvixanthone G

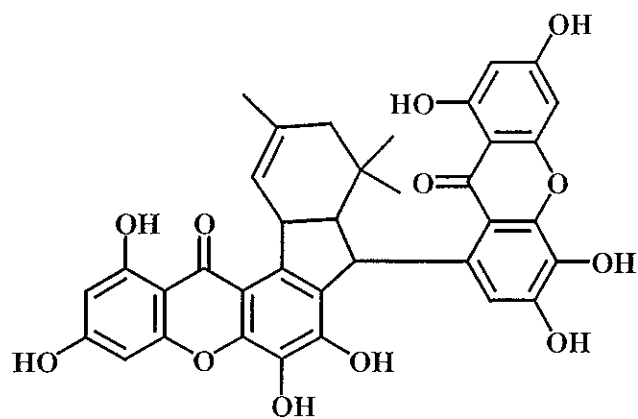


9.2ggg: parvixanthone H



9.2hhh: parvixanthone I

9.3 Bixanthone



9.3a: griffipavixanthone

1.3 The Objective

Based on NAPRALERT database, phytochemical examination on *G. nigrolineata* has not yet been reported. This prompted us to investigate its chemical constituents in order to provide additional information of this plant. This research involved isolation, purification and structure elucidation of the chemical constituents isolated from the stem bark of *G. nigrolineata* which was collected at the Ton Nga Chang Wildlife Sanctuary.

CHAPTER 2

EXPERIMENTAL

2.1 Chemicals and Instruments

Melting points were determined on an electrothermal melting point apparatus (Electrothermal 9100) and reported without correction. Infrared spectra (IR) were obtained on a FTS165 FT-IR spectrometer and Perkin Elmer Spectrum GX FT-IR system and recorded on wavenumber (cm^{-1}). ^1H and ^{13}C -Nuclear magnetic resonance (^1H and ^{13}C NMR) spectra were recorded on a FTNMR, Varian UNITY INOVA 500 MHz by using a solution in either deuteriochloroform or deuteromethanol with tetramethylsilane (TMS) as an internal standard. Spectra were recorded as chemical shift parameter (δ) value in ppm down field from TMS ($\delta 0.00$). Ultraviolet spectra (UV) were measured with UV-160A spectrophotometer (SHIMADZU). Principle bands (λ_{max}) were recorded as wavelengths (nm) and $\log \epsilon$ in methanol solution. Optical rotation was measured in methanol solution with sodium D line (590 nm) on an AUTOPOL[®] II automatic polarimeter. Quick column chromatography, thin-layer chromatography (TLC) and precoated thin-layer chromatography were performed on silica gel 60 GF₂₅₄ (Merck) or reverse-phase C-18. Column chromatography was performed on silica gel (Merck) type 100 (70-230 Mesh ASTM) or reverse-phase C-18. The solvents for extraction and chromatography were distilled at their boiling point ranges prior to use except for petroleum ether (bp. 40-60°C), while diethyl ether and ethyl acetate were analytical grade reagent.

2.2 Plant material

The stem bark of *Garcinia nigrolineata* was collected at the Ton Nga Chang Wildlife Sanctuary, Hat Yai, Songkla, Thailand in June 2000. The plant material was identified by Ajarn Prakart Sawangchote, Department of Biology, Faculty of Science, Prince of Songkla University, Hat Yai, Songkhla, where a voucher specimen has been deposited.

2.3 Isolation and extraction

The stem bark (2,775 g) of *Garcinia nigrolineata*, cut into small segments, was extracted with MeOH (10 L) over the period of 15 days at room temperature for three times. After filtration, the filtrate was evaporated to dryness under reduced pressure to give a crude methanol extract as a dark brown gum in 112.78 g.

2.4 Chemical investigation of the crude methanol extract of the stem bark

Chemical investigation of the crude extract was divided into two parts. The first investigation was a preliminary study to separate and purify the major components as well as to find out the purification process. The objectives of the second one was to increase quantity of minor components, isolated from the first investigation, and to purify other additional minor components which could not be separated in the first investigation.

2.4.1 The First Investigation

The crude extract was primarily tested for its solubility in various solvents at room temperature. The results were demonstrated in Table 4.

Table 4 Solubility of the crude extract in various solvents at room temperature

Solvent	Solubility at room temperature
petroleum ether	+ (brown solid in yellow solution)
dichloromethane	+ (brown solid in brown solution)
diethyl ether	++ (trace of brown solid in brown solution)
ethyl acetate	++ (trace of brown solid in brown solution)
acetone	++ (trace of cream solid in brown solution)
methanol	++ (white solid in brown solution)
water	+ (brown solid in yellow solution)
10% HCl	+ (brown solid in pale brown solution)
10% NaOH	+++ (dark brown solution)

symbol meaning: + slightly soluble, ++ moderately soluble, +++ well soluble

The solubility results indicated that crude extract contained moderately polar constituents which were acidic according to its solubility in base. The crude extract (69.71 g) was then separated into two fractions by dissolving in ethyl acetate. The EtOAc soluble (19.71 g) and insoluble fractions (44.23 g) were obtained as a red-brown and a dark brown solid, respectively. Chromatogram characteristics on normal phase TLC of the EtOAc soluble fraction, using 5% methanol-chloroform as a mobile phase, showed three major UV-active spots with the R_f values of 0.51 (a yellow spot),

0.41 and 0.33. However, chromatogram characteristics on reverse phase TLC with 30% water-methanol showed three major UV-active spots with the R_f values of 0.64 (a yellow spot), 0.48 (a yellow spot) and 0.30. From this information, the EtOAc soluble fraction was separated by column chromatography over reverse phase silica gel. Elution was conducted initially with 50% water-methanol, followed by decreasing amount of water until pure methanol. Fractions with the similar chromatogram characteristics were combined and evaporated to dryness under reduced pressure to afford thirteen subfractions as shown in **Table 5**.

Table 5 Fractions obtained from the EtOAc soluble fraction by column chromatography over reverse phase silica gel

Fraction	Weight (g)	Physical appearance
1	8.266	dark brown gum mixed with brown solid
2	0.702	red-brown solid
3	0.540	red-brown gum mixed with brown solid
4	0.244	red-brown gum mixed with brown solid
5	0.337	red-brown gum mixed with brown solid
6	0.216	yellow-brown gum mixed with yellow solid
7	0.344	yellow-brown gum mixed with yellow solid
8	0.259	yellow-brown gum mixed with yellow solid
9	0.176	yellow-brown gum mixed with yellow solid
10	1.058	dark brown gum
11	0.563	dark brown gum
12	7.161	dark brown gum
13	0.581	dark brown gum

Fraction 1 Chromatogram characteristics on both normal phase TLC with 15% methanol-chloroform and reverse phase TLC with 50% methanol-water showed many highly polar and unseparable components. It was not further investigated.

Fraction 2 Chromatogram characteristics on normal phase TLC with 10% methanol-chloroform) showed many UV-active spots. Further separation by column chromatography over silica gel was performed. Elution was conducted initially with chloroform, followed by increasing amount of methanol and finally with pure methanol. Fractions with the similar chromatogram characteristics were combined and evaporated to dryness under reduced pressure to afford four subfractions, as shown in Table 6.

Table 6 Fractions obtained from the fraction 2 by column chromatography over silica gel

Fraction	Weight (g)	Physical appearance
2.1	0.024	pale yellow gum
2.2	0.038	yellow gum
2.3	0.026	yellow gum
2.4	0.292	dark yellow gum

Fraction 2.1 Chromatogram characteristics on normal phase TLC with 4% methanol-chloroform showed no definite spots on TLC. It was then not investigated further.

Fraction 2.2 Chromatogram characteristics on normal phase TLC with 6% methanol-chloroform showed three major spots under UV with the R_f values of 0.57, 0.53 and

0.31. Upon chromatographic separation using precoated TLC on silica gel plates and 4% methanol-chloroform as a mobile phase (8 runs), three bands were obtained.

Band1 was obtained as a dark yellow gum (0.009 g). Chromatogram characteristics on normal phase TLC with 4% methanol-chloroform (6 runs) showed a single UV-active spot with the R_f value of 0.52. However, its ^1H NMR spectrum in a mixture of CDCl_3 and CD_3OD solution revealed that it was a mixture. It was not further investigated.

Band2 (TR14) was obtained as a yellow solid (0.003 g). Chromatogram characteristics on normal phase TLC with 4% methanol-chloroform (6 runs) showed only one UV-active spot with the R_f value of 0.30, melting at 196.0-197.8 °C.

UV (MeOH) λ_{max} nm (log ϵ)	241 (4.02), 248 (3.96), 262 (4.09), 312 (3.73)
FT-IR (neat) $\nu_{\text{cm}^{-1}}$	3328 (OH stretching), 1649 (C=O stretching)
^1H NMR ($\text{CDCl}_3+\text{CD}_3\text{OD}$) (δ ppm) (500 MHz)	13.40 (<i>s</i>), 7.18 (<i>d</i> , $J = 8.5$ Hz, 1H), 7.11 (<i>d</i> , $J = 8.5$ Hz, 1H), 6.23 (<i>d</i> , $J = 2.0$ Hz, 1H), 6.16 (<i>d</i> , $J = 2.0$ Hz, 1H), 3.39-3.36 (<i>m</i> , 2H), 1.85-1.82 (<i>m</i> , 2H), 1.27 (<i>s</i> , 6H)
^{13}C NMR ($\text{CDCl}_3+\text{CD}_3\text{OD}$) (δ ppm) (125 MHz)	183.26, 164.74, 163.30, 157.50, 151.79, 150.90, 129.80, 123.71, 118.76, 116.13, 103.74, 97.89, 93.50, 71.37, 42.86, 29.19, 21.30
DEPT (135°) ($\text{CDCl}_3+\text{CD}_3\text{OD}$) CH	123.71, 116.13, 97.89, 93.50
CH ₂	42.86, 21.30
CH ₃	29.19

Band3 (TR15) was obtained as yellow crystals (0.002 g). Chromatogram characteristics on normal phase TLC with 4% methanol-chloroform (6 runs) showed only one UV-active spot with the R_f value of 0.26, melting at 230.5-232.9 °C.

UV (MeOH) λ_{\max} nm (log \mathcal{E})	238 (4.53), 262 (4.50), 314 (4.22), 374 (3.81)
FT-IR (neat) $\nu_{\text{cm}^{-1}}$	3365 (OH stretching), 1645 (C=O stretching)
^1H NMR (Acetone- d_6) (δ ppm) (500 MHz)	13.26 (s), 7.57 (d, $J = 3.0$ Hz, 1H), 7.41 (d, $J = 9.0$ Hz, 1H), 7.33 (dd, $J = 9.0, 3.0$ Hz, 1H), 6.48 (s, 1H), 2.78-2.75 (m, 2H), 1.72-1.69 (m, 2H), 1.25 (s, 6H)
^{13}C NMR (Acetone- d_6) (δ ppm) (125 MHz)	182.17, 165.15, 162.18, 157.50, 155.52, 151.40, 125.52, 122.44, 120.16, 112.96, 109.83, 103.89, 94.55, 70.85, 43.22, 30.36, 17.77
DEPT (135 $^\circ$) (Acetone- d_6)	CH 125.52, 120.16, 109.83, 94.55 CH ₂ 43.22, 17.77 CH ₃ 30.36

Fraction 2.3 Chromatogram characteristics on normal phase TLC with 6% methanol-chloroform showed two major spots under UV with the R_f values of 0.20 and 0.16. Attempted purification was performed by precoated TLC on silica gel plates with 6% methanol-chloroform (9 runs) as a mobile phase to afford two bands of which chromatogram characteristics on normal phase TLC with 6% methanol-chloroform (3 runs) showed many spots without major spots.

Fraction 2.4 Chromatogram characteristics on normal phase TLC with 15% methanol-chloroform showed none of well-separated spots. No attempted investigation was carried out.

Fraction 3 Chromatogram characteristics on normal phase TLC with 10% methanol-chloroform showed many UV-active spots. Further separation by column chromatography over silica gel was performed. Elution was conducted initially with chloroform, followed by increasing amount of methanol and finally with pure

methanol. Fractions with the similar chromatogram characteristics were combined and evaporated to dryness under reduced pressure to afford four subfractions, as shown in

Table 7.

Table 7 Fractions obtained from the fraction 3 by column chromatography over silica gel

Fraction	Weight (g)	Physical appearance
3.1	0.019	dark yellow gum
3.2	0.032	dark yellow gum
3.3	0.022	yellow gum mixed with yellow soild
3.4	0.195	brown gum

Fraction 3.1 Chromatogram characteristics on normal phase TLC with 4% methanol-chloroform showed no definite spots. It was then not investigated further.

Fraction 3.2 Chromatogram characteristics on normal phase TLC with 20% ethyl acetate-petroleum ether (6 runs) showed two major UV- active spots with the R_f values of 0.21 and 0.18. Further separation by precoated TLC on silica gel plates with 20% ethyl acetate-petroleum ether (7 runs) as a mobile phase afforded four bands of which chromatogram characteristics on normal phase TLC with 6% chloroform-methanol contained many UV-active spots without any major spots.

Fraction 3.3 Chromatogram characteristics on normal phase TLC with 6% methanol-chloroform showed two major UV- active spots with the R_f values of 0.23 and 0.19. Further separation by precoated TLC on silica gel plates with 6% methanol-chloroform (2 runs) as a mobile phase afforded two bands. Because of low quantity, they were not investigated.

Fraction 3.4 Chromatogram characteristics on normal phase TLC with 6% methanol-chloroform showed no major UV-active spots. It was not investigation further.

Fraction 4 Chromatogram characteristics on normal phase TLC with 10% methanol-chloroform showed many UV-active spots. Further separation by column chromatography over silica gel was performed. Elution was conducted initially with chloroform, followed by increasing amount of methanol and finally with pure methanol. Fractions with the similar chromatogram characteristics were combined and evaporated to dryness under reduced pressure to afford three subfractions of which chromatogram characteristics on normal phase TLC with 3% chloroform-methanol showed many UV-active spots without any major spots.

Fraction 5 Chromatogram characteristics on normal phase TLC with 3% methanol-chloroform showed three major UV-active spots with the R_f values of 0.53, 0.47 and 0.07. Further separation by column chromatography over silica gel was performed. Elution was conducted initially with chloroform, followed by increasing amount of methanol and finally with pure methanol. Fractions with the similar chromatogram characteristics were combined and evaporated to dryness under reduced pressure to afford four subfractions, as shown in **Table 8**.

Table 8 Fractions obtained from the fraction 5 by column chromatography over silica gel

Fraction	Weight (g)	Physical appearance
5.1	0.005	yellow gum
5.2	0.027	dark yellow gum mixed with yellow solid
5.3	0.036	brown gum

Table 8 (Continued)

Fraction	Weight (g)	Physical appearance
5.4	0.087	brown gum

Fraction 5.1 Chromatogram characteristics on normal phase TLC with pure chloroform showed one major UV-active spot with the R_f value of 0.48 and one pale spot which was adjacent to the major spot. No attempted investigation was performed because of low quantity.

Fraction 5.2 Chromatogram characteristics on normal phase TLC with 10% ethyl acetate-petroleum ether (6 runs) showed two major UV-active spots with the R_f values of 0.38 and 0.27 which were visualized as purple spots after dipping the TLC plate in ASA reagent and subsequently heating. Further purification by flash column chromatography over silica gel was performed. Elution was conducted initially with 10% ethyl acetate-petroleum ether, gradually enriched with ethyl acetate until 20% ethyl acetate-petroleum ether. Fractions with the similar chromatogram characteristics were combined and evaporated to dryness under reduced pressure to afford four subfractions, as shown in **Table 9**.

Table 9 Fractions obtained from the fraction 5.2 by flash column chromatography over silica gel

Fraction	Weight (g)	Physical appearance
A1	0.005	yellow crystals
A2	0.006	dark yellow crystals
A3	0.002	dark yellow crystals
A4	0.018	dark yellow crystals

Subfraction A1 (TR9) Chromatogram characteristics on normal phase TLC with 10% ethyl acetate-petroleum ether (5 runs) showed one UV-active spot with the R_f value of 0.50, melting at 207.0-209.0 °C.

UV (MeOH) λ_{\max} nm (log ϵ)	228 (3.34), 269 (3.40), 281 (3.49), 310 (3.20)
FT-IR (neat) $\nu_{\text{cm}^{-1}}$	3360 (OH stretching), 1642 (C=O stretching)
^1H NMR (CDCl_3) (δ ppm) (500 MHz)	13.08 (<i>s</i> , 1H), 7.78 (<i>dd</i> , $J = 8.0, 1.5$ Hz, 1H), 7.33 (<i>dd</i> , $J = 8.0, 1.5$ Hz, 1H), 7.26 (<i>t</i> , $J = 8.0$ Hz, 1H), 6.75 (<i>d</i> , $J = 10.0$ Hz, 1H), 6.39 (<i>s</i> , 1H), 5.63 (<i>d</i> , $J = 10.0$ Hz, 1H), 1.48 (<i>s</i> , 6H)
^{13}C NMR (CDCl_3) (δ ppm) (125 MHz)	180.73, 160.89, 157.94, 156.23, 144.25, 144.12, 127.75, 124.09, 121.10, 120.11, 116.90, 115.30, 105.02, 103.54, 94.95, 78.48, 28.41
DEPT (135°) (CDCl_3)	CH 127.75, 124.09, 120.11, 116.90, 115.30, 94.95 CH ₃ 28.41

Subfraction A2 Chromatogram characteristics on normal phase TLC with 10% ethyl acetate-petroleum ether (5 runs) showed two major UV-active spots with the R_f values of 0.50 and 0.45 which was identified as **TR9** and **TR10**, respectively.

Subfraction A3 (TR10) Chromatogram characteristics on normal phase TLC with 10% ethyl acetate-petroleum ether (5 runs) showed one UV-active spot with the R_f value of 0.45, melting at 236.2-237.7 °C.

UV (MeOH) λ_{\max} nm (log ϵ)	252 (4.54), 270 (4.53), 310 (4.00), 330 (4.05)
FT-IR (neat) $\nu_{\text{cm}^{-1}}$	3376 (OH stretching), 1649 (C=O stretching)
^1H NMR (CDCl_3) (δ ppm) (500 MHz)	13.02 (<i>s</i> , 1H), 7.83 (<i>dd</i> , $J = 8.0, 2.0$ Hz, 1H), 7.37 (<i>dd</i> , $J = 8.0, 2.0$ Hz, 1H), 7.31 (<i>t</i> , $J = 8.0$ Hz, 1H),

		6.82 (<i>dd</i> , $J = 10.0, 0.5$ Hz, 1H), 6.35(<i>d</i> , $J = 0.5$ Hz, 1H), 5.70 (<i>d</i> , $J = 10.0$ Hz, 1H), 1.53 (<i>s</i> , 6H)
^{13}C NMR (CDCl ₃) (δ ppm)		180.75, 163.50, 161.07, 151.04, 144.36, 144.22,
(125 MHz)		127.78, 124.24, 121.29, 120.41, 117.25, 114.63,
		103.65, 101.06, 99.89, 78.34, 28.29
DEPT (135°) (CDCl ₃)	CH	127.78, 124.41, 120.41, 117.25, 114.63, 99.89
	CH ₃	28.29

Subfraction A4 Chromatogram characteristics on normal phase TLC with 10% ethyl acetate-petroleum ether (5 runs) showed one major UV-active spot which was identical to **TR10**. It was further investigated together with the band **2** of the fraction **6.2**.

Fraction 5.3 Chromatogram characteristics on normal phase TLC with 1% methanol-chloroform showed two major UV-active spots which were identical to **TR9** and **TR10**.

Fraction 5.4 Chromatogram characteristics on normal phase TLC with 4% methanol-chloroform showed two major UV-active spots with the R_f values of 0.35 and 0.20. The spot with the R_f value of 0.35 was found to be the major spot of the fraction **4.3** according to their chromatogram characteristics. Further purification by flash column chromatography over silica gel was performed. Elution was conducted with 4% methanol-chloroform. Fractions with the similar chromatogram characteristics were combined and evaporated to dryness under reduced pressure to afford four subfractions of which chromatogram characteristics on normal phase TLC with 4% methanol-chloroform contained many spots.

Fraction 6 Chromatogram characteristics on normal phase TLC with 3% methanol-chloroform showed two major UV-active spots with the R_f values of 0.50 and 0.15. Further separation by column chromatography over silica gel was performed. Elution was conducted initially with chloroform, gradually enriched with methanol and finally with pure methanol. Fractions with the similar chromatogram characteristics were combined and evaporated to dryness under reduced pressure to afford five subfractions, as shown in **Table 10**.

Table 10 Fractions obtained from the fraction 6 by column chromatography over silica gel

Fraction	Weight (g)	Physical appearance
6.1	0.011	pale yellow gum
6.2	0.018	yellow gum mixed with yellow solid
6.3	0.031	yellow gum
6.4	0.029	yellow gum
6.5	0.074	brown gum

Fraction 6.1 Chromatogram characteristics on normal phase TLC with 20% ethyl acetate-petroleum ether (3 runs) showed many pale spots. Therefore it was not further investigated.

Fraction 6.2 Chromatogram characteristics on normal phase TLC with 20% ethyl acetate-petroleum ether (3 runs) showed two major UV-active spots with the R_f values of 0.38 (**TR9**) and 0.18. Further separation by precoated TLC on silica gel plates with 20% ethyl acetate-petroleum ether (6 runs) as a mobile phase afforded three bands.

Band1 was obtained as yellow crystals (0.004 g) which was identical to **TR9**.

Band2 was obtained as dark yellow crystals (0.004 g). Chromatogram characteristics on normal phase TLC with 50% dichloromethane-petroleum ether (6 runs) were similar to that of the fraction A4. They were then combined and separated by flash column chromatography over silica gel. Elution was conducted with 50% dichloromethane-petroleum ether. Fractions with the similar chromatogram characteristics were combined and evaporated to dryness under reduced pressure to afford two subfractions, which contained TR9 as major component.

Band3 was obtained as dark yellow crystals (0.004 g). Chromatogram characteristics on normal phase TLC with 20% ethyl acetate-petroleum ether (2 runs) indicated the presence of TR10. It was not further investigated.

Fraction 6.3 Chromatogram characteristics on normal phase TLC with 2% methanol-chloroform showed no definite spots under UV. No further purification was attempted.

Fraction 6.4 Chromatogram characteristics on normal phase TLC with 4% methanol-chloroform showed one major UV-active spot with the R_f value of 0.28. Further separation by precoated TLC on silica gel plates with 2% methanol-chloroform (6 runs) as a mobile phase gave TR11 as a yellow gum (0.012 g).

UV (MeOH) λ_{\max} nm (log ϵ)	260 (4.11), 264 (4.12), 322 (3.88)
FT-IR (neat) $\nu_{\text{cm}^{-1}}$	3397 (OH stretching), 1638 (C=O stretching)
^1H NMR (Acetone- d_6) (δ ppm) (500 MHz)	13.50 (<i>s</i> , 1H), 7.48 (<i>s</i> , 1H), 6.52 (<i>s</i> , 1H), 5.30 (<i>mt</i> , J = 8.0 Hz, 1H), 5.27 (<i>mt</i> , J = 7.5 Hz, 1H), 3.60 (<i>d</i> , J = 8.0 Hz, 2H), 3.35 (<i>d</i> , J = 7.5 Hz, 2H), 1.87 (<i>s</i> , 3H), 1.76 (<i>s</i> , 3H) 1.64 (<i>s</i> , 3H), 1.63 (<i>s</i> , 3H)
^{13}C NMR (Acetone- d_6) (δ ppm) (125 MHz)	180.77, 163.07, 161.18, 156.62, 151.79, 150.68, 143.12, 136.36, 132.34, 123.49, 122.48, 116.37, 113.40, 110.90, 106.42, 102.99, 93.87, 25.85,

		25.84, 23.06, 21.92, 18.05, 17.86
DEPT (135°) (Acetone- <i>d</i> ₆)	CH	123.49, 122.48, 106.42, 93.87
	CH ₂	23.06, 21.92
	CH ₃	25.85, 25.84, 18.05, 17.86

Fraction 6.5 Chromatogram characteristics on normal phase TLC with 2% methanol-chloroform under UV showed unseparable spots. Further investigation was then not carried out.

Fraction 7 Chromatogram characteristics on normal phase TLC with 3% methanol-chloroform showed many UV-active spots. Further separation by column chromatography over silica gel was performed. Elution was conducted initially with chloroform, gradually enriched with methanol and finally with pure methanol. Fractions with the similar chromatogram characteristics were combined and evaporated to dryness under reduced pressure to afford four subfractions, as shown in **Table 11**.

Table 11 Fractions obtained from the fraction 7 by column chromatography over silica gel

Fraction	Weight (g)	Physical appearance
7.1	0.014	purple-yellow gum
7.2	0.012	yellow gum
7.3	0.018	yellow gum mixed yellow solid
7.4	0.161	orange-yellow gum

Fraction 7.1 Chromatogram characteristics on normal phase TLC with pure chloroform (3 runs) showed many spots under UV. Further investigation was then not carried out.

Fraction 7.2 Chromatogram characteristics on normal phase TLC with 10% ethyl acetate-petroleum ether (4 runs) showed one major UV-active spot with the R_f value of 0.35. Further purification by flash column chromatography over silica gel was performed. Elution was conducted initially with 6% ethyl acetate-petroleum ether and gradually enriched with ethyl acetate until 20% ethyl acetate-petroleum ether. Fractions with the similar chromatogram characteristics were combined and evaporated to dryness under reduced pressure to afford two subfractions, as shown in **Table 12**.

Table 12 Fractions obtained from the fraction 7.2 by flash column chromatography over silica gel

Fraction	Weight (g)	Physical appearance
B1	0.005	yellow crystals
B2	0.017	yellow crystals

Fraction B1 Chromatogram characteristics on normal phase TLC with 10% ethyl acetate-petroleum ether (3 runs) showed one major UV-active spot with the R_f value of 0.46. Because of low quantity, it was not further investigated.

Fraction B2 Chromatogram characteristics on normal phase TLC with 10% ethyl acetate-petroleum ether (3 runs) showed one major UV-active spot with the R_f value of 0.36. Further purification by flash column chromatography over silica gel was performed. Elution was conducted with 50% dichloromethane-petroleum ether.

Fractions with the similar chromatogram characteristics were combined and evaporated to dryness under reduced pressure to afford three subfractions, as shown in

Table 13.

Table 13 Fractions obtained from the fraction **B2** by flash column chromatography over silica gel

Fraction	Weight (g)	Physical appearance
B2.1	0.003	yellow crystals
B2.2	0.008	yellow crystals
B2.3	0.005	yellow crystals

Subfraction B2.1 Chromatogram characteristics on normal phase TLC with 50% dichloromethane-petroleum ether (7 runs) showed many pale UV-active spots. No further purification was performed.

Subfraction B2.2 Chromatogram characteristics on normal phase TLC with 50% dichloromethane-petroleum ether (7 runs) showed one major UV-active spot with the R_f value of 0.31. Further purification by flash column chromatography over silica gel was performed. Elution was conducted with 30% dichloromethane-petroleum ether. Fractions with the similar chromatogram characteristics were combined and evaporated to dryness under reduced pressure to afford two subfractions, as shown in **Table 14**.

Table 14 Fractions obtained from the subfraction **B2.2** by flash column chromatography over silica gel

Fraction	Weight (g)	Physical appearance
BA1	0.003	yellow crystals
BA2	0.003	yellow crystals

Subfraction BA1 Chromatogram characteristics on normal phase TLC with 70% dichloromethane-petroleum ether (2 runs) showed **TR18** as a major UV-active spot. Because of low quantity, it was not further investigated.

Subfraction BA2 (TR18) Chromatogram characteristics on normal phase TLC with 70% dichloromethane-petroleum ether (2 runs) showed only one UV-active spot with the R_f value of 0.48, melting at 223.8-225.5 °C.

UV (MeOH) λ_{\max} nm (log ϵ)	222 (4.32), 264 (4.61), 316 (4.10)
FT-IR (neat) $\nu_{\text{cm}^{-1}}$	3387 (OH stretching), 1629 (C=O stretching)
^1H NMR (CDCl_3) (δ ppm) (500 MHz)	12.14 (<i>s</i> , 1H), 11.26(<i>s</i> , 1H), 7.24 (<i>d</i> , $J = 8.5$, Hz, 1H), 6.75 (<i>d</i> , $J = 10.0$ Hz, 1H), 6.71 (<i>d</i> , $J = 8.5$ Hz, 1H), 6.29 (<i>s</i> , 1H), 5.66 (<i>d</i> , $J = 10.0$ Hz, 1H), 5.01 (<i>brs</i> , 1H), 1.50 (<i>s</i> , 6H)
^{13}C NMR (CDCl_3) (δ ppm) (125 MHz)	174.03, 162.79, 161.70, 154.10, 151.07, 142.80, 135.54, 127.97, 123.56, 114.36, 110.36, 107.70, 102.30, 101.60, 100.06, 78.59, 28.30
DEPT (135°) (CDCl_3)	CH 127.97, 123.56, 114.36, 110.36, 100.06 CH ₃ 28.30

Subfraction B2.3 Chromatogram characteristics on normal phase TLC with 50% dichloromethane-petroleum ether (7 runs) showed two major UV-active spots with the R_f values of 0.31 (TR18) and 0.26. No further purification was performed because of low quantity.

Fraction 7.3 Chromatogram characteristics on normal phase TLC with 10% ethyl acetate-petroleum ether (4 runs) showed many UV-active spots, one of which was TR10. Because of low quantity, it was not further investigated.

Fraction 7.4 Chromatogram characteristics on normal phase TLC with 3% methanol-chloroform showed no definite spot under UV. No attempted investigation was performed because of low quantity.

Fraction 8 Chromatogram characteristics on normal phase TLC with 3% methanol-chloroform showed many UV-active spots. Further separation by column chromatography over silica gel was performed. Elution was conducted initially with chloroform, gradually enriched with methanol and finally with pure methanol. Fractions with the similar chromatogram characteristics were combined and evaporated to dryness under reduced pressure to afford two subfractions, as shown in Table 15.

Table 15 Fractions obtained from the fraction 8 by column chromatography over silica gel

Fraction	Weight (g)	Physical appearance
8.1	0.010	purple gum mixed with yellow solid
8.2	0.155	yellow gum

Fraction 8.1 Chromatogram characteristics on normal phase TLC with pure chloroform (2 runs) showed one major UV-active spot with the R_f values of 0.47. It was further investigated together with fraction 9.1.

Fraction 8.2 Chromatogram characteristics on normal phase TLC with 3% methanol-chloroform showed many major UV-active spots. It was further separated by flash column chromatography over silica gel. Elution was conducted with 1% methanol-chloroform. Fractions with the similar chromatogram characteristics were combined and evaporated to dryness under reduced pressure to afford three subfractions of which chromatogram characteristics on normal phase TLC with 1% methanol-chloroform (3 runs) showed unseparable spots.

Fraction 9 Chromatogram characteristics on normal phase TLC with 3% methanol-chloroform showed many UV-active spots. Further separation by column chromatography over silica gel was performed. Elution was conducted initially with chloroform, gradually enriched with methanol and finally with pure methanol. Fractions with the similar chromatogram characteristics were combined and evaporated to dryness under reduced pressure to afford two subfractions, as shown in **Table 16**.

Table 16 Fractions obtained from the fraction 9 by column chromatography over silica gel

Fraction	Weight (g)	Physical appearance
9.1	0.016	brown gum mixed with yellow solid
9.2	0.105	yellow gum

Fraction 9.1 Chromatogram characteristics on normal phase TLC with 10% ethyl acetate-petroleum ether (2 runs) were similar to those of the fraction 8.1. They were then combined and separated by flash column chromatography over silica gel. Elution was conducted initially with 5% ethyl acetate-petroleum ether and gradually enriched with ethyl acetate until 10% ethyl acetate-petroleum ether. Fractions with the similar chromatogram characteristics were combined and evaporated to dryness under reduced pressure to afford three subfractions, as shown in Table 17.

Table 17 Fractions obtained from the combined fraction of fractions 9.1 and 8.1 by flash column chromatography over silica gel

Fraction	Weight (g)	Physical appearance
C1	0.009	purple gum mixed with yellow solid
C2	0.004	yellow crystals
C3	0.002	yellow crystals

Fraction C1 Chromatogram characteristics on normal phase TLC with 6% ethyl acetate-petroleum ether (6 runs) showed one major UV-active spot with the R_f value of 0.23 and many pale spots above major spot. Because of low quantity, it was not further investigated.

Fraction C2 (TR17) Chromatogram characteristics on normal phase TLC with 6% ethyl acetate-petroleum ether (6 runs) showed one UV-active spot with the R_f value of 0.23, melting at 249.8-250.7 °C.

UV (MeOH) λ_{\max} nm (log ϵ) 280 (4.43), 334 (4.15)

FT-IR (neat) $\nu_{\text{cm}^{-1}}$ 3412 (OH stretching), 1712 (C=O stretching)

^1H NMR (CDCl_3) (δ ppm) (500 MHz)		13.09 (<i>s</i> , 1H), 7.49 (<i>s</i> , 1H), 6.90 (<i>d</i> , $J = 10.0$ Hz, 1H), 6.46 (<i>d</i> , $J = 9.5$ Hz, 1H), 6.27 (<i>s</i> , 1H), 5.75 (<i>d</i> , $J = 9.5$ Hz, 1H), 5.62 (<i>d</i> , $J = 10.0$ Hz, 1H), 5.51 (<i>s</i> , 1H), 1.54 (<i>s</i> , 6H), 1.49 (<i>s</i> , 6H)
^{13}C NMR (CDCl_3) (δ ppm) (125 MHz)		180.30, 163.08, 160.52, 151.57, 145.02, 144.72, 132.38, 131.01, 127.13, 121.42, 117.79, 115.16, 114.13, 113.47, 103.24, 101.36, 99.37, 78.97, 78.19, 28.45, 28.27
DEPT (135°) (CDCl_3)	CH	131.01, 127.13, 121.42, 115.16, 113.47, 99.37
	CH_3	28.45, 28.27

Fraction C3 Chromatogram characteristics on normal phase TLC with 6% ethyl acetate-petroleum ether (6 runs) showed many UV-active spots. It was not further investigated because of low quantity.

Fraction 9.2 Chromatogram characteristics on normal phase TLC with 3% methanol-chloroform showed none of well-separated spots. No attempted investigation was carried out.

Fraction 10 Chromatogram characteristics on normal phase TLC with 3% methanol-chloroform showed many UV-active spots. Further separation by column chromatography over silica gel was performed. Elution was conducted initially with chloroform, gradually enriched with methanol and finally with pure methanol. Fractions with the similar chromatogram characteristics were combined and evaporated to dryness under reduced pressure to afford three subfractions, as shown in **Table 18**.

Table 18 Fractions obtained from the fraction 10 by column chromatography over silica gel

Fraction	Weight (g)	Physical appearance
10.1	0.117	yellow gum mixed with yellow solid
10.2	0.146	yellow solid
10.3	0.734	dark brown solid

Fraction 10.1 Chromatogram characteristics on normal phase TLC with 10% ethyl acetate-petroleum ether (3 runs) showed three major UV-active spots with the R_f values of 0.52, 0.46 and 0.31. Further separation by flash column chromatography over silica gel was performed. Elution was conducted initially with 5% ethyl acetate-petroleum ether, followed by increasing amount of ethyl acetate until 10% ethyl acetate-petroleum ether. Fractions with the similar chromatogram characteristics were combined and evaporated to dryness under reduced pressure to afford seven subfractions of which chromatogram characteristics on normal phase TLC with 10% ethyl acetate-petroleum ether (2 runs) showed many unseparable spots.

Fraction 10.2 Chromatogram characteristics on normal phase TLC with pure chloroform showed three major UV-active spots with the R_f values of 0.63, 0.45 and 0.28. Further separation by flash column chromatography over silica gel was performed. Elution was conducted initially with pure chloroform, followed by increasing amount of methanol until 2% methanol- chloroform. Fractions with the similar chromatogram characteristics were combined and evaporated to dryness under reduced pressure to afford four subfractions as shown in **Table 19**.

Table 19 Fractions obtained from the fraction 10.2 by flash column chromatography over silica gel

Fraction	Weight (g)	Physical appearance
D1	0.005	yellow gum
D2	0.027	yellow crystals
D3	0.045	yellow gum
D4	0.031	yellow gum

Fraction D1 Chromatogram characteristics on normal phase TLC with 2% methanol-chloroform showed many UV-active spots without any major components. No further separation was conducted.

Fraction D2 upon standing at room temperature, afforded yellow crystals (0.004 g) which was identified to be **TR17** on the basis of its chromatogram characteristics.

Fraction D3 Chromatogram characteristics on normal phase TLC with 2% methanol-chloroform showed one major UV-active spot with the R_f value of 0.43. Further separation by flash column chromatography over silica gel was performed. Elution was conducted with 2% methanol-chloroform. Fractions with the similar chromatogram characteristics were combined and evaporated to dryness under reduced pressure to afford three subfractions as shown in **Table 20**.

Table 20 Fractions obtained from the fraction D3 by flash column chromatography over silica gel

Fraction	Weight (g)	Physical appearance
D3.1	0.005	yellow gum
D3.2	0.021	dark yellow gum
D3.3	0.006	yellow gum

Subfraction D3.1 Chromatogram characteristics on normal phase TLC with 2% methanol-chloroform showed many pale UV-active spots. It was not further investigated because of low quantity.

Subfraction D3.2 Chromatogram characteristics on normal phase TLC with 2% methanol-chloroform showed one major UV-active spot with the R_f value of 0.37. Further separation by precoated TLC on silica gel plates with 2% methanol-chloroform (2 runs) as a mobile phase gave **TR19** as a yellow gum (0.006 g).

UV (MeOH) λ_{\max} nm (log ϵ)	258 (4.47), 328 (4.03)
FT-IR (neat) $\nu_{\text{cm}^{-1}}$	3416 (OH stretching), 1627 (C=O stretching)
^1H NMR (CDCl_3) (δ ppm) (500 MHz)	13.35 (<i>s</i> , 1H), 7.73 (<i>d</i> , $J = 9.0$ Hz, 1H), 6.97 (<i>d</i> , $J = 9.0$ Hz, 1H), 6.64 (<i>dd</i> , $J = 18.0, 10.5$ Hz, 1H), 5.30 (<i>mt</i> , $J = 6.0$ Hz, 1H), 5.25 (<i>dd</i> , $J = 18.0, 1.0$ Hz, 1H), 5.05 (<i>dd</i> , $J = 10.5, 1.0$ Hz, 1H), 3.78 (<i>s</i> , 3H), 3.42 (<i>d</i> , $J = 6.0$ Hz, 1H), 1.80 (<i>s</i> , 3H), 1.71 (<i>s</i> , 3H), 1.67 (<i>s</i> , 6H)
^{13}C NMR (CDCl_3) (δ ppm) (125 MHz)	181.28, 164.42, 160.03, 156.79, 152.73, 149.22, 144.78, 132.22, 130.89, 122.54, 118.64, 118.38,

		117.81, 113.79, 112.85, 105.62, 104.27, 62.69, 41.96, 28.74, 25.72, 22.90, 18.01
DEPT (135°) (CDCl ₃)	CH	156.79, 122.54, 117.81, 112.85
	CH ₂	104.27, 22.90
	CH ₃	62.69, 28.74, 25.72, 18.01
MS(<i>m/z</i>) (% rel. int.)		410 (21), 367 (99), 355 (87), 339 (59), 323 (43), 311 (46), 309 (26), 297 (20), 285 (19), 153 (15), 115 (12), 77 (10)

Subfraction D3.3 Chromatogram characteristics on normal phase TLC with 2% methanol-chloroform contained many spots, none of which were major components. Therefore it was not investigated further.

Fraction D4 Chromatogram characteristics on normal phase TLC with 5% methanol-chloroform showed none of well-separated spots. Further purification was therefore not attempted.

Fraction 10.3 Chromatogram characteristics on reverse phase TLC with 10% water-methanol appeared one major yellow spot with the R_f value of 0.27. Further separation of this fraction by column chromatography over reverse phase silica gel was performed. Elution was conducted with 10% water-methanol. Fractions with the similar chromatogram characteristics were combined and evaporated to dryness under reduced pressure to afford ten subfractions in low quantity. Their chromatogram characteristics on normal phase TLC with 2% methanol-chloroform showed many unseparable spots.

Fraction 11 Chromatogram characteristics on reverse phase TLC with 10% water-methanol showed three major spots: two UV-active spots with the R_f values of 0.34 and 0.12, and one yellow spot with the R_f value of 0.07. Further separation by column

chromatography over reverse phase silica gel was performed. Elution was conducted initially with 10% water-methanol, followed by decreasing amount of water until 7% water-methanol. Fractions with the similar chromatogram characteristics were combined and evaporated to dryness under reduced pressure to afford three subfractions, as shown in **Table 21**.

Table 21 Fractions obtained from the fraction **11** by column chromatography over reverse phase silica gel

Fraction	Weight (g)	Physical appearance
11.1	0.067	brown gum
11.2	0.234	yellow-brown gum
11.3	0.241	dark yellow gum

Fraction 11.1 Chromatogram characteristics on reverse phase TLC with 10% water-methanol showed many pale UV-active spots. No further investigation was performed.

Fraction 11.2 Chromatogram characteristics on reverse phase TLC with 10% water-methanol showed one major yellow spot with the R_f value of 0.07. Further separation by column chromatography over reverse phase silica gel was performed. Elution was conducted initially with 30% water-methanol, followed by decreasing amount of water until 100% methanol. Fractions with the similar chromatogram characteristics were combined and evaporated to dryness under reduced pressure to afford seven subfractions in low quantity. Their chromatogram characteristics on reverse phase TLC with 5% water-methanol showed many unseparable spots. Thus, further purification was not performed.

Fraction 11.3 Chromatogram characteristics on reverse phase TLC with 10% water-methanol showed one major yellow spot with the R_f value of 0.25. Further separation

of this fraction (0.156 g) by column chromatography over reverse phase silica gel was performed. Elution was conducted initially with 20% water-methanol, followed by decreasing amount of water until 10% water-methanol. Fractions with the similar chromatogram characteristics were combined and evaporated to dryness under reduced pressure to afford nine subfractions in low quantity. Their chromatogram characteristics on reverse phase TLC with 5% water-methanol showed many unseparable spots. Therefore further purification was not conducted.

Fraction 12 Chromatogram characteristics on normal phase TLC with 3% methanol-chloroform showed many oval UV-active spots. Further separation of this fraction (0.801g) by column chromatography over silica gel was performed. Elution was conducted initially with pure chloroform, gradually enriched with methanol and finally with pure methanol. Fractions with the similar chromatogram characteristics were combined and evaporated to dryness under reduced pressure to afford two subfractions, as shown in **Table 22**.

Table 22 Fractions obtained from the fraction 12 by column chromatography over silica gel

Fraction	Weight (g)	Physical appearance
12.1	0.259	yellow-brown gum
12.2	0.334	brown gum mixed with brown solid

Fraction 12.1 Chromatogram characteristics on normal phase TLC with pure chloroform showed unseparable UV-active spots. No attempted purification was performed.

Fraction 12.2 Chromatogram characteristics on normal phase TLC with 4% methanol-chloroform showed many UV-active spots. It was further separated by flash column chromatography over silica gel. Elution was conducted with 3% methanol-chloroform, gradually enriched with methanol and finally with 8% methanol-chloroform. Fractions with the similar chromatogram characteristics were combined and evaporated to dryness under reduced pressure to afford seven subfractions of which chromatogram characteristics on normal phase TLC with 4% methanol-chloroform showed many unseparable spots. They were then combined. The mixture (0.139 g) were subjected to acetylation reaction with acetic anhydride (9.0 mL) in the presence of pyridine (5.0 mL). The reaction mixture was stirred at room temperature overnight. It was then poured into ice-water and the aqueous solution was extracted with ethyl acetate (3x75 mL). The ethyl acetate layer was consecutively washed with 10% hydrochloric acid (3x75 mL) and aqueous NaHCO₃ (3x75 mL). The combined ethyl acetate extracts were washed with water (2x75 mL) and dried over anhydrous Na₂SO₄. After the removal of ethyl acetate, a yellow gum was obtained in 0.150 g. Chromatogram characteristics on normal phase TLC with 100% dichloromethane showed many major UV-active spots with higher R_f values than those found in the starting material, indicating that the acetylation reaction was complete.

Fraction 13 Chromatogram characteristics on normal phase TLC with 3% methanol-chloroform showed no separation. They were not further investigated.

2.4.2 The Second Investigation

The EtOAc insoluble part obtained from the first MeOH extract was combined with the second MeOH extract. The crude extract (88.81 g) was separated by column chromatography over reverse phase silica gel. Elution was conducted initially with

50% water-methanol, followed by decreasing amount of water until pure methanol. Fractions with the similar chromatogram characteristics were combined and evaporated to dryness under reduced pressure to afford fifteen subfractions, as shown in Table 23.

Table 23 Fractions obtained from the crude extract by column chromatography over reverse phase silica gel

Fraction	Weight (g)	Physical appearance
1'	55.223	dark brown gum
2'	5.452	dark black-brown gum mixed with brown solid
3'	5.384	dark brown solid
4'	3.382	dark brown solid
5'	3.8166	brown solid
6'	1.275	dark brown gum mixed with brown solid
7'	2.183	dark brown gum mixed with brown solid
8'	5.6958	yellow-brown solid
9'	1.198	yellow-brown solid
10'	1.944	yellow-brown gum
11'	1.692	yellow-brown gum
12'	1.399	yellow-brown gum mixed with yellow solid
13'	1.155	yellow-brown gum
14'	1.173	dark yellow-brown gum mixed with brown solid
15'	0.3742	dark yellow-brown gum mixed with brown solid

Fraction 1' Chromatogram characteristics on normal phase TLC with 15% methanol-chloroform showed many highly polar and unseparable components. It was not further investigated.

Fraction 2' Chromatogram characteristics on normal phase TLC with 6% methanol-chloroform showed many components. It was further separated by column chromatography over silica gel. Elution was conducted with pure chloroform, gradually enriched with methanol and finally with pure methanol. Fractions with the similar chromatogram characteristics were combined and evaporated to dryness under reduced pressure to afford three subfractions, as shown in **Table 24**.

Table 24 Fractions obtained from the fraction 2' by column chromatography over silica gel

Fraction	Weight (g)	Physical appearance
2'.1	0.215	yellow gum
2'.2	0.038	brown gum
2'.3	2.120	brown gum mixed with brown solid

Fraction 2'.1 Chromatogram characteristics on normal phase TLC with 6% methanol-chloroform showed three major UV-active spots with the R_f values of 0.47, 0.38 and 0.16. It was further separated by flash column chromatography over silica gel. Elution was conducted with pure chloroform, gradually enriched with methanol and finally with 5% methanol-chloroform. Fractions with the similar chromatogram characteristics were combined and evaporated to dryness under reduced pressure to afford four subfractions, as shown in **Table 25**.

Table 25 Fractions obtained from the fraction 2'.1 by flash column chromatography over silica gel

Fraction	Weight (g)	Physical appearance
A'1	0.039	yellow gum
A'2	0.067	yellow gum mixed with yellow solid
A'3	0.025	dark yellow gum
A'4	0.054	yellow gum

Fraction A'1 Chromatogram characteristics on normal phase TLC with 2% methanol-chloroform (2 runs) showed many major UV-active spots. No attempted purification was carried out.

Fraction A'2 Chromatogram characteristics on normal phase TLC with 2% methanol-chloroform (2 runs) showed three major UV-active spots with the R_f values of 0.37, 0.30 and 0.27. It was further separated by flash column chromatography over silica gel. Elution was conducted with 1% methanol-chloroform, gradually enriched with methanol and finally with 3% methanol-chloroform. Fractions with the similar chromatogram characteristics were combined and evaporated to dryness under reduced pressure to afford five subfractions, as shown in **Table 26**.

Table 26 Fractions obtained from the fraction A'2 by flash column chromatography over silica gel

Fraction	Weight (g)	Physical appearance
A'2.1	0.007	yellow gum
A'2.2	0.014	yellow gum

Table 26 (Continued)

Fraction	Weight (g)	Physical appearance
A'2.3	0.024	yellow gum
A'2.4	0.008	yellow gum
A'2.5	0.008	yellow gum

Subfraction A'2.1 Chromatogram characteristics on normal phase TLC with 20% ethyl acetate-petroleum ether (5 runs) showed many pale UV-active spots. No attempted purification was carried out.

Subfraction A'2.2 Chromatogram characteristics on normal phase TLC with 20% ethyl acetate-petroleum ether (5 runs) showed one major UV- active spot with the R_f value of 0.31. Further separation by precoated TLC on silica gel plates with 20% ethyl acetate-hexane (13 runs) as a mobile phase afforded three bands.

Band1 was obtained as a yellow solid (0.001 g). Chromatogram characteristics on normal phase TLC with 20% ethyl acetate-hexane (12 runs) showed one UV-active spot with the R_f value of 0.31. Because of low quantity, it was not further investigated.

Band2 was obtained as a yellow solid (0.002 g). Chromatogram characteristics on normal phase TLC with 20% ethyl acetate-hexane (12 runs) showed two major UV-active spots with the R_f values of 0.17 and 0.02. Because of low quantity, it was not further investigated.

Band3 (TR1) was obtained as a yellow gum (0.002 g). Chromatogram characteristics on normal phase TLC with 20% ethyl acetate-hexane (12 runs) as a mobile phase showed one UV-active spot with the R_f value of 0.10, melting at 104.5-105.8 °C.

$[\alpha]_D^{29}$	-43.47° ($c = 2.30 \times 10^{-3}$ g/10 cm ³ , EtOH)
UV (MeOH) λ_{\max} nm (log ϵ)	244 (4.41), 258 (4.33), 320 (4.11)
FT-IR (neat) $\nu_{\text{cm}^{-1}}$	3394 (OH stretching), 1645 (C=O stretching)
¹ H NMR (CDCl ₃) (δ ppm) (500 MHz)	12.83 (<i>s</i> , 1H), 7.73 (<i>dd</i> , $J = 7.5, 1.5$ Hz, 1H), 7.29 (<i>dd</i> , $J = 7.5, 1.5$ Hz, 1H), 7.24 (<i>t</i> , $J = 7.5$ Hz, 1H), 6.42 (<i>s</i> , 1H), 3.94 (<i>s</i> , 3H), 3.67 (<i>dd</i> , $J = 8.0, 2.0$ Hz, 1H), 3.30 (<i>dd</i> , $J = 15.0, 2.0$ Hz, 1H), 2.83 (<i>dd</i> , $J = 15.0, 8.0$ Hz, 1H), 1.36 (<i>s</i> , 6H)
¹³ C NMR (CDCl ₃) (δ ppm) (125 MHz)	181.37, 163.85, 162.38, 154.03, 145.43, 144.63, 124.12, 120.79, 120.36, 116.10, 106.08, 103.53, 94.24, 79.60, 74.35, 56.27, 25.70, 24.47
DEPT (135°) (CDCl ₃)	CH 124.12, 120.36, 116.10, 94.24, 79.60 CH ₂ 25.70 CH ₃ 56.27, 24.47

Subfraction A'2.3 Chromatogram characteristics on normal phase TLC with 20% ethyl acetate-petroleum ether (5 runs) showed one major UV- active spot with the R_f value of 0.31. Further separation by flash column chromatography over silica gel was performed. Elution was conducted initially with 20% ethyl acetate-hexane, gradually enriched with ethyl acetate and finally with 30% ethyl acetate-hexane. Fractions with the similar chromatogram characteristics were combined and evaporated to dryness under reduced pressure to afford three subfractions, as shown in Table 27.

Table 27 Fractions obtained from the subfraction A'2.3 by flash column chromatography over silica gel

Fraction	Weight (g)	Physical appearance
AA'1	0.002	yellow solid
AA'2	0.006	yellow solid
AA'3	0.009	yellow gum

Subfraction AA'1 Chromatogram characteristics on normal phase TLC with 20% ethyl acetate-hexane (7 runs) showed two major UV-active spots with the R_f values of 0.35 and 0.32. Because of low quantity, it was not further investigated.

Subfraction AA'2 Chromatogram characteristics on normal phase TLC with 20% ethyl acetate-hexane (7 runs) showed one major UV-active spot with the R_f value of 0.32. Further separation by precoated TLC on silica gel plates with 20% ethyl acetate-hexane (13 runs) as a mobile phase gave **TR2** as a yellow solid (0.003 g), melting at 115.0-116.2 °C.

UV (MeOH) λ_{\max} nm (log \mathcal{E})	244 (4.24), 320 (3.92)
FT-IR (neat) $\nu_{\text{cm}^{-1}}$	3409 (OH stretching), 1646 (C=O stretching)
^1H NMR ($\text{CDCl}_3+\text{CD}_3\text{OD}$) (δ ppm) (500 MHz)	12.85 (<i>s</i> , 1H), 7.69 (<i>dd</i> , $J = 7.5, 1.5$ Hz, 1H), 7.25 (<i>dd</i> , $J = 7.5, 1.5$ Hz, 1H), 7.20 (<i>t</i> , $J = 7.5$ Hz, 1H), 6.26 (<i>s</i> , 1H), 2.95-2.91 (<i>m</i> , 2H), 1.78-1.74 (<i>m</i> , 2H), 1.30 (<i>s</i> , 6H)
^{13}C NMR ($\text{CDCl}_3+\text{CD}_3\text{OD}$) (δ ppm) (125 MHz)	181.32, 162.50, 160.72, 154.75, 146.00, 145.11, 123.90, 121.10, 120.48, 115.99, 108.00, 103.21, 97.76, 71.79, 41.51, 29.30, 16.66

DEPT (135°) (CDCl ₃ +CD ₃ OD)	CH	123.90, 120.48, 115.99, 97.76
	CH ₂	41.51, 16.66
	CH ₃	29.30

Subfraction AA'3 Chromatogram characteristics on normal phase TLC with 20% ethyl acetate-hexane (7 runs) showed three UV-active spot with the R_f values of 0.16, 0.10 and 0.09. Because of low quantity, it was not further investigated.

Subfraction A'2.4 Chromatogram characteristics on normal phase TLC with 20% ethyl acetate-petroleum ether (5 runs) showed one major UV-active spot with the R_f value of 0.10. Further separation by precoated TLC on silica gel plates with 20% ethyl acetate-hexane (13 runs) as a mobile phase gave **TR2** as a yellow solid (0.002 g).

Subfraction A'2.5 Chromatogram characteristics on normal phase TLC with 20% ethyl acetate-petroleum ether (5 runs) showed one major UV-active spot with the R_f value of 0.16. Further separation by precoated TLC on silica gel plates with 20% ethyl acetate-hexane (19 runs) as a mobile phase gave **TR14** as a yellow solid (0.003 g).

Fraction A'3 Chromatogram characteristics on normal phase TLC with 4% methanol-chloroform (2 runs) showed three major UV-active spots with the R_f values of 0.43, 0.36 and 0.32. It was further separated by flash column chromatography over silica gel. Elution was conducted with 30% ethyl acetate-hexane, gradually enriched with ethyl acetate and finally with 40% ethyl acetate-hexane. Fractions with the similar chromatogram characteristics were combined and evaporated to dryness under reduced pressure to afford four subfractions, as shown in **Table 28**.

Table 28 Fractions obtained from the fraction A'3 by flash column chromatography over silica gel

Fraction	Weight (g)	Physical appearance
A'3.1	0.004	yellow solid
A'3.2	0.003	yellow solid
A'3.3	0.008	yellow solid
A'3.4	0.002	dark yellow solid

Subfraction A'3.1 Chromatogram characteristics on normal phase TLC with 30% ethyl acetate-hexane (3 runs) indicated the presence of **TR14** as a major component.

Subfraction A'3.2 Chromatogram characteristics on normal phase TLC with 30% ethyl acetate-hexane (3 runs) indicated the presence of **TR14** and **TR15** as a mixture compounds.

Subfraction A'3.3 Chromatogram characteristics on normal phase TLC with 30% ethyl acetate-hexane (3 runs) indicated the presence of **TR15** as a pure component.

Subfraction A'3.4 Chromatogram characteristics on normal phase TLC with 30% ethyl acetate-hexane (3 runs) indicated the presence of **TR15** and the other minor component with R_f value of 0.13.

Fraction A'4 Chromatogram characteristics on normal phase TLC with 4% methanol-chloroform (2 runs) showed many UV-active spots. It was further separated by flash column chromatography over silica gel. Elution was conducted with 4% methanol-chloroform. Fractions with the similar chromatogram characteristics were combined and evaporated to dryness under reduced pressure to afford seven

subfractions in low quantity. Their chromatogram characteristics on normal phase TLC with 4% methanol-chloroform showed many spots without any major components. They were not further investigated.

Fraction 2'.2 Chromatogram characteristics on normal phase TLC with 6% methanol-chloroform showed many UV-active spots. It was further separated by flash column chromatography over silica gel. Elution was conducted with pure chloroform, gradually enriched with methanol and finally with 15% methanol-chloroform. Fractions with the similar chromatogram characteristics were combined and evaporated to dryness under reduced pressure to afford five subfractions in low quantity. Their chromatogram characteristics on normal phase TLC with 6% methanol-chloroform showed many unseparable spots. They were then not further investigated.

Fraction 2'.3 Chromatogram characteristics on normal phase TLC with 15% methanol-chloroform showed no separation. It was not further investigated.

Fraction 3' Chromatogram characteristics on normal phase TLC with 6% methanol-chloroform) contained many components. It was further separated by column chromatography over silica gel. Elution was conducted with pure chloroform, gradually enriched with methanol and finally with pure methanol. Fractions with the similar chromatogram characteristics were combined and evaporated to dryness under reduced pressure to afford four subfractions, as shown in **Table 29**.

Table 29 Fractions obtained from the fraction 3' by column chromatography over silica gel

Fraction	Weight (g)	Physical appearance
3'.1	0.190	yellow gum
3'.2	0.116	yellow gum
3'.3	0.664	brown solid
3'.4	1.162	dark brown solid

Fraction 3'.1 Chromatogram characteristics on normal phase TLC with 1% methanol-chloroform showed three major UV-active spots with the R_f values of 0.51, 0.36 and 0.11. It was further separated by flash column chromatography over silica gel. Elution was conducted with pure chloroform, gradually enriched with methanol and finally with 10% methanol-chloroform. Fractions with the similar chromatogram characteristics were combined and evaporated to dryness under reduced pressure to afford seven subfractions, as shown in **Table 30**.

Table 30 Fractions obtained from the fraction 3'.1 by flash column chromatography over silica gel

Fraction	Weight (g)	Physical appearance
B'1	0.005	colorless gum
B'2	0.022	dark yellow gum
B'3	0.017	yellow gum
B'4	0.035	yellow gum
B'5	0.041	yellow gum

Table 30 (Continued)

Fraction	Weight (g)	Physical appearance
B'6	0.049	yellow gum
B'7	0.011	dark yellow gum

Fraction B'1 Chromatogram characteristics on normal phase TLC with 30% dichloromethane-hexane (2 runs) showed one major UV-active spot with the R_f value of 0.32. It was separated by precoated TLC on silica gel plates with 30% dichloromethane-petroleum ether (4 runs) as a mobile phase to give **TR20** as a colorless gum in 0.002 g. Chromatogram characteristics on normal phase TLC with 40% dichloromethane-petroleum ether (3 runs) showed one spot under UV with the R_f value of 0.56.

UV (MeOH) λ_{\max} nm (log ϵ)	227 (2.97), 253 (3.64), 260 (3.70), 274 (3.16)
FT-IR (neat) $\nu_{\text{cm}^{-1}}$	1645, 1586 (C=C stretching), 1154 (C-O stretching)
^1H NMR (CDCl_3) (δ ppm) (500 MHz)	6.62 (<i>d</i> , $J = 10.0$ Hz, 1H), 5.97 (<i>s</i> , 1H), 5.47 (<i>d</i> , $J = 10.0$ Hz, 1H), 4.04 (<i>s</i> , 3H), 1.42 (<i>s</i> , 6H)
^{13}C NMR (CDCl_3) (δ ppm) (125 MHz)	169.78, 160.60, 125.91, 115.91, 102.80, 96.75, 93.50, 77.74, 52.50, 28.29
DEPT (135°) (CDCl_3)	CH 125.91, 115.91, 96.75 CH ₃ 52.50, 28.29

Fraction B'2 Chromatogram characteristics on normal phase TLC with pure chloroform showed many spots under UV. Further separation by flash column chromatography over silica gel was performed. Elution was conducted with 50%

chloroform-hexane. Fractions with the similar chromatogram characteristics were combined and evaporated to dryness under reduced pressure to afford four subfractions of which chromatogram characteristics on normal phase TLC with 50% chloroform-hexane (2 runs) showed many unseparable spots.

Fraction B'3 Chromatogram characteristics on normal phase TLC with pure chloroform showed one spot under UV with the R_f value of 0.47. Further separation by precoated TLC on silica gel plates with 10% ethyl acetate-petroleum ether (6 runs) as a mobile phase afforded two bands.

Band1 was obtained as a yellow solid (0.002 g). Chromatogram characteristics on normal phase TLC with 10% ethyl acetate-petroleum ether (4 runs) showed two UV-active spots with the R_f values of 0.37 and 0.30. Because of low quantity, it was not further investigated.

Band2 (TR4) was obtained as a yellow solid (0.006 g). Chromatogram characteristics on normal phase TLC with 10% ethyl acetate-petroleum ether (4 runs) as a mobile phase showed one UV-active spot with the R_f value of 0.18, melting at 142.8-144.6 °C.

UV (MeOH) λ_{\max} nm ($\log \mathcal{E}$)	248 (4.45), 318 (4.13)
FT-IR (neat) $\nu_{\text{cm}^{-1}}$	3358 (OH stretching), 1645 (C=O stretching)
^1H NMR (CDCl_3) (δ ppm) (500 MHz)	12.82 (<i>s</i> , 1H), 7.73 (<i>dd</i> , $J = 8.0, 2.0$ Hz, 1H), 7.28 (<i>dd</i> , $J = 8.0, 2.0$ Hz, 1H), 7.23 (<i>t</i> , $J = 8.0$ Hz, 1H), 6.39 (<i>s</i> , 1H), 3.91 (<i>s</i> , 3H), 2.95-2.92 (<i>m</i> , 2H), 1.77-1.74 (<i>m</i> , 2H), 1.36 (<i>s</i> , 6H)
^{13}C NMR (CDCl_3) (δ ppm) (125 MHz)	181.38, 163.59, 161.78, 153.60, 145.54, 144.65, 123.94, 120.87, 120.36, 115.92, 108.62, 103.47, 94.02, 72.71, 56.01, 41.00, 29.73, 16.42
DEPT (135°) (CDCl_3)	CH 123.94, 120.36, 115.92, 94.02

CH₂ 41.00, 16.42

CH₃ 56.01, 29.73

Fraction B'4 Chromatogram characteristics on normal phase TLC with 20% ethyl acetate-petroleum ether (2 runs) showed one spot under UV with the R_f value of 0.28. Further separation by precoated TLC on silica gel plates with 10% ethyl acetate-petroleum ether (5 runs) as a mobile phase gave a yellow solid (0.003 g), Chromatogram characteristics on normal phase TLC with 20% ethyl acetate-petroleum ether (3 runs) showed only one UV-active spot with the R_f value of 0.36. However, its ¹H NMR spectrum in a mixture of CDCl₃ and CD₃OD solution revealed that it was a mixture. It was not further investigated.

Fraction B'5 Chromatogram characteristics on normal phase TLC with 2% methanol-chloroform showed four major spots under UV with the R_f values of 0.28, 0.25, 0.21 and 0.18. Further separation by precoated TLC on silica gel plates with 20% ethyl acetate-petroleum ether (8 runs) as a mobile phase afforded three bands in low quantity. No attempted purification was performed.

Fraction B'6 Chromatogram characteristics on normal phase TLC with 2% methanol-chloroform showed many spots under UV. Further separation by flash column chromatography over silica gel was performed. Elution was conducted with 20% ethyl acetate-petroleum ether, gradually enriched with ethyl acetate and finally with pure ethyl acetate. Fractions with the similar chromatogram characteristics were combined and evaporated to dryness under reduced pressure to afford four subfractions, as shown in **Table 31**.

Table 31 Fractions obtained from the fraction B'6 by flash column chromatography over silica gel

Fraction	Weight (g)	Physical appearance
B'6.1	0.010	yellow solid
B'6.2	0.012	yellow gum
B'6.3	0.002	yellow gum
B'6.4	0.026	yellow gum

Subfraction B'6.1 Chromatogram characteristics on normal phase TLC with 20% ethyl acetate-petroleum ether (3 runs) showed one major UV- active spot with the R_f value of 0.36. Further separation by flash column chromatography over silica gel was performed. Elution was conducted with 20% ethyl acetate-petroleum ether. Fractions with the similar chromatogram characteristics were combined and evaporated to dryness under reduced pressure to afford three subfractions, as shown in Table 32.

Table 32 Fractions obtained from the subfraction B'6.1 by flash column chromatography over silica gel

Fraction	Weight (g)	Physical appearance
BA'1	0.002	yellow solid
BA'2	0.002	yellow solid
BA'3	0.002	yellow gum

Subfraction BA'1 Chromatogram characteristics on normal phase TLC with 20% ethyl acetate-petroleum ether (4 runs) showed two pale UV-active spots with the R_f values of 0.31 and 0.25. Because of low quantity, it was not further investigated.

Subfraction BA'2 Chromatogram characteristics on normal phase TLC with 20% ethyl acetate-petroleum ether (4 runs) showed one UV-active spot with the R_f value of 0.25, corresponding to **TR1**.

Subfraction BA'3 Chromatogram characteristics on normal phase TLC with 20% ethyl acetate-petroleum ether (4 runs) indicated the presence of **TR1** as a major component.

Subfraction B'6.2 Chromatogram characteristics on normal phase TLC with 20% ethyl acetate-petroleum ether (3 runs) showed many major spots under UV. No attempted purification was performed.

Subfraction B'6.3 Chromatogram characteristics on reverse phase TLC with 20% water-methanol (2 runs) showed only one major UV-active spot with the R_f value of 0.10. It was separated by column chromatography over reverse phase silica gel. Elution was conducted initially with 20% water-methanol, followed by decreasing amount of methanol until 10% water-methanol. Fractions with the similar chromatogram characteristics were combined on the basis of their chromatogram characteristics and evaporated to dryness under reduced pressure to afford three subfractions, as shown in **Table 33**.

Table 33 Fractions obtained from the subfraction **B'6.3** by column chromatography over reverse phase silica gel

Fraction	Weight (g)	Physical appearance
BB'1	0.002	yellow gum

Table 33 (Continued)

Fraction	Weight (g)	Physical appearance
BB'2	0.003	yellow solid
BB'3	0.002	yellow gum

Subfraction BB'1 Chromatogram characteristics on reverse phase TLC with 20% water-methanol showed many pale UV-active spots. It was not further investigated.

Subfraction BB'2 (TR3) Chromatogram characteristics on reverse phase TLC with 20% water-methanol showed one UV-active spot with the R_f value of 0.31, melting at 205.8-207.2 °C.

UV (MeOH) λ_{\max} nm (log \mathcal{E})	228 (4.28), 262 (4.47), 334 (4.04), 376 (3.84)
FT-IR (neat) $\nu_{\text{cm}^{-1}}$	3416 (OH stretching), 1644 (C=O stretching)
^1H NMR (CDCl_3) (δ ppm) (500 MHz)	13.38 (<i>s</i> , 1H), 7.63 (<i>s</i> , 1H), 6.95 (<i>d</i> , $J = 10.0$ Hz, 1H), 6.45 (<i>s</i> , 1H), 5.79 (<i>d</i> , $J = 10.0$ Hz, 1H), 2.85 (<i>t</i> , $J = 6.5$ Hz, 2H), 1.87 (<i>t</i> , $J = 6.5$ Hz, 2H), 1.59 (<i>s</i> , 6H), 1.36 (<i>s</i> , 6H)
^{13}C NMR (CDCl_3) (δ ppm) (125 MHz)	180.05, 162.08, 160.17, 155.76, 146.42, 145.68, 141.69, 129.72, 115.58, 114.78, 111.50, 109.13, 108.74, 102.80, 94.56, 79.24, 72.66, 41.10, 29.27, 28.27, 16.04
DEPT (135°) (CDCl_3)	CH 129.72, 115.58, 108.74, 94.56 CH ₂ 41.10, 16.04 CH ₃ 29.27, 28.27

Subfraction BB'3 Chromatogram characteristics on reverse phase TLC with 20% water-methanol indicated the presence of **TR3** as a major component.

Subfraction B'6.4 Chromatogram characteristics on normal phase TLC with 20% ethyl acetate-petroleum ether (3 runs) showed many pale spots under UV. No attempted purification was performed.

Fraction B'7 Chromatogram characteristics on normal phase TLC with 2% methanol-chloroform showed no separation. It was not further investigated.

Fraction 3'.3 Chromatogram characteristics on normal phase TLC 1% methanol-chloroform showed many major UV-active spots. It was further separated by flash column chromatography over silica gel. Elution was conducted with pure chloroform, gradually enriched with methanol and finally with 20% methanol-chloroform. Fractions with the similar chromatogram characteristics were combined and evaporated to dryness under reduced pressure to afford three subfractions, as shown in **Table 34**.

Table 34 Fractions obtained from the fraction 3'.3 by flash column chromatography over silica gel

Fraction	Weight (g)	Physical appearance
C'1	0.036	yellow gum
C'2	0.021	yellow gum
C'3	0.036	yellow gum

Fraction C'1 Chromatogram characteristics on normal phase TLC with 1% methanol-chloroform showed many pale spots under UV. No attempted purification was performed.

Fraction C'2 Chromatogram characteristics on normal phase TLC with 3% methanol-chloroform (2 runs) showed one major spot under UV with the R_f value of 0.29. Further separation by flash column chromatography over silica gel was performed. Elution was conducted with pure chloroform, gradually enriched with methanol and finally with 5% methanol-chloroform. Fractions with the similar chromatogram characteristics were combined and evaporated to dryness under reduced pressure to afford three subfractions, as shown in **Table 35**.

Table 35 Fractions obtained from the fraction C'2 by flash column chromatography over silica gel

Fraction	Weight (g)	Physical appearance
C'2.1	0.004	yellow gum
C'2.2	0.006	yellow gum
C'2.3	0.10	yellow gum

Subfraction C'2.1 Chromatogram characteristics on normal phase TLC with 2% methanol-chloroform (8 runs) showed many pale spots under UV. No attempted purification was performed.

Subfraction C'2.2 Chromatogram characteristics on normal phase TLC with 10% ethyl acetate-chloroform (8 runs) showed one major UV-active spot with the R_f value of 0.12. Further separation by precoated TLC on silica gel plates with 10% ethyl acetate-chloroform (9 runs) as a mobile phase afforded one major spot as a yellow solid (0.003 g). Because of low quantity, it was not further investigation.

Subfraction C'2.3 Chromatogram characteristics on normal phase TLC with 10% ethyl acetate-chloroform (8 runs) showed many pale spots under UV. No attempted purification was performed.

Fraction C'3 Chromatogram characteristics on normal phase TLC with 3% methanol-chloroform (2 runs) showed three major UV-active spots with the R_f values of 0.17, 0.12 and 0.05. Attempted purification was performed by precoated TLC on silica gel plates with 2% methanol-chloroform (8 runs) as a mobile phase, to afford three bands of which chromatogram characteristics on normal phase TLC with 2% methanol-chloroform (5 runs) showed unseparable spots. Further purification was not carried out.

Fraction 3'4 Chromatogram characteristics on normal phase TLC with 10% methanol-chloroform showed many UV-active spots. It was further separated by flash column chromatography over silica gel. Elution was conducted with pure chloroform, gradually enriched with methanol and finally with pure methanol. Fractions with the similar chromatogram characteristics were combined and evaporated to dryness under reduced pressure to afford five subfractions in low quantity. Their chromatogram characteristics on normal phase TLC with 8% methanol-chloroform showed unseparable spots. They were not further investigated.

Fraction 3'5 Chromatogram characteristics on normal phase TLC with 10% methanol-chloroform showed no separation. It was not further investigated.

Fraction 4' Chromatogram characteristics on normal phase TLC with pure chloroform showed many components. It was further separated by column chromatography over silica gel. Elution was conducted with pure chloroform, gradually enriched with methanol and finally with pure methanol. Fractions with the similar chromatogram

characteristics were combined and evaporated to dryness under reduced pressure to afford eight subfractions, as shown in Table 36.

Table 36 Fractions obtained from the fraction 4' by column chromatography over silica gel

Fraction	Weight (g)	Physical appearance
4'.1	0.008	purple solid
4'.2	0.017	green-brown crystals
4'.3	0.044	yellow gum
4'.4	0.137	yellow solid
4'.5	0.021	yellow solid
4'.6	0.046	yellow gum mixed with yellow solid
4'.7	0.160	dark yellow gum
4'.8	0.981	yellow-brown gum

Fraction 4'.1 Chromatogram characteristics on normal phase TLC with pure chloroform showed one major purple spot with the R_f value of 0.80 and many pale UV-active spots. It was further investigated together with fraction 2'.2.

Fraction 4'.2 Chromatogram characteristics on normal phase TLC with 6% ethyl acetate-petroleum ether showed one yellow major spot with the R_f value of 0.18 and many pale UV-active spots below the major spot. Further separation by precoated TLC on silica gel plates with 5% ethyl acetate-petroleum ether (7 runs) as a mobile phase afforded three bands.

Band1 was obtained as a yellow gum (0.002 g). Chromatogram characteristics on normal phase TLC with 5% ethyl acetate-petroleum ether (6 runs) showed many spots under UV. It was not further investigated.

Band2 (TR12) was obtained as a yellow solid (0.002 g). Chromatogram characteristics on normal phase TLC with 5% ethyl acetate-petroleum ether (6 runs) as a mobile phase showed one yellow spot with the R_f value of 0.25, melting at 216.5-218.1 °C.

UV (MeOH) λ_{\max} nm (log ϵ)	242 (4.31), 264 (4.15), 316 (4.01)
FT-IR (neat) $\nu_{\text{cm}^{-1}}$	3446 (OH stretching), 1642 (C=O stretching)
^1H NMR (CDCl_3) (δ ppm) (500 MHz)	13.10 (<i>s</i> , 1H), 8.02 (<i>d</i> , $J = 10.5$ Hz, 1H), 7.52 (<i>t</i> , $J = 8.0$ Hz, 1H), 6.88 (<i>s</i> , 1H), 6.85 (<i>dd</i> , $J = 8.0, 1.0$ Hz, 1H), 6.75 (<i>dd</i> , $J = 8.0, 1.0$ Hz, 1H), 6.30 (<i>brs</i> , 1H), 5.86 (<i>d</i> , $J = 10.5$ Hz, 1H), 1.51 (<i>s</i> , 6H)
^{13}C NMR (CDCl_3) (δ ppm) (125 MHz)	183.63, 161.89, 155.68, 153.45, 151.55, 136.97, 135.76, 132.54, 120.81, 119.69, 110.10, 109.00, 108.77, 106.28, 102.36, 77.10, 27.33
DEPT (135°) (CDCl_3)	CH 135.76, 132.54, 120.81, 110.10, 106.28, 102.39 CH ₃ 27.33

Band3 was obtained as a yellow gum (0.003 g). Chromatogram characteristics on normal phase TLC with 5% ethyl acetate-petroleum ether (6 runs) showed two spots under UV with the R_f values of 0.25 and 0.17. It was not further investigated because of low quantity.

Fraction 4.3 Chromatogram characteristics on normal phase TLC with pure chloroform indicated the presence of TR9 and TR10 as major components.

Fraction 4'.4 Chromatogram characteristics on normal phase TLC with pure chloroform showed **TR9** and **TR10** as major components. It was further separated by flash column chromatography over silica gel. Elution was conducted with 50% dichloromethane-petroleum ether, gradually enriched with dichloromethane and finally with pure dichloromethane. Fractions with the similar chromatogram characteristics were combined and evaporated to dryness under reduced pressure to afford two subfractions as shown in **Table 37**.

Table 37 Fractions obtained from the fraction 4'.4 by flash column chromatography over silica gel

Fraction	Weight (g)	Physical appearance
D'1	0.003	yellow crystals
D'2	0.131	yellow gum mixed with yellow crystals

Fraction D'1 Chromatogram characteristics on normal phase TLC with 50% dichloromethane-petroleum indicated the presence of **TR9** as a pure compound.

Fraction D'2 Chromatogram characteristics on normal phase TLC with 50% dichloromethane-petroleum (4 runs) indicated the presence of **TR9** and **TR10** as major components. Further separation by precoated TLC on silica gel plates with 50% dichloromethane-petroleum (13 runs) as a mobile phase afforded two bands.

Band1 was obtained as yellow crystals (0.013 g). Chromatogram characteristics on normal phase TLC with 50% dichloromethane-petroleum (8 runs) indicated the presence of **TR9** as a pure component.

Band2 was obtained as yellow crystals (0.042 g). Chromatogram characteristics on normal phase TLC with 50% dichloromethane-petroleum (8 runs)

showed two yellow spots with the R_f values of 0.68 and 0.66 (**TR10**). Further chromatography by precoated TLC on silica gel plates with 15% ethyl acetate-petroleum ether (19 runs) as a mobile phase gave four isolated bands.

Band2.1 was obtained as yellow crystals (0.001 g). Chromatogram characteristics on normal phase TLC with 15% ethyl acetate-petroleum ether (9 runs) showed one pale major spot under UV. It was not further investigated because of low quantity.

Band2.2 was obtained as yellow crystals (0.020 g). Chromatogram characteristics on normal phase TLC with 15% ethyl acetate-petroleum ether (9 runs) was the similar to that of the original mixture. It was further investigated together with fraction 4'.5.

Band2.3 was obtained as yellow crystals (0.015 g). Chromatogram characteristics on normal phase TLC with 15% ethyl acetate-petroleum ether (9 runs) indicated the presence of **TR10** as a pure component.

Band2.4 was obtained as yellow crystals (0.003 g). Chromatogram characteristics on normal phase TLC with 15% ethyl acetate-petroleum ether (9 runs) indicated the presence of **TR10** as a major component.

Fraction 4'.5 Chromatogram characteristics on normal phase TLC with 15% ethyl acetate-petroleum ether (9 runs) were similar to that of the band 2.2 of the fractions **D'2**. They were then combined and separated by column chromatography over reverse phase silica gel. Elution was initially conducted with 20% water-methanol, followed by decreasing amount of water until 10% water-methanol. Fractions with the similar chromatogram characteristics were combined and evaporated to dryness under reduced pressure to afford three subfractions, as shown in **Table 38**.

Table 38 Fractions obtained from the combined fraction of fraction 4'5 and band 2.2 of fraction D'2 by column chromatography over reverse phase silica gel

Fraction	Weight (g)	Physical appearance
E'1	0.003	yellow crystals
E'2	0.012	yellow crystals
E'3	0.029	yellow crystals

Fraction E'1 Chromatogram characteristics on reverse phase TLC with 20% water-methanol (3 runs) showed one major UV-active spot with the R_f value of 0.41 (**TR10**). Because of low quantity, it was not further investigated.

Fraction E'2 Chromatogram characteristics on reverse phase TLC with 20% water-methanol (3 runs) indicated the presence of **TR10** as a pure component.

Fraction E'3 Chromatogram characteristics on reverse phase TLC with 20% water-methanol (3 runs) indicated the presence of **TR10** as a major component and the other minor component below **TR10** with the R_f value of 0.30.

Fraction 4'6 Chromatogram characteristics on normal phase TLC with pure chloroform showed three major UV-active spots with the R_f values of 0.53, 0.41 and 0.28. Further purification was performed by precoated TLC on silica gel plates with pure chloroform (4 runs) as a mobile phase afforded five bands.

Band1 was obtained as a yellow gum (0.009 g). Chromatogram characteristics on normal phase TLC with pure chloroform showed one major UV-active spot with the R_f value of 0.48. Further purification was performed by precoated TLC on silica gel plates with 70% dichloromethane-petroleum ether (9 runs) as a mobile phase, to give **TR5** as a yellow solid (0.006 g), melting at 220.1-222.5 °C.

UV (MeOH) λ_{\max} nm (log ϵ)	256 (4.62), 338 (4.05), 384 (4.00)
FT-IR (neat) $\nu_{\text{cm}^{-1}}$	3409 (OH stretching), 1642 (C=O stretching)
^1H NMR (CDCl_3) (δ ppm) (500 MHz)	12.85 (<i>s</i> , 1H), 7.63 (<i>s</i> , 1H), 7.54 (<i>t</i> , $J = 8.5$ Hz, 1H), 6.94 (<i>d</i> , $J = 10.0$ Hz, 1H), 6.91 (<i>dd</i> , $J = 8.5, 0.5$ Hz, 1H), 6.78 (<i>dd</i> , $J = 8.5, 0.5$ Hz, 1H), 5.78 (<i>d</i> , $J =$ 10.0 Hz, 1H), 5.52 (<i>brs</i> , 1H), 1.56 (<i>s</i> , 6H)
^{13}C NMR (CDCl_3) (δ ppm) (125 MHz)	181.27, 161.80, 156.12, 146.90, 146.45, 142.07, 135.89, 129.88, 115.40, 114.10, 110.25, 109.24, 108.72, 108.51, 106.68, 79.54, 28.30
DEPT (135°) (CDCl_3)	CH 135.89, 129.88, 115.40, 110.25, 108.72, 106.68 CH ₃ 28.30

Band2 was obtained as a yellow gum (0.006 g). Chromatogram characteristics on normal phase TLC with pure chloroform indicated the presence of **TR10** as a major component.

Band3 was obtained as a yellow gum (0.004 g). Chromatogram characteristics on normal phase TLC with pure chloroform showed one major UV-active spot with the R_f value of 0.32. Further purification was performed by precoated TLC on silica gel plates with 70% dichloromethane-petroleum ether (8 runs) as a mobile phase to give **TR7** as a yellow gum (0.002 g).

UV (MeOH) λ_{\max} nm (log ϵ)	268 (4.36) 336 (3.92) 374 (3.72)
FT-IR (neat) $\nu_{\text{cm}^{-1}}$	3439 (OH stretching) 1648 (C=O stretching)
^1H NMR (CDCl_3) (δ ppm) (500 MHz)	13.44 (<i>s</i> , 1H), 7.61 (<i>s</i> , 1H), 6.91 (<i>d</i> , $J = 10.5$ Hz, 1H), 6.39 (<i>s</i> , 1H), 5.76 (<i>d</i> , $J = 10.5$ Hz, 1H), 5.47 (<i>brs</i> , 1H), 5.31(<i>mt</i> , $J = 7.0$ Hz, 1H), 3.48 (<i>d</i> , $J =$ 7.0 Hz, 1H), 1.85 (<i>s</i> , 3H), 1.78 (<i>s</i> , 3H), 1.55 (<i>s</i> , 6H)

^{13}C NMR (CDCl_3) (δ ppm) (125 MHz)	180.09, 161.98, 160.28, 155.75, 146.40, 141.75, 132.94, 129.78, 121.25, 115.49, 114.00, 109.10, 108.77, 108.42, 102.50, 93.97, 79.30, 28.25, 25.86, 21.44, 17.94
DEPT (135°) (CDCl_3)	CH 129.78, 121.25, 115.49, 108.77, 93.97 CH ₂ 21.44 CH ₃ 28.25, 25.86, 17.94

Band4 was obtained as a yellow gum (0.003 g). Chromatogram characteristics on normal phase TLC with pure chloroform showed one major UV-active spot with the R_f value of 0.31. Further purification was performed by precoated TLC on silica gel plates with 70% dichloromethane-form-petroleum ether (6 runs) as a mobile phase, to give **TR8** as a yellow solid (0.002 g), melting at 165.0-167.2 °C.

UV (MeOH) λ_{max} nm (log \mathcal{E})	240 (4.18), 274 (4.50), 322 (4.04)
FT-IR (neat) $\nu_{\text{cm}^{-1}}$	3439 (OH stretching), 1644 (C=O stretching)
^1H NMR (CDCl_3) (δ ppm) (500 MHz)	12.96 (<i>s</i> , 1H), 7.45 (<i>s</i> , 1H), 6.44 (<i>d</i> , $J = 10.0$ Hz, 1H), 6.37 (<i>s</i> , 1H), 5.73 (<i>d</i> , $J = 10.0$ Hz, 1H), 3.91 (<i>s</i> , 3H), 2.95-2.92 (<i>m</i> , 2H), 1.78-1.74 (<i>m</i> , 2H), 1.54 (<i>s</i> , 6H), 1.34 (<i>s</i> , 6H)
^{13}C NMR (CDCl_3) (δ ppm) (125 MHz)	180.68, 163.28, 161.66, 153.51, 145.70, 145.44, 138.67, 131.04, 121.59, 118.34, 113.95, 113.11, 108.67, 103.20, 93.99, 78.19, 72.20, 55.99, 41.40, 29.63, 28.46, 16.55
DEPT (135°) (CDCl_3)	CH 131.04, 121.59, 113.11, 93.99 CH ₂ 41.40, 16.55

CH₃ 55.99, 29.63, 28.46

Band5 was obtained as a yellow solid (0.003 g). Chromatogram characteristics on normal phase TLC with pure chloroform showed many UV-active spots. Because of low quantity, it was not further investigated.

Fraction 4'.7 Chromatogram characteristics on normal phase TLC with pure chloroform demonstrated many components. It was further separated by flash column chromatography over silica gel. Elution was conducted with pure chloroform, gradually enriched with methanol and finally with pure methanol. Fractions with the similar chromatogram characteristics were combined and evaporated to dryness under reduced pressure to afford two subfractions, as shown in **Table 39**.

Table 39 Fractions obtained from the fraction 4'.7 by flash column chromatography over silica gel

Fraction	Weight (g)	Physical appearance
F'1	0.091	yellow gum
F'2	0.062	yellow-brown gum

Fraction F'1 Chromatogram characteristics on normal phase TLC with 2% methanol-chloroform showed many UV-active spots. It was further separated by flash column chromatography over silica gel. Elution was conducted with 15% ethyl acetate-hexane, gradually enriched with ethyl acetate and finally 20% ethyl acetate-hexane. Fractions with the similar chromatogram characteristics were combined and evaporated to dryness under reduced pressure to afford four subfractions, as shown in **Table 40**.

Table 40 Fractions obtained from the fraction F'1 by flash column chromatography over silica gel

Fraction	Weight (g)	Physical appearance
F'1.1	0.016	yellow solid
F'1.2	0.019	yellow solid
F'1.3	0.032	yellow gum

Subfraction F'1.1 Chromatogram characteristics on normal phase TLC with 20% ethyl acetate-hexane showed one major UV-active spot with the R_f value of 0.56. It was separated by precoated TLC on silica gel plates with 70% dichloromethane-petroleum ether (7 runs) as a mobile phase to give TR6 as a yellow solid in 0.003 g. Chromatogram characteristics on normal phase TLC with 70% dichloromethane-petroleum ether (8 runs) showed one spot under UV with the R_f value of 0.25, melting at 235.9-236.5 °C.

UV (MeOH) λ_{\max} nm (log ϵ)	230 (4.47), 276 (4.25), 328 (3.82)
FT-IR (neat) $\nu_{\text{cm}^{-1}}$	3446 (OH stretching), 1644 (C=O stretching)
^1H NMR (CDCl_3) (δ ppm) (500 MHz)	12.92 (<i>s</i> , 1H), 7.60 (<i>d</i> , $J = 3.0$ Hz, 1H), 7.39 (<i>d</i> , $J = 8.5$ Hz, 1H), 7.28 (<i>dd</i> , $J = 8.5, 3.0$ Hz, 1H), 6.83 (<i>dd</i> , $J = 10.0, 0.5$ Hz, 1H), 6.27 (<i>d</i> , $J = 0.5$ Hz, 1H), 5.61 (<i>d</i> , $J = 10.0$ Hz, 1H), 1.48 (<i>s</i> , 6H)
^{13}C NMR (CDCl_3) (δ ppm) (125 MHz)	180.46, 163.01, 160.92, 152.06, 151.90, 150.30, 127.04, 123.84, 121.05, 119.09, 114.98, 109.30, 103.47, 100.93, 99.20, 78.25, 28.29

DEPT (135°) (CDCl ₃)	CH	127.04, 123.84, 119.09, 114.98, 109.30, 99.20
	CH ₃	28.29

Subfraction F'1.2 Chromatogram characteristics on normal phase TLC with 20% ethyl acetate-hexane (3 runs) showed two major UV-active spots with the R_f values of 0.56 and 0.50 (**TR6**). It was separated by precoated TLC on silica gel plates with 20% ethyl acetate-hexane (7 runs) as a mobile phase to afford **TR6** (0.008 g) as a yellow solid.

Subfraction F'1.3 Chromatogram characteristics on normal phase TLC with 20% ethyl acetate-hexane (3 runs) showed many UV-active spots. It was not further investigated.

Fraction F'2 Chromatogram characteristics on normal phase TLC with 2% methanol-chloroform showed many UV-active spots. No attempted purification was performed.

Fraction 4'.8 Chromatogram characteristics on normal phase TLC with 8% methanol-chloroform showed many components. It was further separated by flash column chromatography over silica gel. Elution was conducted with pure chloroform, gradually enriched with methanol and finally with pure methanol. Fractions with the similar chromatogram characteristics were combined and evaporated to dryness under reduced pressure to afford seven subfractions of which chromatogram characteristics on normal phase TLC with 4% methanol-chloroform showed many unseparable spots.

Fraction 5' Chromatogram characteristics on normal phase TLC with 100% chloroform showed many components. It was further separated by column chromatography over silica gel. Elution was conducted with pure chloroform, gradually enriched with methanol and finally with pure methanol. Fractions with the

similar chromatogram characteristics were combined and evaporated to dryness under reduced pressure to afford six subfractions, as shown in **Table 41**.

Table 41 Fractions obtained from the fraction 5' by column chromatography over silica gel

Fraction	Weight (g)	Physical appearance
5'.1	0.018	pale yellow solid
5'.2	0.022	yellow gum
5'.3	0.160	red-yellow gum
5'.4	0.087	yellow gum mixed with yellow solid
5'.5	0.799	brown gum
5'.6	2.359	dark brown solid

Fraction 5'.1 Chromatogram characteristics on normal phase TLC with 50% dichloromethane-petroleum ether showed one major purple pale spot with the R_f value of 0.57. It was then not further investigated.

Fraction 5'.2 Chromatogram characteristics on normal phase TLC with 50% dichloromethane-petroleum ether was similar to that of the fraction 4'.1. They were then combined and separated by column chromatography over silica gel. Elution was conducted with 30% dichloromethane-petroleum ether. Fractions with the similar chromatogram characteristics were combined on the basis of their chromatogram characteristics and evaporated to dryness under reduced pressure to afford five subfractions in low quantity. The first fraction was identified as **TR20** by chromatogram characteristic. The remaining fractions were therefore not investigated further.

Fraction 5'3 Chromatogram characteristics on normal phase TLC with 50% dichloromethane-petroleum ether showed three major spots with the R_f values of 0.45, 0.24 and 0.20 (TR17). Further separation by flash column chromatography over silica gel was performed. Elution was conducted with 30% dichloromethane-petroleum ether. Fractions with the similar chromatogram characteristics were combined on the basis of their chromatogram characteristics and evaporated to dryness under reduced pressure to afford seven subfractions, as shown in **Table 42**.

Table 42 Fractions obtained from the fraction 5'3 by flash column chromatography over silica gel

Fraction	Weight (g)	Physical appearance
G'1	0.005	yellow gum
G'2	0.007	yellow-purple gum
G'3	0.036	yellow gum
G'4	0.045	pink gum
G'5	0.011	dark pink gum
G'6	0.006	yellow solid
G'7	0.014	yellow gum mixed with yellow solid

Fraction G'1 Chromatogram characteristics on normal phase TLC with 5% ethyl acetate-petroleum ether (6 runs) indicated the presence of TR20 as a major component.

Fraction G'2 Chromatogram characteristics on normal phase TLC with 5% ethyl acetate-petroleum ether (6 runs) showed many pale spots under UV. No further purification was performed.

Fraction G'3 Chromatogram characteristics on normal phase TLC with 5% ethyl acetate-petroleum ether (6 runs) showed one major UV-active spot with the R_f value of 0.26. Further separation by flash column chromatography over silica gel was performed. Elution was conducted with 5% ethyl acetate-petroleum ether. Fractions with the similar chromatogram characteristics were combined and evaporated to dryness under reduced pressure to afford two subfractions as shown in **Table 43**.

Table 43 Fractions obtained from the fraction G'3 by flash column chromatography over silica gel

Fraction	Weight (g)	Physical appearance
G'3.1	0.022	yellow liquid
G'3.2	0.007	yellow solid

Subfraction G'3.1 Chromatogram characteristics on normal phase TLC with 5% ethyl acetate-petroleum ether (4 runs) showed many pale spots under UV. No further purification was performed.

Subfraction G'3.2 Chromatogram characteristics on normal phase TLC with 5% ethyl acetate-petroleum ether (4 runs) showed one major spot under UV with the R_f value of 0.24. It was separated by precoated TLC on silica gel plates with 5% ethyl acetate-petroleum ether (5 runs) as a mobile phase to give **TR16** as a yellow solid in 0.003 g. Chromatogram characteristics on normal phase TLC with 5% ethyl acetate-petroleum ether (4 runs) showed one spot under UV with the R_f value of 0.22, melting at 215.9-217.1 °C.

UV (MeOH) λ_{\max} nm (log ϵ) 216 (3.35), 268 (3.40), 298 (3.25), 330 (3.15)

FT-IR (neat) $\nu_{\text{cm}^{-1}}$	3394 (OH stretching), 1638 (C=O stretching)
^1H NMR (CDCl_3) (δ ppm) (500 MHz)	13.42 (<i>s</i> , 1H), 8.02 (<i>d</i> , $J = 10.5$ Hz, 1H), 6.87 (<i>s</i> , 1H), 6.78 (<i>d</i> , $J = 10.0$ Hz, 1H), 6.22 (<i>s</i> , 1H), 5.84 (<i>d</i> , $J = 10.5$ Hz, 1H), 5.58 (<i>d</i> , $J = 10.0$ Hz, 1H), 1.50 (<i>s</i> , 6H), 1.47 (<i>s</i> , 6H)
^{13}C NMR (CDCl_3) (δ ppm) (125 MHz)	182.48, 163.10, 159.97, 152.90, 151.91, 150.91, 136.88, 132.41, 126.80, 120.86, 119.76, 115.05, 108.48, 103.83, 102.30, 100.38, 99.05, 77.98, 77.00, 28.22, 27.32
DEPT (135°) (CDCl_3)	CH 132.41, 126.80, 120.86, 115.05, 102.30, 99.05 CH ₃ 28.22, 27.32

Fraction G'4 Chromatogram characteristics on normal phase TLC with 5% ethyl acetate-petroleum ether (6 runs) showed many pale spots under UV. No further purification was performed.

Fraction G'5 Chromatogram characteristics on normal phase TLC with 5% ethyl acetate-petroleum ether (6 runs) showed two major spots with the R_f values of 0.30 and 0.21. Further separation by flash column chromatography over silica gel was performed. Elution was conducted with 5% ethyl acetate-petroleum ether. Fractions with the similar chromatogram characteristics were combined on the basis of chromatogram characteristics and evaporated to dryness under reduced pressure to afford three subfractions, as shown in **Table 44**.

Table 44 Fractions obtained from the fraction G'5 by flash column chromatography over silica gel

Fraction	Weight (g)	Physical appearance
G'5.1	0.003	purple gum
G'5.2	0.003	yellow solid
G'5.3	0.003	yellow gum

Subfraction G'5.1 Chromatogram characteristics on normal phase TLC with 5% ethyl acetate-petroleum ether (4 runs) showed many pale spots under UV. No further purification was performed.

Subfraction G'5.2 Chromatogram characteristics on normal phase TLC with 5% ethyl acetate-petroleum ether (4 runs) showed one UV-active spot with the R_f value of 0.29. It decomposed at room temperature. Thus, it was not investigated further.

Subfraction G'5.3 Chromatogram characteristics on normal phase TLC with 5% ethyl acetate-petroleum ether (4 runs) showed one major UV-active spot with the R_f value of 0.24 and many pale UV-active spots above the major spot. Because of low quantity, it was not further investigated.

Fraction G'6 Chromatogram characteristics on normal phase TLC with 5% ethyl acetate-petroleum ether (6 runs) showed three major spots under UV with the R_f values of 0.30, 0.26 and 0.24. No attempted investigation was performed because of low quantity.

Fraction G'7 Chromatogram characteristics on normal phase TLC with 5% ethyl acetate-petroleum ether (6 runs) indicated the presence of TR17 as a pure component.

Fraction 5'.4 Chromatogram characteristics on normal phase TLC with 5% ethyl acetate-petroleum ether (6 runs) indicated the presence of **TR17** as a major component.

Fraction 5'.5 was separated into two parts: a yellow solid (**5'.5S**) and a yellow solution (**5'.5L**), upon standing at room temperature.

SubFraction 5'.5S was obtained as yellow crystals (0.018 g). It was chromatographed on TLC with 10% water-methanol as a mobile phase. It showed one major UV-active spot with R_f the value of 0.18. Further separation by column chromatography over reverse phase silica gel was performed. Elution was conducted with 20% water-methanol. Fractions with the similar chromatogram characteristics were combined on the basis of their chromatogram characteristics and evaporated to dryness under reduced pressure to afford two subfractions, as shown in **Table 45**.

Table 45 Fractions obtained from the fraction **5'.5S** by column chromatography over reverse phase silica gel

Fraction	Weight (g)	Physical appearance
5S1	0.005	yellow gum
5S2	0.010	yellow solid

SubFraction 5S1 Chromatogram characteristics on reverse phase TLC with 10% water-methanol (2 runs) showed one major yellow spot with the R_f value of 0.14. Because of low quantity, it was not further investigated.

SubFraction 5S2 (TR13) Chromatogram characteristics on reverse phase TLC with 10% water-methanol (2 runs) showed one yellow spot with the R_f value of 0.14, melting at 241.7-243.5 °C.

UV (MeOH) λ_{\max} nm (log ϵ)	222 (4.62), 346 (4.50)
FT-IR (neat) $\nu_{\text{cm}^{-1}}$	3424 (OH stretching), 1646 (C=O stretching)
^1H NMR (CDCl_3) (δ ppm) (500 MHz)	13.34 (<i>s</i> , 1H), 7.58 (<i>s</i> , 1H), 6.88 (<i>d</i> , $J = 10.0$ Hz, 1H), 6.75 (<i>d</i> , $J = 10.0$ Hz, 1H), 6.33 (<i>s</i> , 1H), 5.75 (<i>d</i> , $J = 10.0$ Hz, 1H), 5.59 (<i>d</i> , $J = 10.0$ Hz, 1H), 5.50 (<i>brs</i> , 1H), 1.55 (<i>s</i> , 6H), 1.47 (<i>s</i> , 6H)
^{13}C NMR (CDCl_3) (δ ppm) (125 MHz)	180.02, 160.08, 157.55, 156.86, 146.33, 145.74, 141.85, 129.87, 127.36, 115.56, 115.42, 113.99, 109.16, 108.69, 104.53, 103.21, 94.77, 79.30, 78.05, 28.31, 28.24
DEPT (135°) (CDCl_3)	CH 129.87, 127.36, 115.56, 115.42, 108.69, 94.77 CH ₃ 28.31, 28.24

SubFraction 5'.5L Chromatogram characteristics on normal phase TLC with 2% methanol-chloroform showed many components. It was further separated by flash column chromatography over silica gel. Elution was initially conducted with pure chloroform, gradually enriched with methanol and finally with pure methanol. Fractions with the similar chromatogram characteristics were combined and evaporated to dryness under reduced pressure to afford three subfractions, as shown in Table 46.

Table 46 Fractions obtained from the fraction 5'.5L by flash column chromatography over silica gel

Fraction	Weight (g)	Physical appearance
5L1	0.067	yellow gum mixed with yellow solid
5L2	0.094	yellow solid
5L3	0.598	dark brown gum

SubFraction 5L1 Chromatogram characteristics on normal phase TLC with 20% ethyl acetate-petroleum ether showed three major UV-active spots with the R_f values of 0.42, 0.35 and 0.12. It was further separated by flash column chromatography over silica gel. Elution was conducted with 20% ethyl acetate-petroleum ether. Fractions with the similar chromatogram characteristics were combined and evaporated to dryness under reduced pressure to afford five subfractions in low quantity. The third fraction contained **TR18** according to its chromatogram characteristics. The chromatogram characteristics of the remaining fractions on normal phase TLC with 4% methanol-chloroform showed many spots. They were not further investigated.

SubFraction 5L2 Chromatogram characteristics on normal phase TLC with 70% chloroform-petroleum ether (2 runs) showed one major UV-active spot with the R_f value of 0.29. It was further separated by flash column chromatography over silica gel. Elution was conducted with 80% chloroform-petroleum ether. Fractions with the similar chromatogram characteristics were combined and evaporated to dryness under reduced pressure to afford three subfractions, as shown in **Table 47**.

Table 47 Fractions obtained from the fraction **5L2** by flash column chromatography over silica gel

Fraction	Weight (g)	Physical appearance
H'1	0.004	yellow gum
H'2	0.082	brown gum mixed with yellow solid
H'3	0.007	brown gum mixed with yellow solid

Subfraction H'1 Chromatogram characteristics on normal phase TLC with 70% chloroform-petroleum ether (2 runs) showed many pale UV-active spots. No further purification was performed.

Subfraction H'2 Chromatogram characteristics on normal phase TLC with 70% chloroform-petroleum ether (2 runs) showed one major UV-active spot with the R_f value of 0.29. It was further separated by flash column chromatography over silica gel. Elution was conducted with 80% chloroform-petroleum ether. Fractions with the similar chromatogram characteristics were combined and evaporated to dryness under reduced pressure to afford three subfractions, as shown in **Table 48**.

Table 48 Fractions obtained from the fraction **H'2** by flash column chromatography over silica gel

Fraction	Weight (g)	Physical appearance
H'2.1	0.026	yellow gum
H'2.2	0.042	brown gum mixed with yellow solid
H'2.3	0.018	brown gum mixed with yellow solid

Subfraction H'2.1 Chromatogram characteristics on normal phase TLC with 20% ethyl acetate-petroleum ether showed many pale UV-active spots. No further purification was performed.

Subfraction H'2.2 Chromatogram characteristics on normal phase TLC with 20% ethyl acetate-petroleum ether demonstrated one major UV-active spots with the R_f value of 0.21. It was further separated by flash column chromatography over silica gel. Elution was conducted with 10% dichloromethane-petroleum ether. Fractions with the similar chromatogram characteristics were combined and evaporated to dryness under reduced pressure to afford three subfractions, as shown in **Table 49**.

Table 49 Fractions obtained from the subfraction **H'2.2** by flash column chromatography over silica gel

Fraction	Weight (g)	Physical appearance
HA'1	0.007	yellow gum mixed with yellow solid
HA'2	0.016	yellow solid
HA'3	0.008	yellow solid

Subfraction HA'1 Chromatogram characteristics on normal phase TLC with 10% dichloromethane-petroleum ether showed many pale UV-active spots. No further purification was performed.

Subfraction HA'2 Chromatogram characteristics on normal phase TLC with 10% dichloromethane-petroleum ether indicated the presence of **TR13** as a pure component.

Subfraction HB'3 Chromatogram characteristics on normal phase TLC with 1% methanol-chloroform indicated the presence of **TR19** as a pure component.

SubFraction 5L3 Chromatogram characteristics on normal phase TLC with 30% ethyl acetate-petroleum ether showed many major UV-active spots. It was further separated by flash column chromatography over silica gel. Elution was conducted with 30% ethyl acetate-petroleum ether. Fractions with the similar chromatogram characteristics were combined and evaporated to dryness under reduced pressure to afford five subfractions in low quantity. Their chromatogram characteristics on normal phase TLC with 4% methanol-chloroform showed many spots. They were not further investigated.

Fraction 5'.6 Chromatogram characteristics on reverse phase TLC with 20% water-methanol showed many spots under UV. Further separation by column chromatography over reverse phase silica gel was performed. Elution was conducted with 20% water-methanol. Fractions with the similar chromatogram characteristics were combined on the basis of their chromatogram characteristics and evaporated to dryness under reduced pressure to afford nine subfractions of which chromatogram characteristics on reverse phase TLC with 20% water-methanol (4 runs) showed many unseparable spots.

Fraction 6' Chromatogram characteristics on normal phase TLC with 100% chloroform contained many components. It was further separated by column chromatography over silica gel. Elution was conducted with pure chloroform, gradually enriched with methanol and finally with pure methanol. Fractions with the similar chromatogram characteristics were combined and evaporated to dryness under reduced pressure to afford five subfractions, as shown in **Table 51**.

Table 51 Fractions obtained from the fraction 6' by column chromatography over silica gel

Fraction	Weight (g)	Physical appearance
6'.1	0.010	pale yellow solid
6'.2	0.037	pale yellow gum mixed with purple solid
6'.3	0.036	yellow gum mixed with yellow solid
6'.4	0.386	yellow gum
6'.6	0.456	brown gum

Fraction 6'.1 Chromatogram characteristics on normal phase TLC with 50% dichloromethane-petroleum ether showed no spot under UV. It was not further investigated.

Fraction 6'.2 Chromatogram characteristics on normal phase TLC with 50% dichloromethane-petroleum ether showed many spots under UV. No attempted investigation was performed because of low quantity.

Fraction 6'.3 Chromatogram characteristics on normal phase TLC with pure chloroform showed three major spots with the R_f values of 0.52, 0.42 and 0.17. Further separation by flash column chromatography over silica gel was performed. Elution was conducted with pure chloroform, gradually enriched with methanol and finally with 5% methanol-chloroform. Fractions with the similar chromatogram characteristics were combined on the basis of their chromatogram characteristics and evaporated to dryness under reduced pressure to afford three subfractions, as shown in **Table 52**.

Table 52 Fractions obtained from the fraction 6'.3 by flash column chromatography over silica gel

Fraction	Weight (g)	Physical appearance
I'1	0.003	pale yellow gum
I'2	0.026	yellow gum
I'3	0.005	yellow solid

Subfraction I'1 Chromatogram characteristics on normal phase TLC with pure chloroform showed many UV-active spots. No further purification was performed.

Subfraction I'2 Chromatogram characteristics on normal phase TLC with pure chloroform showed three major UV-active spots with the R_f values of 0.85 (TR9), 0.73 (TR18) and 0.25 (TR17).

Subfraction I'3 Chromatogram characteristics on normal phase TLC with pure chloroform showed no definite spots under UV. No further purification was attempted.

Fraction 6'.4 Chromatogram characteristics on normal phase TLC with 2% methanol-chloroform showed many major UV-active spots. It was further separated by flash column chromatography over silica gel. Elution was conducted with pure chloroform, gradually enriched with methanol and finally with pure methanol. Fractions with the similar chromatogram characteristics were combined and evaporated to dryness under reduced pressure to afford six subfractions of which chromatogram characteristics on normal phase TLC with 4% methanol-chloroform showed many unseparable spots. They were not further investigated.

Fraction 6'.5 Chromatogram characteristics on normal phase TLC with 5% methanol-chloroform showed no separation. No further separation was conducted.

Fraction 7'-15' They were not further investigated because of limitation of time.

CHAPTER 3

RESULTS AND DISCUSSION

The stem bark of *G. nigrolineata* was extracted with MeOH. The first MeOH extract was separated into two parts with EtOAc. The EtOAc soluble part, upon repeated chromatography, afforded eight xanthenes. The EtOAc insoluble part was combined with the second MeOH extract and then subjected to chromatographic purification. Eleven additional xanthenes together with one dibenzofuran derivative were obtained. Ten xanthenes (TR1, TR3, TR4, TR5, TR6, TR8, TR11, TR13, TR14 and TR19) and the dibenzofuran (TR20) were found to be new. However, two of them (TR3 and TR6) were previously reported as synthetic xanthenes. All structures were elucidated using 1D and 2D NMR spectroscopic data. The ^{13}C NMR signals were assigned from DEPT, HMQC and HMBC spectra. For known xanthenes, their ^1H and/or ^{13}C spectral data were compared with those reported in the literature.

3.1 Compound TR4

Compound TR4 was isolated as a yellow solid, melting at 142.8-144.6 $^{\circ}\text{C}$. The IR spectrum (Figure 3.2) exhibited absorption bands at 3358 and 1645 cm^{-1} for hydroxyl and conjugated carbonyl functionalities. The absorption bands at λ_{max} 248 and 318 nm in the UV spectrum (Figure 3.1) indicated that TR4 has a xanthone chromophore. The ^1H NMR spectrum (Figure 3.3) (Table 53) showed characteristic peaks of a 1,2,3-trisubstituted benzene ring [δ 7.73 and 7.28 (1H each, *dd*, $J = 8.0$ and 2.0 Hz) and 7.23 (1H, *t*, $J = 8.0$ Hz)], a 3-hydroxy-3-methylbutyl unit [δ 2.95-2.92

(2H, *m*), 1.77-1.74 (2H, *m*) and 1.36 (6H, *s*)] in addition to a chelated hydroxy proton [δ 12.82 (1-OH, *s*)]. The remaining one-proton singlet at δ 6.39 was attributed to an aromatic proton. The ^{13}C NMR spectrum (Figure 3.4) (Table 53) showed 18 resonances for 19 carbon atoms: ten quaternary carbons (δ 181.38, 163.59, 161.78, 153.60, 145.54, 144.65, 120.87, 108.62, 103.47 and 72.71), four methine carbons (δ 123.94, 120.36, 115.92 and 94.02), two methylene carbons (δ 41.00 and 16.42) and three methyl carbons [δ 56.01 (OCH₃), 29.73 (2xC)]. The lowest-field aromatic proton (δ 7.73) of the 1,2,3-trisubstituted benzene ring gave cross peaks with a carbonyl carbon (δ 181.38, C-9) and the *O*-linked carbon signal at δ 144.65 (C-10a), indicating that it was located at a *peri*-position (δ 115.92, C-8) to a carbonyl group. Two other aromatic protons at δ 7.28 and 7.23 were then attributed to H-6 and H-7, respectively, according to their splitting pattern and the value of coupling constants. H-6 gave cross peaks with a methine carbon (C-8) and an oxygenated carbon (C-10a) while H-7 showed correlation with an oxygenated aromatic carbon (δ 145.54, C-5) and a quaternary aromatic carbon (δ 120.87, C-8a). These indicated that the C-5 position was substituted by a hydroxyl group. The chelated hydroxy proton (1-OH) caused a cross peak with a methine aromatic carbon at (δ 94.02, C-2) which correlated to the aromatic proton (δ 6.39, H-2) in the HMQC spectrum (Figure 3.7). Irradiation of H-2, in the NOE experiment (Figure 3.6), enhanced the singlet signals of the methoxy protons (δ 3.91) and chelated hydroxy proton (δ 12.85). Subsequently, the methoxyl group was assigned to be at C-3 (δ 163.59). The correlation of the methoxy protons with an oxyquaternary carbon (C-3), in the HMBC spectrum (Figure 3.8) (Table 53), confirmed the location of the methoxyl group. Therefore, 3-hydroxy-3-methylbutyl unit was substituted at C-4. The HMBC correlation, H-11/C-3 and H-12/C-4, confirmed the linkage of this unit at C-4. Accordingly, TR4 was assigned as 1,5-dihydroxy-3-methoxy-4-(3-hydroxy-3-methylbutyl)xanthone (1), a new naturally occurring xanthone.

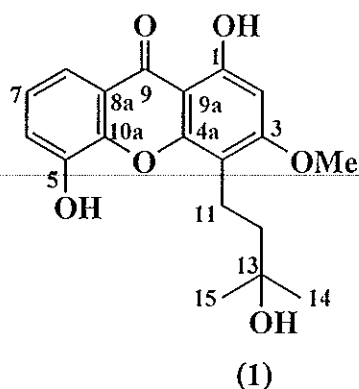


Table 53 The NMR data of compound TR4 in CDCl₃

Position	δ_{H} (<i>mult.</i> , J_{Hz})	δ_{C} (C-Type)	HMBC correlation
1-OH	12.82 (<i>s</i>)	161.78 (C)	C-1, C-2, C-9a
2	6.39 (<i>s</i>)	94.02 (CH)	C-1, C-3, C-4, C-9a
3		163.59 (C)	
3-OCH ₃	3.91 (<i>s</i>)	56.01 (CH ₃)	C-3
4		108.62 (C)	
4a		153.60 (C)	
5-OH		145.54 (C)	
6	7.28 (<i>dd</i> , 8.0 and 2.0)	120.36 (CH)	C-8, C-10a
7	7.23 (<i>t</i> , 8.0)	123.94 (CH)	C-5, C-8a
8	7.73 (<i>dd</i> , 8.0 and 2.0)	115.92 (CH)	C-6, C-9, C-10a
8a		120.87 (C)	
9		181.38 (C=O)	
9a		103.47 (C)	
10a		144.65 (C)	
11	2.95-2.92 (<i>m</i>)	16.42 (CH ₂)	C-3, C-4, C-4a, C-11, C-13
12	1.77-1.74 (<i>m</i>)	41.00 (CH ₂)	C-4, C-11, C-13, C-14, C-15
13-OH		72.71 (C)	
14,15	1.36 (<i>s</i>)	29.73 (CH ₃)	C-11, C-12, C-13, C-14, C-15

3.2 Compound TR2

Compound **TR2** was obtained as a pale yellow solid, melting at 115.0-116.2 °C. The IR spectrum (Figure 3.10) exhibited absorption bands at 3409 and 1646 cm^{-1} for hydroxyl and carbonyl functionalities. Its UV spectrum with absorption bands at λ_{max} 244 and 320 nm (Figure 3.9) indicated the presence of xanthone chromophore. Its ^1H NMR spectrum (Figure 3.11) (Table 54) was similar to that of **TR4** except for the absence of the methoxy proton signal. The ^{13}C NMR spectrum (Figure 3.12) showed the same number and type of quaternary, methine and methylene carbons as those found in **TR4** but with only one resonance of a methyl carbon for two geminal-dimethyl groups. It was shown by the HMBC spectrum (Figure 3.15) (Table 54) that the methylene protons, H-11 (δ 2.95-2.91), of a 3-hydroxy-3-methylbutyl unit correlated with an oxygenated aromatic carbon (δ 162.50, C-3) while the other methylene protons, H-12 (δ 1.78-1.74), gave a cross peak with C-4 (δ 108.00). These data revealed that C-3 and C-4 were substituted by a hydroxyl group and 3-hydroxy-3-methylbutyl group, respectively. Thus, **TR2** was determined as 1,3,5-trihydroxy-4-(3-hydroxy-3-methylbutyl)xanthone (**2**) which was previously isolated from *Anaxagorea luzonensis* A. GRAY, (Gonda, *et al.*, 2000).

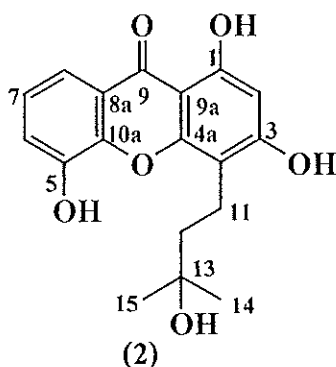


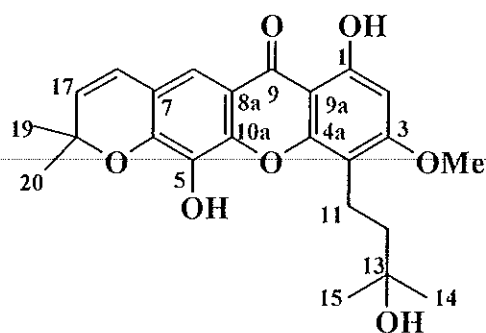
Table 54 The NMR data of compound TR2 in CDCl₃/CD₃OD

Position	TR2		HMBC correlation	TR 2 (reported data)	
	δ_{H} (<i>mult.</i> , J_{Hz})	δ_{C} (C-Type)		δ_{H} (<i>mult.</i> , J_{Hz})*	δ_{C} (C-Type)*
1-OH	12.85 (<i>s</i>)	160.72 (C)	C-1, C-2, C-9a	12.83 (<i>s</i>)	160.1 (C)
2	6.26 (<i>s</i>)	97.76 (CH)	C-1, C-3, C-4, C-9a	6.27 (<i>s</i>)	97.6 (CH)
3-OH		162.50 (C)			164.2 (C)
4		108.00 (C)			107.6 (C)
4a		154.72 (C)			154.2 (C)
5-OH		146.00 (C)			146.3 (C)
6	7.25 (<i>dd</i> , 7.5 and 1.5)	120.48 (CH)	C-8, C-10a	7.28 (<i>dd</i> , 7.9 and 1.8)	120.1 (CH)
7	7.20 (<i>t</i> , 7.5)	123.90 (CH)	C-5, C-8a	7.24 (<i>dd</i> , 7.9 and 7.3)	127.7 (CH)
8	7.69 (<i>dd</i> , 7.5 and 1.5)	115.99 (CH)	C-6, C-9, C-10a	7.53 (<i>dd</i> , 7.3 and 1.8)	114.3 (CH)
8a		121.10 (C)			120.6 (C)
9		181.32 (C=O)			180.0 (C=O)
9a		103.21 (C)			101.7 (C)
10a		145.11 (C)			144.9 (C)
11	2.95-2.91 (<i>m</i>)	16.66 (CH ₂)	C-3, C-4, C-4a, C-12	2.79 (<i>dd</i> , 8.6 and 4.9)	17.2 (CH ₂)
12	1.78-1.74 (<i>m</i>)	41.51 (CH ₂)	C-4, C-11, C-13, C-14, C-15	1.61 (<i>dd</i> , 8.6 and 4.9)	42.6 (CH ₂)
13-OH		71.79 (C)			69.2 (C)
14,15	1.30 (<i>s</i>)	29.30 (CH ₃)	C-12, C-13, C-14, C-15	1.21 (<i>s</i>)	28.9 (CH ₃)

* ¹H and ¹³C NMR data of 1,3,5-trihydroxy-4-(3-hydroxy-3-methylbutyl)xanthone in DMSO-*d*₆.

3.3 Compound TR8

Compound **TR8** was isolated as yellow crystals, melting at 165.0-167.2 °C. The xanthone chromophore was evident by its UV (Figure 3.16) absorption bands at λ_{max} 240, 274 and 322 nm and the pyrone carbonyl stretching frequency was found in the region of 1644 cm^{-1} in the IR spectrum (Figure 3.17). Its ^1H NMR spectrum (Figure 3.18) (Table 55) was similar to that of **TR4** except for the fact that two high-field aromatic protons of the 1,2,3-trisubstituted benzene ring of **TR4** were replaced, in **TR8**, by a dimethylchromene ring [δ 6.44 and 5.73 (1H each, *d*, $J = 10.0$ Hz) and 1.54 (6H, *s*)]. A singlet signal of the lowest-field aromatic proton at δ 7.45 was assigned to H-8, *peri* to the carbonyl functionality. Irradiation of H-8 caused an NOE enhancement (Figure 3.21) of the olefinic methine proton (δ 6.44, H-16), suggesting that dimethylchromene ring was fused in a linear fashion to the xanthone nucleus. Important observations from the HMBC experiment (Figure 3.24) (Table 55) were as follows. The correlation between H-16 and C-6 (δ 145.44) and C-18 (δ 78.19) suggested that the oxygen atom of the dimethylchromene ring was attached to C-6. The C-3/H-11 and C-4/H-12 correlation established the linkage of the 3-hydroxy-3-methylbutyl unit at C-4. The enhancement of both chelated hydroxy and methoxy proton signals, after irradiation of H-2 (Figure 3.22), confirmed the location of this side chain. The methoxy proton signal showed a correlation to an oxyaromatic carbon signal (δ 163.28, C-3), indicating the attachment of the methoxyl group at C-3. One remaining carbon resonance at δ 138.67 was then assigned to C-5. Since no more proton signal was observed, the substituent at C-5 must be a hydroxyl group. Thus, **TR8** was assigned as 1,5-dihydroxy-3-methoxy-4-(3-hydroxy-3-methylbutyl)-6',6'-dimethylpyrano(2',3':6,7) xanthone (**3**), a new naturally occurring xanthone.



(3)

Table 55 The NMR data of compound TR8 in CDCl_3

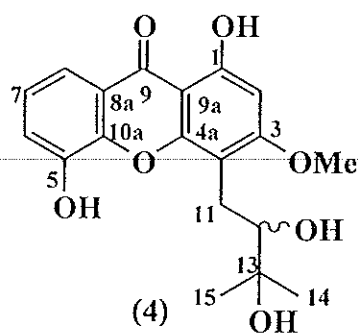
Position	δ_{H} (<i>mult.</i> , J_{Hz})	δ_{C} (C-Type)	HMBC correlation
1-OH	12.96 (<i>s</i>)	161.66 (C)	C-1, C-2, C-9a
2	6.37 (<i>s</i>)	93.99 (CH)	C-1, C-3, C-4, C-9a
3		163.28 (C)	
3-OCH ₃	3.91 (<i>s</i>)	55.99 (OCH ₃)	C-3
4		108.67 (C)	
4a		153.51 (C)	
5-OH		138.67 (C)	
6		145.44 (C)	
7		118.34 (C)	
8	7.45 (<i>s</i>)	113.11 (CH)	C-9, C-6, C-10a, C-16
8a		113.95 (C)	
9		180.68 (C=O)	
9a		103.20 (C)	
10a		145.70 (C)	
11	2.95-2.92 (<i>m</i>)	16.55 (CH ₂)	C-3, C-4, C-4a, C-12
12	1.78-1.74 (<i>m</i>)	41.40 (CH ₂)	C-11, C-13
13-OH		72.20 (C)	
14,15	1.34 (<i>s</i>)	29.63 (CH ₃)	C-12, C-13, C-14, C-15
16	6.44 (<i>d</i> , 10.0)	121.59 (CH)	C-6, C-18

Table 55 (Continued)

Position	δ_{H} (mult., J_{Hz})	δ_{C} (C-Type)	HMBC correlation
17	5.73 (<i>d</i> , 10.0)	131.04 (CH)	C-7, C-18
18		78.19 (C)	
19,20	1.54 (<i>s</i>)	28.46 (CH ₃)	C-17, C-18, C-19, C-20

3.4 Compound TR1

Compound **TR1** was obtained as a pale yellow solid, melting at 104.5-105.8 °C. Its UV spectrum (Figure 3.25) (λ_{max} 244, 258 and 326 nm) indicated the presence of a xanthone nucleus while the IR spectrum (Figure 3.26) showed absorption bands at 3394 (OH) and 1645 (α, β -unsaturated C=O) cm^{-1} . Its ^1H (Figure 3.27) (Table 56) and ^{13}C NMR spectra (Figure 3.28) (Table 56) were similar to those of **TR4**, suggesting that **TR1** was also 1,3,5-trioxygenated xanthone. Direct comparison of their ^1H NMR spectra revealed that the methylene proton signal of H-12 of **TR4** was replaced, in **TR1**, by an oxymethine proton. The presence of an additional oxymethine carbon at δ 79.60 (C-12) supported this conclusion. Thus, the side chain became 2,3-dihydroxy-3-methylbutyl unit [δ 3.67 (1H, *dd*, $J = 8.0$ and 2.0 Hz), 3.30 (1H, *dd*, $J = 15.0$ and 2.0 Hz), 2.83 (1H, *dd*, $J = 15.0$ and 8.0 Hz) and 1.36 (6H, *s*)]. In the HMBC spectrum (Figure 3.32) (Table 56), this oxymethine proton (H-12) gave a cross peak with C-4 (δ 106.08), suggesting the substituent at C-4 to be 2,3-dihydroxy-3-methylbutyl unit. Irradiation of H-2, in the NOE spectrum (Figure 3.30), enhanced signals of both the chelated hydroxy and methoxy protons, supporting the attachment of the methoxyl group at C-3. Thus, **TR1** was identified as 1,5-dihydroxy-3-methoxy-4-(2,3-dihydroxy-3-methylbutyl)xanthone (**4**), a new naturally occurring xanthone.

Table 56 The NMR data of compound TR1 in CDCl₃

Position	δ_{H} (<i>mult.</i> , J_{Hz})	δ_{C} (C-Type)	HMBC correlation
1-OH	12.83 (<i>s</i>)	162.38 (C)	C-1, C-2, C-9a
2	6.42 (<i>s</i>)	94.24 (CH)	C-1, C-3, C-4, C-9a
3		163.85 (C)	
3-OCH ₃	3.94 (<i>s</i>)	56.27 (OCH ₃)	C-3
4		106.08 (C)	
4a		154.03 (C)	
5-OH		145.43 (C)	
6	7.29 (<i>dd</i> , 7.5 and 1.5)	120.36 (CH)	C-8, C-10a
7	7.24 (<i>t</i> , 7.5)	124.12 (CH)	C-5, C-8a
8	7.73 (<i>dd</i> , 7.5 and 1.5)	116.10 (CH)	C-6, C-9, C-10a
8a		120.79 (C)	
9		181.37 (C=O)	
9a		103.53 (C)	
10a		144.63 (C)	
11	3.30 (<i>dd</i> , 15.0 and 2.0) 2.83 (<i>dd</i> , 15.0 and 8.0)	25.70 (CH ₂)	C-3, C-4, C-4a, C-12, C13
12-OH	3.67 (<i>dd</i> , 8.0 and 2.0)	79.60 (CH)	C-4, C-11, C-13
13-OH		74.35 (C)	
14,15	1.36 (<i>s</i>)	24.47 (CH ₃)	C-11, C-12, C-13, C-14, C-15

3.5 Compound TR14

Compound TR14 was isolated as a pale yellow solid, melting at 196.0-197.8 °C. Its UV (Figure 3.33) and IR (Figure 3.34) spectra indicated the presence of a hydroxylated xanthone skeleton. The ¹H NMR spectrum (Figure 3.35) (Table 57) showed characteristic peaks of a chelated hydroxy proton [δ 13.40 (*s*)], two sets of doublet signal of two *ortho*-aromatic protons [δ 7.11 and 7.18 (1H each, *d*, $J = 8.5$ Hz)] and two sets of doublet signal of two *meta*-aromatic protons [δ 6.16 and 6.23 (1H each, *d*, $J = 2.0$ Hz)], in addition to typical proton signals of 3-hydroxy-3-methylbutyl unit [δ 3.39-3.36 (2H, *m*), 1.85-1.82 (2H, *m*) and 1.27 (6H, *s*)]. The ¹³C NMR spectrum (Figure 3.36) (Table 57) showed 17 resonances for 18 carbon atoms: ten quaternary carbons (δ 183.26, 164.74, 163.30, 157.50, 151.79, 150.90, 129.80, 118.76, 103.74 and 71.37), four methine carbons (δ 123.71, 116.13, 97.89 and 93.50), two methylene carbons (δ 42.86 and 21.30) and two methyl carbons [δ 29.19 (2xC)]. The highly-deshielded position of the methylene protons of the 3-hydroxy-3-methylbutyl unit [δ 3.37, H-11] suggested that this side chain was at a *peri* position to a carbonyl group. These methylene protons, H-11, showed cross peaks, in the HMBC spectrum (Figure 3.39) (Table 57), with an oxyaromatic carbon (δ 150.90, C-7) and a quaternary aromatic carbon (δ 118.76, C-8a) while the other methylene protons (δ 1.84, H-12) showed a cross peak with a quaternary aromatic carbon at δ 129.80 (C-8). These data indicated that the 3-hydroxy-3-methylbutyl unit linked with the carbon signal at δ 129.80 which was assigned to C-8. Two sets of doublet signal of two-*ortho* aromatic protons (δ 7.11 and 7.18) were attributed to H-5 and H-6, respectively, according to the HMBC correlation between H-5 and C-7. The signal of the chelated hydroxyl group at δ 13.40 established the substituent at C-1 to be a hydroxyl group. Two-*meta* aromatic protons (δ 6.16 and 6.23) were then located at C-2 and C-4. The ²*J* correlation between the aromatic methine protons, H-2 and H-4, and an oxyaromatic carbon (δ 164.73, C-3) indicated the presence of a

hydroxyl group at C-3. Accordingly, the structure of **TR14** was determined as 1,3,7-trihydroxy-8-(3-hydroxy-3-methylbutyl)xanthone (**5**), a new trioxygenated xanthone.

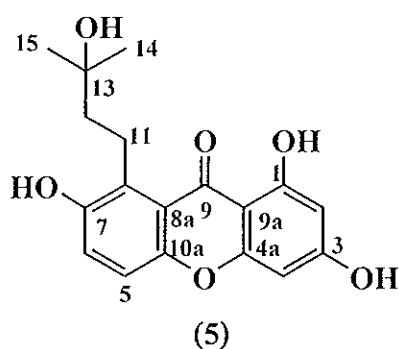
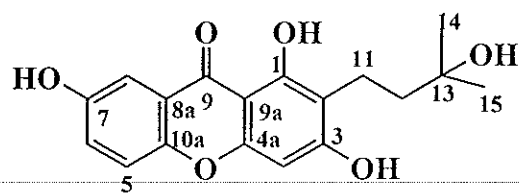


Table 57 The NMR data of compound **TR14** in $\text{CDCl}_3/\text{CD}_3\text{OD}$

Position	δ_{H} (mult., J_{Hz})	δ_{C} (C-Type)	HMBC correlation
1-OH	13.40 (<i>s</i>)	163.30 (C)	
2	6.16 (<i>d</i> , 2.0)	97.89 (CH)	C-1, C-2, C-4, C-9a
3-OH		164.74 (C)	
4	6.23 (<i>d</i> , 2.0)	93.50 (CH)	C-2, C-3, C-4a, C-9a
4a		157.50 (C)	
5	7.11 (<i>d</i> , 8.5)	116.13 (CH)	C-7, C-8a
6	7.18 (<i>d</i> , 8.5)	123.71 (CH)	C-8, C-10a
7-OH		150.90 (C)	
8		129.80 (C)	
8a		118.76 (C)	
9		183.26 (C=O)	
9a		103.74 (C)	
10a		151.79 (C)	
11	3.39-3.36 (<i>m</i>)	21.30 (CH_2)	C-7, C-8, C-8a, C-12, C-13
12	1.85-1.82 (<i>m</i>)	42.86 (CH_2)	C-8, C-11, C-13, C-14, C-15
13-OH		71.37 (C)	
14,15	1.27 (<i>s</i>)	29.19 (CH_3)	C-12, C-13, C-14, C-15

3.6 Compound TR15

Compound **TR15** was isolated as a pale yellow solid, melting at 230.5-232.9 °C. Its UV (Figure 3.40) and IR (Figure 3.14) spectra indicated the presence of a hydroxylated xanthone skeleton. The ¹H NMR spectrum (Figure 3.42) (Table 58) showed characteristic peaks of a chelated hydroxy proton (δ 13.26, 1-OH), typical proton signals of a 1,2,4-trisubstituted benzene [δ 7.57 (1H, *d*, *J* = 3.0 Hz), 7.41 (1H, *d*, *J* = 9.0 Hz) and 7.33 (1H, *dd*, *J* = 9.0 and 3.0 Hz)], 3-hydroxy-3-methylbutyl unit [δ 2.78-2.75 (2H, *m*), 1.72-1.69 (2H, *m*) and 1.25 (6H, *s*)] and a singlet signal of an aromatic proton (δ 6.48). The ¹³C NMR spectrum (Figure 3.43) (Table 58) showed 17 resonances for 18 carbon atoms. The lowest-field aromatic proton (δ 7.57) of the 1,2,4-trisubstituted benzene ring was attributed to H-8 based on its chemical shift and a cross peak between this aromatic proton and a carbonyl carbon (δ 182.17, C-9) in the HMBC spectrum (Figure 3.46) (Table 58). Consequently, other aromatic protons at δ 7.41 and 7.33 were assigned to H-5 and H-6, respectively. The ³*J* correlation between H-5 and an oxyaromatic carbon (δ 155.52, C-7) revealed the presence of a hydroxyl group at C-7. The chelated hydroxy proton (1-OH) caused cross peaks with two aromatic carbons at δ 112.96 (C-2) and 103.89 (C-9a) while the methylene protons (δ 2.78-2.75, H-11) of 3-hydroxy-3-methylbutyl unit gave cross peaks with the two oxyaromatic carbons [δ 162.18, C-1 and δ 165.15, C-3] and an aromatic carbon (δ 112.96, C-2), indicating that a hydroxyl group and 3-hydroxy-3-methylbutyl unit were substituted at C-3 and C-2, respectively. The remaining aromatic proton (δ 6.48) was then located at C-4. Therefore, **TR15** was assigned as 1,3,7-trihydroxy-2-(3-hydroxy-3-methylbutyl)xanthone (**6**) which was previously isolated from *Kielmeyera coriacea* (Garcia cortex, *et al.*, 1998).



(6)

Table 58 The NMR data of compound TR15 in $(\text{CD}_3)_2\text{C}=\text{O}$

Position	TR15		HMBC correlation	TR 15 (reported data)	
	δ_{H} (mult., J_{Hz})	δ_{C} (C-Type)		δ_{H} (mult., $J_{\text{Hz}})^{\text{a}}$	δ_{C} (C-Type) ^b
1-OH	13.26 (s)	162.18 (C)	C-1, C-2, C-9a	13.26 (s)	159.45 (C)
2		112.96 (C)			110.61 (C)
3-OH		165.15 (C)		9.00 (brs)	162.70 (C)
4	6.48 (s)	94.55 (CH)	C-2, C-3, C-4a, C-9a	6.51 (s)	92.93 (CH)
4a		157.50 (C)			155.04 (C)
5	7.41 (d, 9.0)	120.16 (CH)	C-6, C-7, C-8a, C-10a	7.42 (d, 8.6)	117.72 (CH)
6	7.33 (dd, 9.0 and 3.0)	125.52 (CH)	C-7, C-8, C-10a	7.33 (dd, 9.0 and 2.8)	123.31 (CH)
7-OH		155.52 (C)		9.00 (brs)	152.94 (C)
8	7.57 (d, 3.0)	109.83 (CH)	C-6, C-7, C-9, C-10a	7.59 (d, 3.0)	108.14 (CH)
8a		122.44 (C)			120.24 (C)
9		182.17 (C=O)			179.69 (C=O)
9a		103.89 (C)			101.83 (C)
10a		151.40 (C)			148.90 (C)
11	2.78-2.75 (m)	17.77 (CH ₂)	C-1, C-2, C-3, C-12, C-13	2.78 (m)	16.92 (CH ₂)
12	1.72-1.69 (m)	43.22 (CH ₂)	C-2, C-11, C-13, C-14, C-15	1.71 (m)	42.06 (CH ₂)
13-OH		70.85 (C)			69.83 (C)
14,15	1.25 (s)	30.36 (CH ₃)	C-12, C-13, C-14, C-15	1.26 (s)	29.14 (CH ₃)

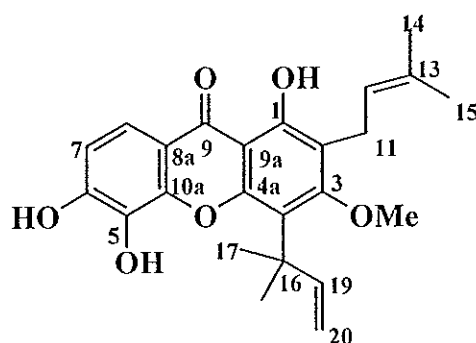
^a ¹H NMR data of 1,3,7-trihydroxy-2-(3-hydroxy-3-methylbutyl)xanthone in $(\text{CD}_3)_2\text{C}=\text{O}$.

^b ¹³C NMR data of 1,3,7-trihydroxy-2-(3-hydroxy-3-methylbutyl)xanthone in $\text{CDCl}_3/\text{DMSO}-d_6$.

3.7 Compound TR19

Compound TR19 was isolated as a pale yellow solid, melting at 102.5-103.8 °C. Its UV (Figure 3.47) and IR (Figure 3.48) spectra indicated the presence of a hydroxylated xanthone skeleton. The mass spectrum (Figure 3.55) showed the molecular ion peak at m/z 410 for the formula $C_{24}H_{26}O_6$. The 1H NMR spectrum (Figure 3.49) (Table 59) consisted of one hydrogen-bonded hydroxyl signal [δ 13.35 (1H, *s*)], two *ortho*-coupled aromatic signals [δ 7.73 and 6.79 (1H each, *d*, $J = 9.0$ Hz)], one methoxy proton signal [δ 3.78 (3H, *s*)] and characteristic signals of a 1,1-dimethylallyl group [δ 6.64 (1H, *dd*, $J = 18.0$ and 10.5 Hz), δ 5.25 (1H, *dd*, $J = 18.0$ and 1.0 Hz), δ 5.05 (1H, *dd*, $J = 10.5$ and 1.0 Hz) and 1.67 (6H, *s*)]. Signals of an isoprenyl unit [δ 5.30 (1H, *mt*, $J = 6.0$ Hz), 3.42 (2H, *d*, $J = 6.0$ Hz), 1.80 and 1.71 (each 3H, *s*)] were also observed. The appearance of the chelated hydroxy proton at δ 13.35 suggested that the hydroxyl group was located at a *peri* position to a carbonyl group. According to their splitting pattern and chemical shift's value, the *ortho* coupled aromatic protons (δ 7.73 and 6.79) were attributed to H-8 and H-7, respectively. The position of deshielded aromatic proton, H-8, was supported by the correlation between H-8 and C-6 (δ 149.22), C-9 (δ 181.28) and C-10a (δ 144.78) and H-7 to C-5 (δ 130.89), C-6 (δ 149.22) and C-8a (δ 113.79). These results also indicated that C-5 and C-6 were substituted by hydroxyl groups. The location of the isoprenyl unit was assigned to be at C-2 (δ 118.38) by the correlation between H-11 (δ 3.42) and C-1 (δ 160.03), C-2 and C-3 (δ 164.42) in the HMBC spectrum (Figure 3.54) (Table 59). In addition, the enhancement of the signal of vinylic methyl protons, Me-14 (δ 1.71), upon irradiation at δ 5.30 [olefinic proton (H-12)] in the NOE spectrum (Figure 3.52), indicated that these methyl protons were *cis* to the olefinic proton. The linkage of the methoxyl group at C-3 was established by a 3J correlation between the methoxy protons and C-3. Thus, the remaining 1,1-dimethylallyl group was assigned to be at C-4 based on the correlation between the *gem*-

dimethyl protons, Me-17 and Me-18 (δ 1.67), and C-4 (δ 118.64). Therefore, **TR19** was assigned as 1,5,6-trihydroxy-3-methoxy-2-(3-methyl-2-butenyl)-4-(1,1-dimethylallyl)xanthone (**7**), a new tetraoxygenated xanthone.



(7)

Table 59 The NMR data of compound **TR19** in CDCl_3

Position	δ_{H} (mult., J_{Hz})	δ_{C} (C-Type)	HMBC correlation
1-OH	13.35 (s)	160.03 (C)	C-1, C-2, C-9a
2		118.38 (C)	
3		164.42 (C)	
3-OCH ₃	3.78 (s)	62.69 (OCH ₃)	C-3
4		118.64 (C)	
4a		152.73 (C)	
5-OH		130.89 (C)	
6-OH		149.22 (C)	
7	6.97 (d, 9.0)	112.85 (CH)	C-5, C-6, C-8a
8	7.73 (d, 9.0)	117.81 (CH)	C-6, C-9, C-10a
8a		113.79 (C)	
9		181.28 (C=O)	
9a		105.62 (C)	
10a		144.78 (C)	
11	3.42 (d, 6.0)	22.90 (CH ₂)	C-1, C-2, C-3, C-12, C-13
12	5.30 (mt, 6.0)	122.54 (CH)	C-11, C-14, C-15
13		132.22 (C)	

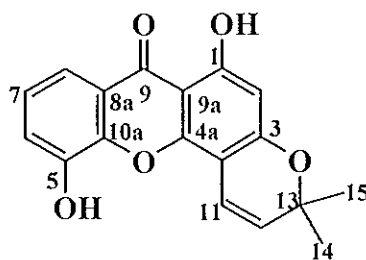
Table 59 (Continued)

Position	δ_{H} (mult., J_{Hz})	δ_{C} (C-Type)	HMBC correlation
14	1.71 (<i>s</i>)	25.72 (CH ₃)	C-12, C-13
15	1.80 (<i>s</i>)	18.01 (CH ₃)	C-12, C-13
16		41.96 (C)	
17,18	1.67 (<i>s</i>)	28.74 (CH ₃)	C-4, C-16, C-17, C-18, C-19
19	6.64 (<i>dd</i> , 18.0 and 10.5)	156.79 (CH)	C-4, C-16, C-17, C-18
20	5.25 (<i>dd</i> , 18.0 and 1.0)	104.27 (CH ₂)	C-16, C-19
	5.05 (<i>dd</i> , 10.5 and 1.0)		

3.8 Compound TR10

Compound TR 10 was isolated as yellow crystals, melting at 236.2-237.7 °C. The xanthone chromophore was evident by its UV absorption bands (Figure 3.56) at λ_{max} 252, 270, 310 and 330 nm and the pyrone carbonyl stretching frequency was found in the region of 1649 cm⁻¹ in the IR spectrum (Figure 3.57). The ¹H NMR spectrum (Figure 3.58) (Table 60) showed characteristic peaks of a 1,2,3-trisubstituted benzene ring [δ 7.83 and 7.37 (1H each, *dd*, $J = 8.0$ and 2.0 Hz) and 7.31 (1H, *t*, $J = 8.0$ Hz)] and a dimethylchromene ring [δ 6.82 (H, *dd*, $J = 10.0$ and 0.5 Hz), 5.70 (1H, *d*, $J = 10.0$ Hz) and 1.53 (6H, *s*)] in addition to a chelated hydroxy proton [δ 13.02 (1-OH, *s*)]. One remaining proton-singlet at δ 6.35 was attributed to an aromatic proton. The ¹³C NMR spectrum (Figure 3.59) (Table 60) showed 17 resonances for 18 carbon atoms. The lowest-field aromatic proton (δ 7.83) of the 1,2,3-trisubstituted benzene ring gave cross peaks with a methine aromatic carbon (δ 120.41, C-6), a carbonyl carbon (δ 180.75, C-9) and an *O*-linked carbon (δ 144.22, C-10a), indicating that this aromatic proton was located at a *peri*-position (C-8) to a carbonyl group. Two other aromatic protons at δ 7.37

and 7.31 were then attributed to H-6 and H-7, respectively. The aromatic protons, H-6 and H-7, gave cross peaks, in the HMBC spectrum (Figure 3.62) (Table 60), with oxygenated aromatic carbons (δ 144.22, C-10a and δ 144.36, C-5), respectively. These indicated that the C-5 position was substituted by a hydroxyl group. The chelated hydroxy proton caused a cross peak with the methine aromatic carbon at δ 99.89 which correlated to the aromatic proton, H-2 (δ 6.35) in the HMQC spectrum (Figure 3.61). This aromatic proton and one of olefinic protons of the dimethylchromene ring at δ 5.70 (H-12) showed correlation with the same quaternary carbon (δ 101.06, C-4) while the other olefinic proton (δ 6.82, H-11) showed a cross peak with an oxyaromatic carbon (δ 161.07, C-3). These data suggested that the dimethylchromene ring formed an ether linkage with C-3. TR10 was then identified as 6-deoxyjacareubin (8) which was previously isolated from *Pentapthalangium solomonse* Warb. (Owen, P.J. and Scheinamann, F. 1974).



(8)

Table 60 The NMR data of compound TR10 in CDCl_3

Position	TR10		HMBC correlation	6-deoxyisojacareubin
	δ_{H} (mult., J_{Hz})	δ_{C} (C-Type)		δ_{H} (mult., $J_{\text{Hz}})^*$
1-OH	13.02 (s)	163.50(C)	C-1, C-2, C-9a	12.95 (s)
2	6.35 (d, 0.5)	99.89 (CH)	C-1, C-3, C-4, C-9a	6.08 (s)
3		161.07 (C)		
4		101.06 (C)		
4a		151.04 (C)		3.58 (br)

Table 60 (Continued)

Position	TR10		HMBC correlation	6-deoxyisojacareubin
	δ_{H} (mult., J_{Hz})	δ_{C} (C-Type)		δ_{H} (mult., $J_{\text{Hz}})^*$
5-OH		144.36 (C)		
6	7.37 (<i>dd</i> , 8.0 and 2.0)	120.41 (CH)	C-8, C-10a	7.20 (<i>m</i>)
7	7.31 (<i>t</i> , 8.0)	124.24 (CH)	C-5, C-8a	7.20 (<i>m</i>)
8	7.83 (<i>dd</i> , 8.0 and 2.0)	117.25 (CH)	C-6, C-9, C-10a	7.57 (<i>q</i>)
8a		121.29 (C)		
9		180.75 (C=O)		
9a		103.65 (C)		
10a		144.22 (C)		
11	6.82 (<i>dd</i> , 10.0 and 0.5)	114.63 (CH)	C-3, C-4, C-4a, C-13	6.94 (<i>d</i>)
12	5.70 (<i>d</i> , 10.0)	127.78 (CH)	C-4, C-13, C-14, C-15	5.65 (<i>d</i>)
13		78.34 (C)		
14,15	1.53 (<i>s</i>)	28.29 (CH ₃)	C-12, C-13, C-14, C-15	1.42 (<i>s</i>)

* ¹H NMR data of 6-deoxyisojacareubin in (CD₃)₂C=O.

3.9 Compound TR6

Compound **TR6** was obtained as yellow crystals, melting at 235.9-236.5 °C. Its UV spectrum (**Figure 3.63**) (λ_{max} 230, 276 and 328 nm) showed the presence of a xanthone nucleus. Its IR spectrum (**Figure 3.64**) showed absorption bands at 3346 (OH) and 1644 (α , β -unsaturated C=O) cm⁻¹. Its ¹H NMR spectrum (**Figure 3.65**) (**Table 61**) showed characteristic signals for a chelated hydroxy proton (δ 12.92, 1-OH), an aromatic proton (δ 6.27, *d*, J = 0.5 Hz, H-2) and a dimethylchromene protons [δ 6.83 (*dd*, J = 10.0 and 0.5 Hz, H-11), δ 5.61 (*d*, J = 10.0 Hz, H-12) and two methyl groups (δ 1.48, *s*, Me-14, 15)]. These signals were similar to those of **TR10**. The

location of the dimethylchromene ring was established by HMBC data (Figure 3.69) (Table 61) which showed two cross peaks: H-11/C-3 (δ 160.92) and H-12/C-4 (δ 100.93), to have the same arrangement as found in TR10. In addition, the typical signals of a 1,2,4-trisubstituted benzene ring [δ 7.60 (1H, *d*, $J = 3.0$ Hz, H-8), 7.39 (1H, *d*, $J = 8.5$ Hz, H-5) and 7.28 (1H, *dd*, $J = 8.5$ and 3.0 Hz)] were observed. The ^{13}C NMR spectrum (Figure 3.66) (Table 61) showed 17 signals for 18 carbon atoms. The lowest-field aromatic proton (δ 7.60) of the 1,2,4-trisubstituted benzene ring was assigned to H-8 by the value of chemical shift and confirmed by a HMBC cross peak between H-8 and a carbonyl carbon (δ 180.46, C-9). Consequently, other aromatic protons at δ 7.39 and 7.28 were assigned to H-5 and H-6, respectively. The 3J correlation between H-5 and an oxyaromatic carbon (C-7, δ 152.06) established the substituent at C-7 to be a hydroxyl group. TR6 was therefore assigned as 1,7-dihydroxy-6',6'-dimethylpyrano(2',3':3,4)xanthone (9), a new naturally occurring xanthone. However, the synthesis of TR6 was previously reported (Clarke, *et al.*, 1974).

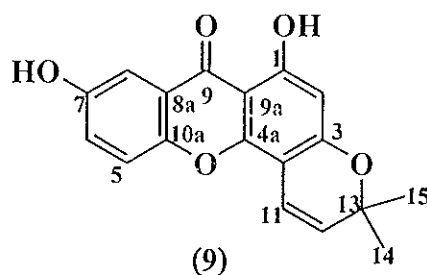


Table 61 The NMR data of compound TR6 in CDCl_3

Position	δ_{H} (<i>mult.</i> , J_{Hz})	δ_{C} (C-Type)	HMBC correlation
1-OH	12.92 (<i>s</i>)	163.01 (C)	C-1, C-2, C-9a
2	6.27 (<i>d</i> , 0.5)	99.20 (CH)	C-1, C-3, C-4, C-9a
3		160.92 (C)	
4		100.93 (C)	

Table 61 (Continued)

Position	δ_{H} (mult., J_{Hz})	δ_{C} (C-Type)	HMBC correlation
4a		151.90 (C)	
5	7.39 (<i>d</i> , 8.5)	119.09 (CH)	C-7, C-8a, C-10a
6	7.28 (<i>dd</i> , 8.5 and 3.0)	123.84 (CH)	C-7, C-10a
7-OH		152.06 (C)	
8	7.60 (<i>d</i> , 3.0)	109.30 (CH)	C-6, C-9, C-10a
8a		121.05 (C)	
9		180.46 (C=O)	
9a		103.47 (C)	
10a		150.30 (C)	
11	6.83 (<i>dd</i> , 10.0 and 0.5)	114.98 (CH)	C-3, C-4a, C-13
12	5.61 (<i>d</i> , 10.0)	127.04 (CH)	C-4, C-13, C-14, C-15
13		78.25 (C)	
14,15	1.48 (<i>s</i>)	28.29 (CH ₃)	C-12, C-13, C-14, C-15

3.10 Compound TR18

Compound TR18 was isolated as yellow crystals, melting at 223.8-225.5 °C. The IR spectrum (Figure 3.71) suggested the presence of hydroxyl (3387 cm⁻¹) and conjugated carbonyl (1629 cm⁻¹) groups. The UV spectrum (Figure 3.70) (λ_{max} 222, 264 and 316 nm) suggested a chromenoxanthone chromophore (Ishiguro, *et al.*, 1993). Compound TR18 showed the similar ¹H NMR characteristic signals of the 1-hydroxy-6',6'-dimethylpyrano(2',3':3,4)xanthone moiety to those found in TR6. The HMBC correlation (Figure 3.76) (Table 62) between the *cis*-olefinic protons of chromene ring and C-3 and C-4 of the xanthone skeleton confirmed the location of the chromene ring.

One additional chelated hydroxy proton (δ 11.26), one non-chelated hydroxy proton (δ 5.01) and two sets of doublet signal of two *ortho*-aromatic protons (δ 7.24 and 6.71) were also observed. The additional chelated hydroxyl group was definitely substituted at C-8 of the xanthone skeleton. The chelated hydroxy proton (8-OH) caused 3J cross peaks with two quaternary carbons at δ 110.36 (C-7) and 107.70 (C-8a). The HMQC spectrum (Figure 3.75) revealed that the carbon at δ 110.36 carried the aromatic methine proton (δ 6.71), which was then attributed to H-7. Furthermore, the HMBC correlation between H-7 and an oxygenated aromatic carbon at δ 135.54 (C-5) established the substituent at C-5 to be a hydroxyl group. This hydroxy proton (δ 5.01) also showed cross peaks with C-5, C-6 (δ 123.56) and C-10a (δ 142.80). TR18 was then identified as morusignin C (10) which was isolated from *Morus insignis* (Hano, *et al.*, 1990).

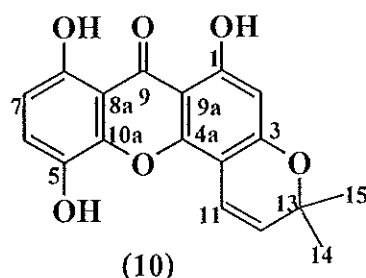


Table 62 The NMR data of compound TR18 in CDCl_3

Position	TR18		HMBC correlation	morusignin C	
	δ_{H} (mult., J_{Hz})	δ_{C} (C-Type)		δ_{H} (mult., J_{Hz}^*)	δ_{C} (C-Type)*
1-OH	12.14 (s)	162.79 (C)	C-1, C-2, C-9a	12.10 (s)	162.5 (C)
2	6.29 (s)	100.06 (CH)	C-1, C-3, C-4, C-9a	6.19 (d, 0.7)	100.0 (CH)
3		161.70 (C)			161.8 (C)
4		101.60 (C)			103.2 (C)
4a		151.07 (C)			154.3 (C)
5-OH	5.01 (brs)	135.54 (C)	C-5, C-6, C-10a		138.1 (C)
6	7.24 (d, 8.5)	123.56 (CH)	C-5, C-8, C-10a	7.32 (d, 9.0)	125.5 (CH)

Table 62 (Continued)

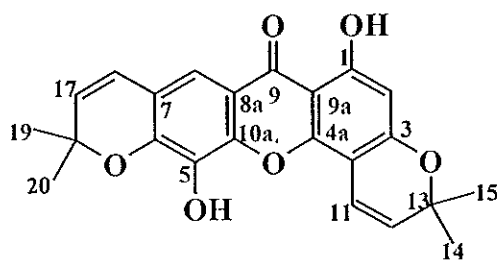
Position	TR18		HMBC correlation	morusignin C	
	δ_{H} (mult., J_{Hz})	δ_{C} (C-Type)		δ_{H} (mult., J_{Hz}^*)	δ_{C} (C-Type)*
7	6.71 (<i>d</i> , 8.5)	110.36 (CH)	C-5, C-8a	6.65 (<i>d</i> , 9.0)	110.8 (CH)
8-OH	11.26 (<i>s</i>)	154.10 (C)	C-7, C-8, C-8a	11.17 (<i>s</i>)	152.7 (C)
8a		107.70 (C)			108.4 (C)
9		174.03 (C=O)			185.9 (C=O)
9a		102.30 (C)			102.4 (C)
10a		142.80 (C)			144.6 (C)
11	6.75 (<i>d</i> , 10.0)	114.36 (CH)	C-3, C-4a, C-13	7.01 (<i>dd</i> , 10.0 and 0.7)	115.5 (CH)
12	5.66 (<i>d</i> , 10.0)	127.97 (CH)	C-4, C-13	5.78 (<i>d</i> , 10.0)	128.2 (CH)
13		78.59 (C)			79.2 (C)
14,15	1.50 (<i>s</i>)	28.30 (CH ₃)	C-12, C-13, C-14, C-15	1.49 (<i>s</i>)	28.5 (CH ₃)

* ¹H and ¹³C NMR data of morusignin C in (CD₃)₂C=O.

3.11 Compound TR17

Compound TR17 was obtained as yellow crystals, melting at 249.8-250.7 °C. It contained xanthone chromophore according to its UV (Figure 3.77) absorption bands at λ_{max} 280 and 334 nm. In addition, the pyrone carbonyl stretching frequency was found in the region of 1712 cm⁻¹ in the IR spectrum (Figure 3.78). Its ¹H NMR spectrum (Figure 3.79) (Table 63) was similar to that of TR10. Direct comparison of their ¹H NMR spectra revealed that two aromatic protons of the 1,2,3-trisubstituted benzene ring of TR10 was replaced, in TR17, by 2,2-dimethylchromene ring of which the signal of *gem*-dimethyl protons resonated as a singlet at δ 1.54 and two doublet signals of two *cis*-olefinic protons (H-16 and H-17) appeared at δ 6.46 and 5.75. These

olefinic protons, H-16 and H-17, showed strong cross peaks with C-6, 8 (δ 144.72 and 113.47) and C-7 (δ 117.79), respectively. The methine aromatic carbon at δ 113.47 (C-8) also correlated to the lowest-field aromatic proton at δ 7.49 in the HMQC spectrum (Figure 3.82). These confirmed that two aromatic protons (H-6 and H-7) of the 1,2,3-trisubstituted benzene ring in the structure of TR10 was replaced by the 2,2-dimethylchromene ring which fused in a linear fashion to the xanthone nucleus. The HMBC correlation (Figure 3.83) (Table 63) between C-3/H-11 and C-4/H/12 established the linkage of the other chromene ring at C-3 and C-4, as found in TR10. TR17 was then identified as rheediaxanthone A (11) which was previously isolated from *Rheedia benthamiana* (Delle Monache, *et al.*, 1981)



(11)

Table 63 The NMR data of compound TR17 in CDCl_3

Position	TR17		HMBC correlation	rheediaxanthone A	
	δ_{H} (mult., J_{Hz})	δ_{C} (C-Type)		δ_{H} (mult., $J_{\text{Hz}})^*$	δ_{C} (C-Type)*
1-OH	13.09 (s)	163.08 (C)	C-1, C-2, C-9a	13.15 (s)	166.5 (C)
2	6.27 (s)	99.37 (CH)	C-1, C-3, C-4, C-9a	6.15 (s)	98.1 (CH)
3		160.52 (C)			162.1 (C)
4		101.36 (C)			100.6 (C)
4a		151.57 (C)			159.5 (C)
5-OH	5.52 (s)	132.38 (C)	C-5, C-6, C-10a		133.0 (C)
6		144.72 (C)			150.9 (C)
7		117.79 (C)			118.2 (C)

Table 63 (Continued)

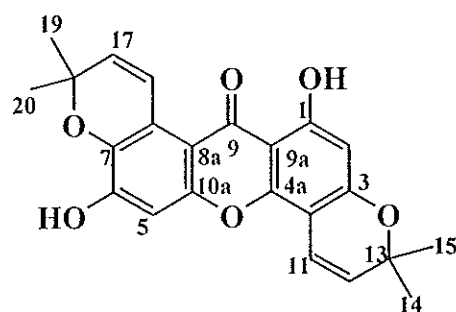
Position	TR17		HMBC correlation	rheediaxanthone A	
	δ_{H} (mult., J_{Hz})	δ_{C} (C-Type)		δ_{H} (mult., $J_{\text{Hz}})^*$	δ_{C} (C-Type)*
8	7.49 (s)	113.47 (CH)	C-6, C-9, C-10a, C-16	7.37 (s)	120.9 (CH)
8a		114.13 (C)			113.4 (C)
9		180.30 (C=O)			179.5 (C=O)
9a		103.24 (C)			102.2 (C)
10a		145.02 (C)			145.8 (C)
11	6.90 (d, 10.0)	115.16 (CH)	C-3, C-4a, C-13	6.90 (d, 10.0)	111.8 (CH)
12	5.62 (d, 10.0)	127.13 (CH)	C-4, C-13	5.62 (d, 10.0)	131.0 (CH)
13		78.19 (C)			77.3 (C)
14,15	1.49 (s)	28.45 (CH ₃)	C-12, C-13	1.49 (s)	27.7 (CH ₃)
16	6.46 (d, 9.5)	121.42 (CH)	C-6, C-7, C-8, C-18	6.46 (d, 9.5)	114.8 (CH)
17	5.75 (d, 9.5)	131.01 (CH)	C-7, C-18	5.75 (d, 9.5)	126.5 (CH)
18		78.97 (C)			77.6 (C)
19,20	1.54 (s)	28.27 (CH ₃)	C-17, C-18	1.54 (s)	27.7 (CH ₃)

* ¹H and ¹³C NMR data of rheediaxanthone A in (CD₃)₂C=O.

3.12 Compound TR16

Compound TR16 was obtained as yellow crystals, melting at 215.9-217.1 °C, Its UV spectrum (Figure 3.84) (λ_{max} 216, 268, 298 and 330 nm) showed the presence of a xanthone nucleus. Its IR spectrum (Figure 3.85) showed absorption bands at 3394 (OH) and 1638 (α, β -unsaturated C=O) cm⁻¹. The ¹H (Figure 3.86) (Table 64) and ¹³C (Figure 3.87) (Table 64) NMR spectra were similar to those of TR17, containing typical signals of a chelated hydroxyl group (δ 13.42, 1-OH), two chromene rings [$\{\delta$ 8.02 (d, J =10.5 Hz, 1H), 5.84 (d, J =10.5 Hz, 1H) and 1.50 (6H, s)] and $\{\delta$ 6.78 (d, J

=10.0 Hz, 1H), 5.58 (*d*, $J=10.0$ Hz, 1H) and 1.47 (6H, *s*)] and two aromatic protons (δ 6.87 and 6.22, 1H each, *s*). One of the chromene ring contained a lower-field *cis* olefinic proton (δ 8.02, H-16), suggesting that this olefinic proton was located in the deshielding zone of a carbonyl group (Marques, *et al.*, 2000). The *cis*-olefinic protons, H-16 and H-17, showed two cross peaks: H-16/C-7 (δ 136.88) and H-17/C-8 (δ 119.76), indicating that the chromene ring formed an ether linkage with C-7, not C-8. A singlet signal at δ 6.87 was attributed to H-5 of an aromatic proton, due to its cross peaks in the HMBC spectrum (Figure 3.90) (Table 64) with quaternary carbons at 152.90 (C-10a), 150.91 (C-6), 136.88 (C-7) and 108.48 (C-8a). Therefore, C-6 was substituted by a hydroxyl group. In addition, C-3/H-11 and C-4/H-12 correlation confirmed the attachment of the other chromene ring to be at the same position as found in TR17. TR16 was then identified as brasilixanthone A (12) which was isolated from *Tovomita brasiliensis* (Marques, *et al.*, 2000).



(12)

Table 64 The NMR data of compound TR16 in CDCl_3

Position	TR16		HMBC correlation	brasilixanthone A	
	δ_{H} (<i>mult.</i> , J_{Hz})	δ_{C} (C-Type)		δ_{H} (<i>mult.</i> , J_{Hz})*	δ_{C} (C-Type)*
1-OH	13.42 (<i>s</i>)	163.10 (C)	C-1, C-2, C-9a	13.40 (<i>s</i>)	163.30 (C)
2	6.22 (<i>s</i>)	99.05 (CH)	C-1, C-3, C-4, C-9a	6.20 (<i>s</i>)	99.26 (CH)

Table 64 (Continued)

Position	TR16		HMBC correlation	brasilixanthone A	
	δ_{H} (mult., J_{Hz})	δ_{C} (C-Type)		δ_{H} (mult., $J_{\text{Hz}})^*$	δ_{C} (C-Type)*
3		159.97 (C)			160.17 (C)
4		100.38 (C)			100.59 (C)
4a		151.91 (C)			151.38 (C)
5	6.87 (<i>s</i>)	102.30 (CH)	C-6, C-7, C-8a, C-9, C-10a	6.83 (<i>s</i>)	102.52 (CH)
6-OH		150.91 (C)			151.15 (C)
7		136.88 (C)			137.12 (C)
8		119.76 (C)			119.97 (C)
8a		108.48 (C)			108.65 (C)
9		182.48 (C=O)			180.64 (C=O)
9a		103.83 (C)			104.03 (C)
10a		152.90 (C)			153.08 (C)
11	6.78 (<i>d</i> , 10.0)	115.05 (CH)	C-3, C-4a, C-13	6.76 (<i>d</i> , 10.0)	115.28 (CH)
12	5.58 (<i>d</i> , 10.0)	126.80 (CH)	C-4, C-13	5.57 (<i>d</i> , 10.0)	126.98 (CH)
13		77.98 (C)			78.19 (C)
14,15	1.47 (<i>s</i>)	28.22 (CH ₃)	C-12, C-13, C-14, C-15	1.47 (<i>s</i>)	28.46 (CH ₃)
16	8.02 (<i>d</i> , 10.5)	120.86 (CH)	C-7, C-18	7.99 (<i>d</i> , 10.5)	121.08 (CH)
17	5.84 (<i>d</i> , 10.5)	132.41 (CH)	C-8, C-18	5.82 (<i>d</i> , 10.5)	132.58 (CH)
18		77.00 (C)			77.23 (C)
19,20	1.50 (<i>s</i>)	27.32 (CH ₃)	C-17, C-18, C-19, C-20	1.49 (<i>s</i>)	27.53 (CH ₃)

* ¹H and ¹³C NMR data of brasilixanthone A in CDCl₃.

3.13 Compound TR12

Compound **TR12** was obtained as yellow crystals, melting at 216.5-218.1 °C. Its UV (Figure 3.91) and IR (Figure 3.92) spectra indicated the presence of a hydroxylated xanthone skeleton. The ^1H NMR spectrum (Figure 3.93) (Table 65) was similar to that of **TR16**. Comparison of the ^1H NMR spectra revealed that the signals of 2,2-dimethylchromene ring of **TR16** at the right-handed side were replaced, in **TR12**, by two aromatic protons (δ 7.52 and 6.85). These aromatic protons were part of 1,2,3-trisubstituted benzene ring [δ 6.75 and 6.85 (1H each, *dd*, $J = 8.0$ and 1.0 Hz) and 7.52 (1H, *t*, $J = 8.0$ Hz)]. The chelated OH proton (δ 13.10) caused cross peaks with carbons at δ 161.89 (C-1), 110.10 (C-2) and 109.00 (C-9a). As C-2 correlated, in the HMQC spectrum (Figure 3.96), with the aromatic proton at δ 6.75, the remaining protons (δ 6.85 and 7.52) were then attributed to H-4 and H-5, respectively, due to their splitting pattern. In addition, the location of the chromene ring with an ether linkage at C-7 was established by HMBC data (Figure 3.97) (Table 65), which showed two cross peaks: H-11/C-7 (δ 136.97) and H-12/C-8 (δ 119.69). Therefore, **TR12** was assigned as 1,6-dihydroxy-6',6'-dimethylpyrano(2',3':7,8)xanthone, known as tovoxanthone (**13**) which was previously isolated from *Tovomita choisyana*, (Gabriel, S.J. and Gottlieb, O.R., 1972).

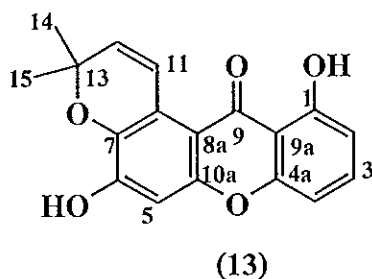


Table 65 The NMR data of compound TR12 in CDCl₃

Position	TR12		HMBC correlation	tovoxanthone
	δ_{H} (mult., J_{Hz})	δ_{C} (C-Type)		δ_{H} (mult., $J_{\text{Hz}})$ *
1-OH	13.10 (<i>s</i>)	161.89 (C)	C-1, C-2, C-9a	13.10 (<i>s</i>)
2	6.75 (<i>dd</i> , 8.0 and 1.0)	110.10 (CH)	C-1, C-4, C-9a	6.67 (<i>dd</i> , 8.0 and 1.5)
3	7.52 (<i>t</i> , 8.0)	135.76 (CH)	C-1	7.45 (<i>t</i> , 8.0)
4	6.85 (<i>dd</i> , 8.0 and 1.0)	106.28 (CH)	C-2, C-4a, C-9a	6.77 (<i>dd</i> , 8.0 and 1.5)
4a		155.68 (C)		
5	6.88 (<i>s</i>)	102.36 (CH)	C-7, C-8a, C-10a	6.80 (<i>s</i>)
6-OH	6.30 (<i>brs</i>)	151.55 (C)	C-4a, C-7	
7		136.97 (C)		
8		119.69 (C)		
8a		108.77 (C)		
9		183.63 (C=O)		
9a		109.00 (C)		
10a		153.45 (C)		
11	8.02 (<i>d</i> , 10.0)	120.81 (CH)	C-7, C-8a, C-13	7.95 (<i>d</i> , 10.0)
12	5.86 (<i>d</i> , 10.0)	132.54 (CH)	C-8, C-13	5.78 (<i>d</i> , 10.0)
13		77.10 (C)		
14,15	1.51 (<i>s</i>)	27.33 (CH ₃)	C-11, C-12, C-13, C-14, C-15	1.49 (<i>s</i>)

* ¹H and ¹³C NMR data of tovoxanthone in (CD₃)₂C=O.

3.14 Compound TR7

Compound TR7 was obtained as a yellow gum. Its UV (Figure 3.98) spectrum (λ_{max} 268, 336 and 374 nm) showed the presence of a xanthone nucleus. Its IR spectrum (Figure 3.99) showed absorption bands at 3439 (OH) and 1648 (α, β -unsaturated C=O)

cm⁻¹. **TR7** showed the similar ¹H NMR characteristic signals of 5-hydroxy-6'',6''-dimethylpyrano(2'',3'':7,8)xanthone moiety to those found in **TR17**. The HMBC data (**Figure 3.105**) (**Table 66**) between the *cis*-olefinic protons of the chromene ring and C-7 and C-8 of the xanthone skeleton confirmed the arrangement of the chromene ring with an ether linkage at C-6. Two sharp singlets in aromatic region at δ 7.61 and 6.39 were assigned to the isolated aromatic protons, H-8 and H-4, respectively, according to the correlation between H-4/C-2 (δ 108.42) and C-4a (δ 155.75) and H-8/C-6 (δ 146.40), C-9 (δ 180.09) and C-10a (δ 141.75). The characteristic signals of an isoprenyl side chain were observed in the ¹H NMR spectrum (**Figure 3.100**) (**Table 66**); two singlet signals of *gem*-dimethyl protons (Me-14 and Me-15) at δ 1.85 and 1.78, a doublet signal of benzylic methylene protons (H-11) at δ 3.48 and a broad triplet signal of an olefinic methine proton (H-12) at δ 5.31. One of the *gem*-dimethyl groups (Me-15, δ 1.78) was found to be *cis* to the olefinic proton (H-12), in the NOE spectrum (**Figure 3.103**), due to the enhancement of the signal of these methyl protons after irradiation of the olefinic proton. The HMBC correlation between the methylene protons, H-11 and C-1 (δ 160.28) and C-3 (δ 161.98) indicated that the isoprenyl side chain was located at C-2. Based on their ¹³C chemical shift value, C-1 and C-3 were substituted by hydroxyl groups. Thus, **TR7** was assigned as 1,3,5-trihydroxy-2-(3-methyl-2-butenyl)-6',6'-dimethylpyrano(2',3':6,7)xanthone (latisxanthone D) (**14**) which was previously isolated from *Garcinia latissima* (Ito, *et. al.*, 1997).

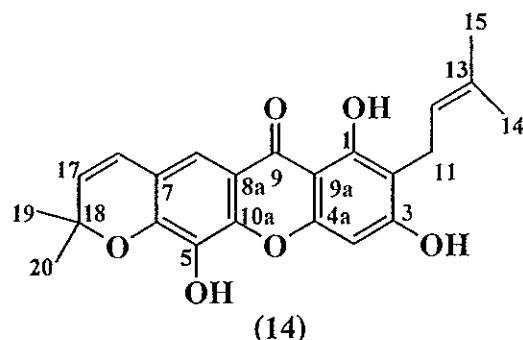


Table 66 The NMR data of compound TR7 in CDCl₃

Position	TR7		HMBC correlation	Latisxanthone D	
	δ_{H} (mult., J_{Hz})	δ_{C} (C-Type)		δ_{H} (mult., $J_{\text{Hz}})^*$	δ_{C} (C-Type)*
1-OH	13.44 (s)	160.28 (C)	C-1, C-2, C-9a	13.32 (s)	160.47 (C)
2		108.42 (C)			108.81 (C)
3-OH		161.98 (C)		6.10 (brs)	162.18 (C)
4	6.39 (s)	93.97 (CH)	C-2, C-3, C-4a, C-9a	6.42 (s)	94.48 (CH)
4a		155.75 (C)			152.96 (C)
5-OH	5.47 (brs)	132.94 (C)	C-7	5.51 (brs)	131.96 (C)
6		146.40 (C)			144.65 (C)
7		109.10 (C)			117.65 (C)
8	7.61 (s)	115.49 (CH)	C-6, C-9, C-10a	7.43 (s)	113.57 (CH)
8a		114.00 (C)			114.65 (C)
9		180.09 (C=O)			180.25 (C=O)
9a		102.50 (C)			103.28 (C)
10a		141.75 (C)			145.11(C)
11	3.48 (d, 7.0)	21.44 (CH ₂)	C-1, C-3, C-12, C-13, C-15	3.40 (d, 7.0)	21.42 (CH ₂)
12	5.31 (mt, 7.0)	121.25 (CH)	C-11, C-14, C-15	5.24 (m)	121.36 (CH)
13		132.94 (C)			136.08(C)
14	1.85 (s)	17.94 (CH ₃)	C-12, C-13, C-15	1.78 (s)	17.90 (CH ₃)
15	1.78 (s)	25.86 (CH ₃)	C-12, C-13, C-14	1.71 (s)	25.82 (CH ₃)
16	6.91 (d, 10.5)	108.77 (CH)	C-6, C-18	6.37 (d, 10.3)	121.18 (CH)
17	5.76 (d, 10.5)	129.78 (CH)	C-7, C-18	5.66 (d, 10.3)	130.93 (CH)
18		79.30 (C)			78.89 (C)
19,20	1.55 (s)	28.25 (CH ₃)	C-17, C-18, C-19, C-20	1.47 (s)	28.46 (CH ₃)

* ¹H and ¹³C NMR data of Latisxanthone D in CDCl₃.

3.15 Compound TR11

Compound **TR11** was obtained as a dark yellow gum. The UV spectrum (**Figure 3.106**) showed maximum absorption bands at λ_{\max} 260, 264 and 322 nm. The IR spectrum (**Figure 3.107**) showed absorption bands of hydroxyl group at 3397 cm^{-1} and conjugate carbonyl group at 1638 cm^{-1} . The ^1H NMR spectrum (**Figure 3.108**) (**Table 67**) showed a sharp singlet signal of a chelated hydroxyl group (1-OH) at δ 13.50 (*s*) and two singlet signals of aromatic protons at δ 7.48 (*s*) and 6.52 (*s*). The deshielding aromatic-proton signal (δ 7.48) was assigned to H-8, according to an anisotropic effect of a carbonyl group. The remaining signals appeared as typical signals of two isoprenyl units. The signals of the first isoprenyl unit consisted of two singlets of *gem*-dimethyl protons, Me-14 and Me-15, at δ 1.63 and 1.76, a broad triplet of an olefinic proton, H-12, at δ 5.27 and a doublet of benzylic methylene protons, H-11, at δ 3.35. The signals of the second isoprenyl unit consisted of two singlets of *gem*-dimethyl protons, Me-19 and Me-20, at δ 1.64 and 1.87, a broad triplet of olefinic proton, H-17, at δ 5.30 and a doublet of benzylic methylene protons, H-16, at δ 3.60. Furthermore, irradiation of both olefinic protons (H-12 and H-17), in the NOE spectrum (**Figure 3.111**), enhanced only signals of vinylic methyl protons, Me-15 (δ 1.63) and Me-19 (δ 1.64), respectively, indicating that olefinic protons, H-12 and H-17, were *cis* to the vinylic methyl protons. The ^{13}C NMR spectra data (**Figure 3.109**) (**Table 67**) deduced from DEPT (**Figure 3.110**) and HMQC (**Figure 3.112**) spectra showed 23 signals for 24 carbon atoms: a carbonyl carbon (δ 180.77), four methyl carbons (δ 25.85, 25.84, 18.05 and 17.86), two methylene carbons (δ 23.06 and 21.92), four methine carbons (δ 123.49, 122.48, 106.42 and 93.87) and twelve quaternary carbons (δ 163.07, 161.18, 156.62, 151.79, 150.68, 143.12, 132.34, 131.36, 116.37, 113.40, 110.90 and 102.99). In the HMBC spectrum (**Figure 3.113**) (**Table 67**), the aromatic proton, H-8, gave cross peaks with the carbonyl carbon (δ 180.77, C-9), and

three oxyquaternary carbon [δ 151.79 (C-10a), 150.68 (C-6) and 143.12 (C-7)], suggesting that C-6 and C-7 were substituted by hydroxyl groups. The methylene protons, H-11, correlated to C-1 (δ 161.18), C-2 (δ 110.90) and C-3 (δ 163.07) whereas the methylene protons, H-16, correlated to C-5, C-6 (δ 150.68 or 151.79) and C-10a. Consequently, two isoprenyl units were located at C-2 and C-5. The remaining high-field aromatic proton (δ 6.52) was attributed to H-4 according to its cross peaks with C-2 (δ 110.90) and C-9a (δ 102.99). These results revealed that TR11 was 1,3,6,7-tetrahydroxy-2,5-bis(3-methyl-2-butenyl)xanthone (15), a new natural occurring xanthone.

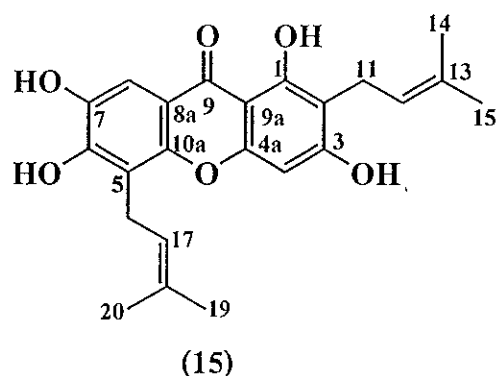


Table 67 The NMR data of compound TR11 in $(\text{CD}_3)_2\text{C}=\text{O}$

Position	δ_{H} (mult., J_{Hz})	δ_{C} (C-Type)	HMBC correlation
1-OH	13.50 (s)	161.18 (C)	C-1, C-2, C-9a
2		110.90 (C)	
3-OH		163.07 (C)	
4	6.52 (s)	93.87 (CH)	C-2, C-3, C-4a, C-9a
4a		156.62 (C)	
5		116.37 (C)	
6-OH		150.68*	
7-OH		143.12 (C)	
8	7.48 (s)	106.42 (CH)	C-6, C-7, C-9, C-10a

Table 67 (Continued)

Position	δ_{H} (mult., J_{Hz})	δ_{C} (C-Type)	HMBC correlation
8a		113.40 (C)	
9		180.77 (C=O)	
9a		102.99 (C)	
10a		151.79(C)*	
11	3.35 (<i>d</i> , 7.5)	21.92 (CH ₂)	C-1, C-2, C-3, C-12, C-13
12	5.27 (<i>mt</i> , 7.5)	123.49 (CH)	C-15
13		136.36 (C)	
14	1.76 (<i>s</i>)	17.86 (CH ₃)	C-12, C-13
15	1.63 (<i>s</i>)	25.84 (CH ₃)	C-12, C-13
16	3.60 (<i>d</i> , 8.0)	23.06 (CH ₂)	C-5, C-6, C-10a, C-17, C-18
17	5.30 (<i>mt</i> , 8.0)	122.48 (CH)	C-19
18		132.34 (C)	
19	1.64 (<i>s</i>)	25.85 (CH ₃)	C-17, C-18
20	1.87 (<i>s</i>)	18.05 (CH ₃)	C-17, C-18

* Interchangeable

3.16 Compound TR3

Compound **TR3** was obtained as yellow crystals, melting at 205.8-207.2 °C. The xanthone chromophore was evident by its UV (Figure 3.114) absorption bands at λ_{max} 228, 262, 334 and 376 nm while the pyrone carbonyl stretching frequency was found in the region of 1644 cm⁻¹ in the IR spectrum (Figure 3.115). Its ¹H NMR spectrum (Figure 3.116) (Table 68) showed characteristic signals for a chelated hydroxyl group (δ 13.38, 1-OH), two aromatic protons (δ 7.63 and 6.45, 1H each, *s*) and typical *cis*-olefinic protons of a chromene ring [δ 6.95 and 5.79 (1H each, *d*, $J = 10.0$ Hz)] and one methyl singlet (δ 1.59, 6H). The spectrum further showed the presence of two

methylene-proton signals as triplets [δ 2.85 and 1.87 (2H each, t , $J = 6.5$ Hz) and two methyl groups as a singlet (δ 1.36), implying the presence of a dimethylchromane ring. In the HMBC spectrum (Figure 3.120) (Table 68), a chelated hydroxy proton at δ 13.38 and a methylene protons (δ 2.85, H-11) of a chromane ring gave cross peak with the same oxyaromatic carbon, (δ 160.17, C-1), while the other methylene protons (δ 1.87, H-12) correlated with a quaternary aromatic carbon, (δ 115.58, C-2). These data indicated that the dimethylchromane ring was fused to C-2 and C-3 (δ 162.08) of xanthone nucleus. The lowest-field aromatic proton (δ 7.63) gave cross peaks with a carbonyl carbon (δ 180.05, C-9) and two *O*-linked carbons at δ 145.68 (C-6) and 141.69 (C-10a), indicating that this aromatic proton was located at a *peri*-position (C-8) to the carbonyl group. The *cis*-olefinic protons of the chromene unit (δ 6.95 and 5.79, H-16 and H-17) showed cross peaks with an oxyaromatic carbon at δ 145.68 (C-6) and a quaternary aromatic carbon at δ 109.13 (C-7), respectively, suggesting that the dimethylchromene ring was fused to C-6 and C-7 of the xanthone nucleus. The remaining aromatic proton (δ 6.45) was then assigned to H-4 due to its cross peaks with C-2, C-3, C-9a (δ 102.80) and C-10a. The remaining carbon signal (δ 146.42) was attributed to C-5 which was definitely substituted by a hydroxyl group. The ^{13}C NMR spectral data (Figure 3.117) (Table 68) deduced from DEPT (Figure 3.118) and HMQC spectra (Figure 3.119) showed 21 signals for 23 carbon atoms. TR3 was then assigned as 1,5-dihydroxy-6',6'-dimethyldihydropyrano(2',3':3,2)-6'',6''-dimethylpyrano(2'',3'':6,7)xanthone (16) which was previously obtained by synthesis (Delle Monache, *et al.*, 1984). Therefore, it was a new naturally occurring xanthone.

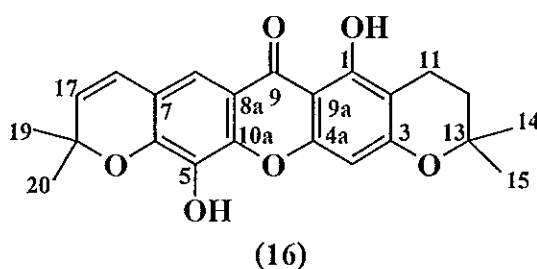


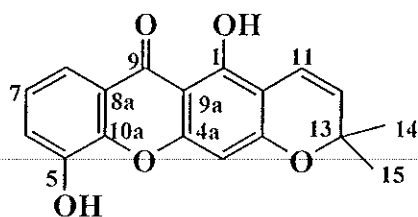
Table 68 The NMR data of compound TR3 in CDCl₃

Position	TR3		HMBC correlation	TR3 (reported data)
	δ_{H} (mult., J_{Hz})	δ_{C} (C-Type)		δ_{H} (mult., $J_{\text{Hz}})$ *
1-OH	13.38 (s)	160.17 (C)	C-1, C-2, C-9a	13.40 (s)
2		111.50 (C)		
3		162.08 (C)		
4	6.45 (s)	94.56 (CH)	C-2, C-3, C-4a, C-9a	6.42 (s)
4a		155.76 (C)		
5-OH		146.42 (C)		
6		145.68 (C)		
7		109.13 (C)		
8	7.63 (s)	108.74 (C)	C-6, C-9, C-10a	7.44 (s)
8a		114.78 (C)		
9		180.05 (C=O)		
9a		102.80 (C)		
10a		141.69 (C)		
11	2.85 (t, 6.5)	16.04 (CH ₂)	C-1, C-2, C-3, C-12, C-13	2.70 (t, 6.0)
12	1.87 (t, 6.5)	41.10 (CH ₂)	C-2, C-11, C-13, C-14, C-15	1.89 (t, 6.0)
13		72.66 (C)		
14,15	1.36 (s)	29.27 (CH ₃)	C-11, C-12, C-13, C-14, C-15	1.38 (s)
16	6.95 (d, 10.0)	115.58 (CH)	C-6, C-18	6.58 (d, 10.0)
17	5.79 (d, 10.0)	129.72 (CH)	C-7, C-18	5.90 (d, 10.0)
18		79.24 (C)		
19,20	1.59 (s)	28.27 (CH ₃)	C-16, C-17, C-18, C-19, C-20	1.49 (s)

* ¹H NMR data of 1,5-dihydroxy-6',6'-dimethyldihydropyrano(2',3':3,2)-6'',6''-dimethylpyrano-(2'',3'':6,7)xanthone in (CD₃)₂C=O

3.17 Compound TR9

Compound **TR9**, obtained as yellow crystals, melting at 207.0-209.0 °C. Its UV (Figure 3.121) and IR (Figure 3.122) spectral data suggested the presence of a xanthone skeleton. The ¹H NMR spectrum (Figure 3.123) (Table 69) exhibited a singlet signal of a chelated hydroxyl group at δ 13.08 which was attributed to 1-OH. It gave cross peaks with C-1 (δ 157.94), C-2 (δ 105.02) and C-9a (δ 103.54). This hydroxy proton and one of olefinic protons of the dimethylchromene ring at δ 5.62 (H-12) showed correlation with the same quaternary carbon (δ 105.02, C-2) while the other olefinic proton (δ 6.75, H-11) showed a cross peak with an oxyaromatic carbon (δ 160.89, C-3). These suggested that the dimethylchromene ring formed an ether linkage with C-3, not C-2. A singlet signal of aromatic proton, δ 6.39, was then assigned for the signal of H-4 according to its correlation to C-2, C-3, C-4a (δ 156.23) and C-9a in the HMBC experiment (Figure 3.127) (Table 69). Three aromatic protons at δ 7.78 and 7.33 (1H each, *dd*, J = 8.0 and 1.5 Hz) and 7.26 (1H, *t*, J = 8.0 Hz) were then proposed for H-8, H-6 and H-7, respectively. The most deshielded-aromatic proton signal was assigned for H-8 according to an anisotropic effect of a carbonyl group. The assignment of these aromatic protons was supported by the ³ J correlation between H-8 and C-6 (δ 120.11), C-9 (δ 180.73) and C-10a (δ 144.12); H-7 and C-5 (δ 144.25) and C-8a (δ 121.10) and H-6 and C-8 (δ 116.90) and C-10a, in HMBC experiment. The ¹³C NMR spectrum (Figure 3.124) (Table 69) showed 17 signals for 18 carbon atoms. Therefore, **TR9** was assigned as 1,5-dihydroxy-6',6'dimethylpyrano(2',3':3,2)xanthone (17). Its spectral data and melting point were in agreement with those of 6-deoxyjacareubin (Burkhardt, *et al.*, 1992).



(17)

Table 69 The NMR data of compound TR9 in CDCl_3

Position	TR9		HMBC correlation	6-deoxyjacareubin
	δ_{H} (mult., J_{Hz})	δ_{C} (C-Type)		δ_{H} (mult., $J_{\text{Hz}})^*$
1-OH	13.08 (s)	157.94 (C)	C-1, C-2, C-9a	13.34 (s)
2		105.02 (C)		
3		160.89 (C)		
4	6.39 (s)	94.95 (CH)	C-2, C-3, C-4a, C-9a	6.40 (s)
4a		156.23 (C)		
5-OH		144.25 (C)		
6	7.33 (dd, 8.0 and 1.5)	120.11 (CH)	C-8, C-10a	7.36 (dd, 7.9 and 1.6)
7	7.26 (t, 8.0)	124.09 (CH)	C-5, C-8a	7.29 (t, 7.9)
8	7.78 (dd, 8.0 and 1.5)	116.90 (CH)	C-6, C-9, C-10a	7.67 (dd, 7.9 and 1.6)
8a		121.10 (C)		
9		180.73 (C=O)		
9a		103.54 (C)		
10a		144.12 (C)		
11	6.75 (d, 10.0)	115.30 (CH)	C-3, C-13	6.70 (d, 10.0)
12	5.63 (d, 10.0)	127.75 (CH)	C-2, C-13	5.77 (d, 10.0)
13		78.48 (C)		
14,15	1.48 (s)	28.41 (CH_3)	C-12, C-13, C-14, C-15	1.48 (s)

* ^1H NMR data of 6-deoxyjacareubin in $(\text{CD}_3)_2\text{C}=\text{O}$.

3.18 Compound TR5

Compound TR5 was obtained as yellow crystals, melting at 220.1-222.5 °C. The UV spectrum (Figure 3.128) showed absorption bands at λ_{\max} 252, 338 and 384 nm. The IR spectrum (Figure 3.129) showed absorption bands of hydroxyl group at 3409 cm^{-1} and conjugated carbonyl group at 1642 cm^{-1} . The ^1H NMR spectrum (Figure 3.130) (Table 70) showed a sharp singlet of a chelated hydroxy proton (1-OH) at δ 12.85, a broad singlet signal of a free hydroxy proton at δ 5.52, an aromatic proton (δ 7.63, *s*) and typical *cis*-olefinic protons of a chromene ring [δ 6.94 and 5.78 (1H each, *d*, $J = 10.0$ Hz)] and one methyl singlet (δ 1.56)], in addition to the presence of a 1,2,3-trisubstituted-benzene signals [δ 7.54 (1H, *t*, $J = 8.5$ Hz), 6.91 and 6.74 (1H each, *dd*, $J = 8.5$ and 0.5 Hz)]. The ^{13}C NMR spectrum (Figure 3.131) (Table 70) showed 17 signals for 18 carbon atoms, indicating that there were two equivalent carbons. In the HMBC data (Figure 3.135) (Table 70), the chelated hydroxy proton (1-OH) caused a cross peak with the aromatic methine carbon at δ 110.25 which correlated to an aromatic proton at δ 6.78 of 1,2,3-trisubstituted benzene ring in the HMQC spectrum (Figure 3.134) (Table 70). These results indicated that aromatic proton (δ 6.78) was located at C-2 position. Two aromatic protons at δ 7.54 and 6.91 were then attributed to H-3 and H-4, respectively. These were supported by cross peaks between H-3/C-1 (δ 161.80) and C-4a (δ 156.12) and H-4/C-2 and C-9a (δ 108.51). The deshielded-aromatic proton at δ 7.63 was assigned to H-8 due to an anisotropic effect of a carbonyl group. Its cross peaks with three oxyaromatic carbons [(δ 146.90, C-7), (δ 146.45, C-6) and (δ 142.00, C-10a)] and a carbonyl carbon (δ 181.27, C-9) confirmed the assigned position. Moreover, irradiation of the hydroxy proton at δ 5.52, in the NOE spectrum (Figure 3.133), affected H-8, indicating the presence of a hydroxyl group at C-7. The linkage of the chromene ring at C-5 (δ 109.24) and C-6 with an ether linkage at C-6

was established by HMBC data which showed two cross peaks: H-11 (δ 6.94)/C-6 and H-12 (δ 5.78)/C-5. Therefore, TR5 was determined as 1,7-dihydroxy-6',6'-dimethylpyrano(2',3':6,5)xanthone (18), a new trioxygenated xanthone.

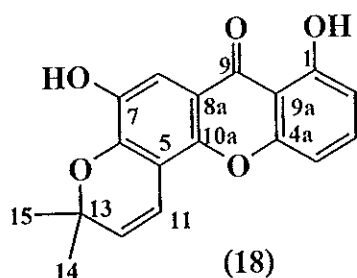


Table 70 The NMR data of compound TR5 in CDCl_3

Position	δ_{H} (mult., J_{Hz})	δ_{C} (C-Type)	HMBC correlation
1-OH	12.85 (s)	161.80 (C)	C-1, C-2, C-9a
2	6.78 (dd, 8.5 and 0.5)	110.25 (CH)	C-1, C-4, C-9a
3	7.54 (t, 8.5)	135.89 (CH)	C-1, C-4a, C-9a
4	6.91 (dd, 8.5 and 0.5)	106.68 (CH)	C-2, C-4a, C-9a
4a		156.12 (C)	
5		109.24 (C)	
6		146.45 (C)	
7-OH	5.52 (brs)	146.90 (C)	
8	7.63 (s)	108.72 (CH)	C-6, C-7, C-9, C-10a
8a		114.10 (C)	
9		181.27 (C=O)	
9a		108.51 (C)	
10a		142.07 (C)	
11	6.94 (d, 10.0)	115.40 (CH)	C-6, C-13
12	5.78 (d, 10.0)	129.88 (CH)	C-5, C-13, C-14, C-15
13		79.54 (C)	
14,15	1.56 (s)	28.30 (CH ₃)	C-11, C-12, C-13, C-14, C-15

3.19 Compound TR13

Compound **TR13** was obtained as a yellow solid, melting at 241.7-243.5 °C. The UV spectrum (**Figure 3.136**) (λ_{\max} 222 and 346) showed the presence of a xanthone chromophore. Its IR spectrum (**Figure 3.137**) showed absorption bands at 3424 (OH) and 1646 (α, β -unsaturated C=O) cm^{-1} . The ^1H NMR spectrum (**Figure 3.138**) (**Table 71**) was similar to that of **TR5**. Comparison of their ^1H NMR spectra revealed that **TR13** contained two unit of chromene rings. This implied that two aromatic protons (δ 7.54 and 6.73) of a 1, 2, 3-trisubstituted benzene ring of **TR5** was replaced, in **TR13**, by a dimethylchromene ring of which the signal of *gem*-dimethyl protons resonated as a singlet at δ 1.47 and two doublet signals of two *cis*-olefinic protons (H-16 and H-17) at δ 6.75 and 5.59. In the HMBC spectrum (**Figure 3.142**) (**Table 71**), the *cis*-olefinic protons (δ 6.75 and 5.59) showed strong cross peaks with C-3 (δ 160.08) and C-2 (δ 104.53), respectively, indicating the arrangement of the chromene ring at C-2 and C-3 with an ether linkage at C-3. The linkage of the other chromene ring at C-5 (δ 109.16) and C-6 (δ 145.74 or 146.33), as found in **TR5**, was established by HMBC correlation between C-5/H-17 and C-6/H-16. The ^{13}C NMR spectrum (**Figure 3.139**) (**Table 71**) appeared 21 signals for 23 carbon atoms. The structure of **TR13** was then elucidated as 1,7-dihydroxy-6',6'-dimethylpyrano(2',3':3,2)-6'',6''-dimethylpyrano(2'',3'':6,5)xanthone (**19**), a new naturally occurring xanthone.

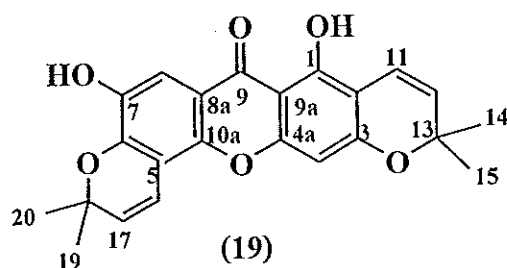


Table 71 The NMR data of compound TR13 in CDCl₃

Position	δ_{H} (mult., J_{H_2})	δ_{C} (C-Type)	HMBC correlation
1-OH	13.34 (s)	157.55 (C)	C-1, C-2, C-9a
2		104.53 (C)	
3		160.08 (C)	
4	6.33 (s)	94.77 (CH)	C-2, C-3, C-4a, C-9a
4a		156.86 (C)	
5		109.16 (C)	
6		145.74 (C)*	
7-OH	5.50 (brs)	141.85 (C)	C-6, C-7, C-8
8	7.58 (s)	108.69 (CH)	C-6, C-8a, C-9, C-10a
8a		113.99 (C)	
9		180.02 (C=O)	
9a		103.21 (C)	
10a		146.33 (C)*	
11	6.75 (d, 10.0)	115.56 (CH)	C-1, C-2, C-3, C-13
12	5.59 (d, 10.0)	127.36 (CH)	C-2, C-12, C-13, C-14, C-15
13		78.05 (C)	
14,15	1.47 (s)	28.31 (CH ₃)	C-12, C-13, C-14, C-15
16	6.88 (d, 10.0)	115.42 (CH)	C-5, C-6, C10a, C-18
17	5.75 (d, 10.0)	129.87 (CH)	C-5, C-18, C-19, C-20
18		79.30 (C)	
19,20	1.55 (s)	28.24 (CH ₃)	C-17, C-18, C-19, C-20

* Interchangeable

3.20 Compound TR20

Compound **TR20** was isolated as a colorless gum. The UV spectrum (Figure 3.143) (λ_{\max} 227, 253, 260, 274 and 328) showed the presence of a conjugated chromophore. Its IR spectrum (Figure 3.144) showed absorption bands at 1645, 1586 (C=C) and 1154 (C-O) cm^{-1} . The ^1H NMR spectrum (Figure 3.145) (Table 72) showed typical signals of a chromene ring [δ 6.62, 5.47 (1H each, *d*, $J = 10.0$ Hz, H-7, 8) and two methyl groups (δ 1.42, 6-H, *s*, Me-10, 11)], an aromatic proton at δ 5.97 (H-5) and a methoxyl group at δ 4.04 (3-H, *s*). In the HMBC spectrum (Figure 3.149) (Table 72), the *cis*-olefinic protons, H-7 and H-8, showed strong cross peaks with C-3 (δ 160.60) and C-4 (δ 102.80), respectively, indicating that C-3 and C-4 positions were substituted by a chromene ring. The aromatic proton, H-5, gave cross peaks with C-1 (δ 93.50), C-3 (δ 160.60), C-4 (δ 102.80) and C-6 (δ 160.60) while the methoxy protons gave a cross peak with a quaternary aromatic carbon at δ 169.72 (C-2). No NOE enhancement was observed after irradiation of the methoxy protons, suggesting that **TR20** was 6',6'-dimethylpyrano(2',3':3,4)xanthone with the methoxyl group and an oxysubstituent at C-2 and C-6, respectively. Since the aromatic carbon, C-1, appeared at much higher field, δ 93.50, it was not substituted by any oxygen substituents. These results suggested that **TR20** was a symmetrical molecule, two possible structures (**20** and **21**) were proposed. However the biphenyl structure (**21**) was excluded due to the absence of an absorption band of a hydroxyl group in the IR spectrum. Therefore, **TR20** was proposed to have a dibenzofuran structure (**20**), a new naturally occurring dibenzofuran.

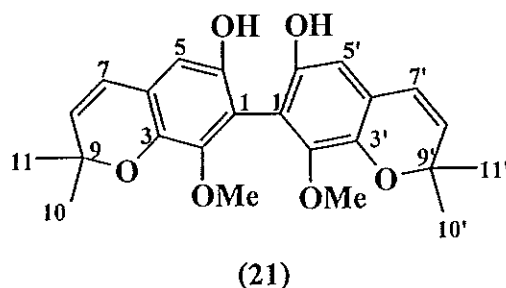
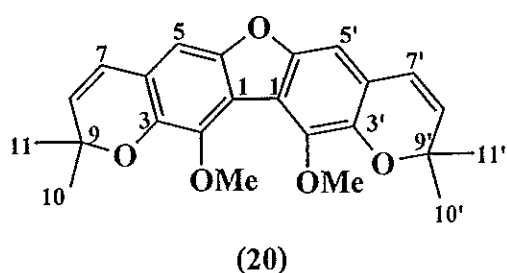


Table 72 The NMR data of compound TR20 in CDCl₃

Position	δ_{H} (<i>mult.</i> , J_{Hz})	δ_{C} (C-Type)	HMBC correlation
1, 1'		93.50 (C)	
2, 2'		169.78 (C)	
2, 2'-OMe	4.04 (<i>s</i>)	52.50 (OCH ₃)	C-2, 2'
3, 3'		160.60 (C)	
4, 4'		102.80 (C)	
5, 5'	5.97 (<i>s</i>)	96.75 (CH)	C-1, 1', C-3, 3', C-4, 4', C-6, 6'
6, 6'		160.60 (C)	
7, 7'	6.62 (<i>d</i> , 10.0)	115.91 (CH)	C-3, 3', C-9, 9'
8, 8'	5.47 (<i>d</i> , 10.0)	125.91 (CH)	C-4, 4', C-9, 9'
9, 9'		77.74 (C)	
10, 10', 11, 11'	1.42 (<i>s</i>)	28.29 (CH ₃)	C-7, 7', C-8, 8', C-9, 9', C-10, 10', 11, 11'

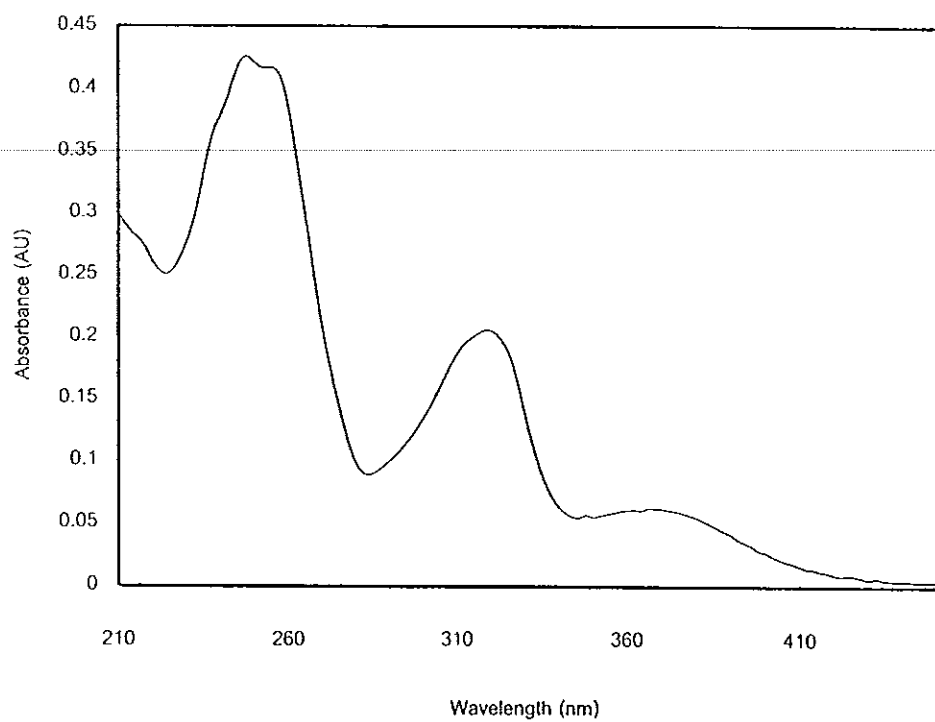


Figure 3.1 UV (MeOH) spectrum of TR4

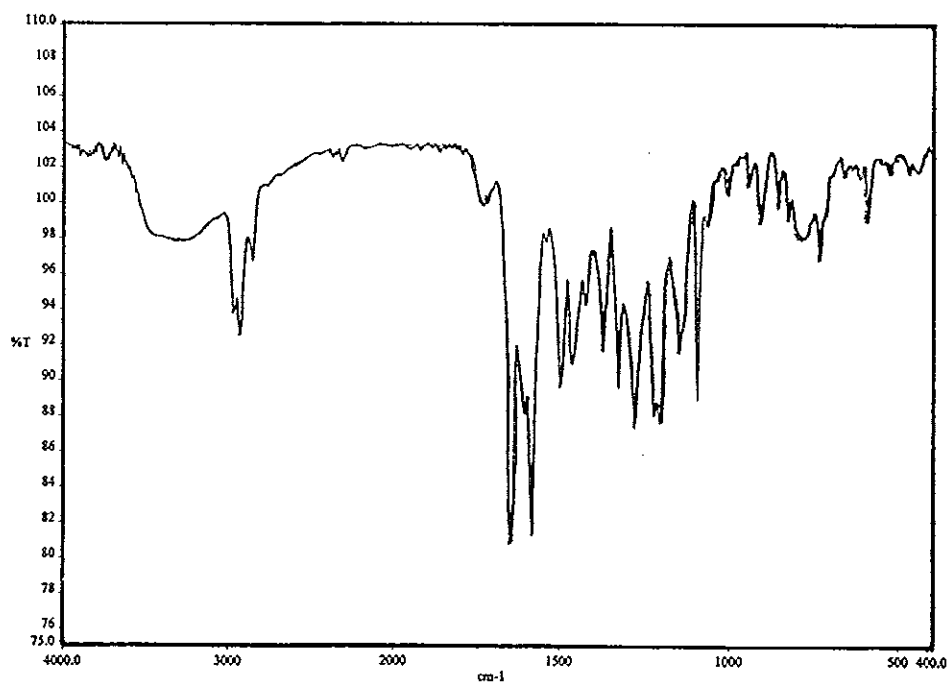


Figure 3.2 FT-IR (neat) spectrum of TR4

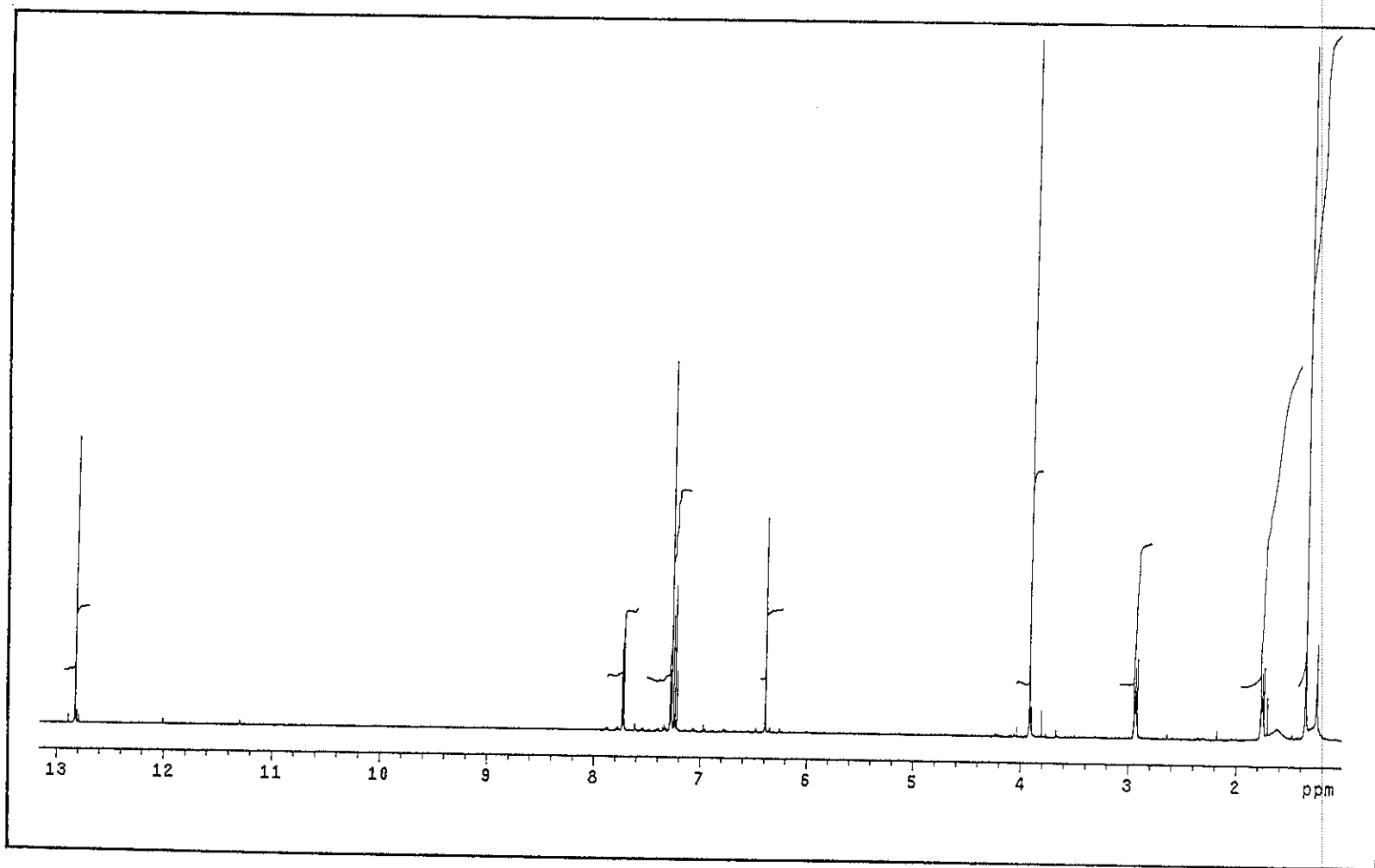


Figure 3.3 ^1H NMR (500 MHz)(CDCl_3) spectrum of TR4

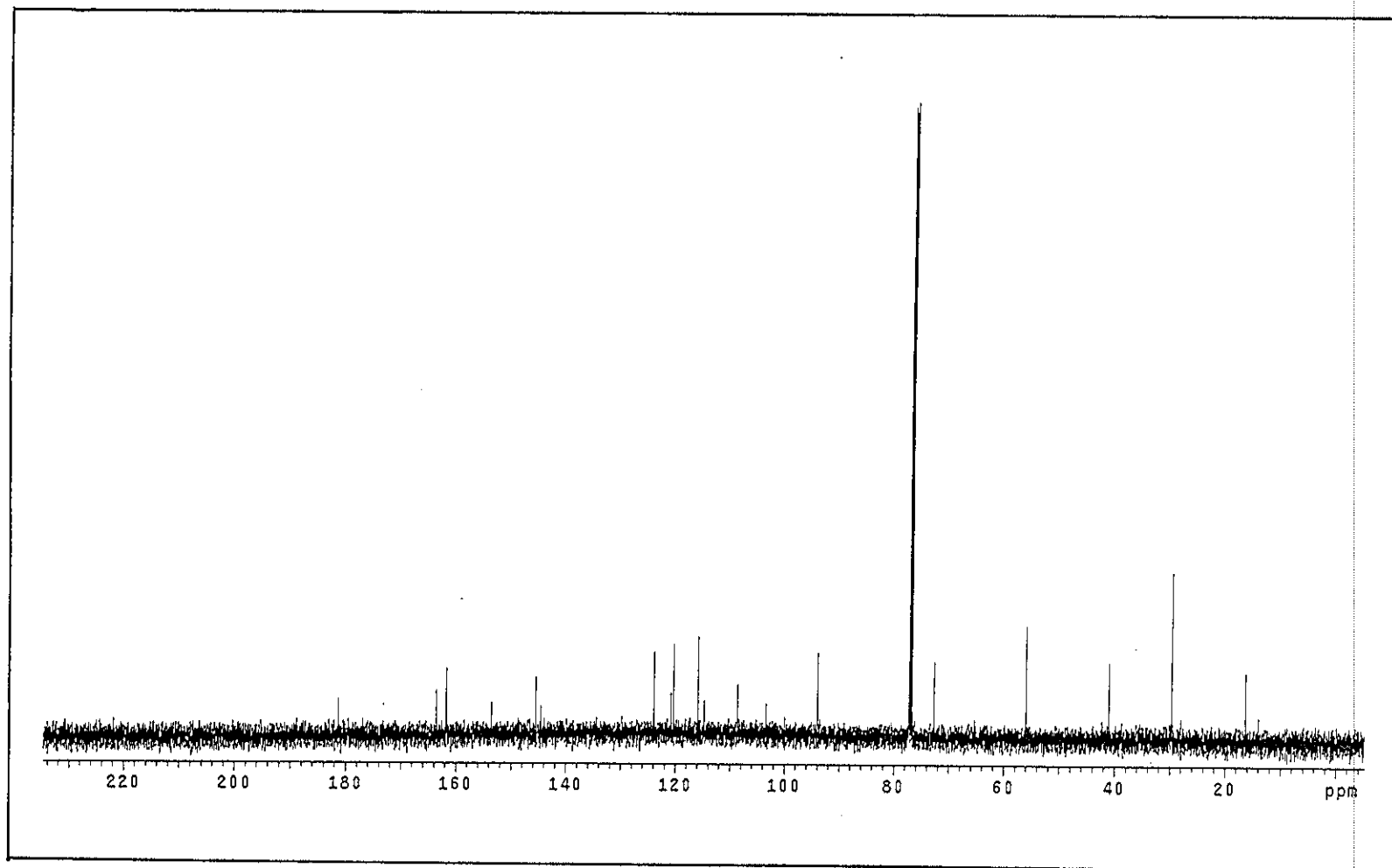


Figure 3.4 ^{13}C NMR (125 MHz)(CDCl_3) spectrum of TR4

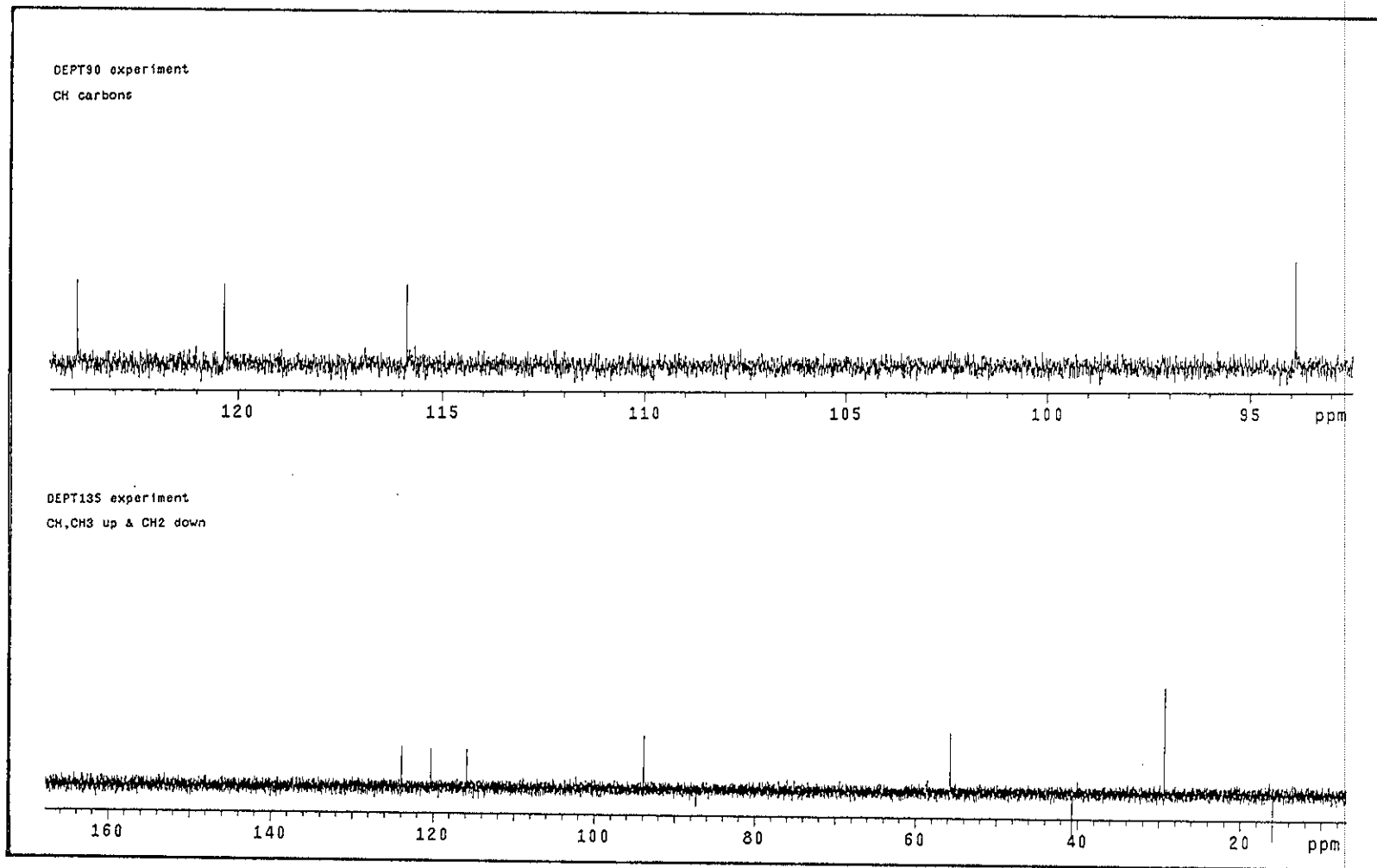


Figure 3.5 DEPT spectrum of TR4

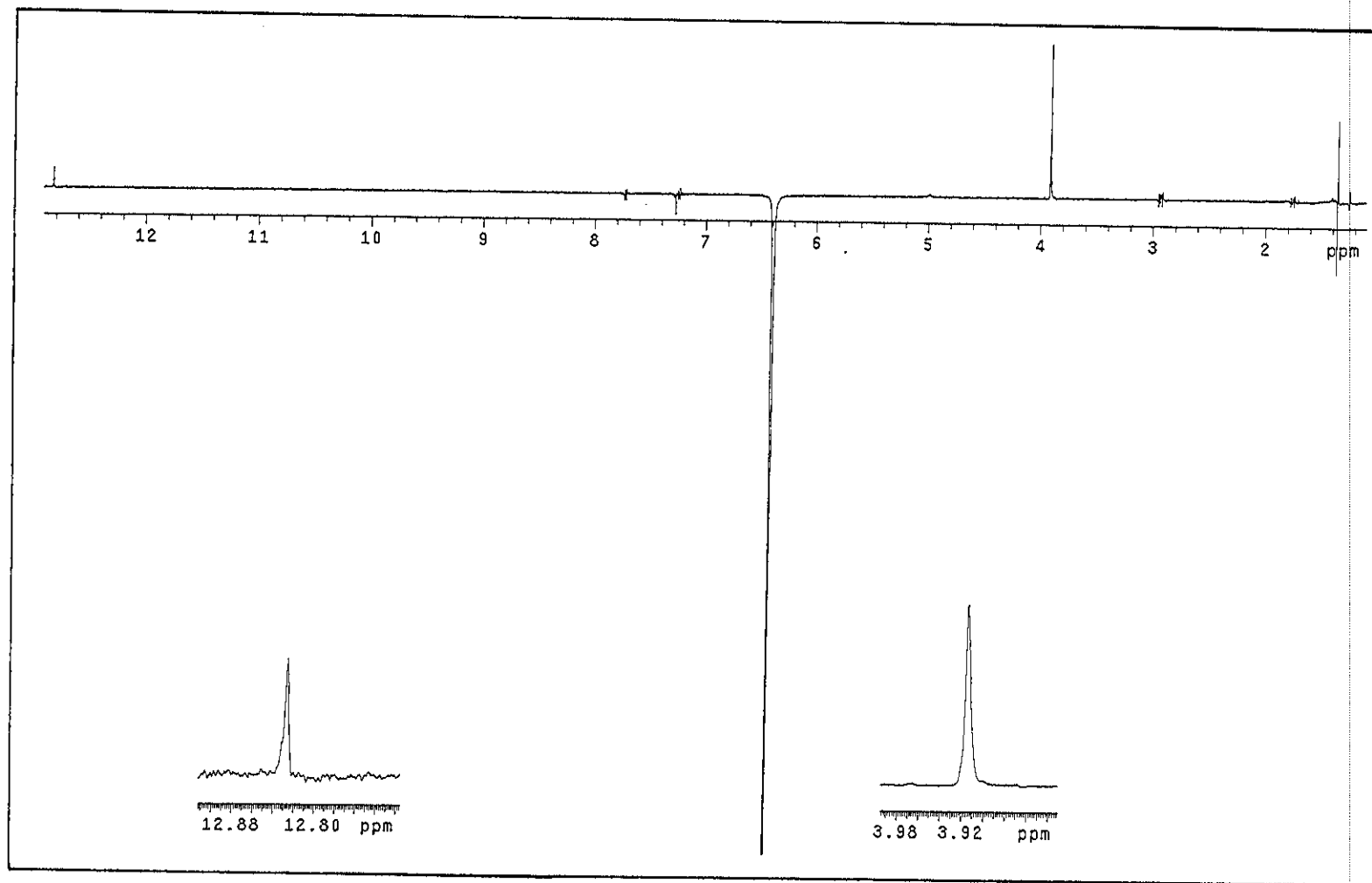


Figure 3.6 NOEDIFF spectrum of TR4 after irradiation at δ_H 6.39

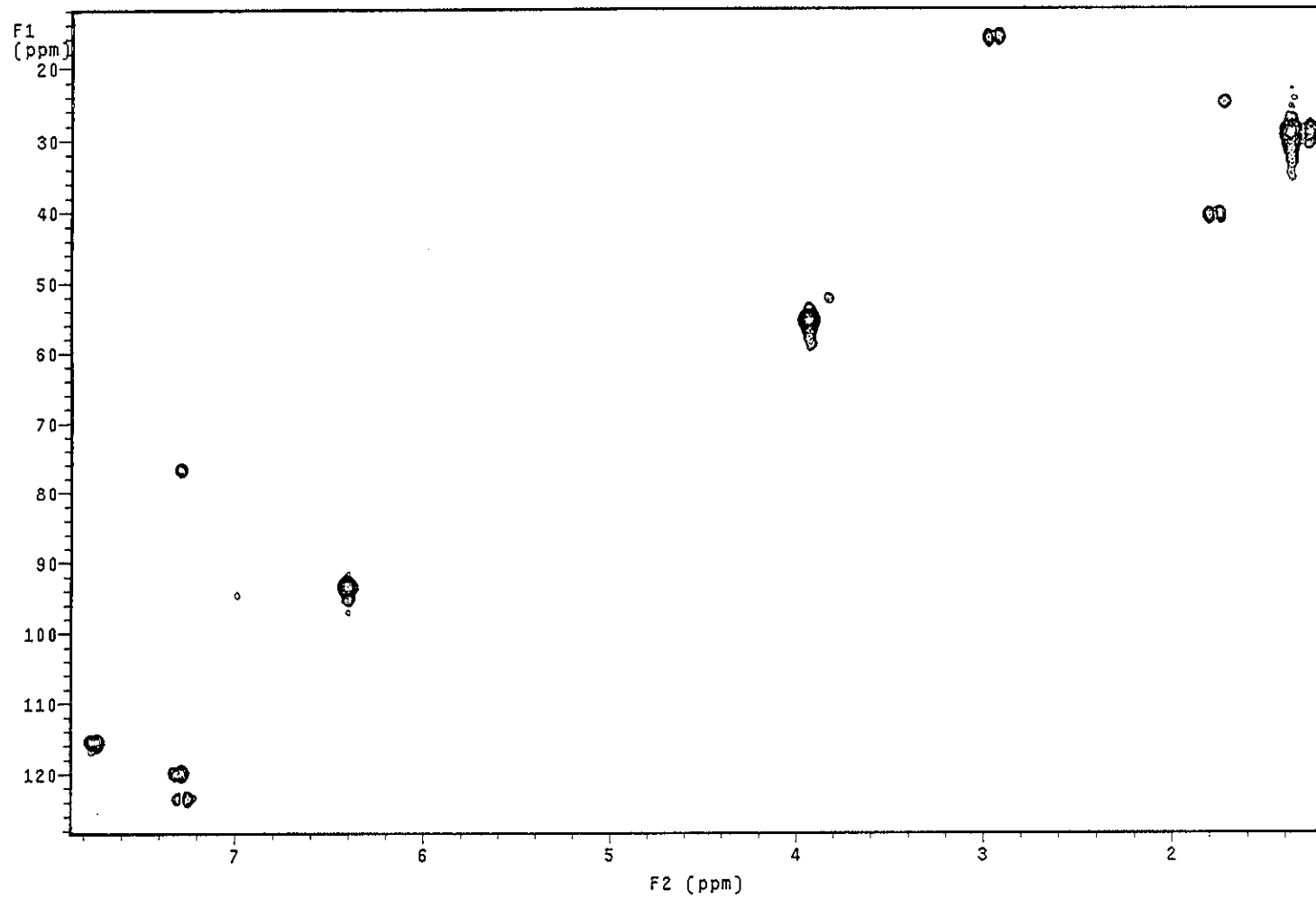


Figure 3.7 2D HMQC spectrum of TR4

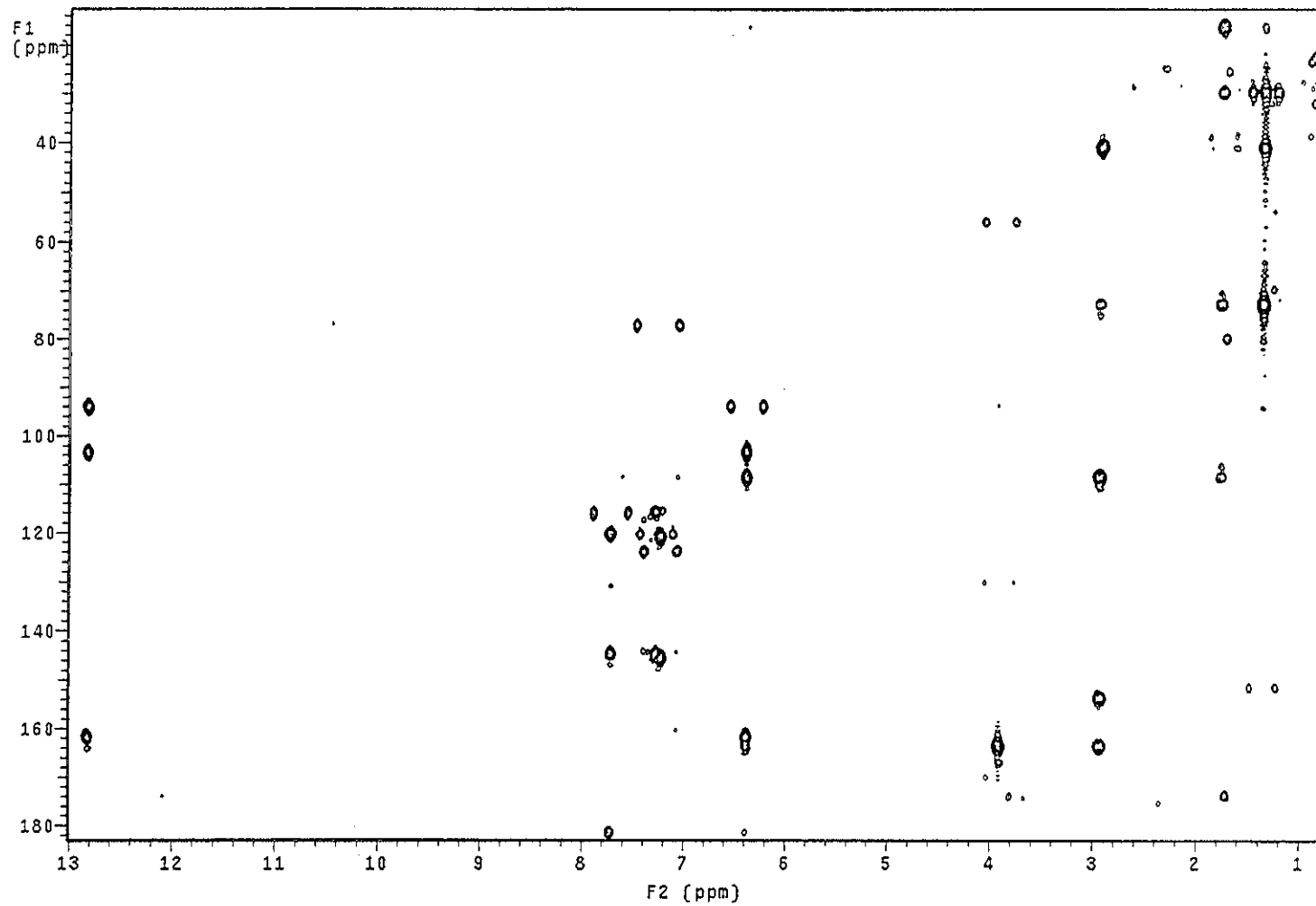


Figure 3.8 2D HMBC spectrum of TR4

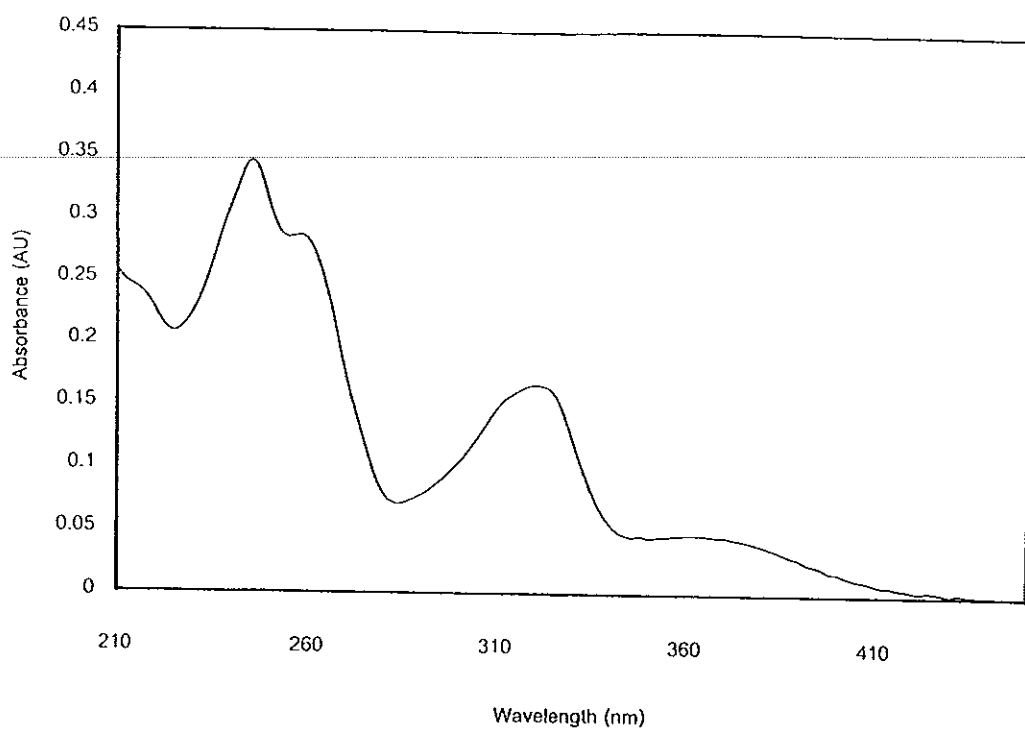


Figure 3.9 UV (MeOH) spectrum of TR2

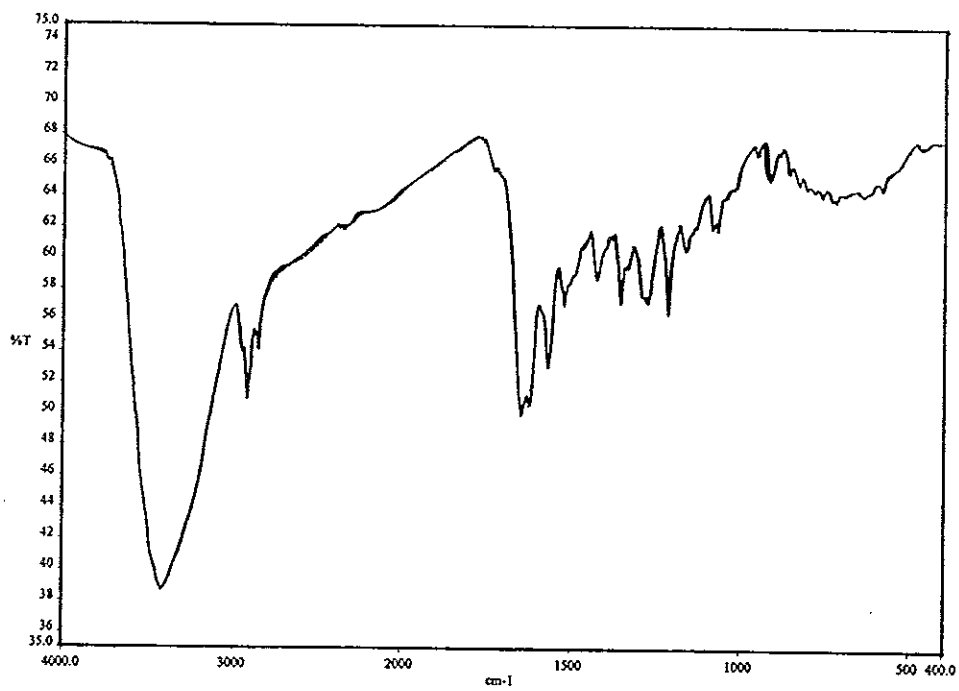


Figure 3.10 FT-IR (neat) spectrum of TR2

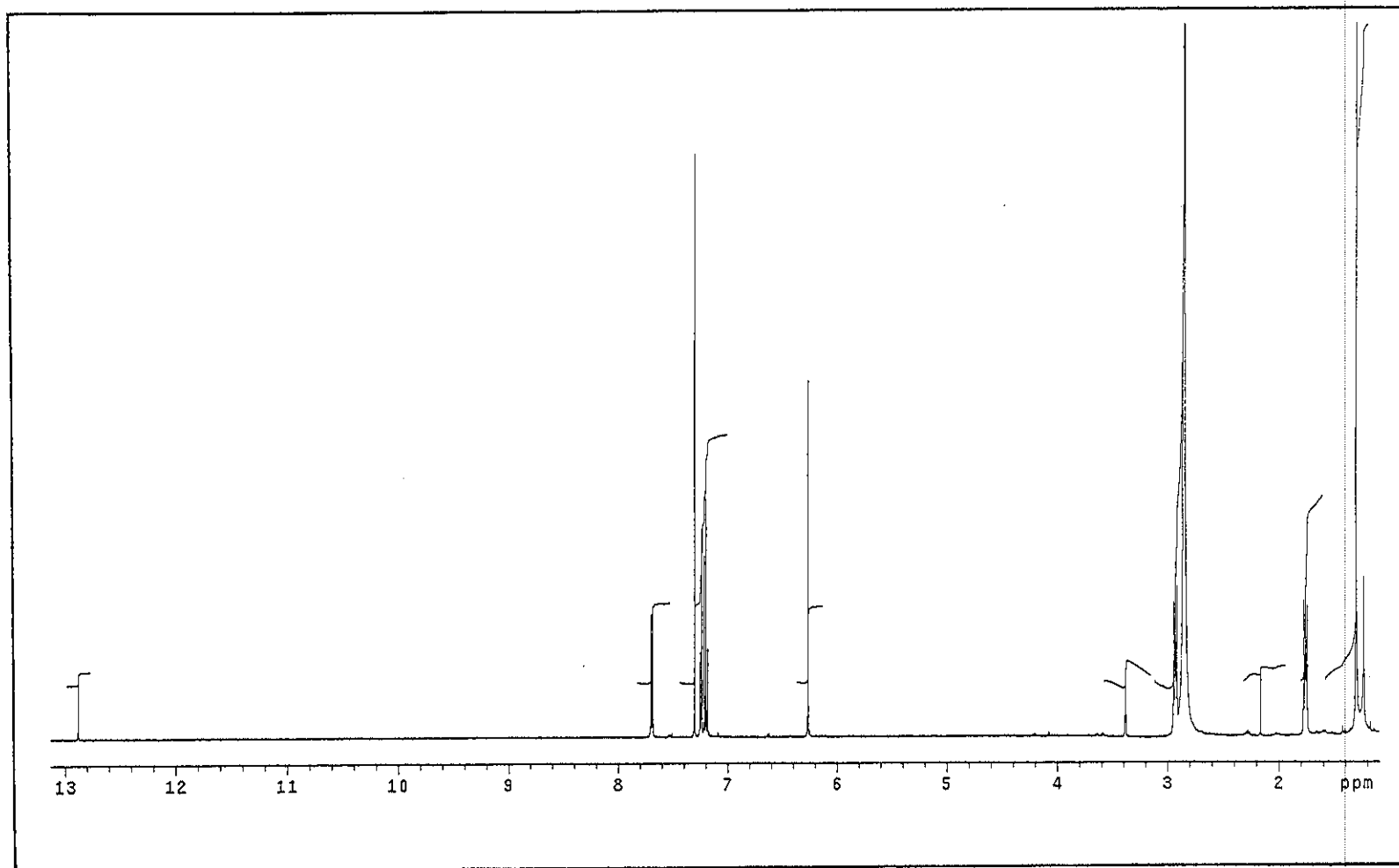


Figure 3.11 ^1H NMR (500MHz)($\text{CDCl}_3+\text{CD}_3\text{OD}$) spectrum of TR2

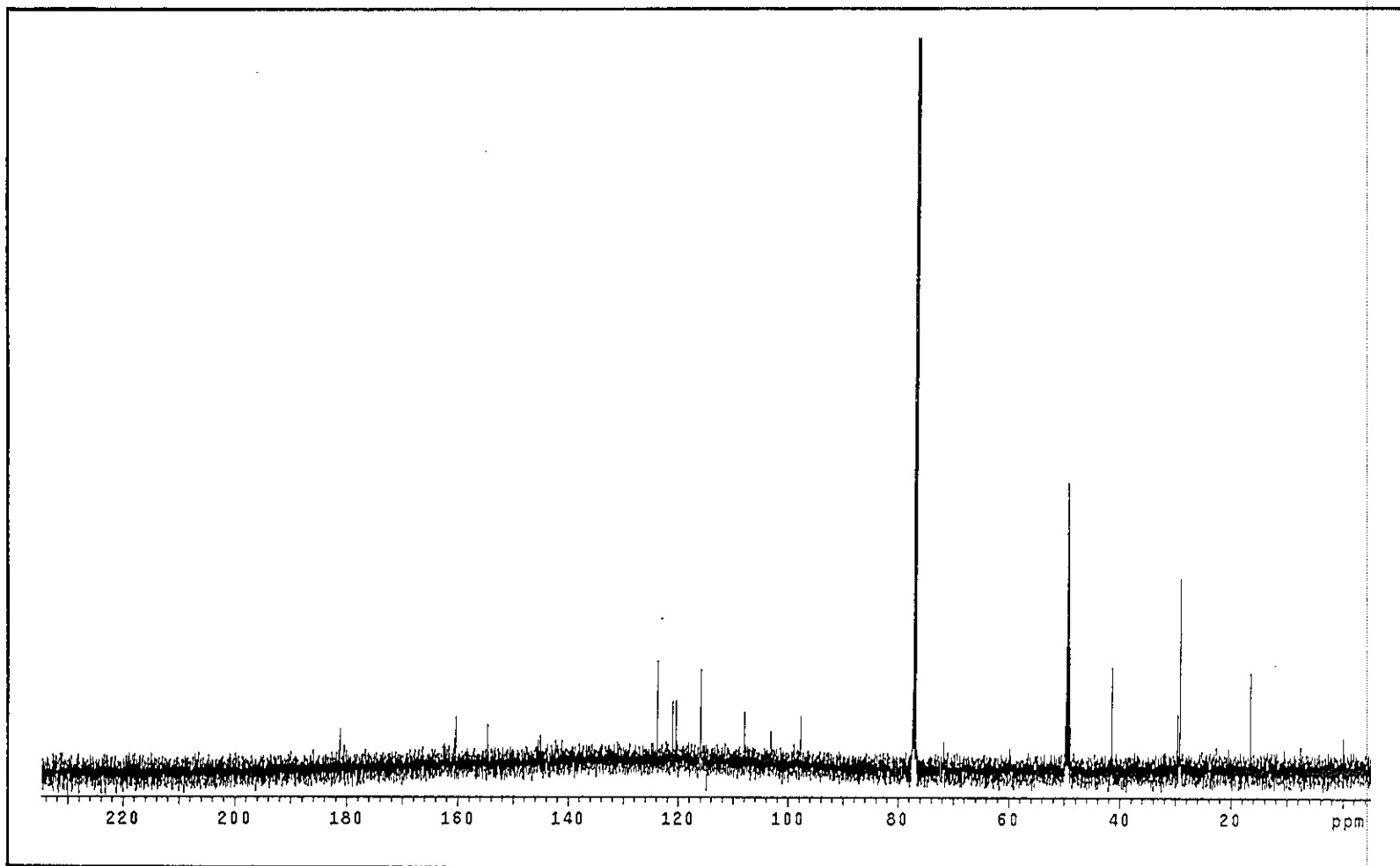


Figure 3.12 ^{13}C NMR (125MHz)($\text{CDCl}_3+\text{CD}_3\text{OD}$) spectrum of TR2

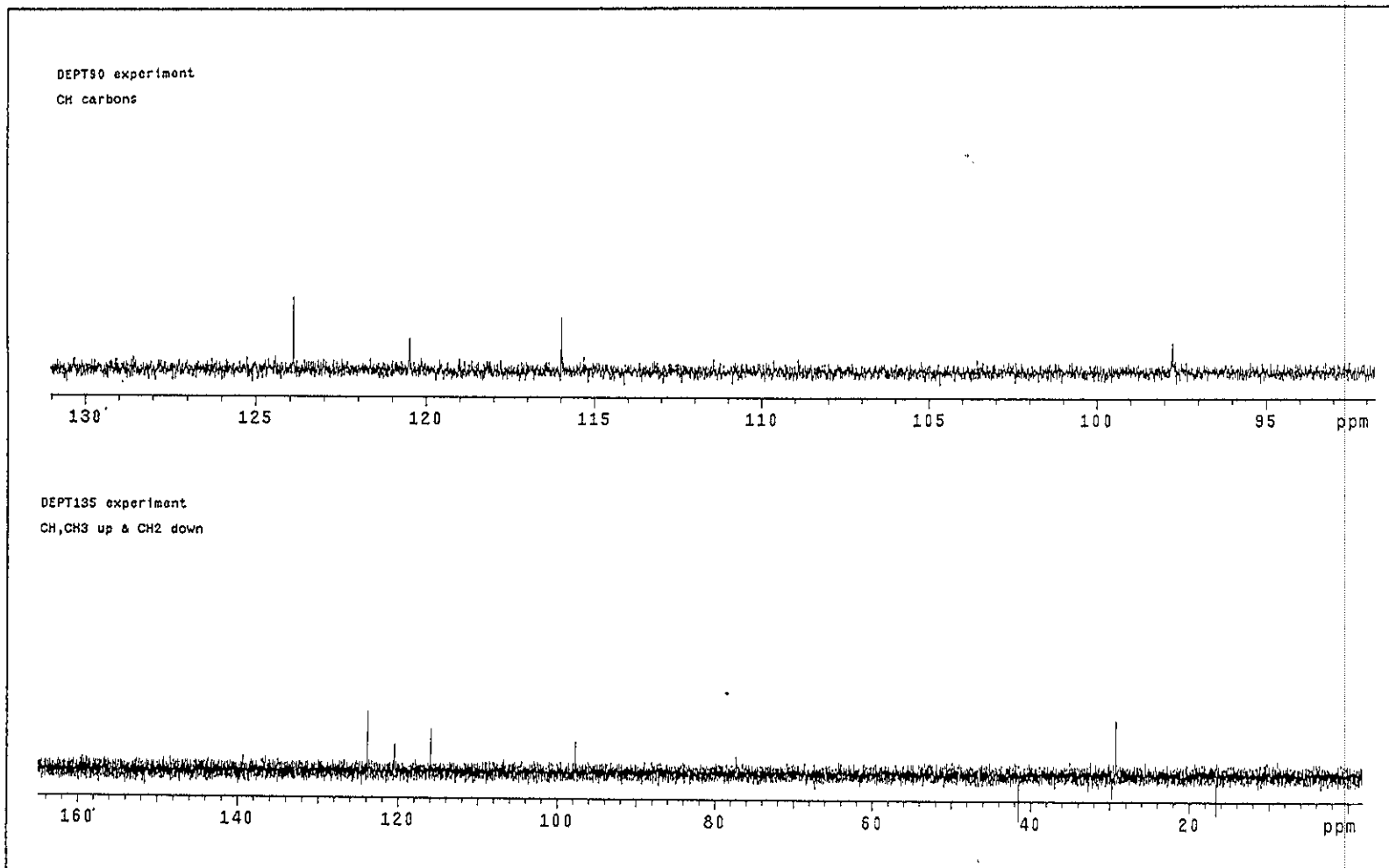


Figure 3.13 DEPT spectrum of TR2

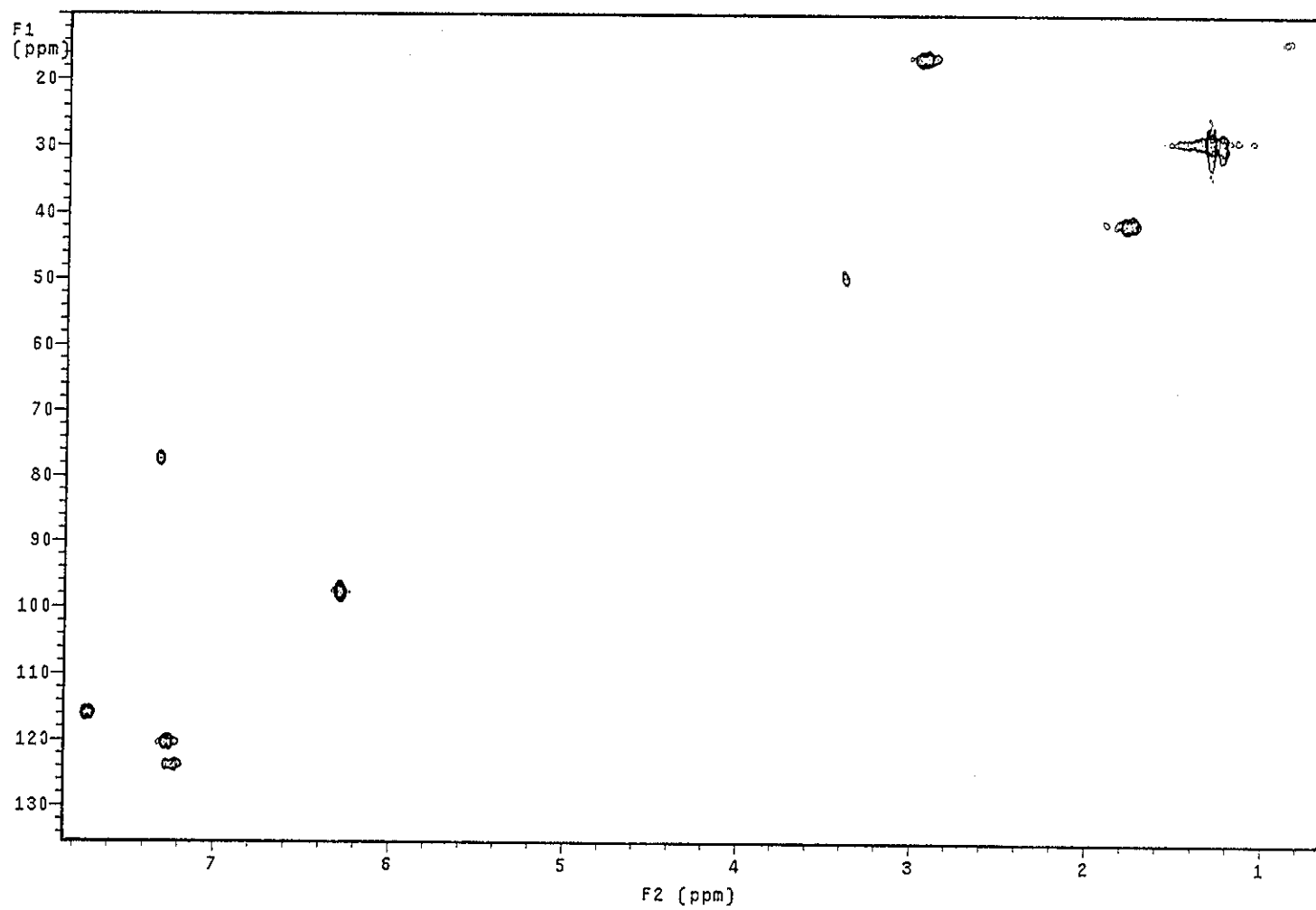


Figure 3.14 2D HMQC spectrum of TR2

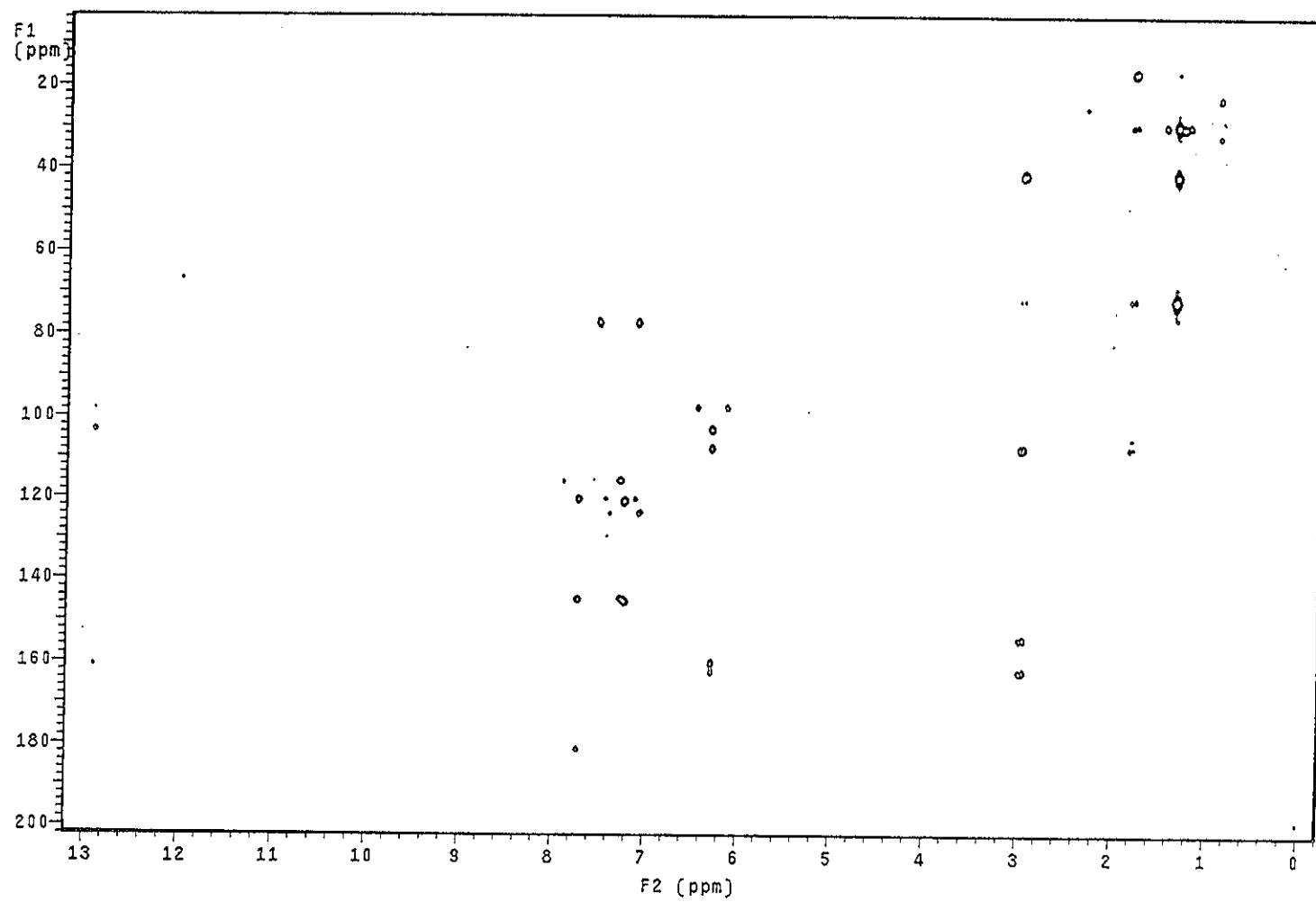


Figure 3.15 2D HMBC spectrum of TR2

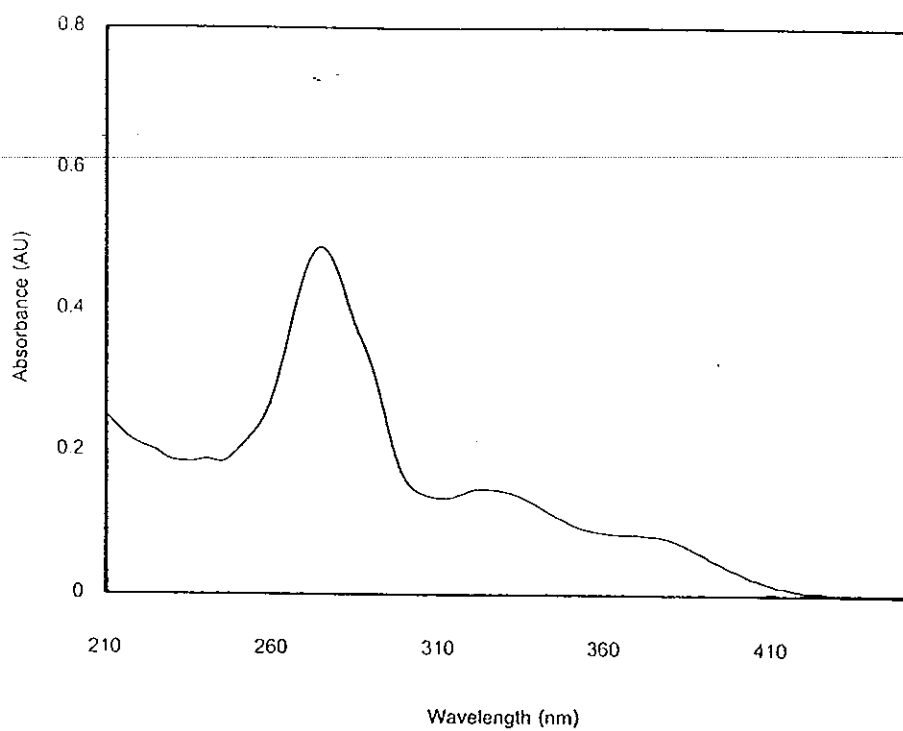


Figure 3.16 UV (MeOH) spectrum of TR8

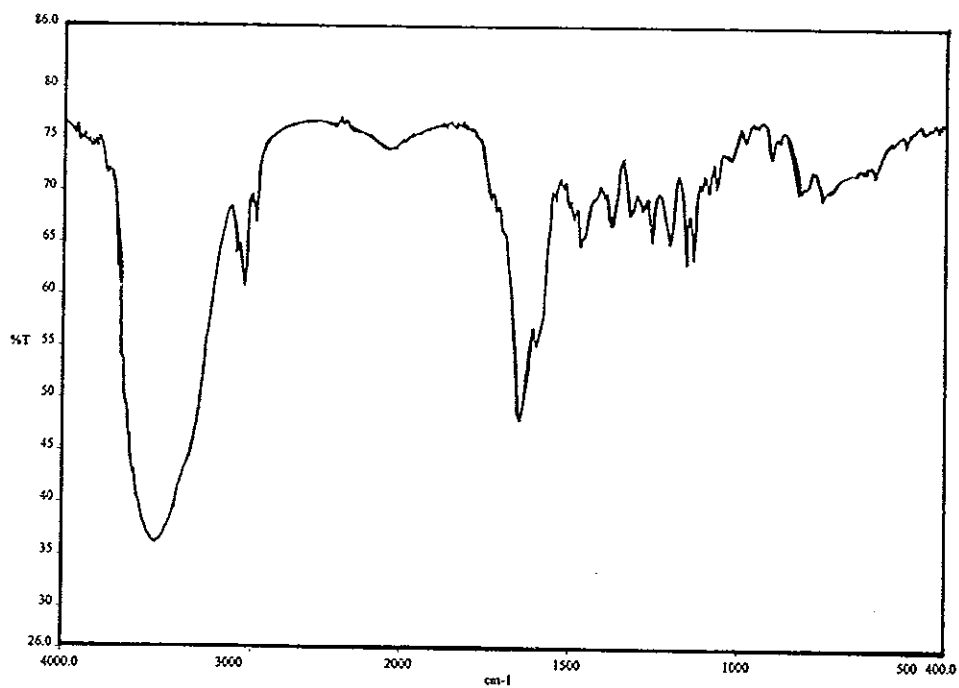


Figure 3.17 FT-IR (neat) spectrum of TR8

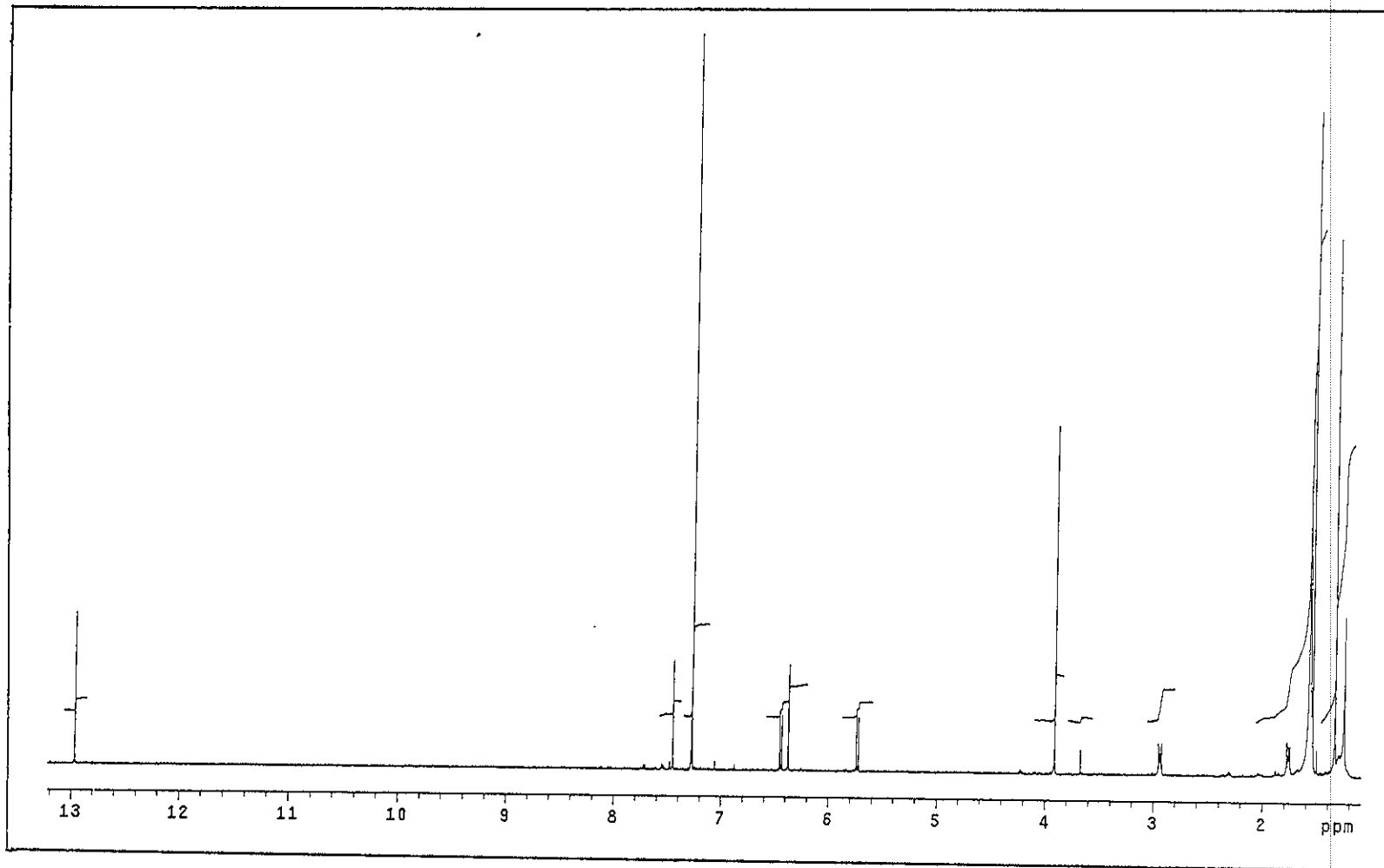


Figure 3.18 ^1H NMR (500 MHz)(CDCl_3) spectrum of TR8

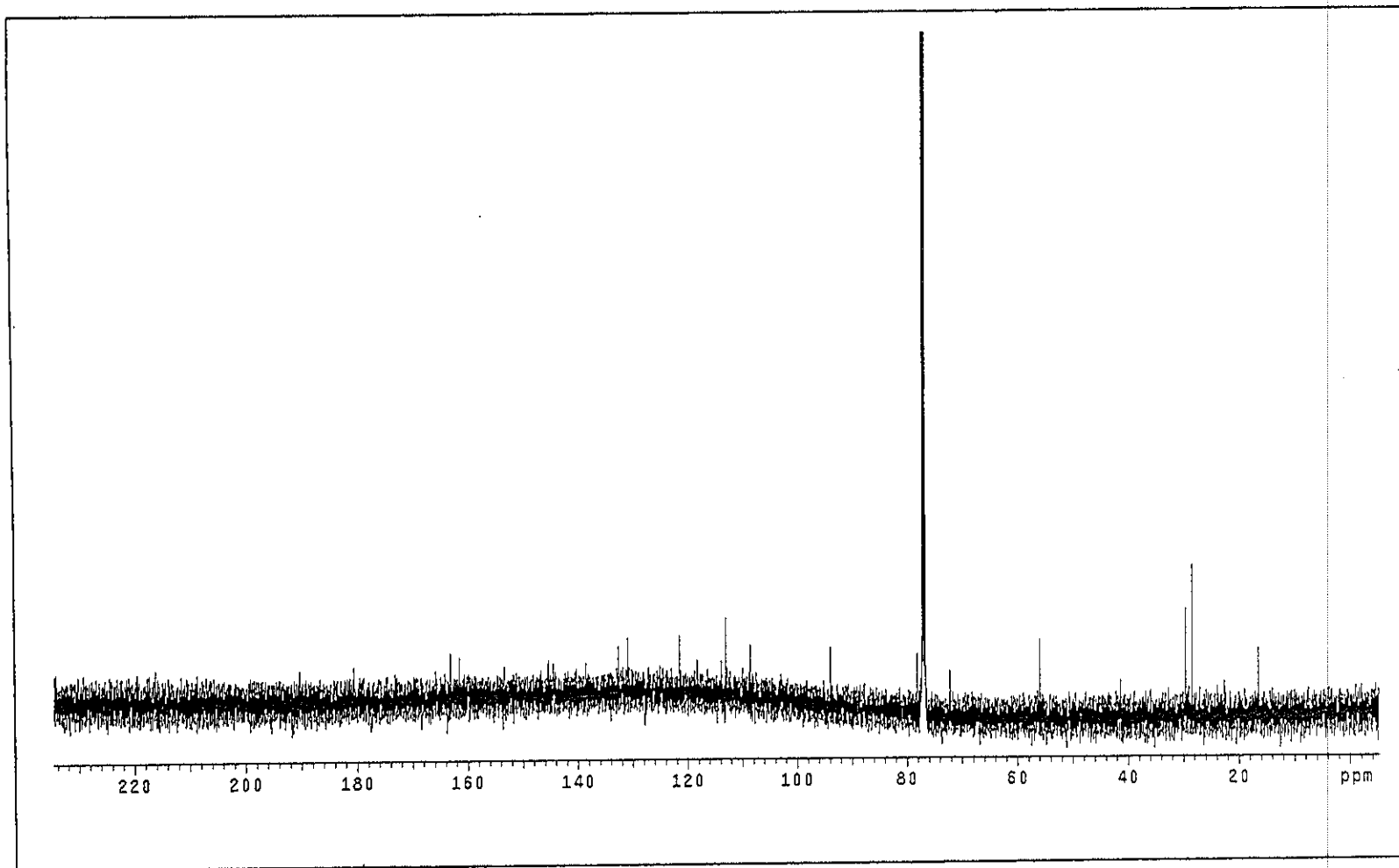


Figure 3.19 ^{13}C NMR (125 MHz)(CDCl_3) spectrum of TR8

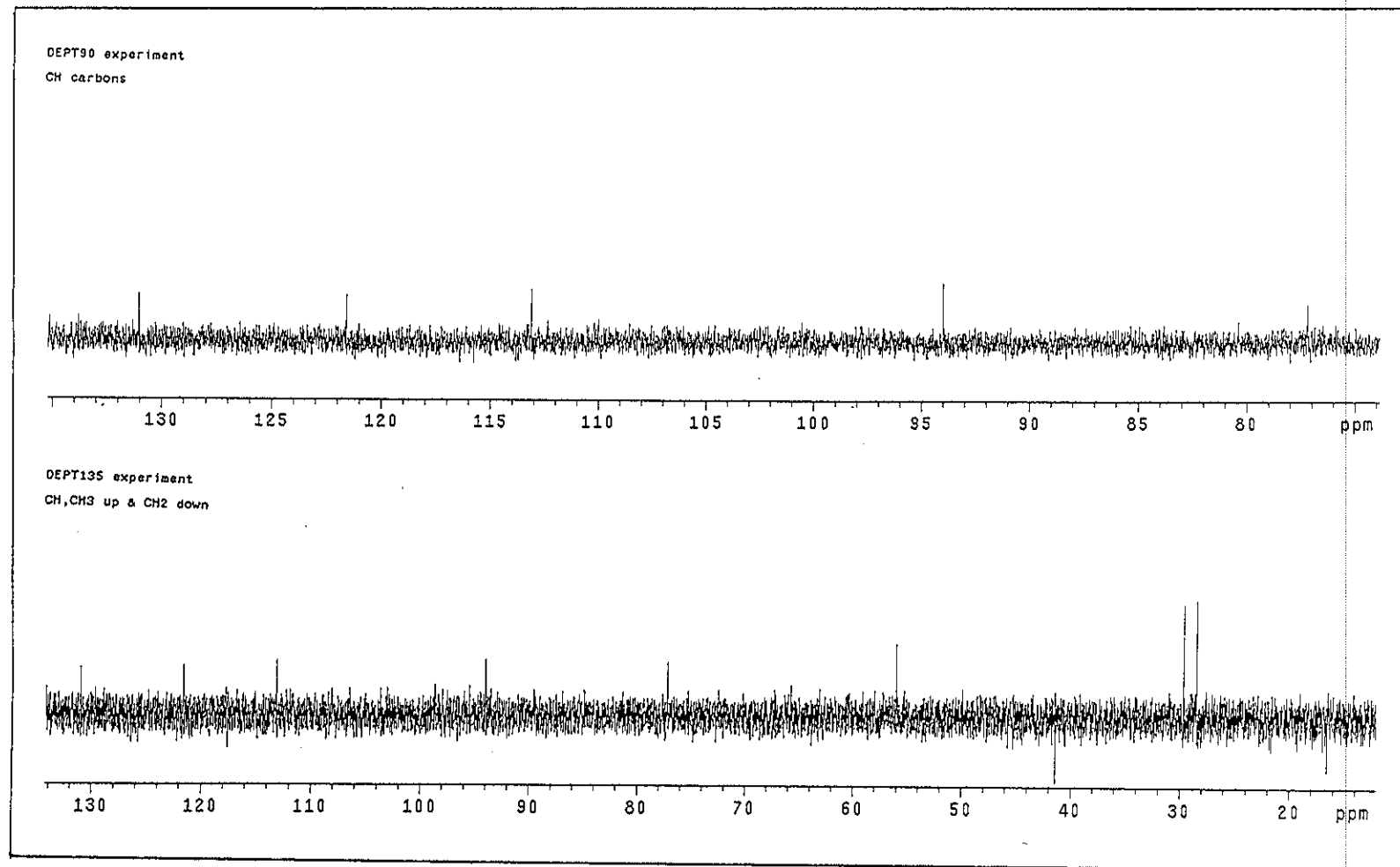


Figure 3.20 DEPT spectrum of TR8

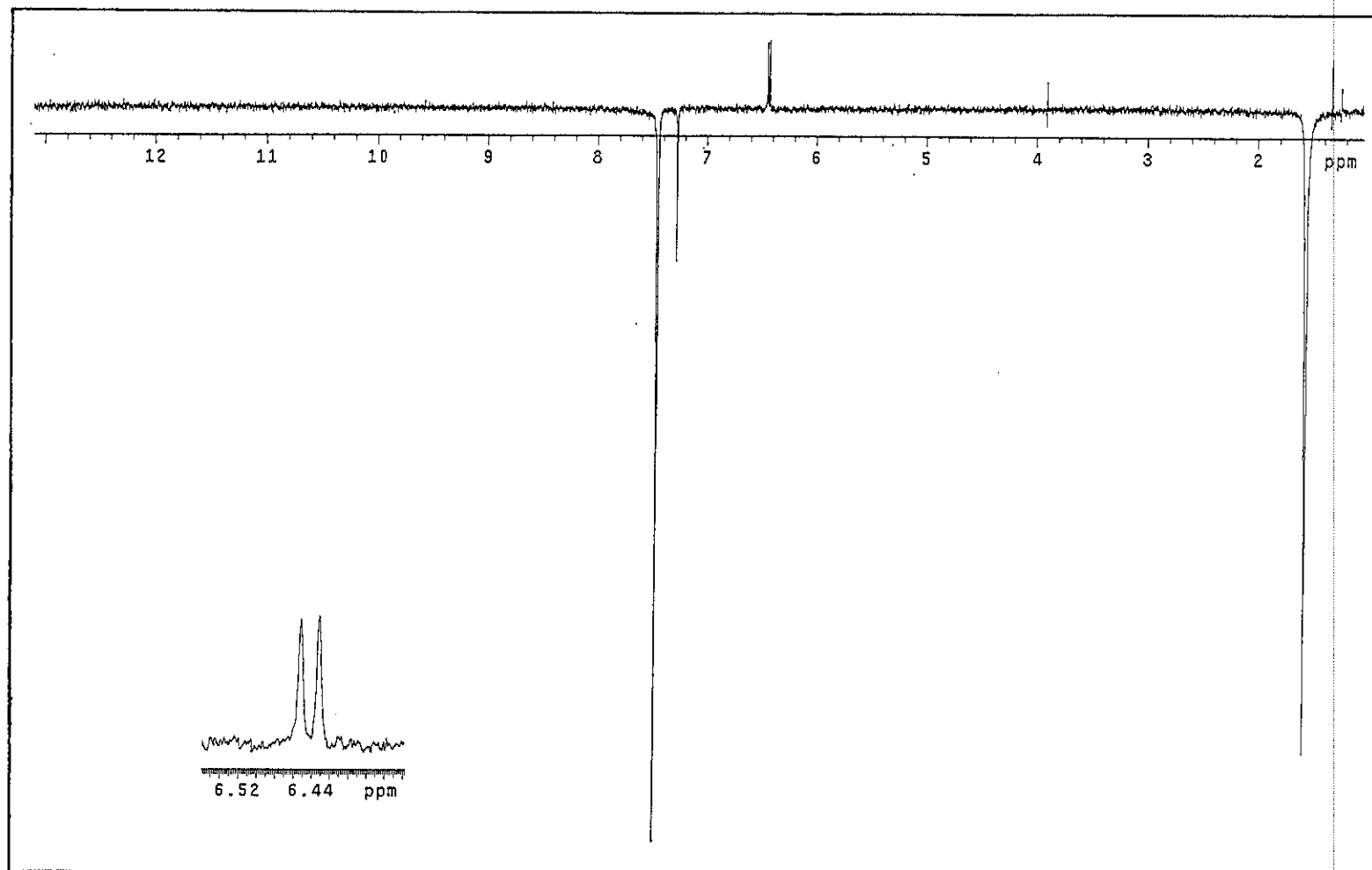


Figure 3.21 NOEDIFF spectrum of TR8 after irradiation at δ_H 7.45

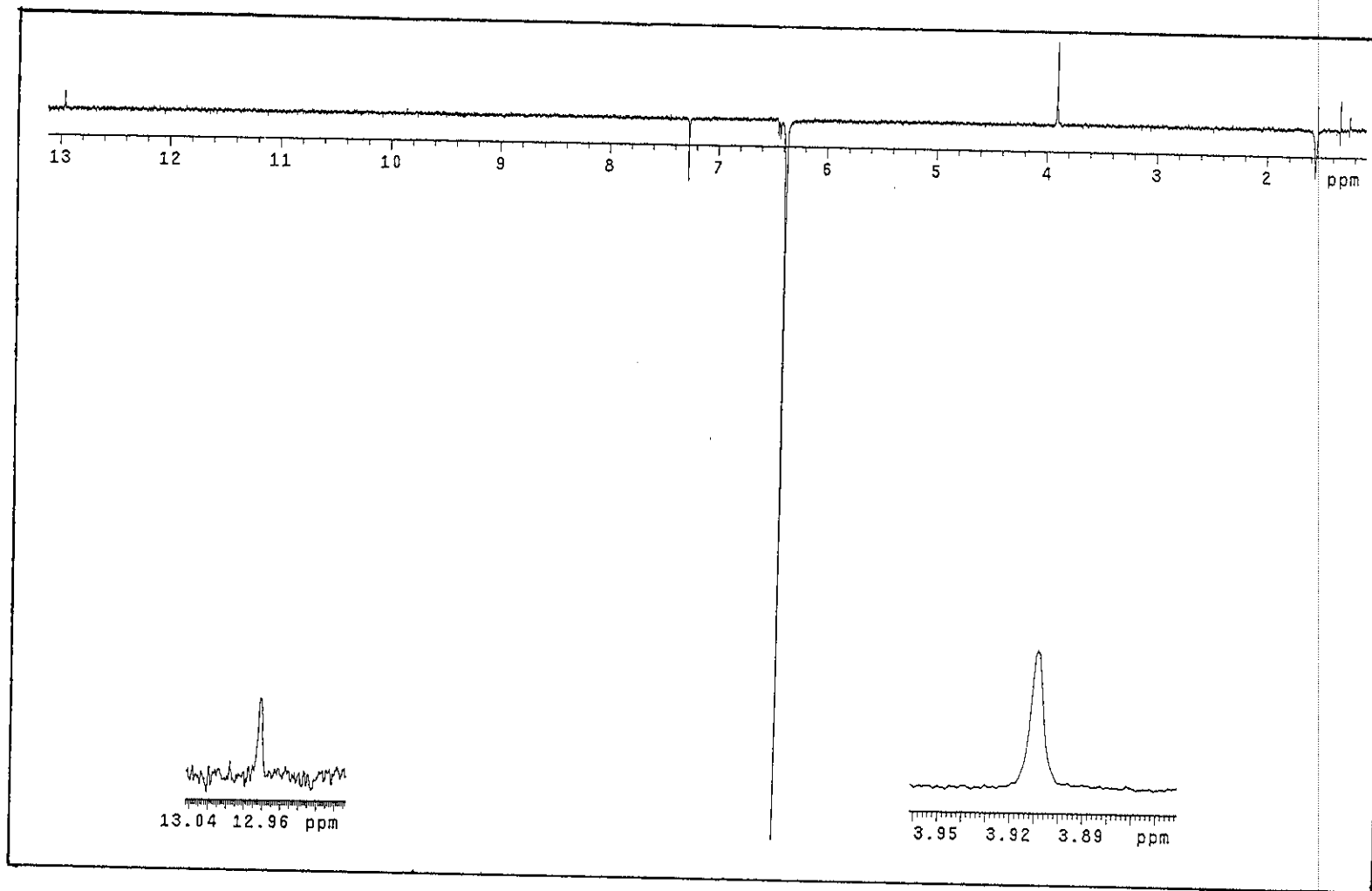


Figure 3.22 NOEDIFF spectrum of TR8 after irradiation at δ_{H} 6.37

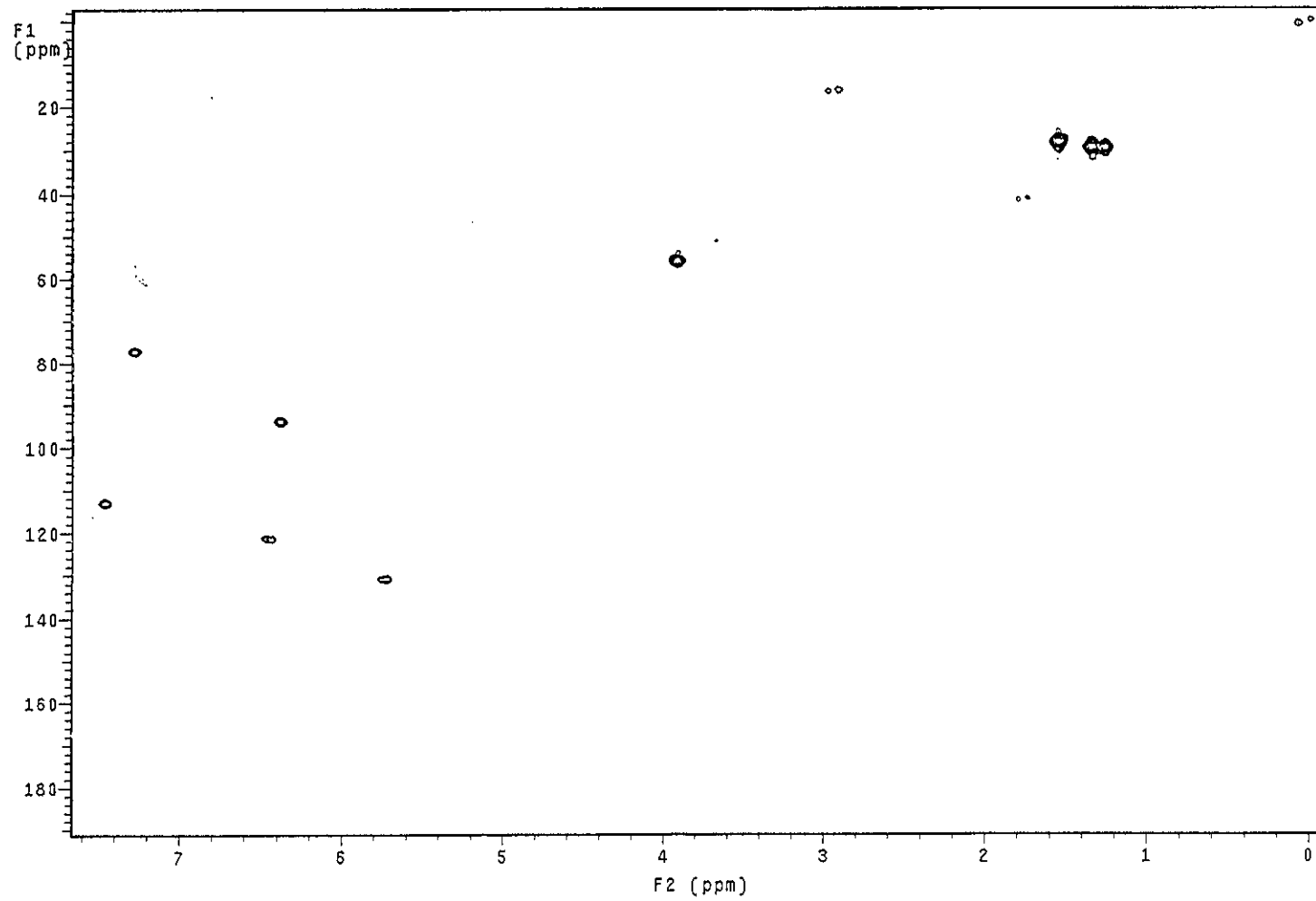


Figure 3.23 2D HMQC spectrum of TR8

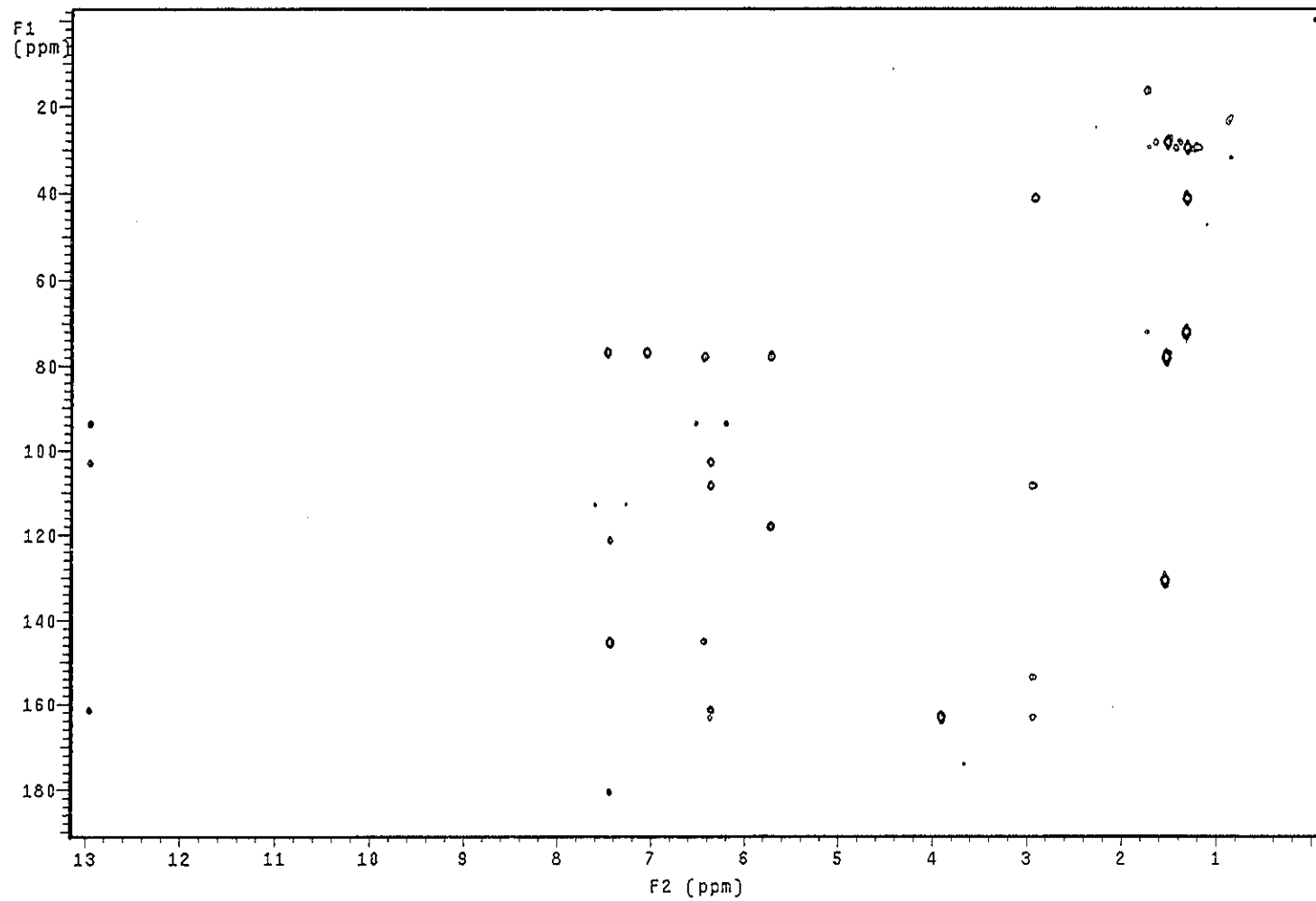


Figure 3.24 2D HMBC spectrum of TR8

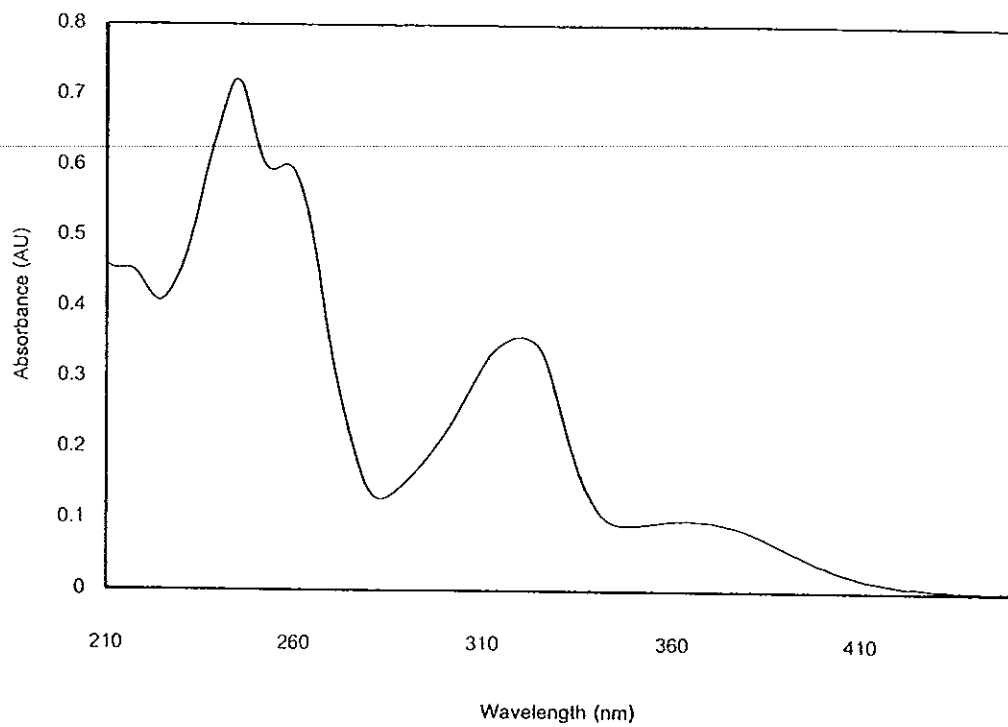


Figure 3.25 UV (MeOH) spectrum of TR1

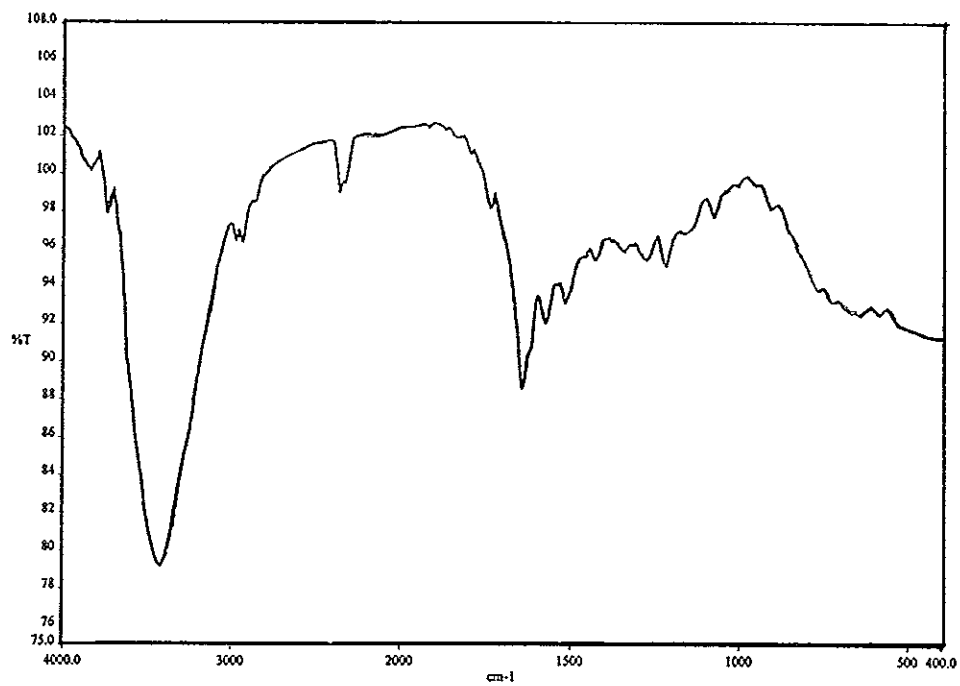


Figure 3.26 FT-IR (neat) spectrum of TR1

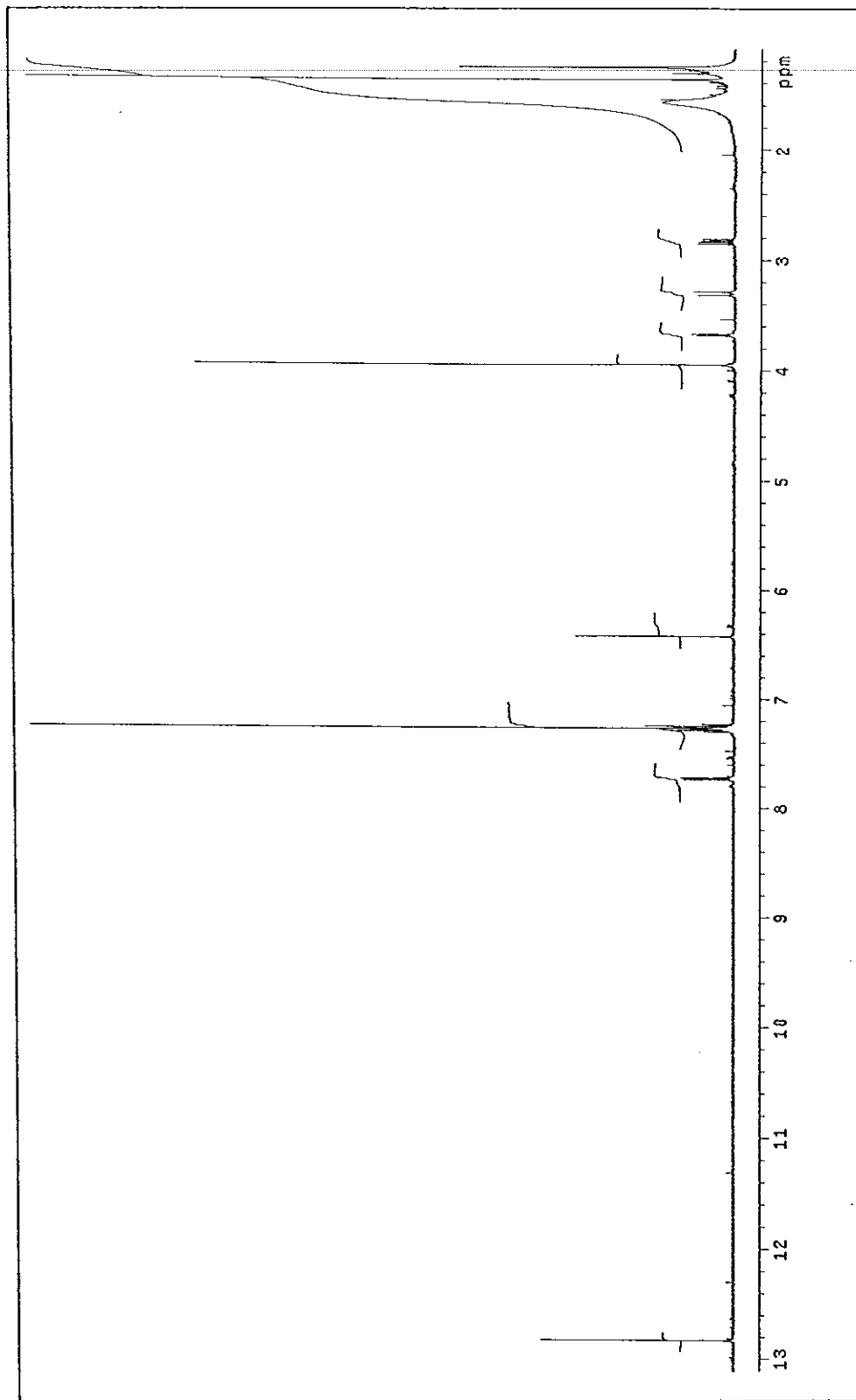


Figure 3.27 ^1H NMR (500 MHz)(CDCl_3) spectrum of TRI

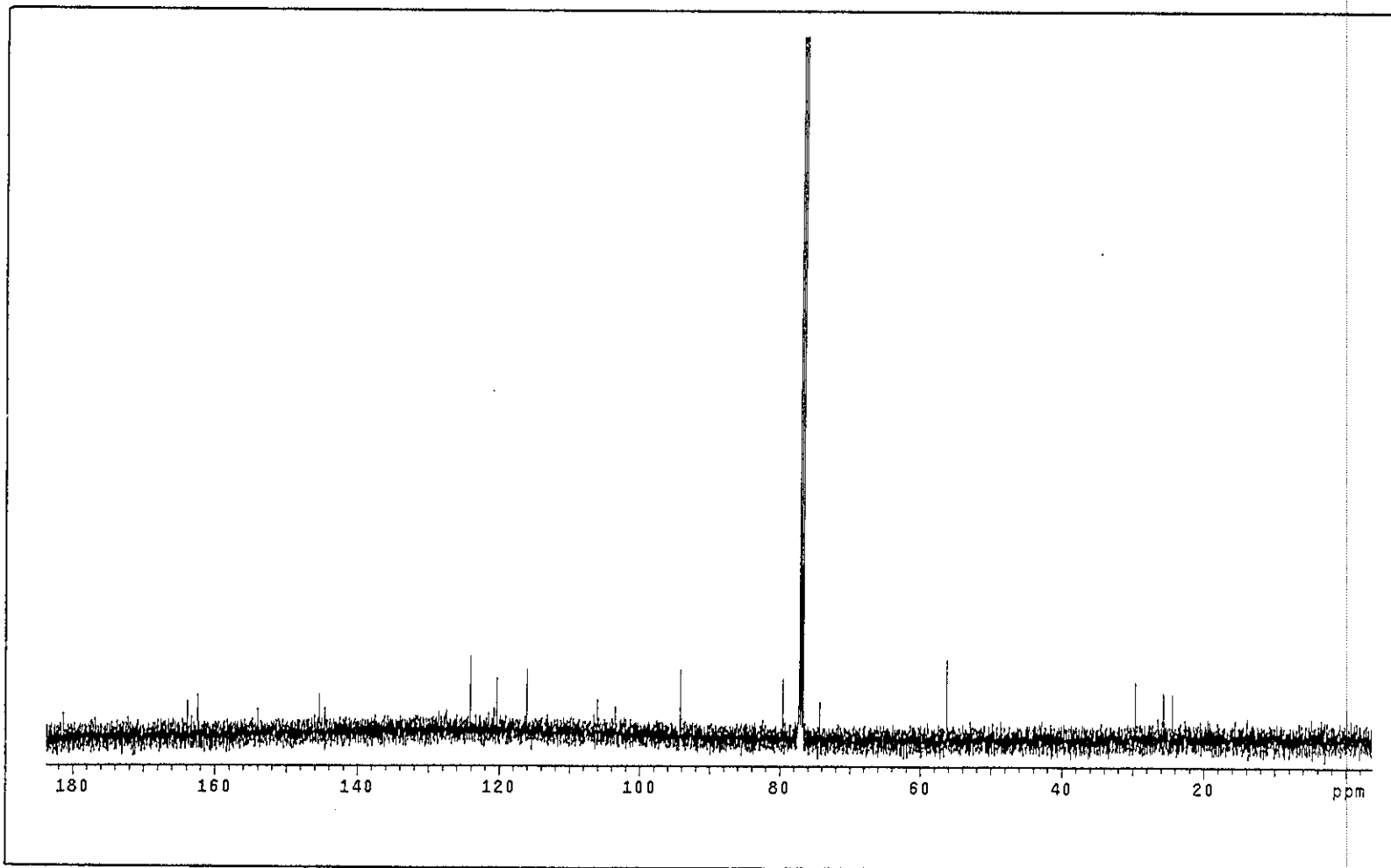


Figure 3.28 ^{13}C NMR (125 MHz)(CDCl_3) spectrum of TR1

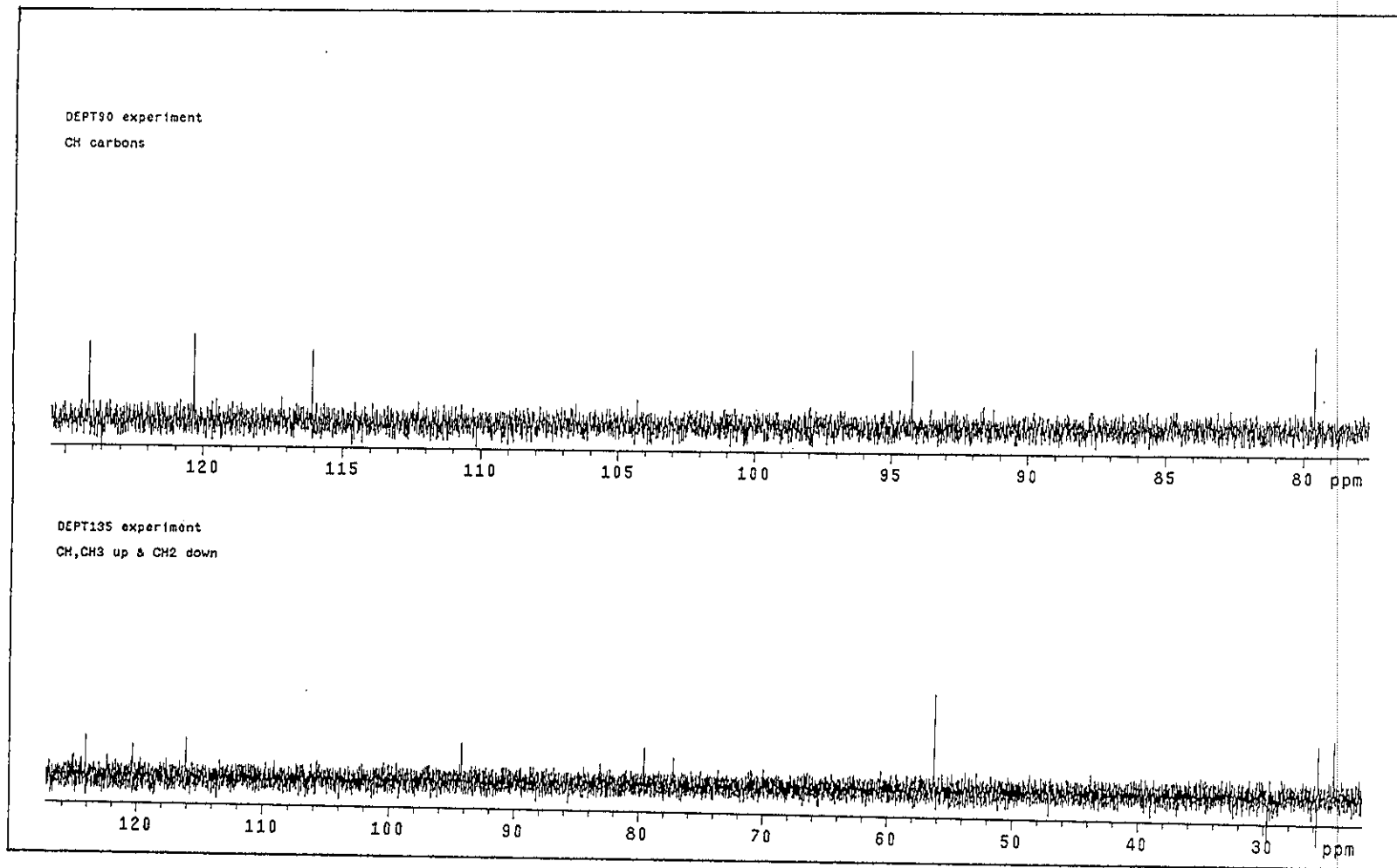


Figure 3.29 DEPT spectrum of TR1

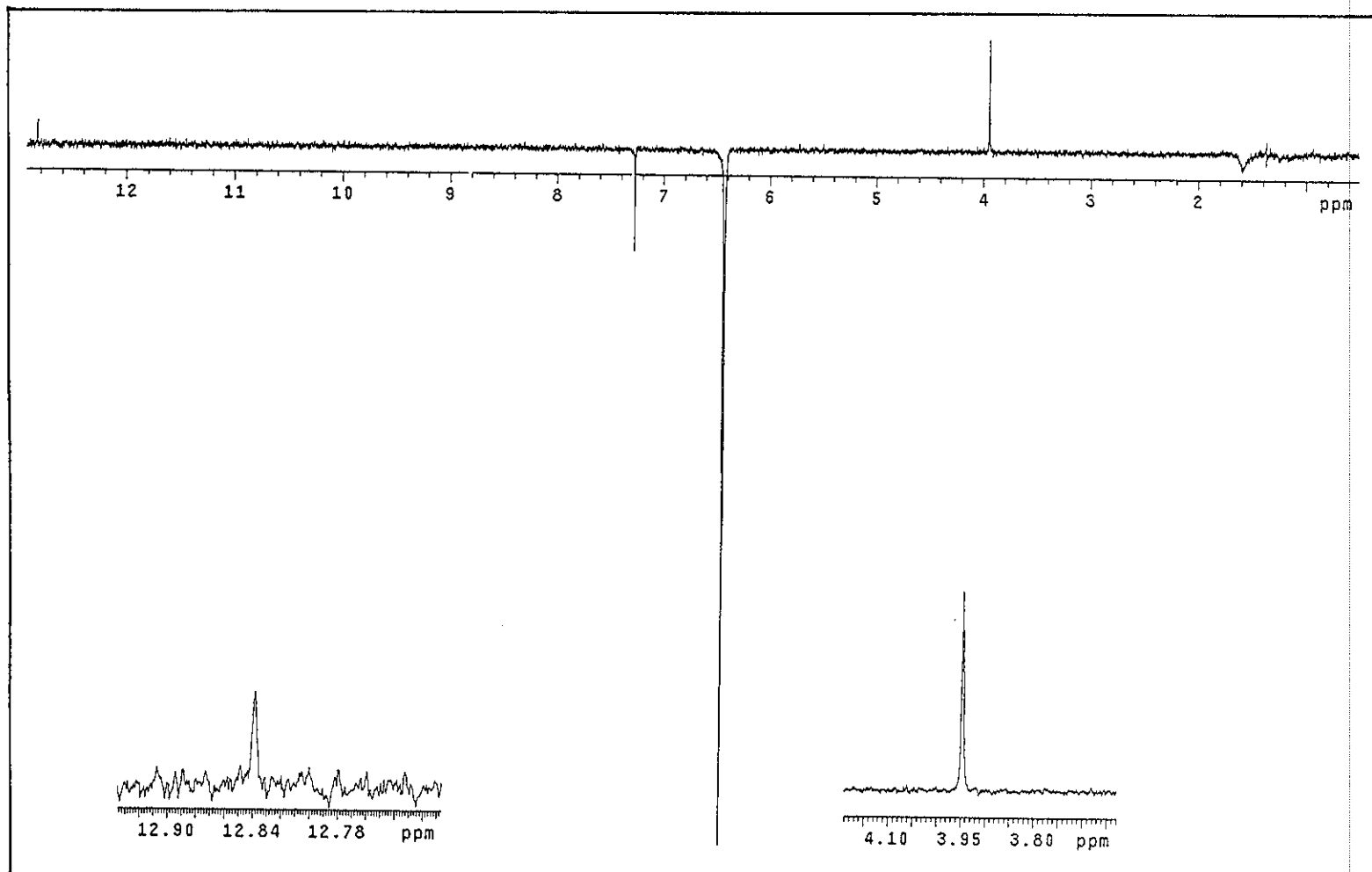


Figure 3.30 NOEDIFF spectrum of TR1 after irradiation at δ_H 6.43

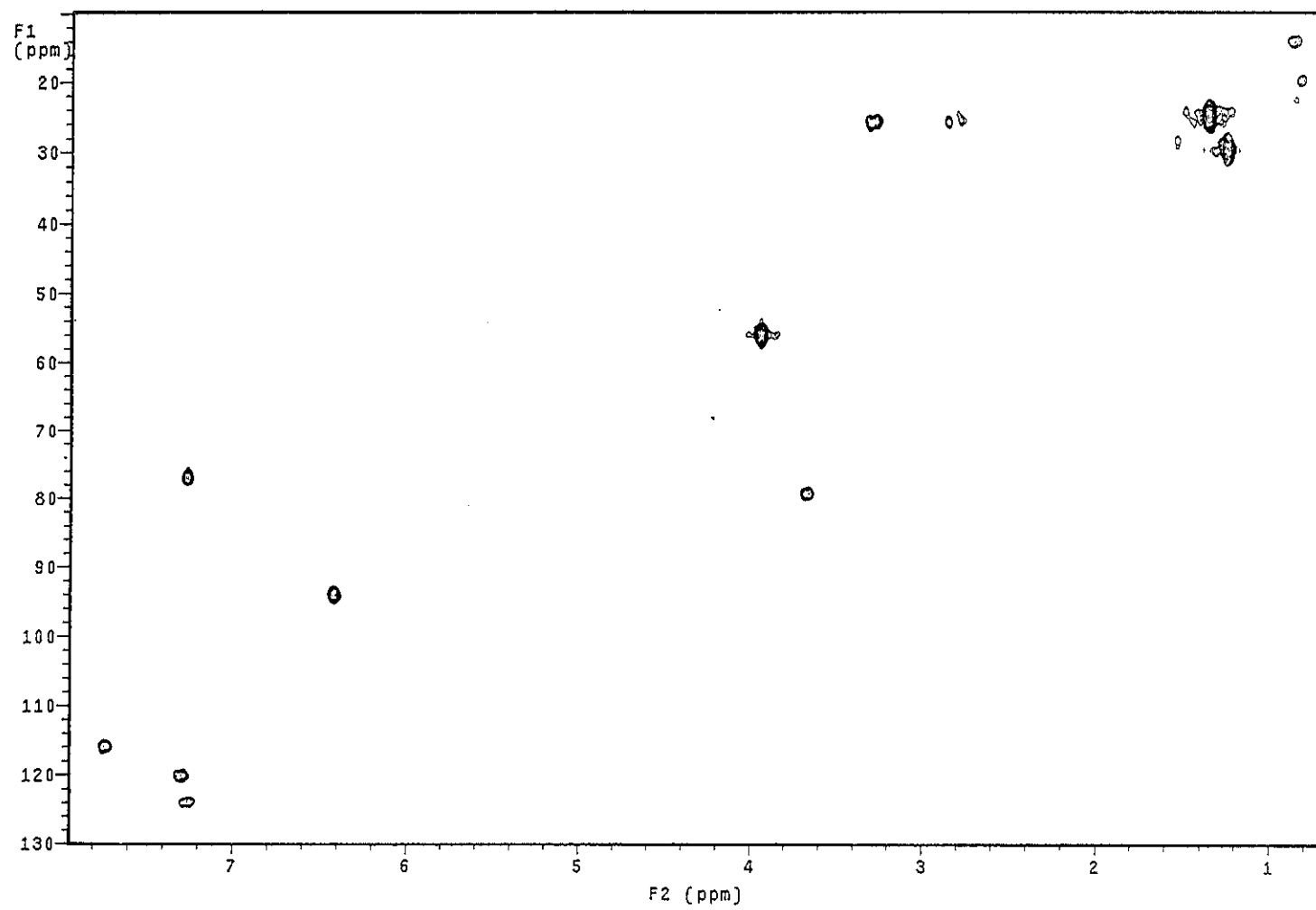


Figure 3.31 2D HMQC spectrum of TRI

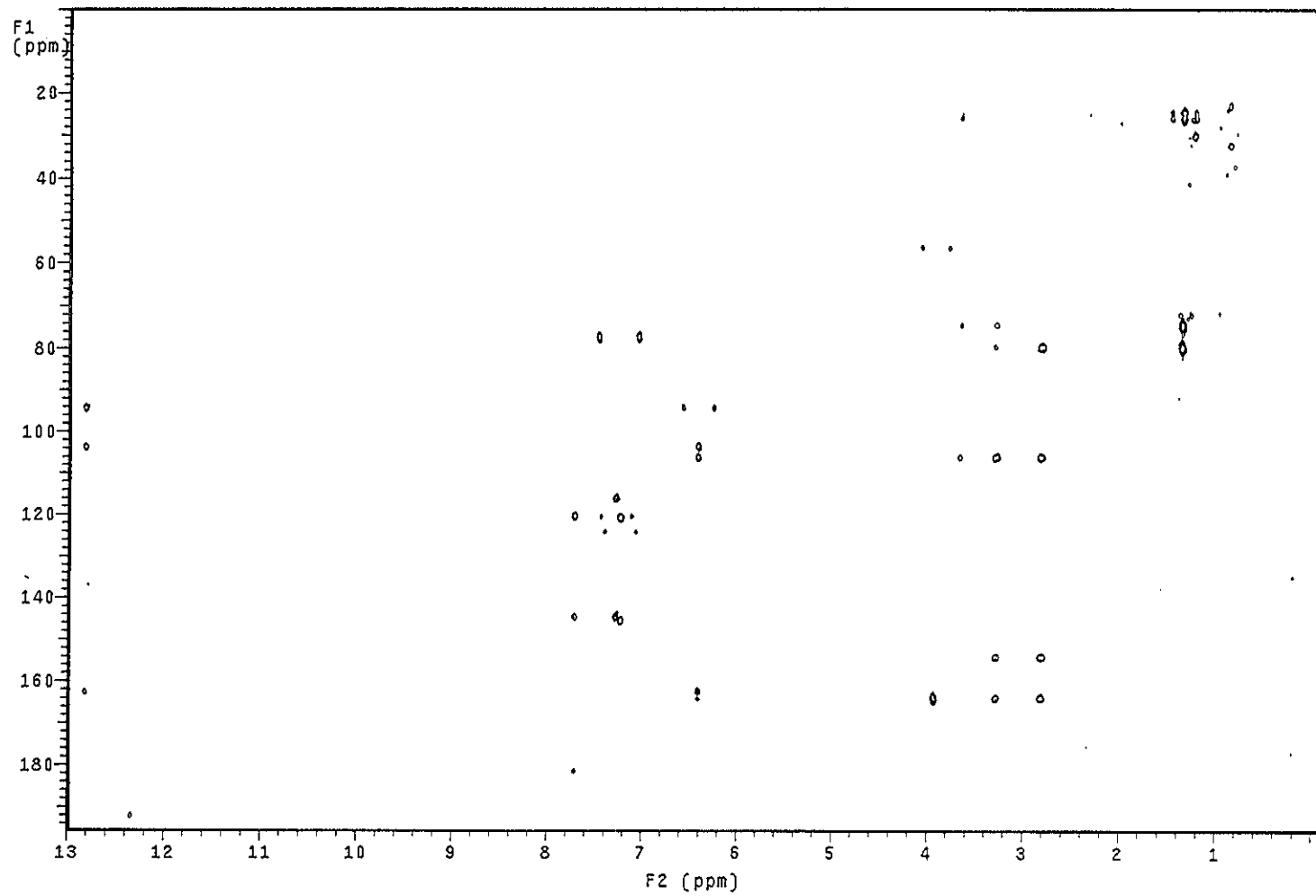


Figure 3.32 2D HMBC spectrum of TR1

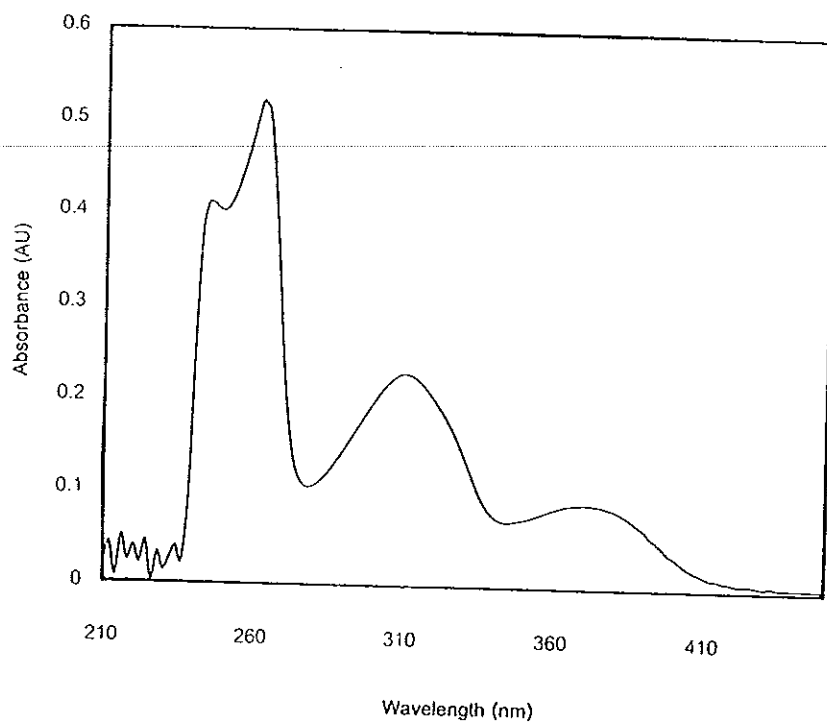


Figure 3.33 UV (MeOH) spectrum of TR14

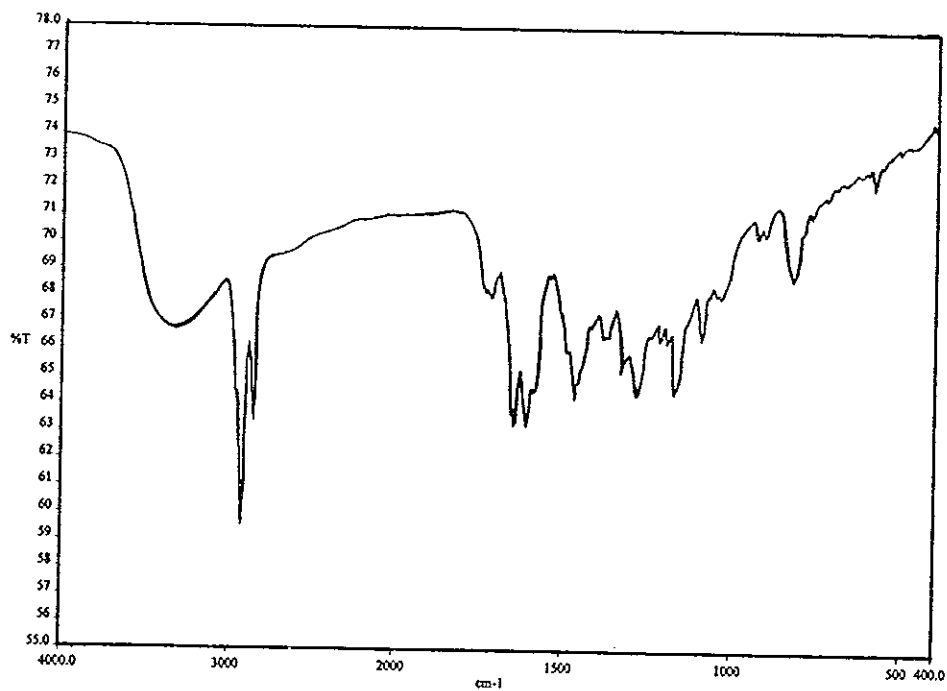


Figure 3.34 FT-IR (neat) spectrum of TR14

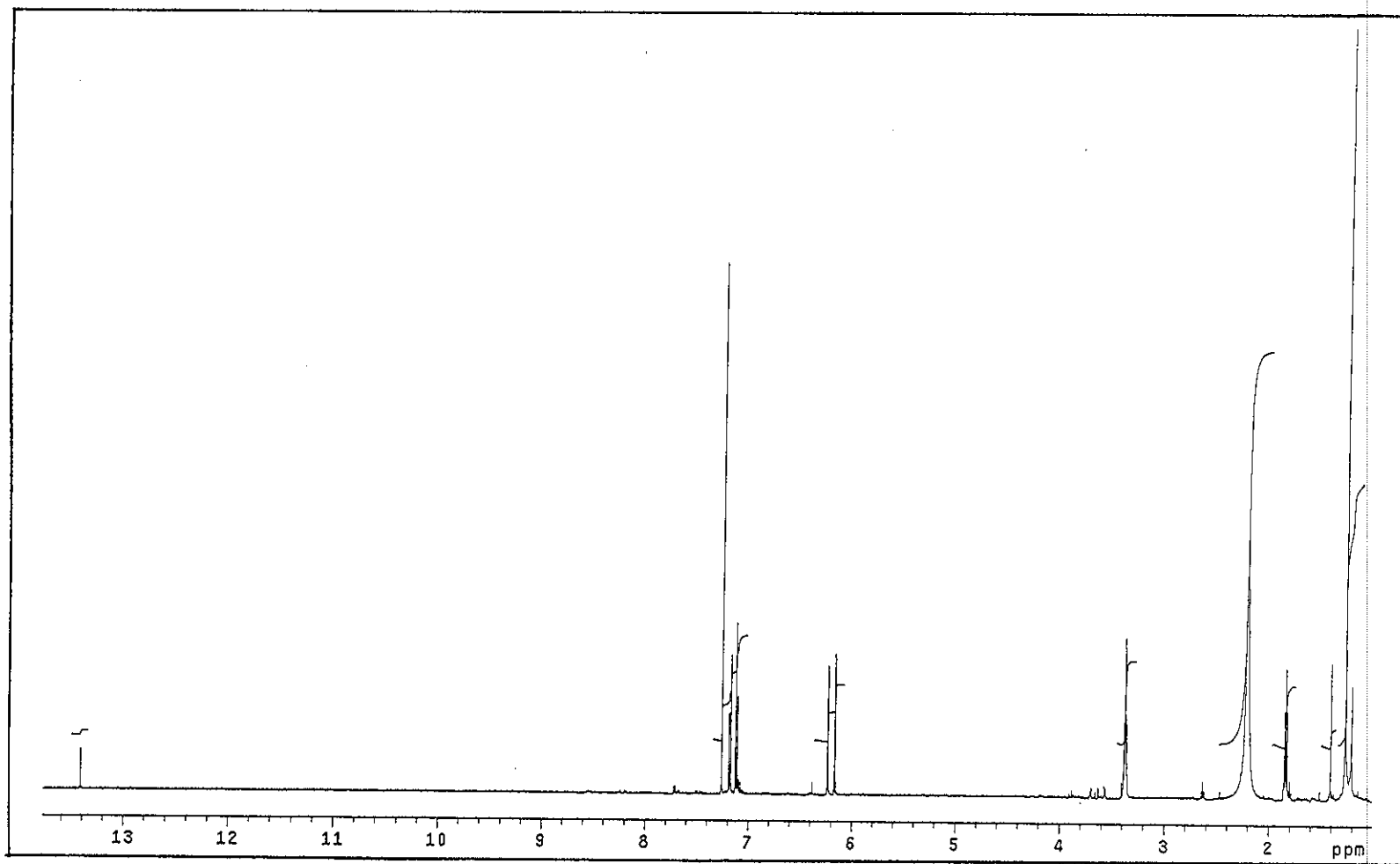


Figure 3.35 ^1H NMR (500 MHz)($\text{CDCl}_3 + \text{CD}_3\text{OD}$) spectrum of TR14

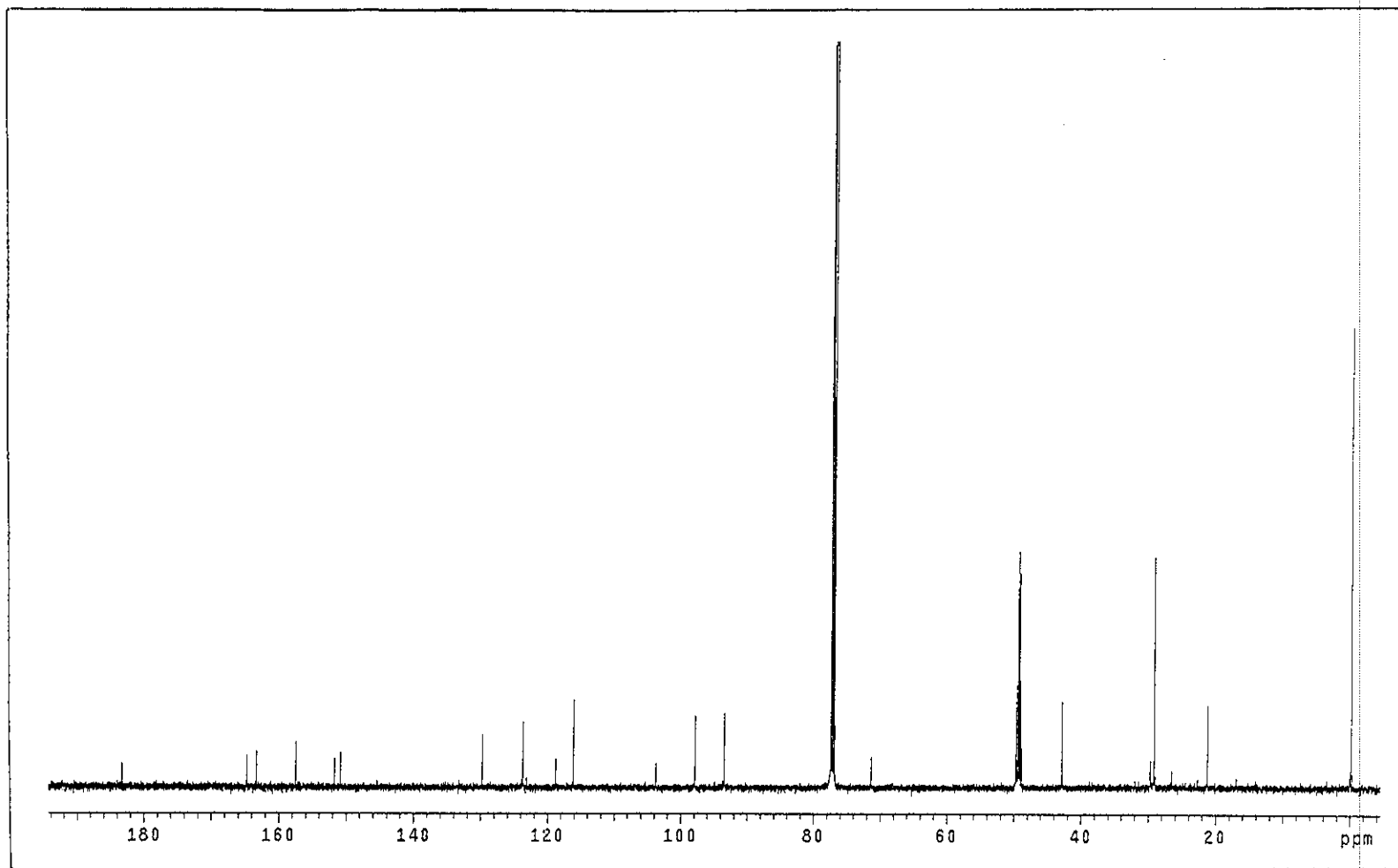


Figure 3.36 ^{13}C NMR (125 MHz)($\text{CDCl}_3 + \text{CD}_3\text{OD}$) spectrum of TR14

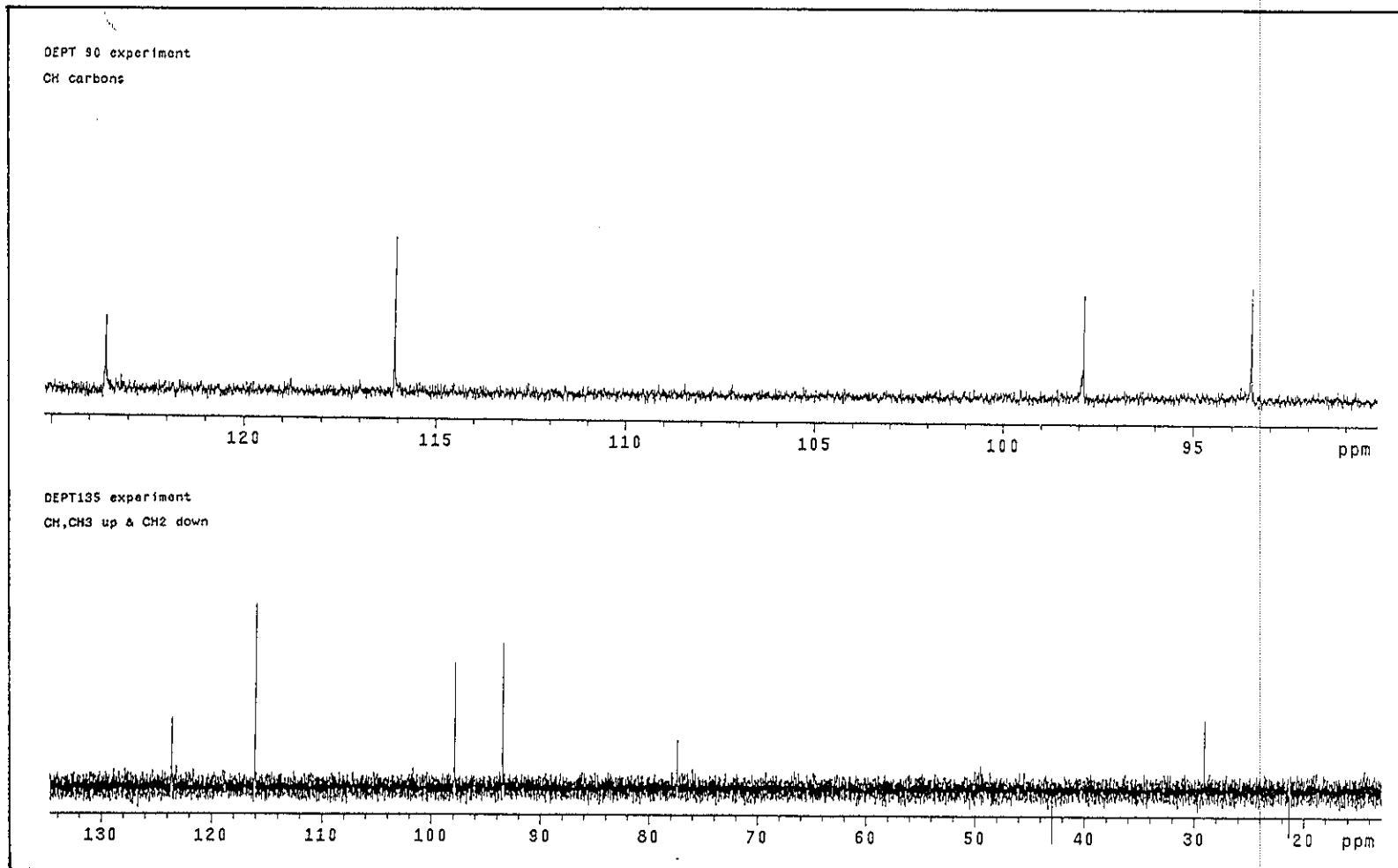


Figure 3.37 DEPT spectrum of TR14

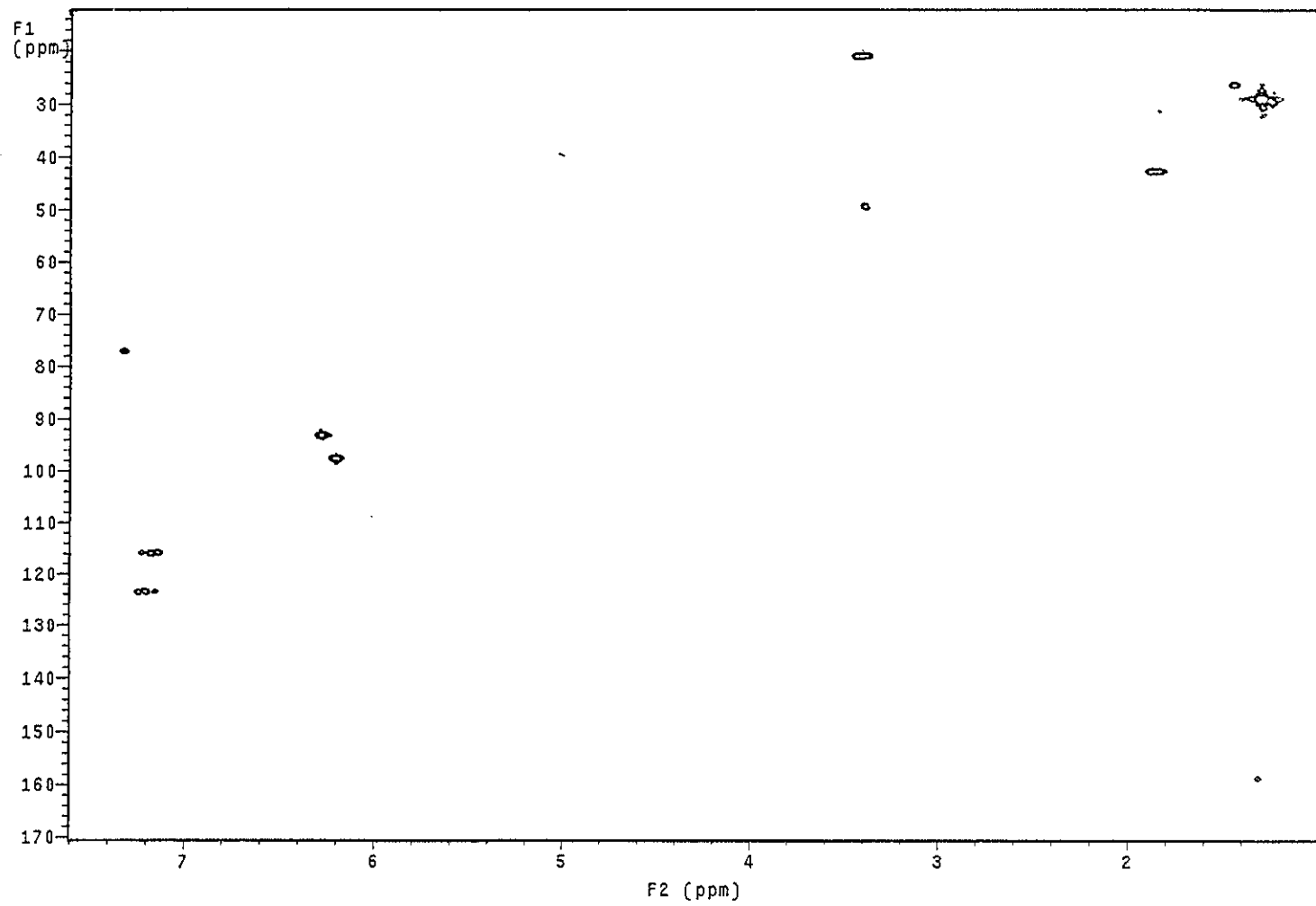


Figure 3.38 2D HMQC spectrum of TR14

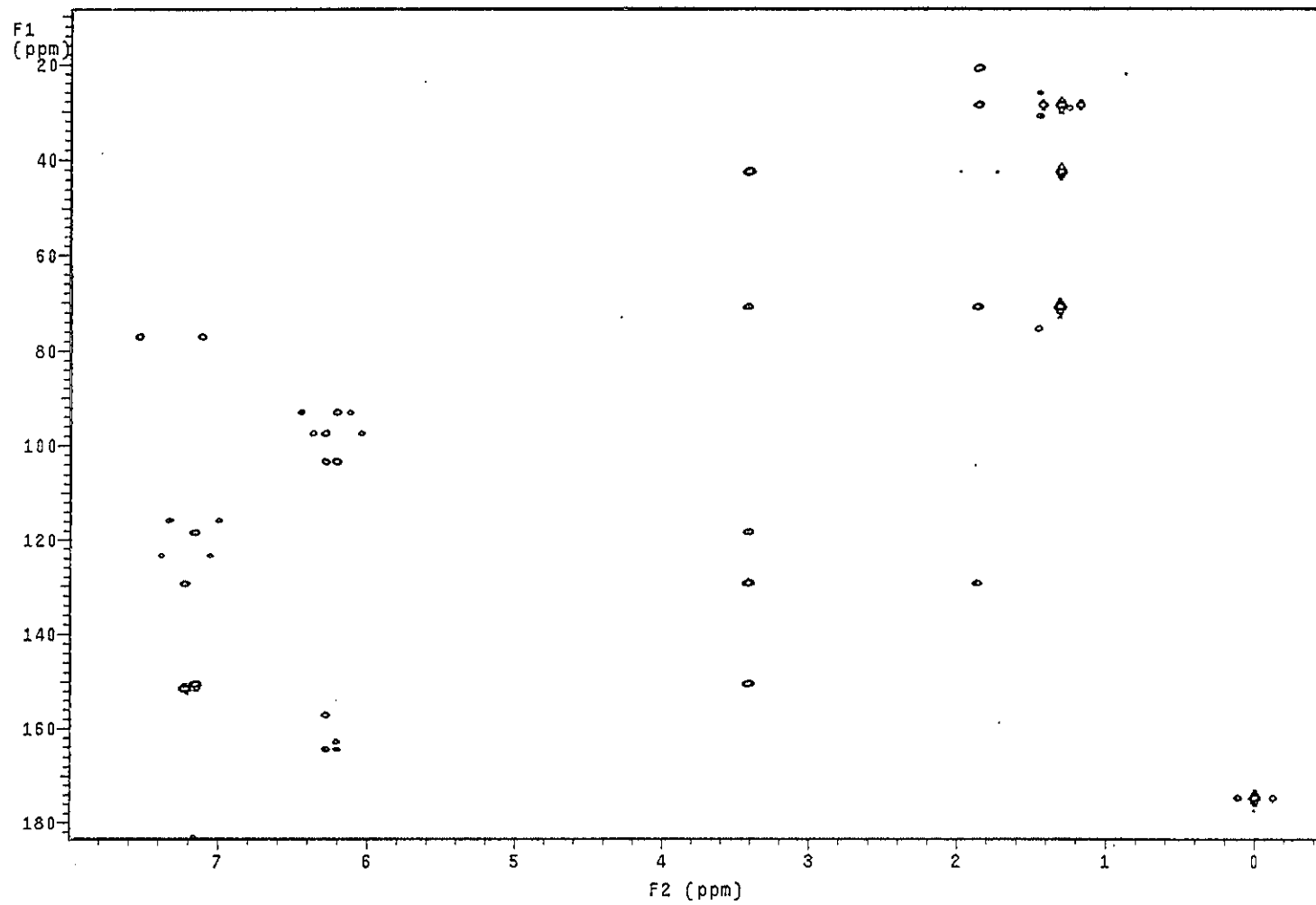


Figure 3.39 2D HMBC spectrum of TR14

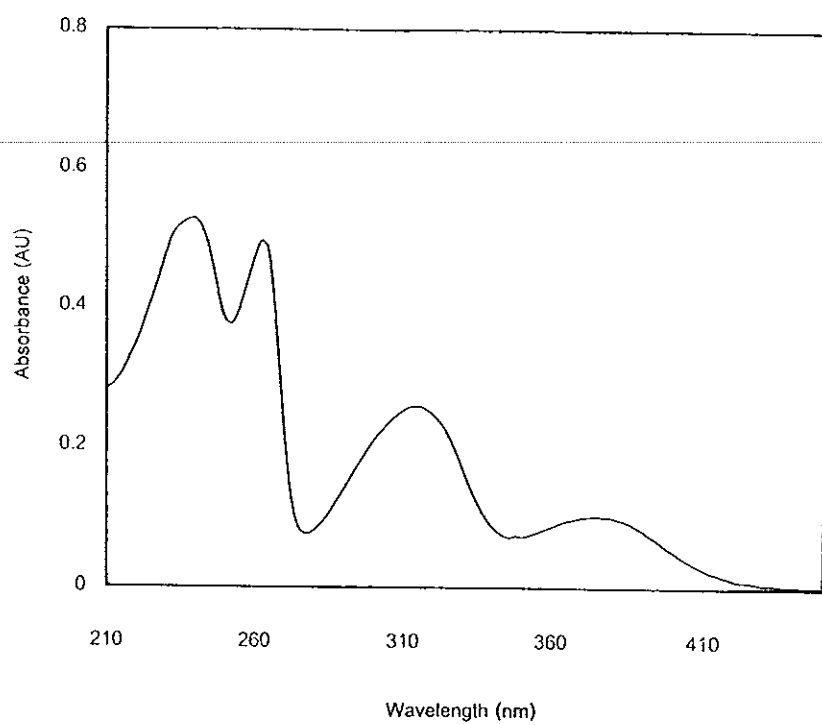


Figure 3.40 UV (MeOH) spectrum of TR15

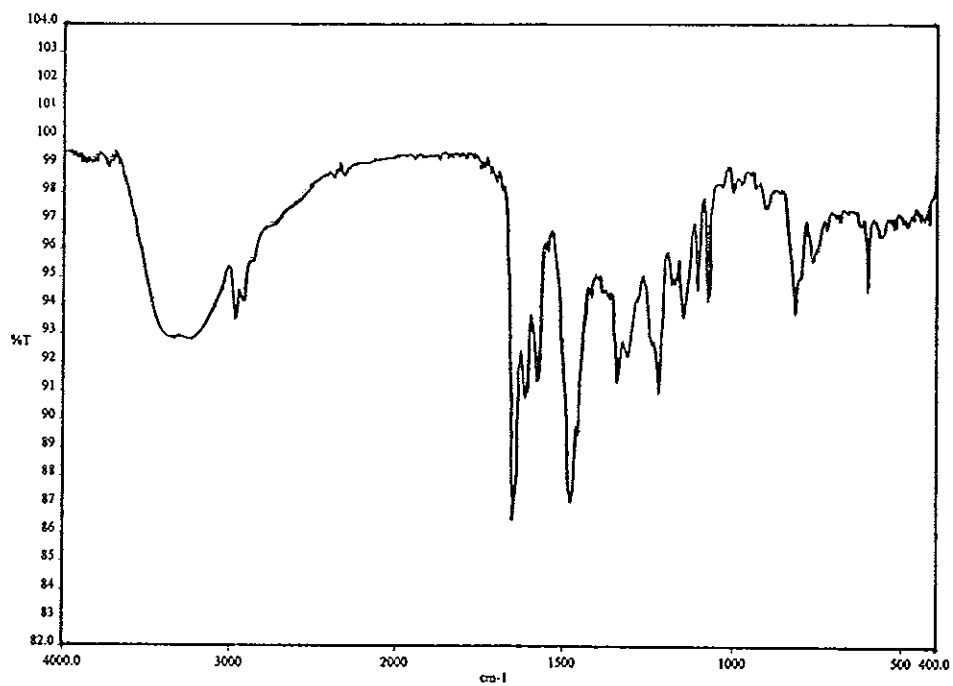


Figure 3.41 FT-IR (neat) spectrum of TR15

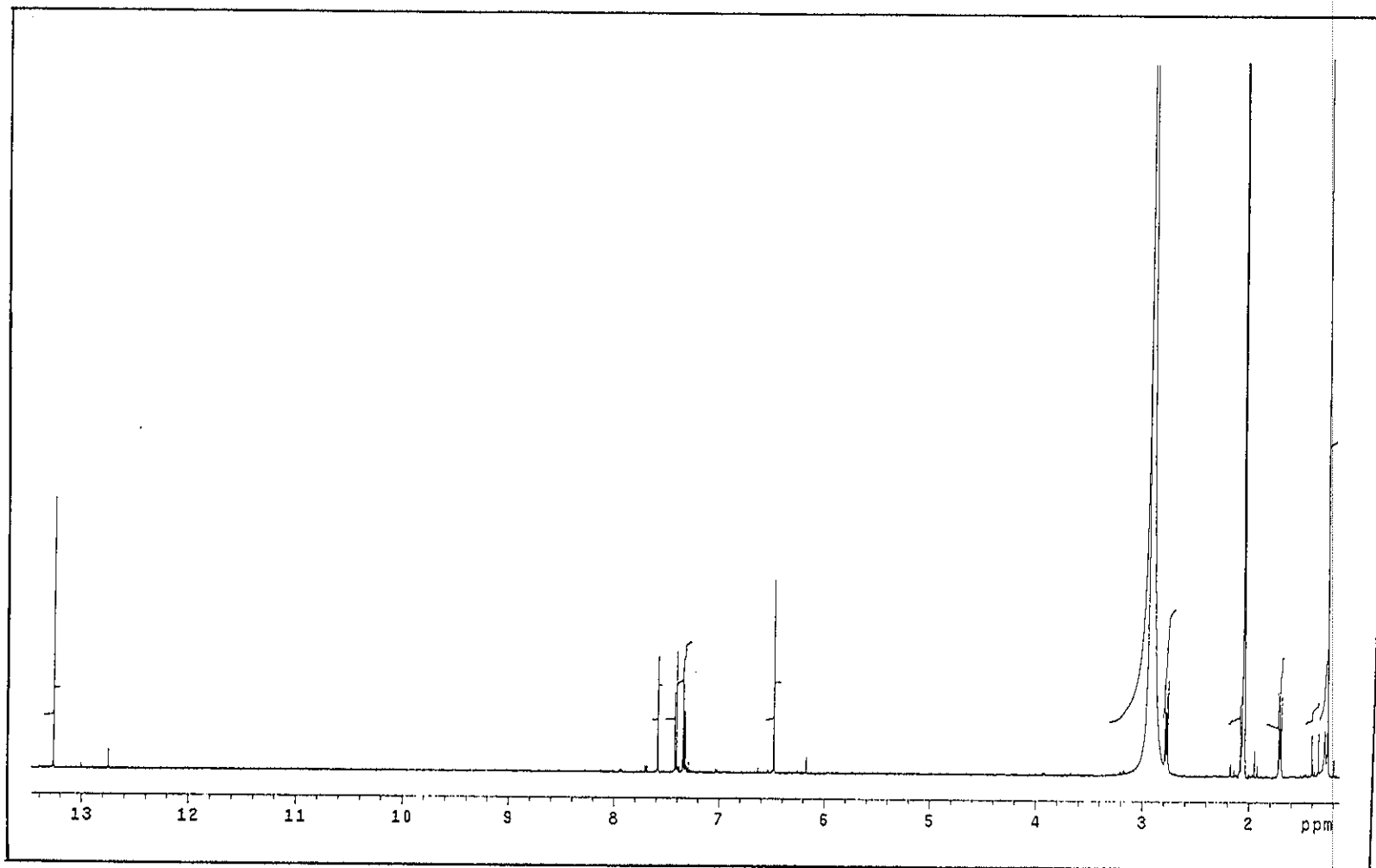


Figure 3.42 ^1H NMR (500 MHz)(Acetone- d_6) spectrum of TR15

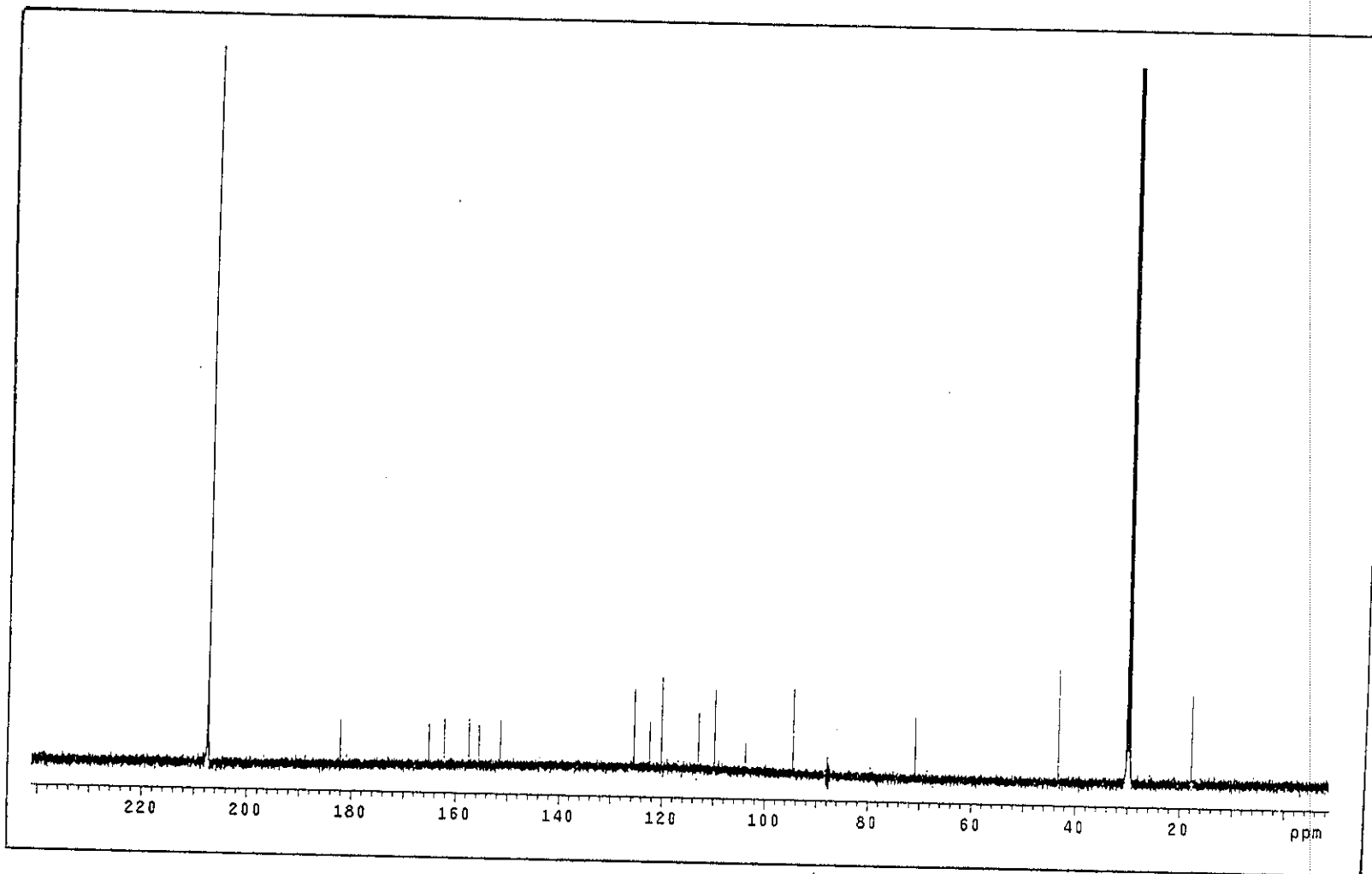


Figure 3.43 ^{13}C NMR (125 MHz)(Acetone- d_6) spectrum of TR15

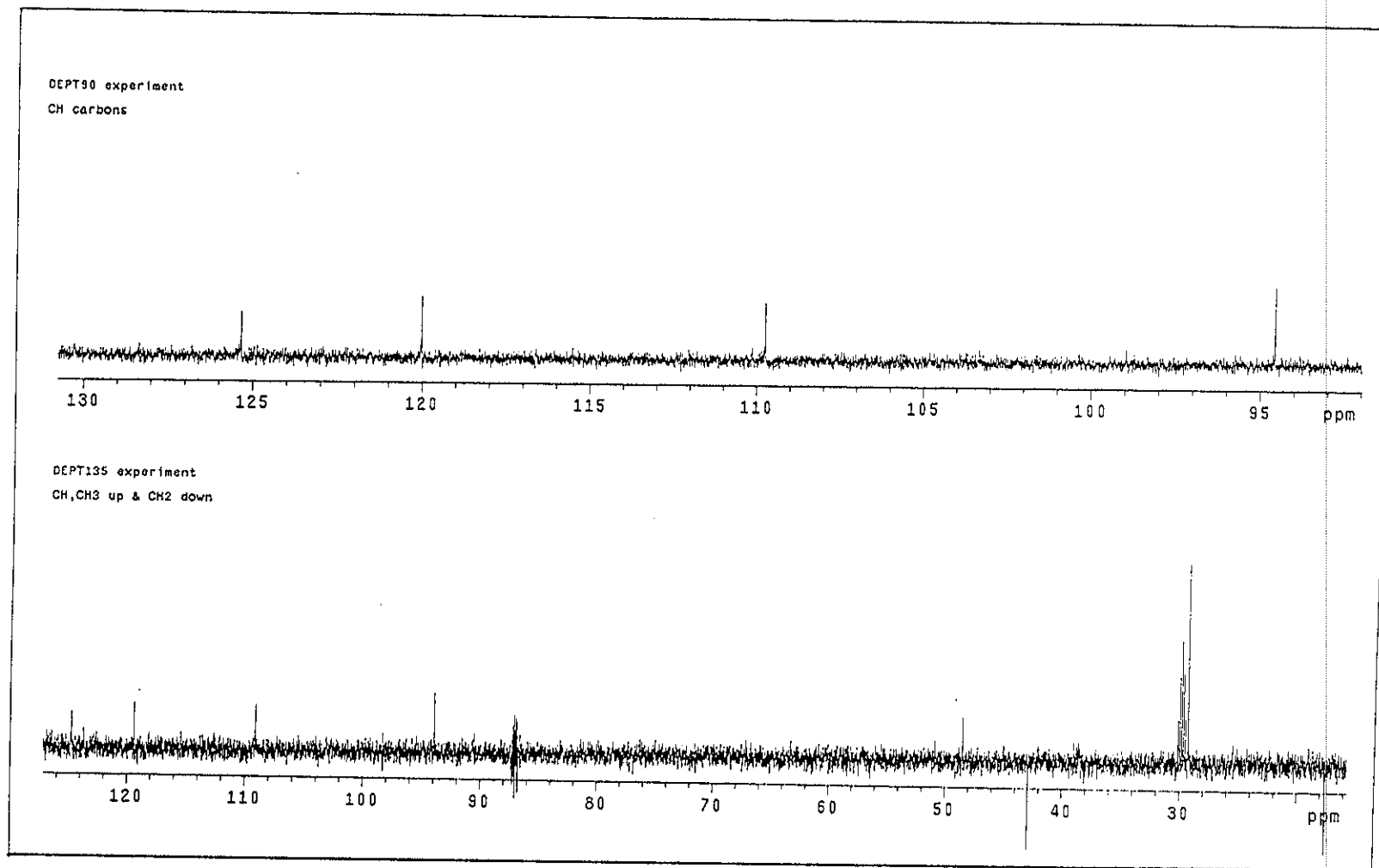


Figure 3.44 DEPT spectrum of TR15

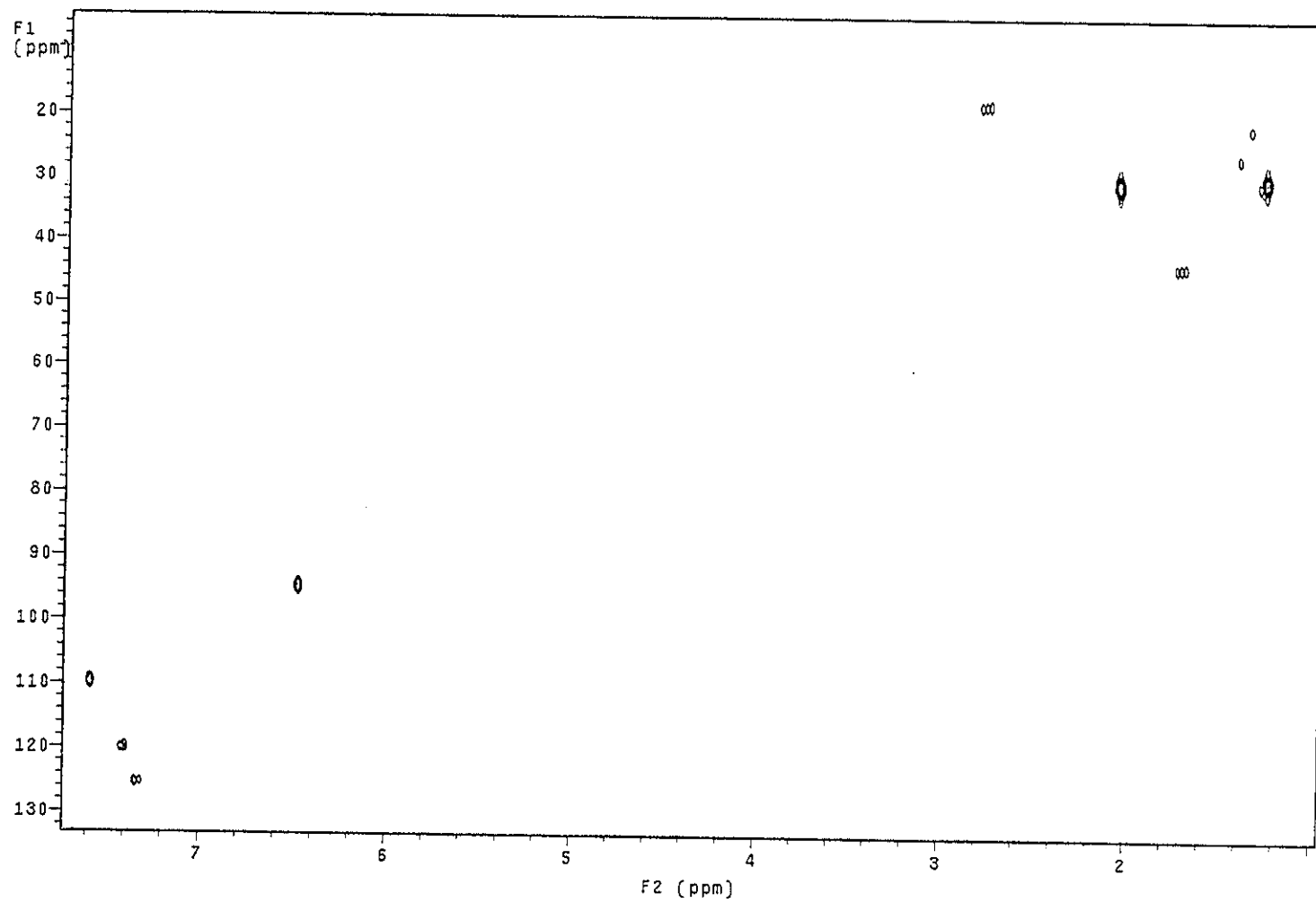


Figure 3.45 2D HMQC spectrum of TR15

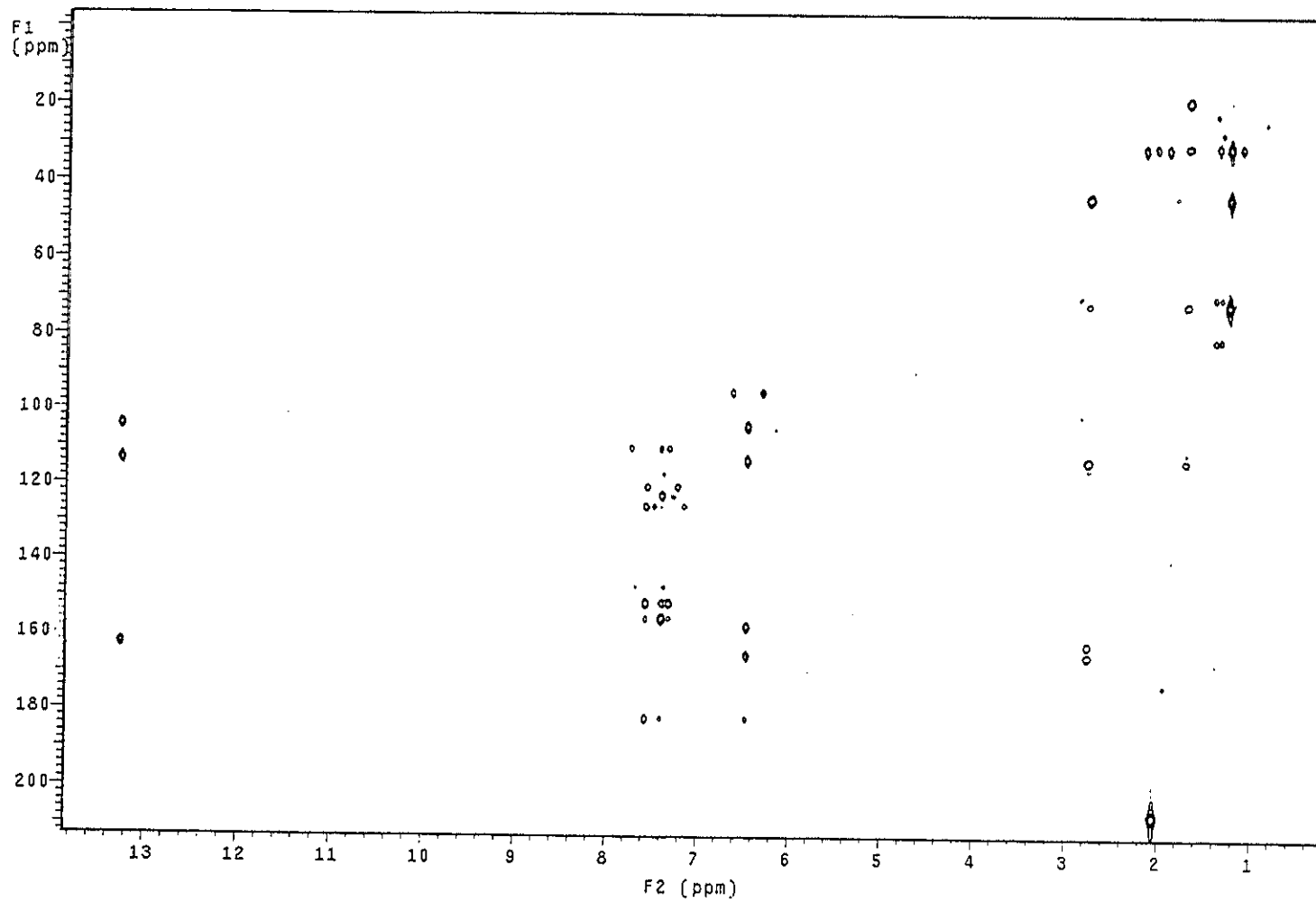


Figure 3.46 2D HMBC spectrum of TR15

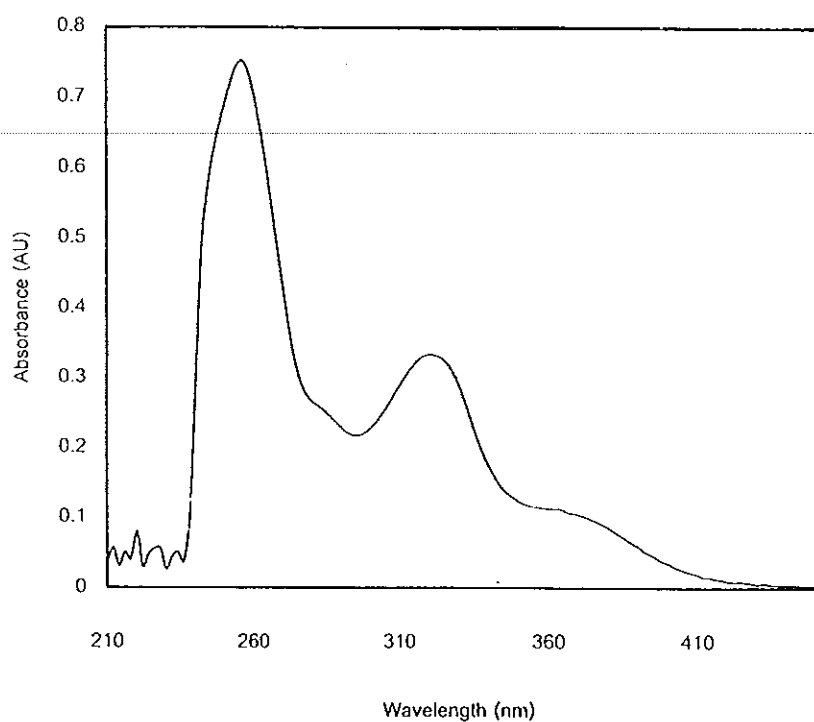


Figure 3.47 UV (MeOH) spectrum of TR19

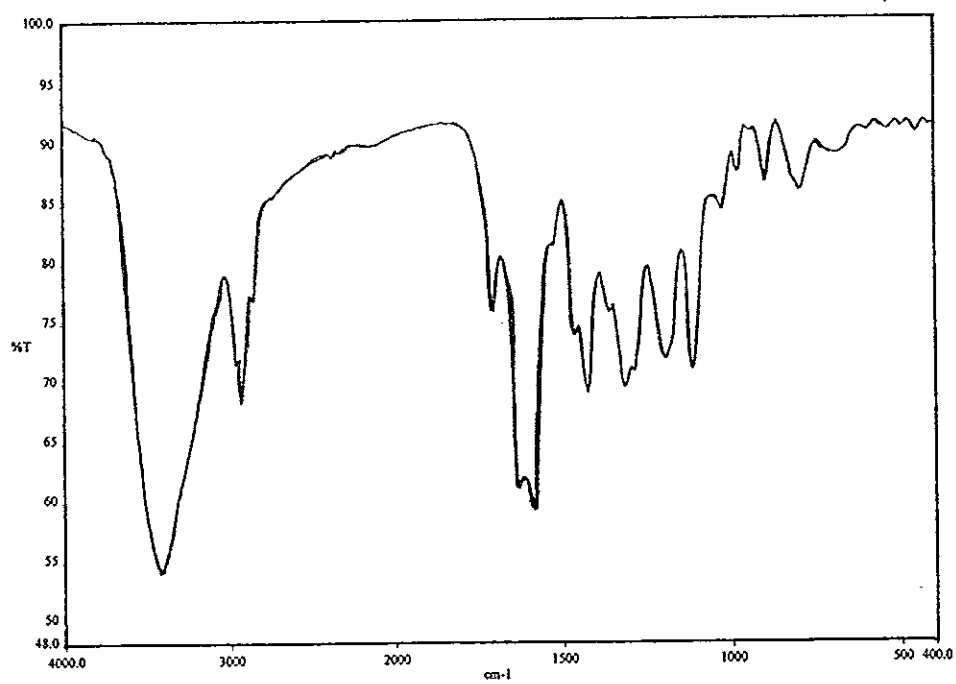


Figure 3.48 FT-IR (neat) spectrum of TR19

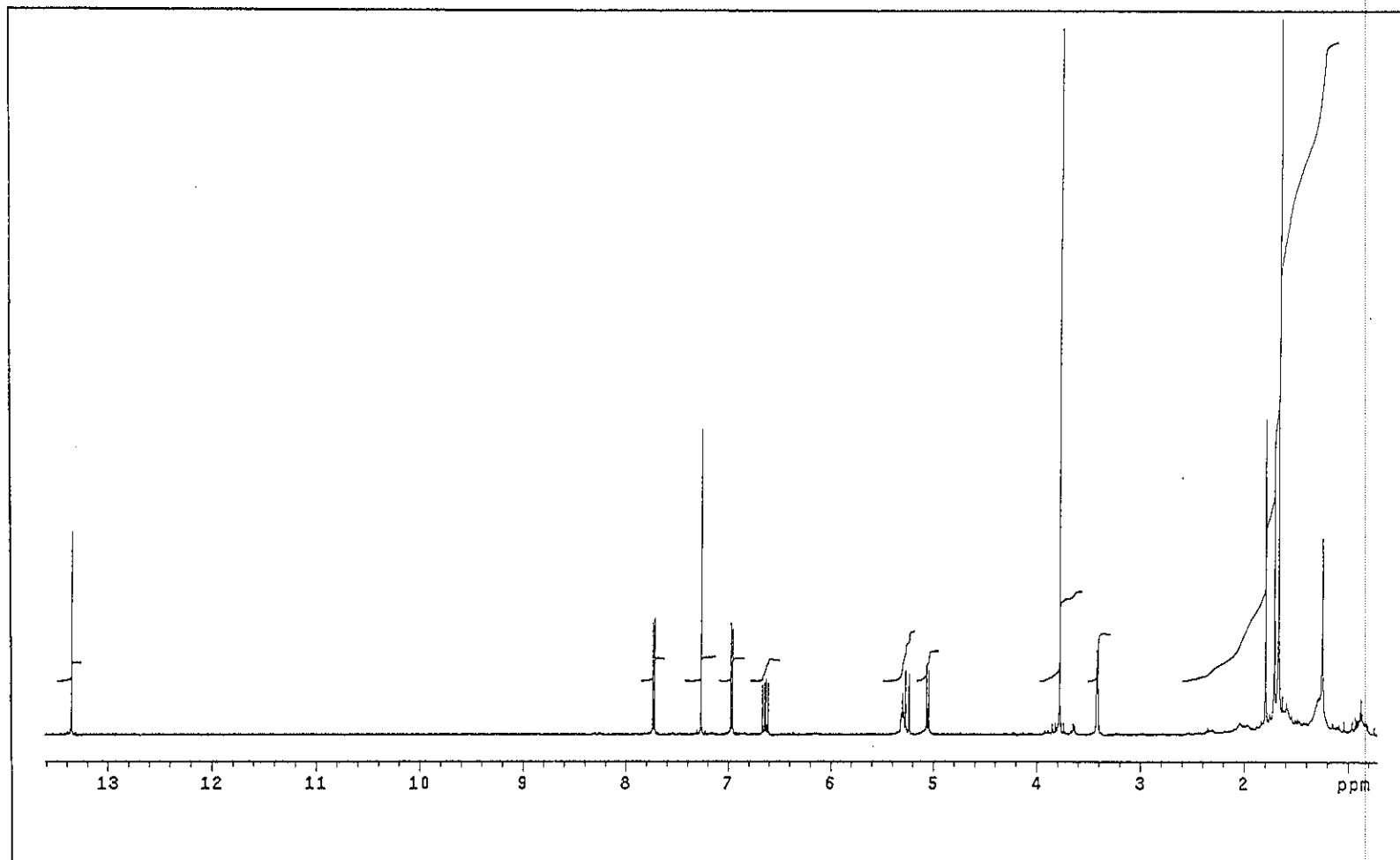


Figure 3.49 ^1H NMR (500 MHz)(CDCl_3) spectrum of TR19

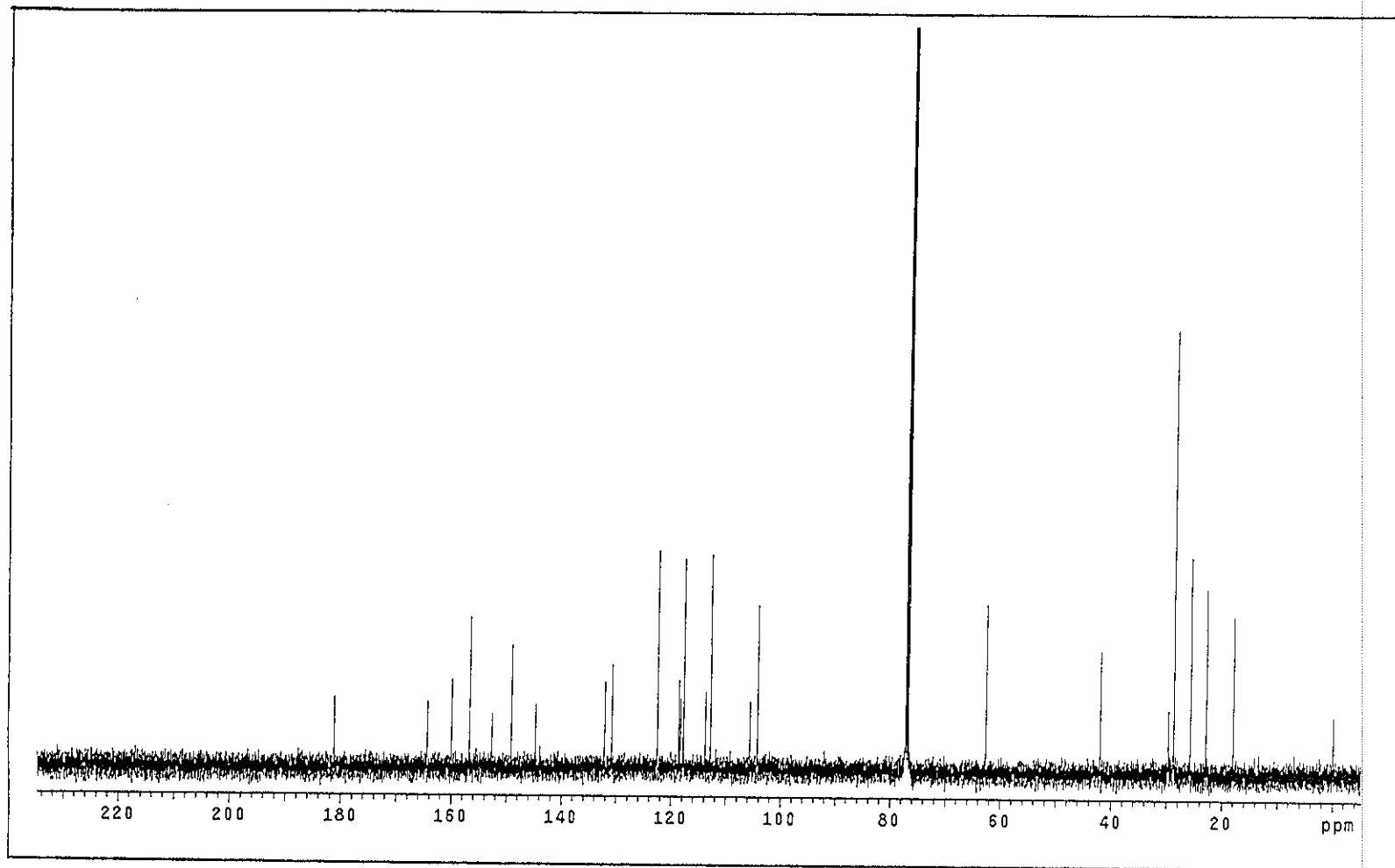


Figure 3.50 ^{13}C NMR (125 MHz)(CDCl_3) spectrum of TR19

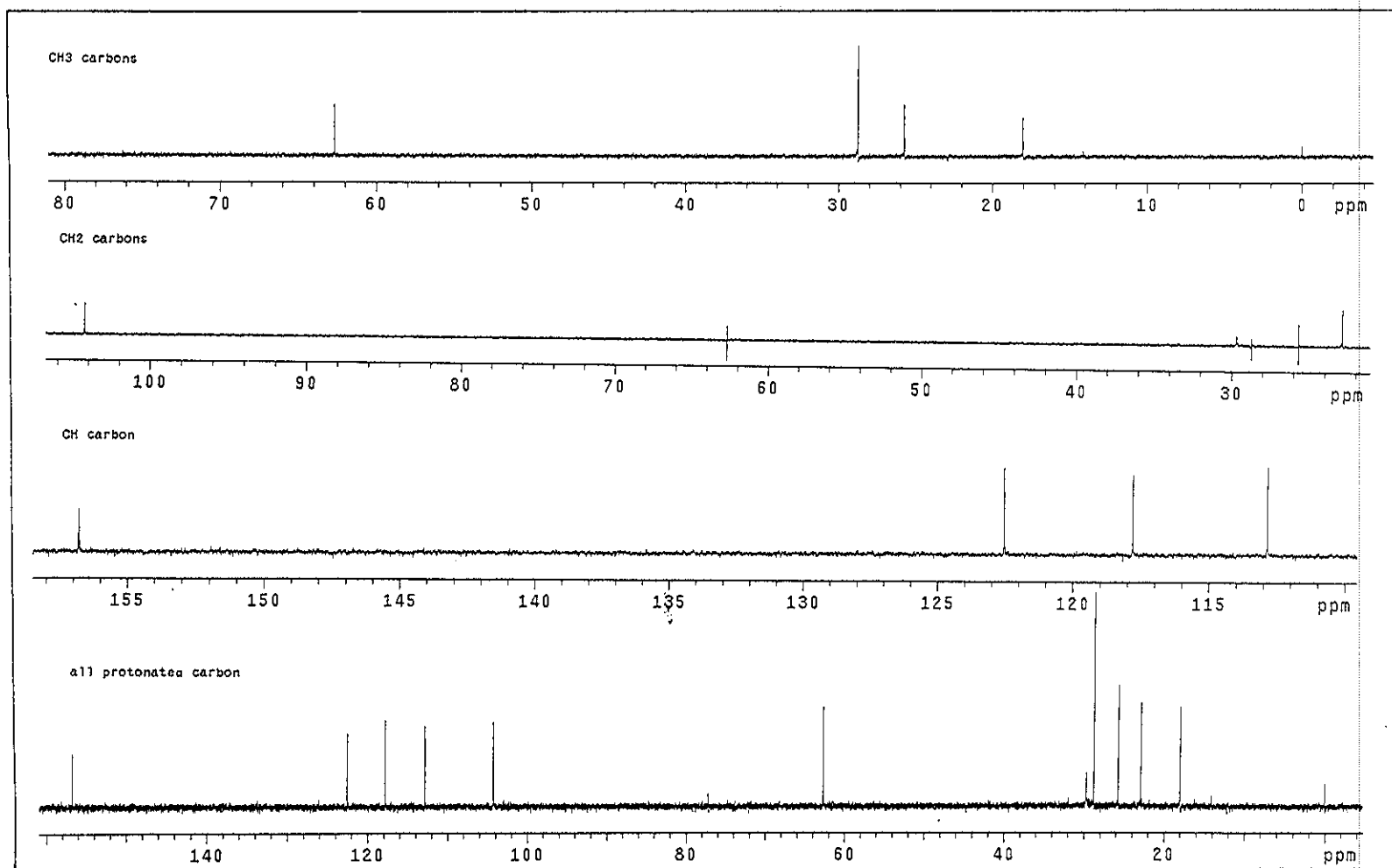


Figure 3.51 DEPT spectrum of TR19

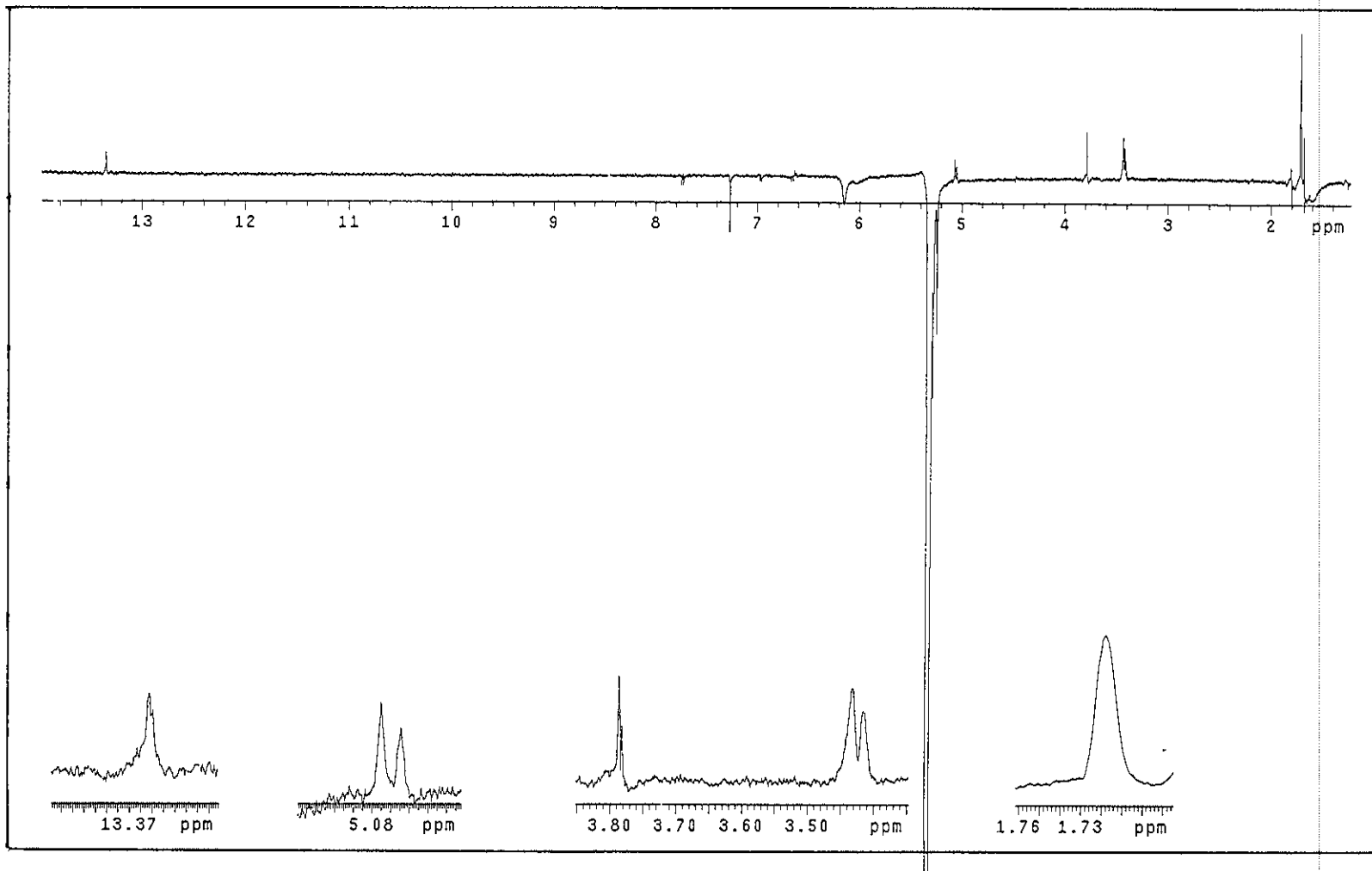


Figure 3.52 NOEDIFF spectrum of TR19 after irradiation at δ_{H} 5.30

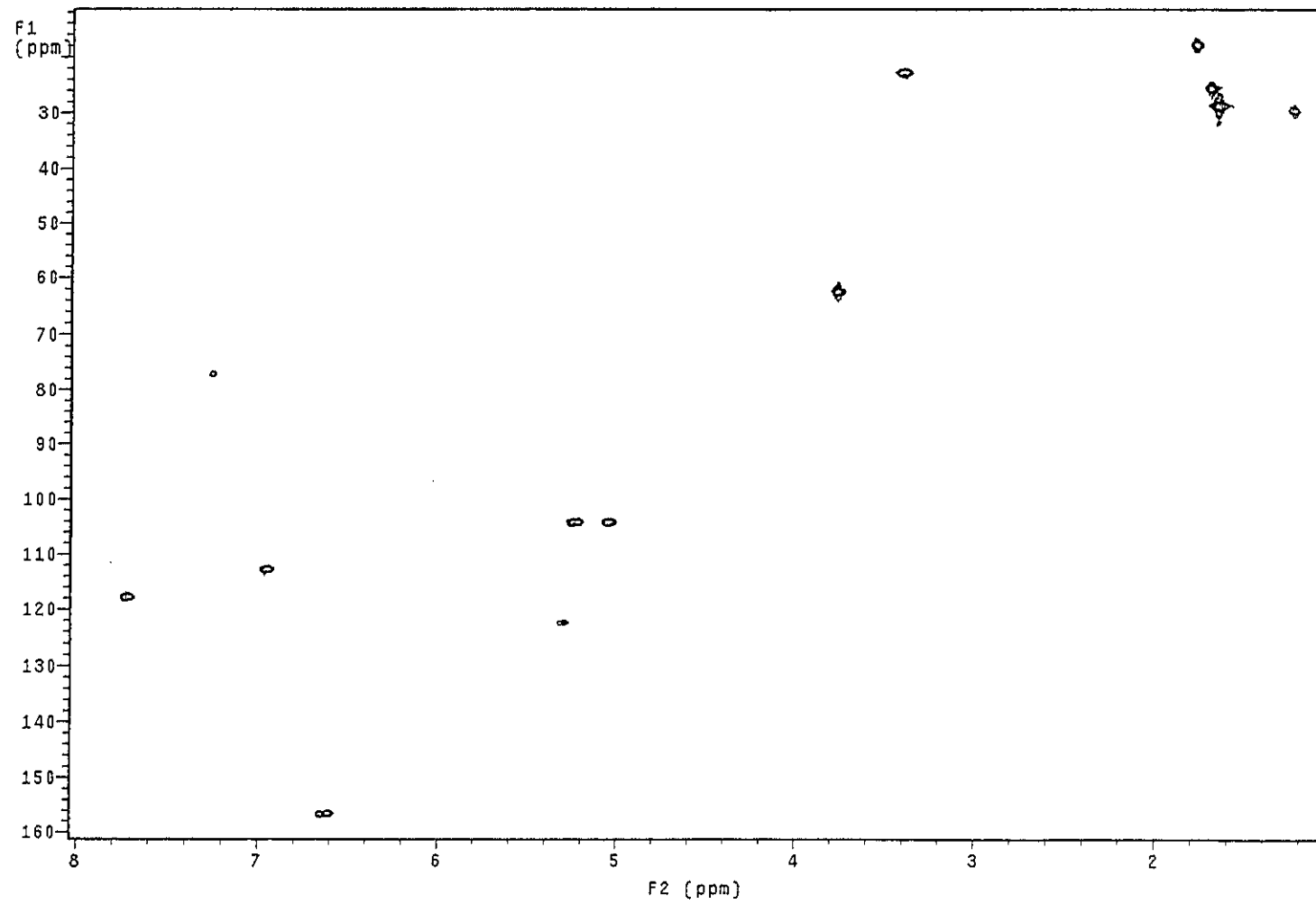


Figure 3.53 2D HMQC spectrum of TR19

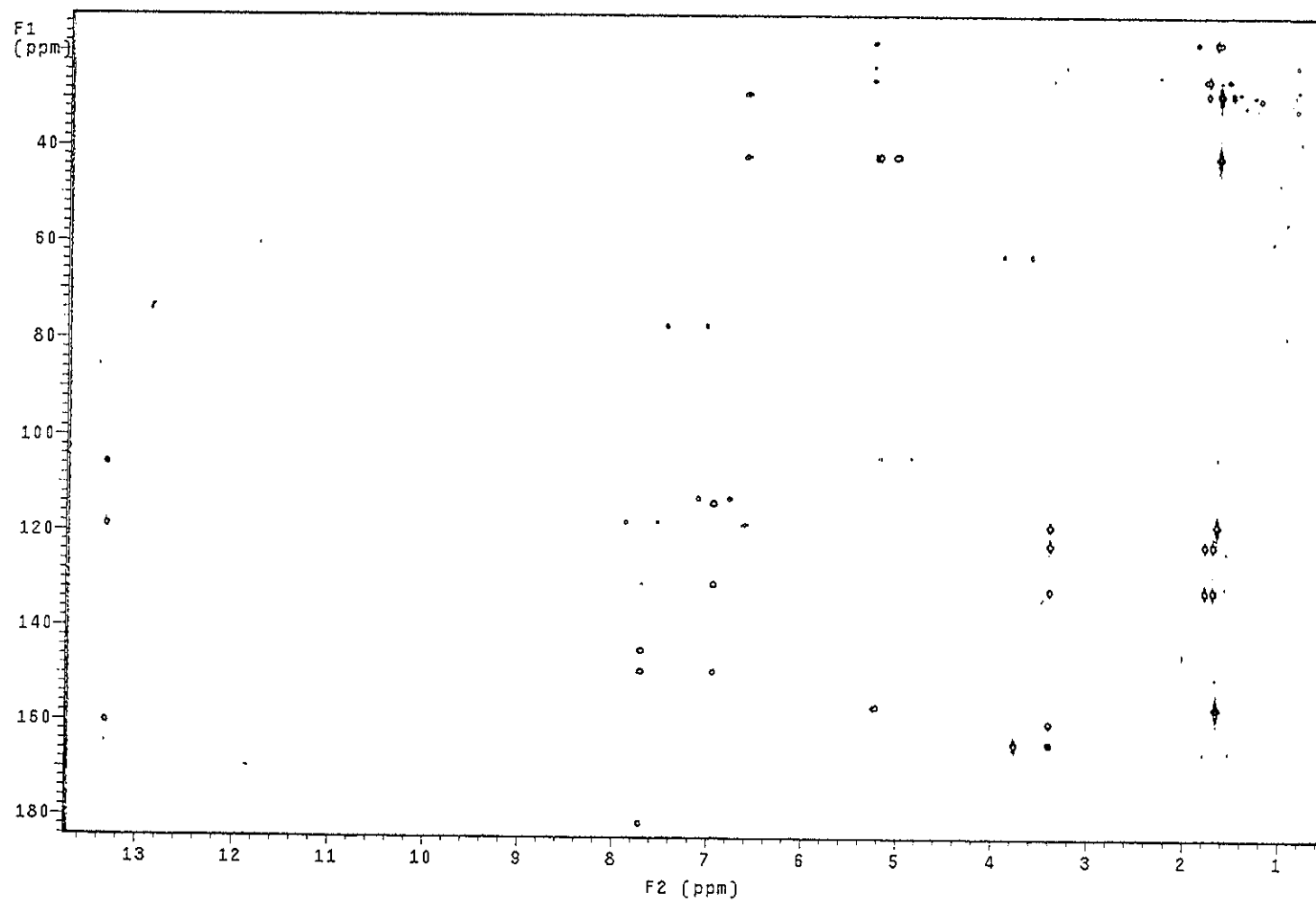


Figure 3.54 2D HMBC spectrum of TR19

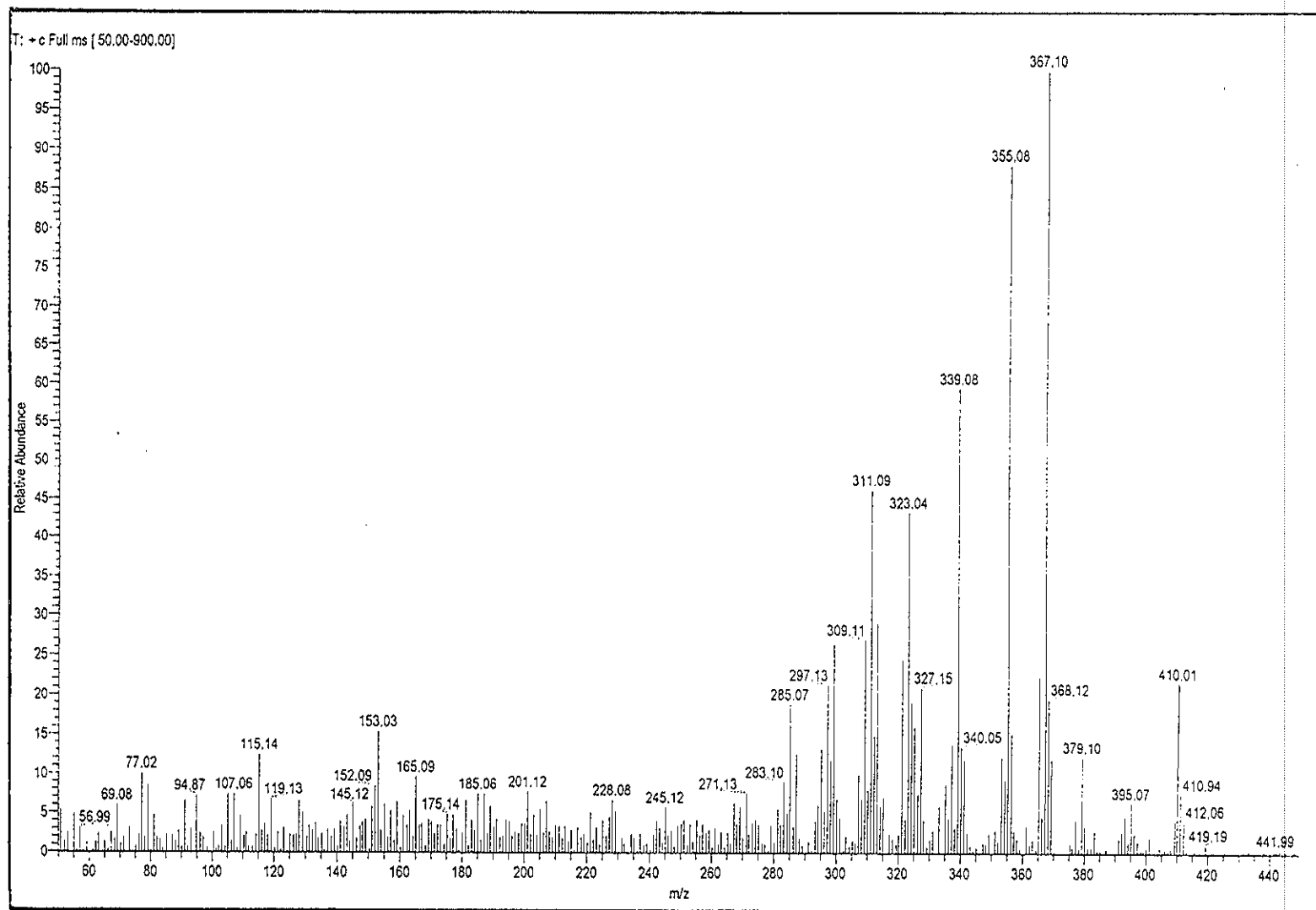


Figure 3.55 Mass spectrum of TR19

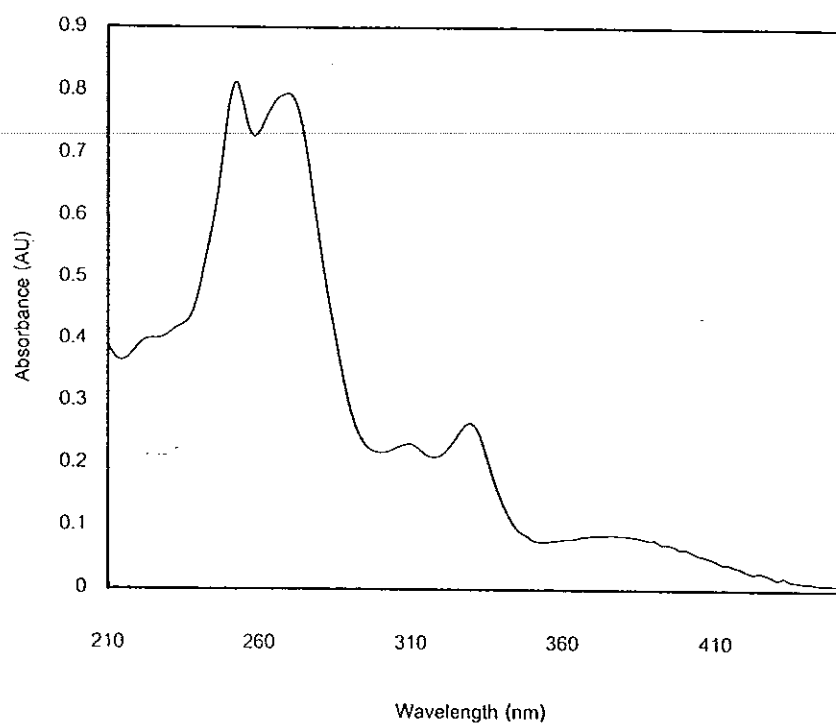


Figure 3.56 UV (MeOH) spectrum of TR10

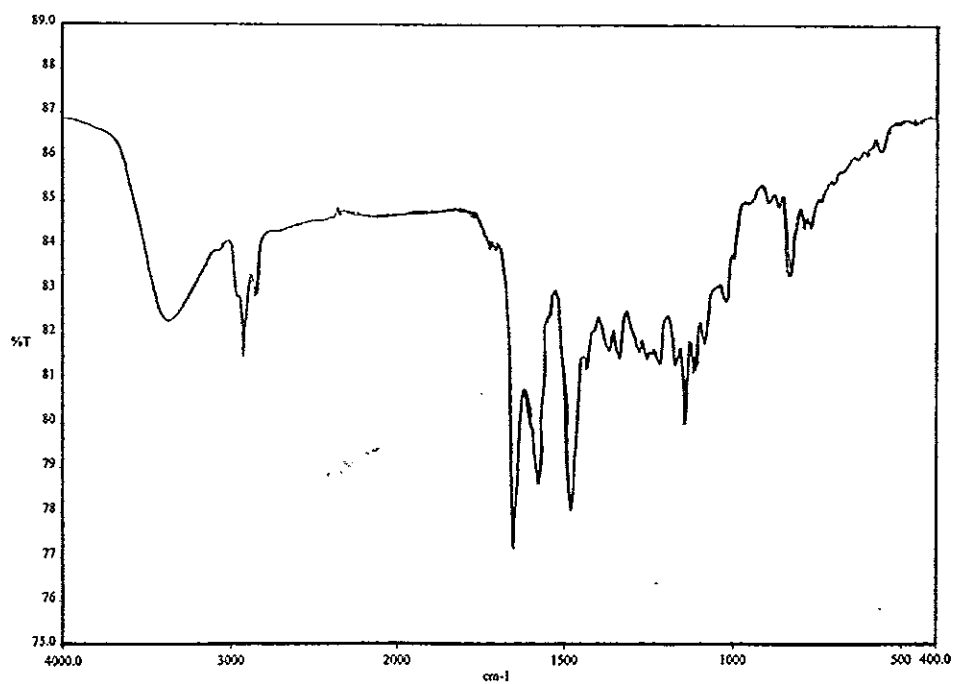


Figure 3.57 FT-IR (neat) spectrum of TR10

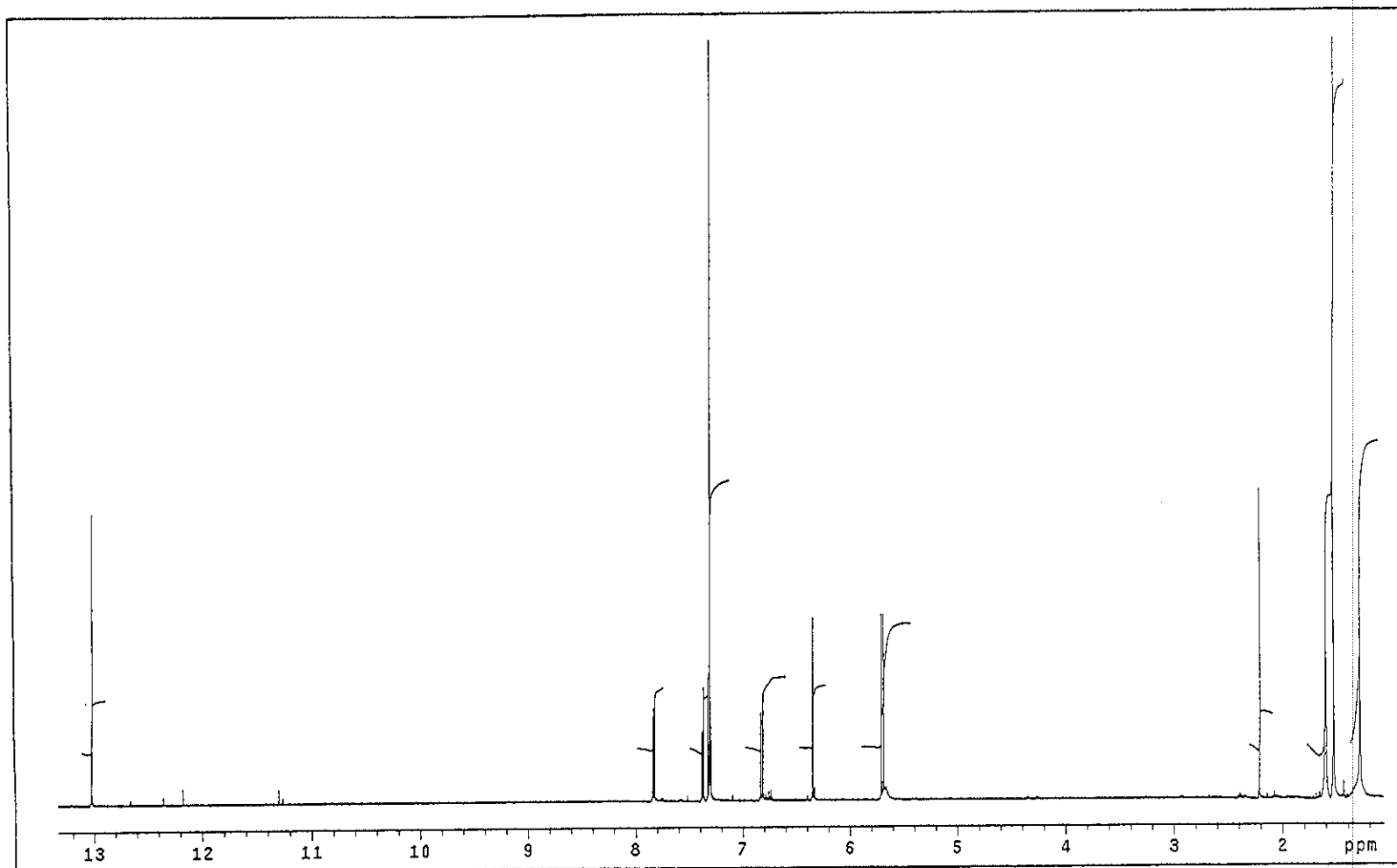


Figure 3.58 ^1H NMR (500 MHz)(CDCl_3) spectrum of TR10

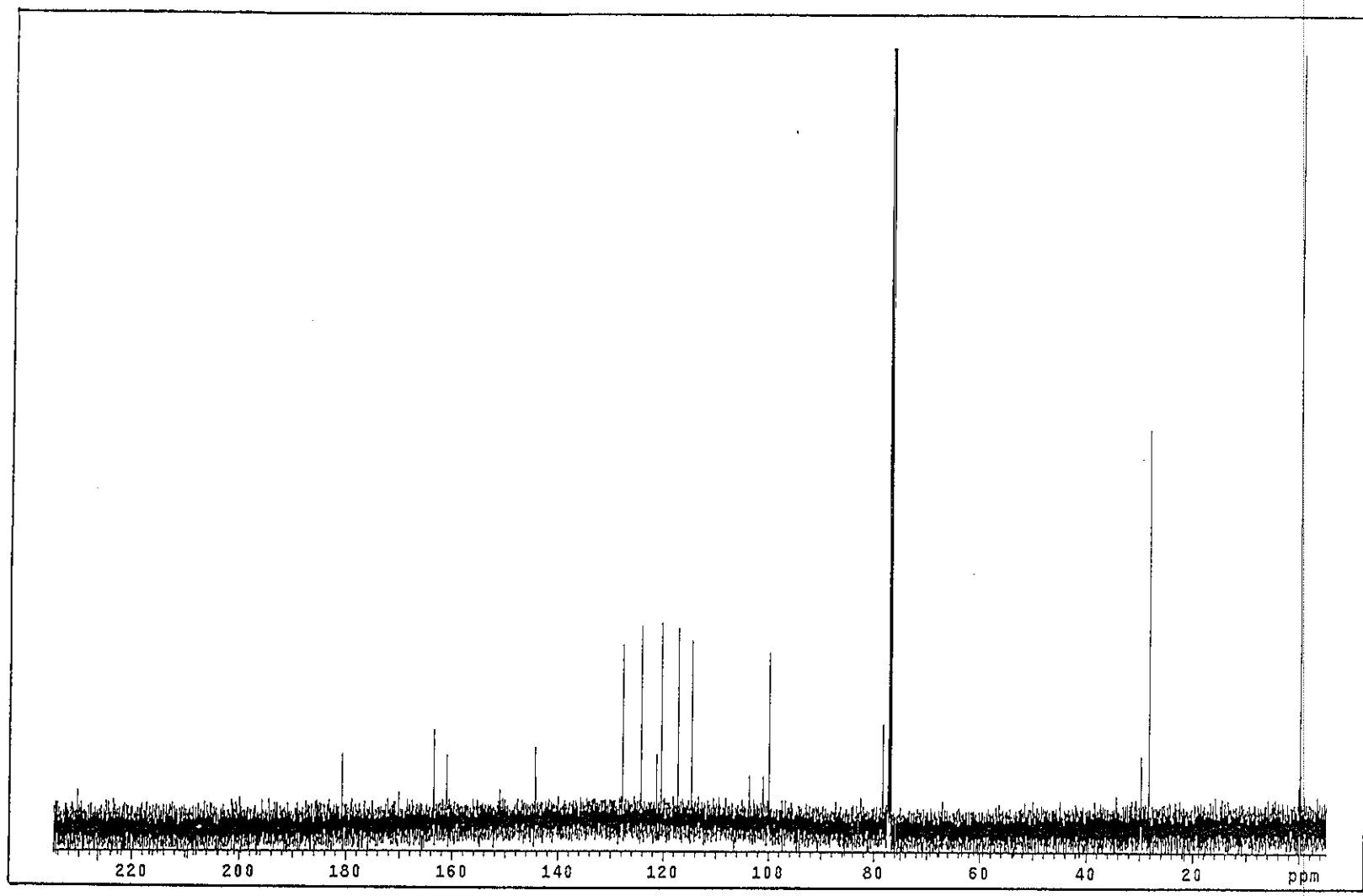


Figure 3.59 ^{13}C NMR (125 MHz)(CDCl_3) spectrum of TR10

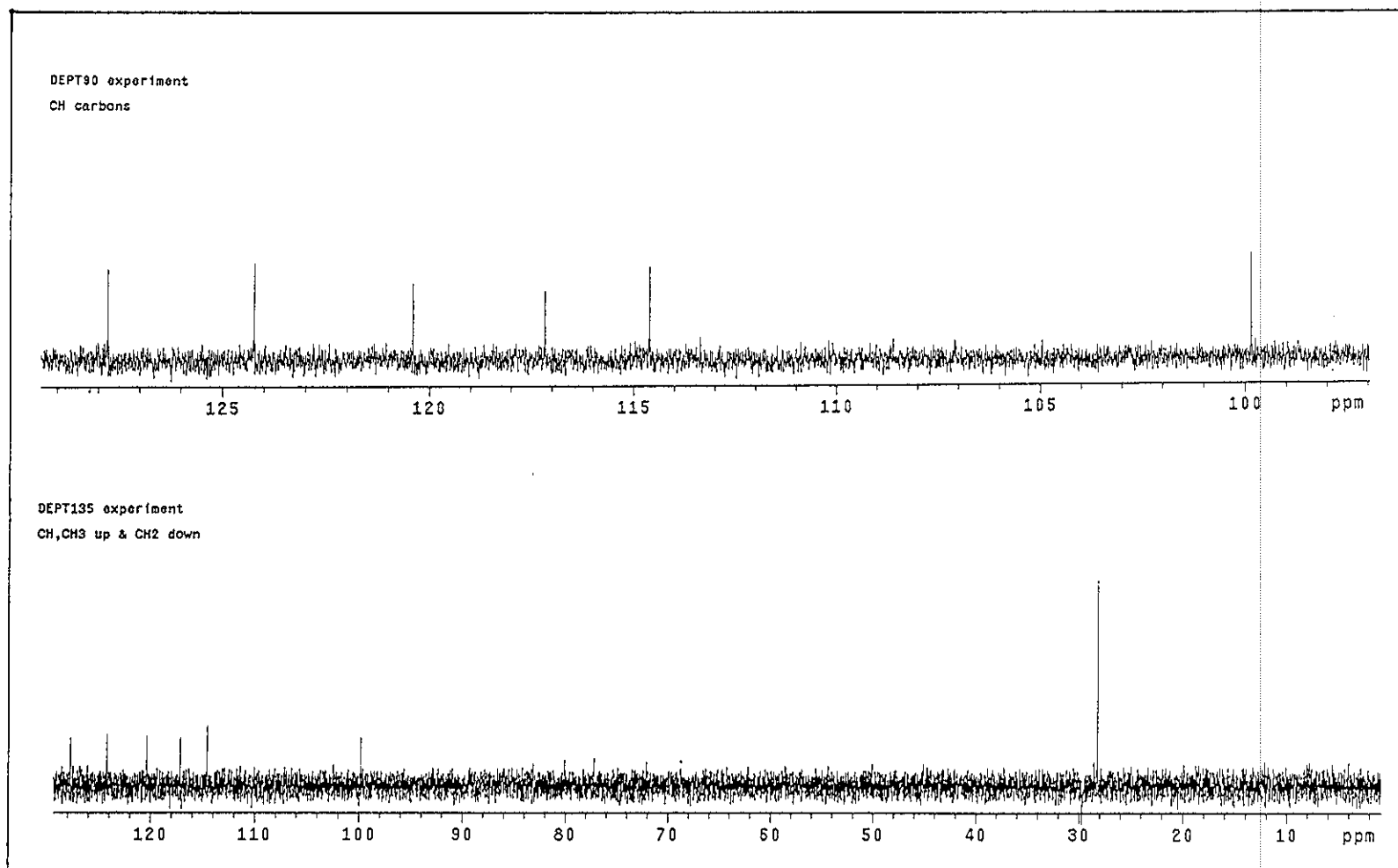


Figure 3.60 DEPT spectrum of TR10

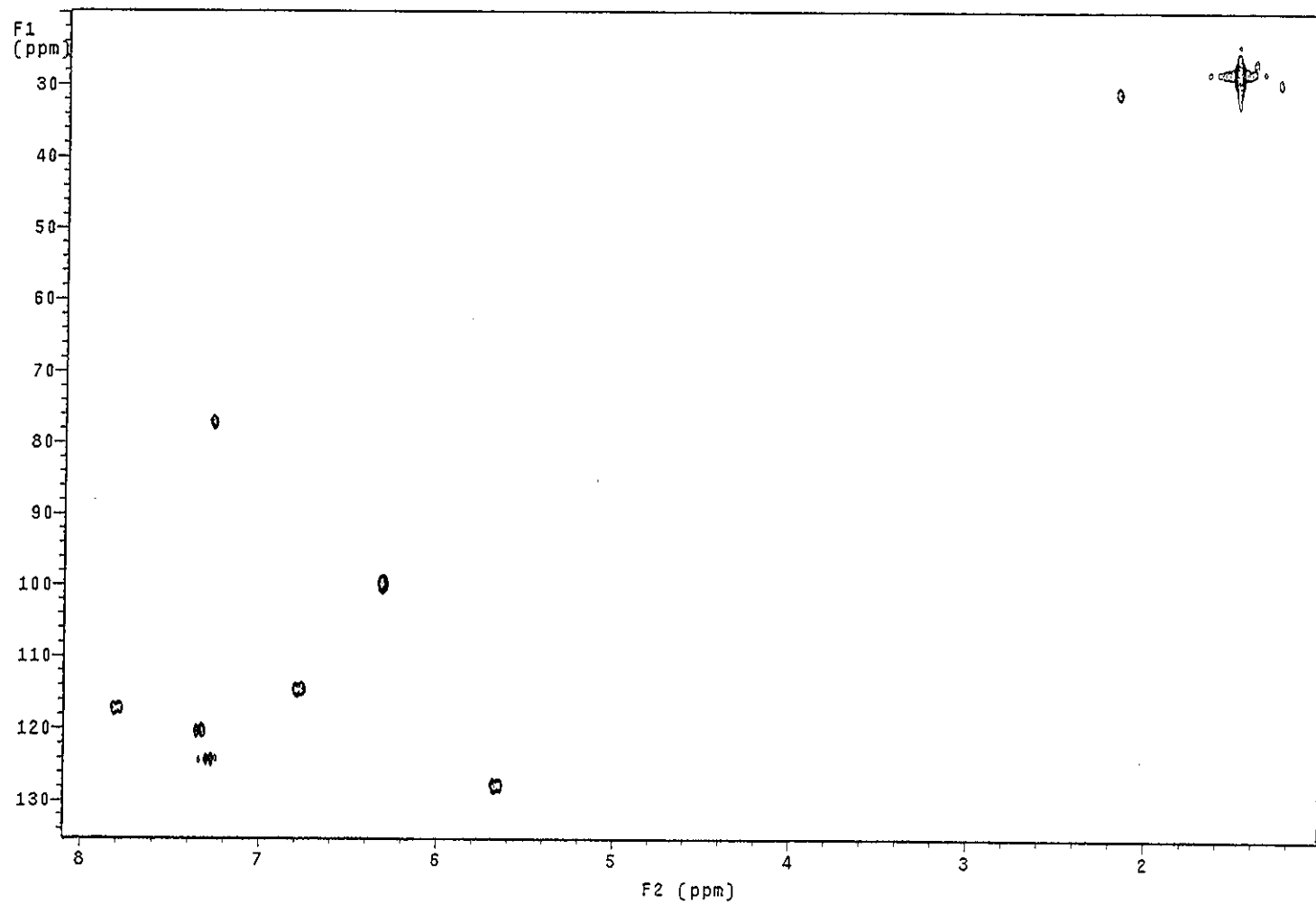


Figure 3.61 2D HMQC spectrum of TR10

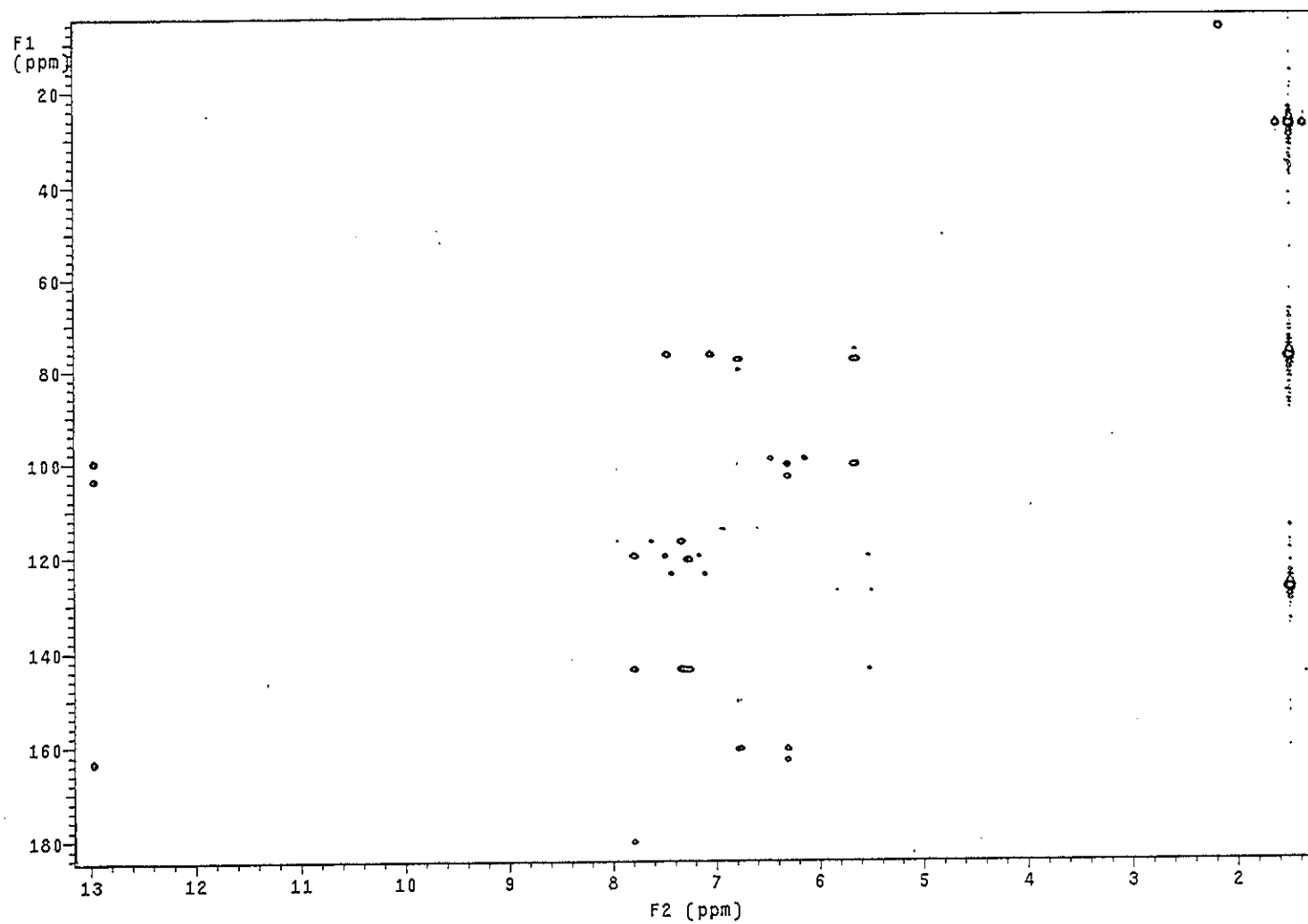


Figure 3.62 2D HMBC spectrum of TR10

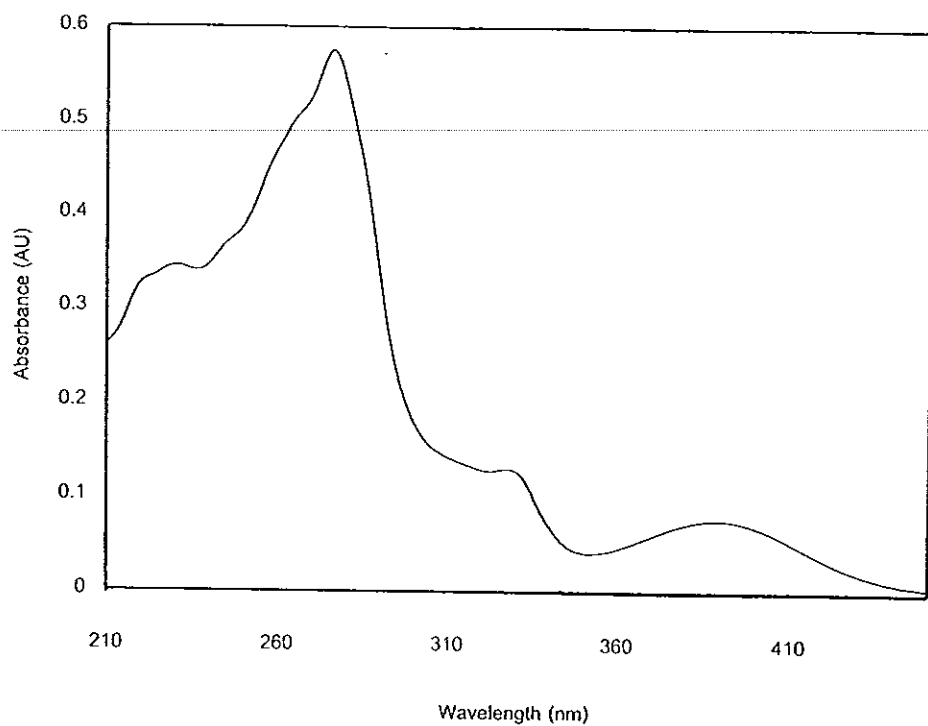


Figure 3.63 UV (MeOH) spectrum of TR6

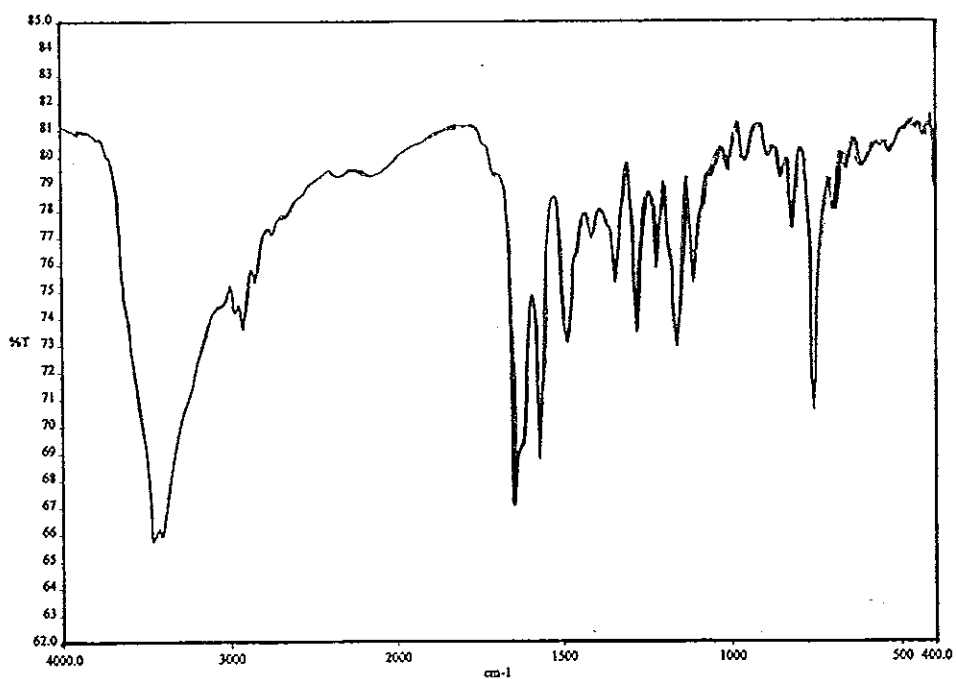


Figure 3.64 FT-IR (neat) spectrum of TR6

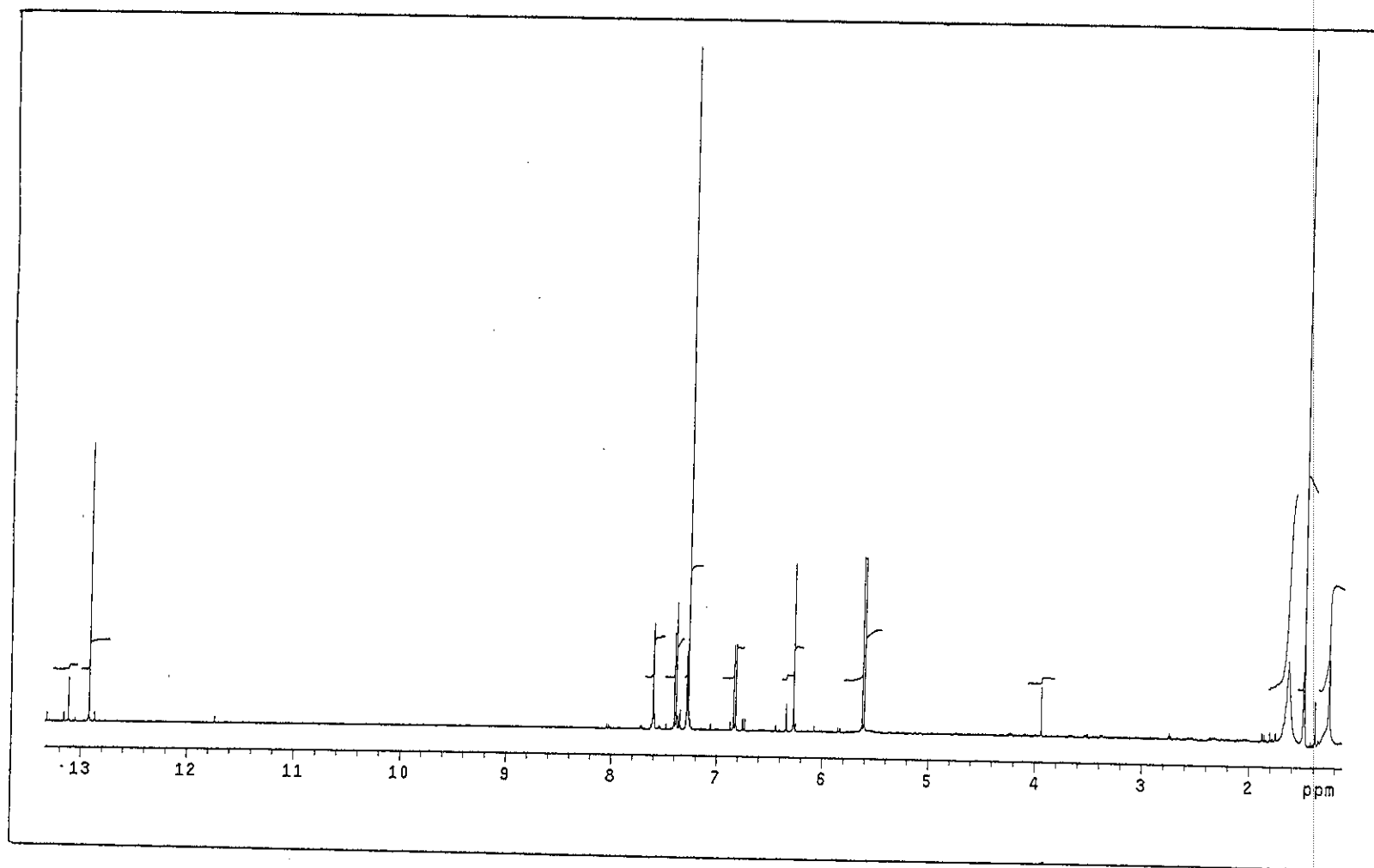


Figure 3.65 ^1H NMR (500 MHz)(CDCl_3) spectrum of TR6

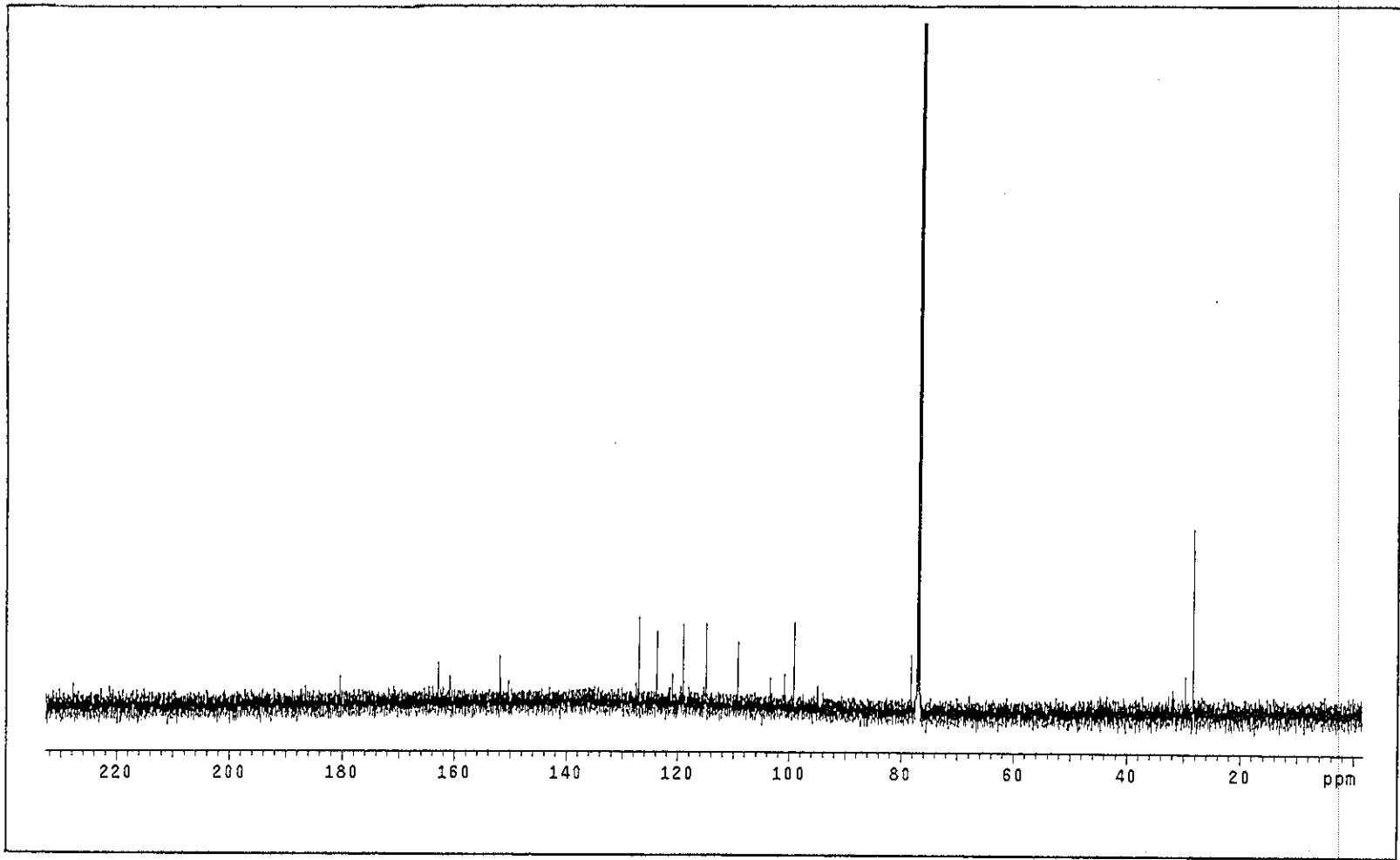


Figure 3.66 ^{13}C NMR (125 MHz)(CDCl_3) spectrum of TR6

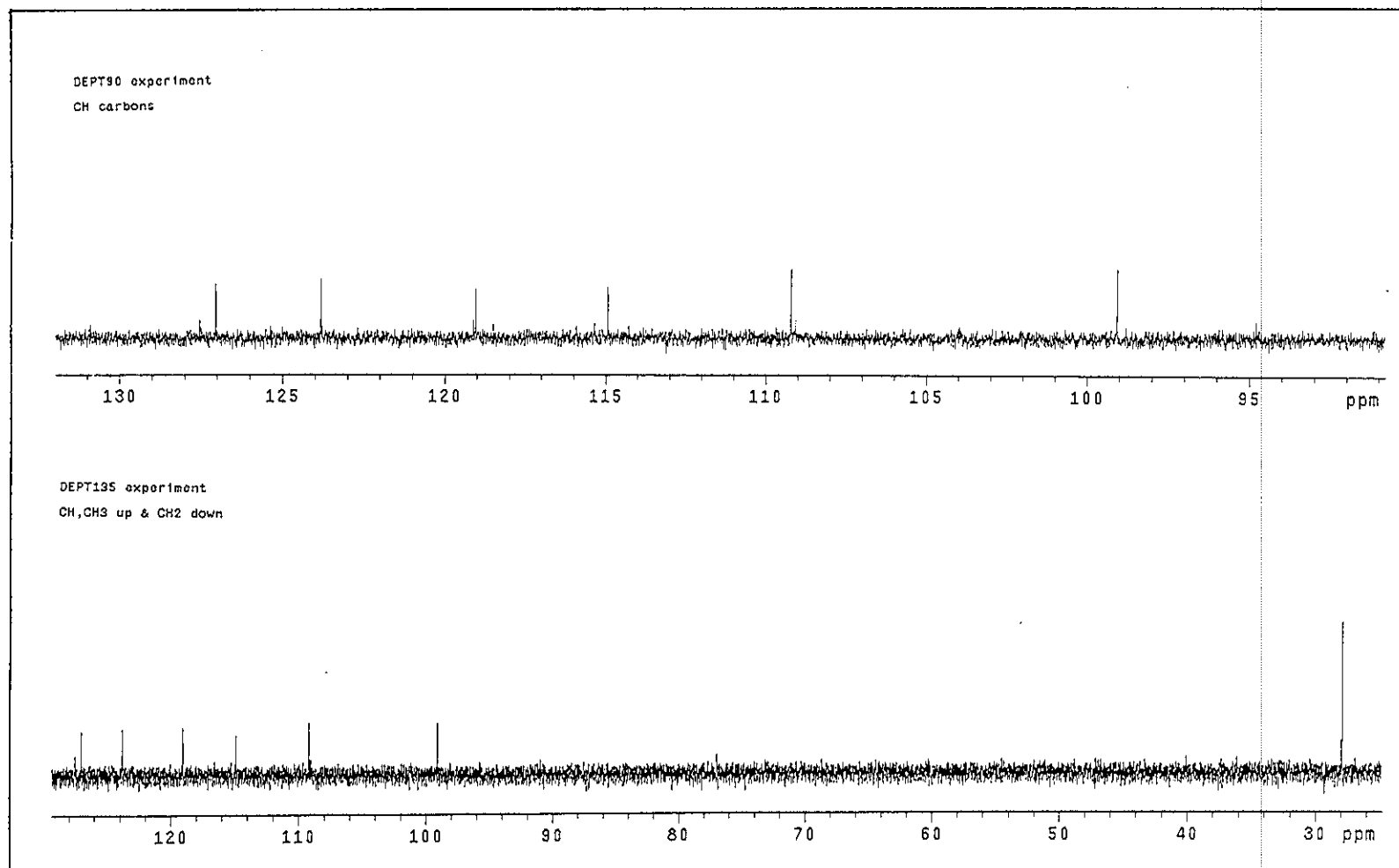


Figure 3.67 DEPT spectrum of TR6

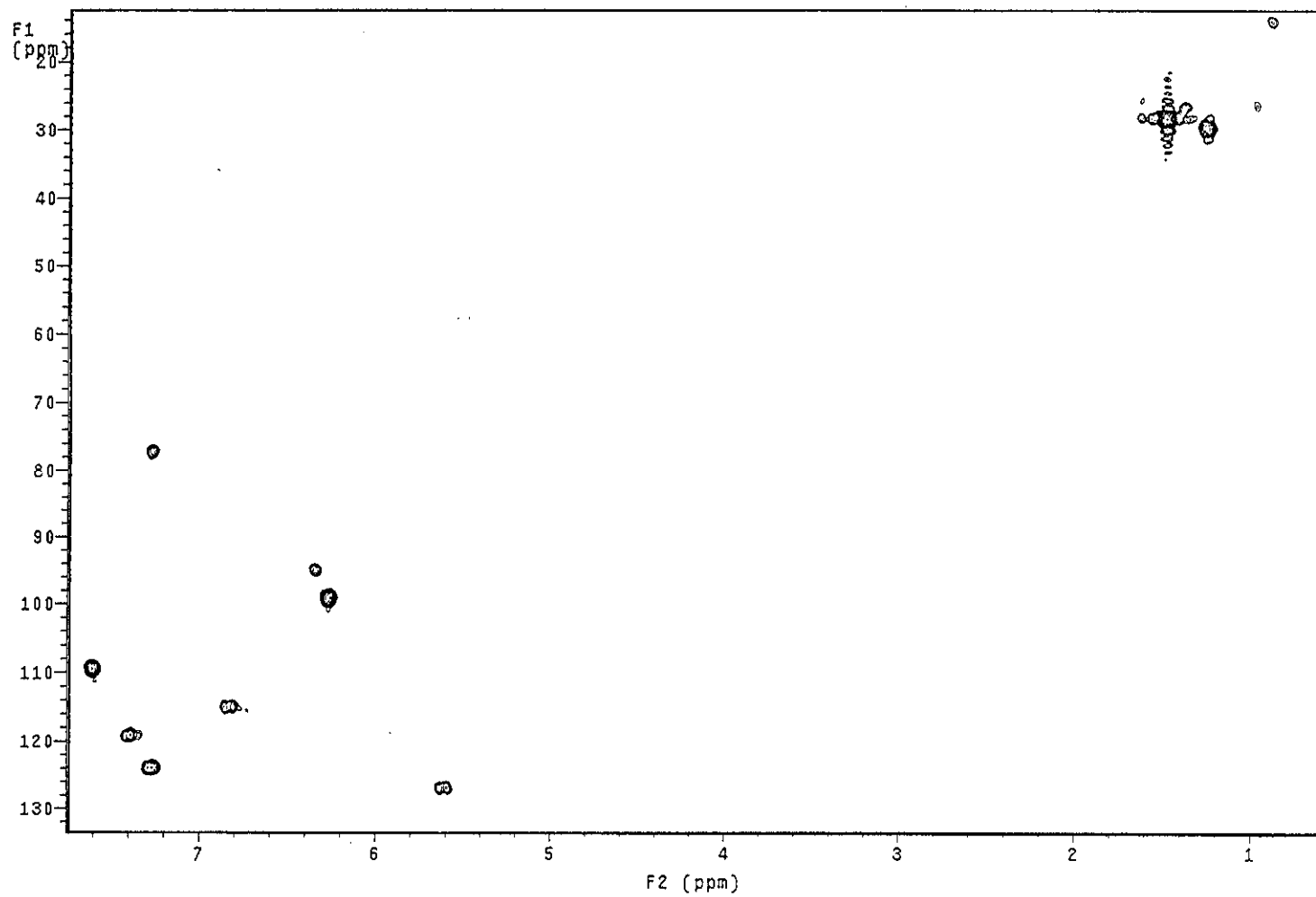


Figure 3.68 2D HMQC spectrum of TR6

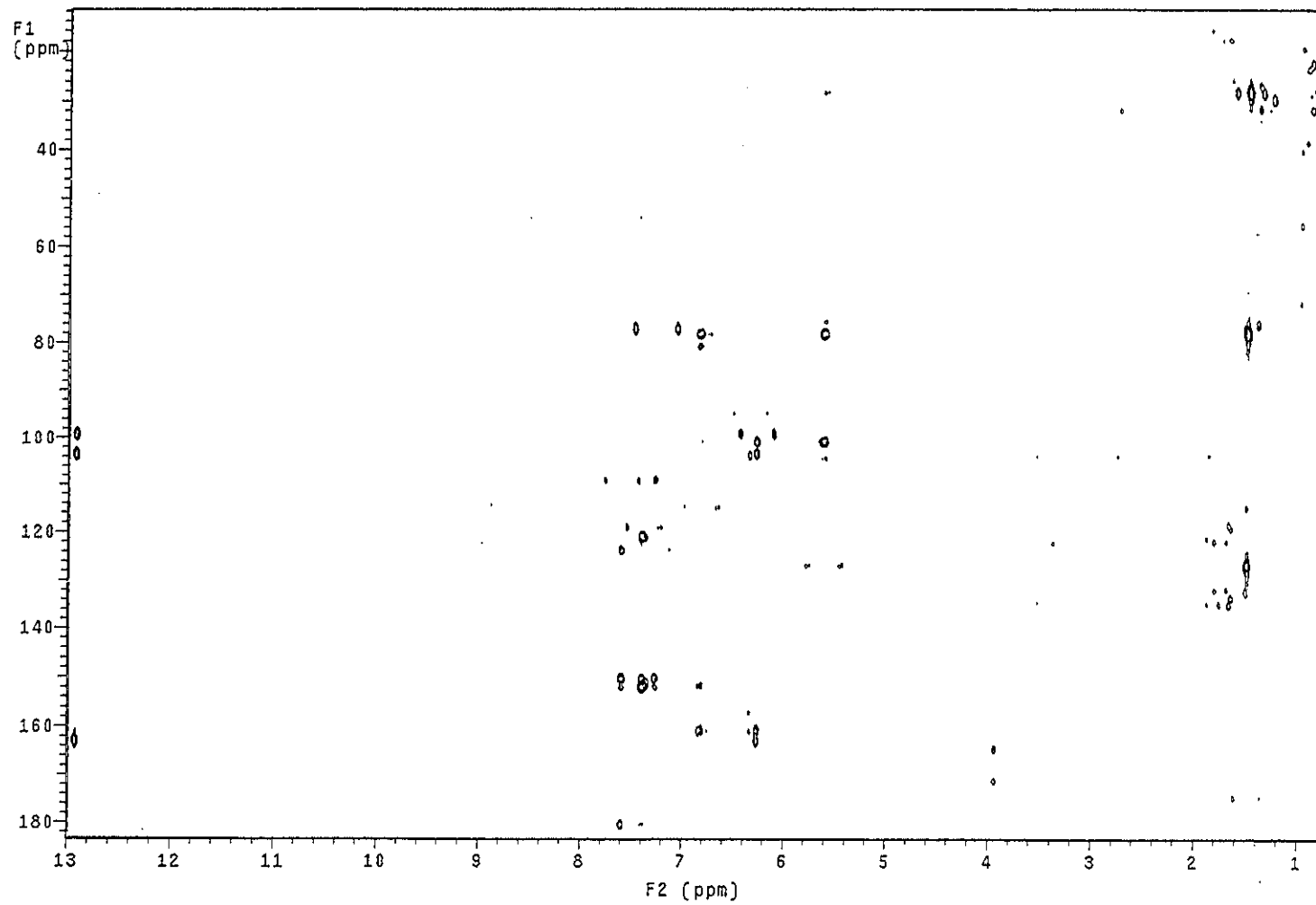


Figure 3.69 2D HMBC spectrum of TR6

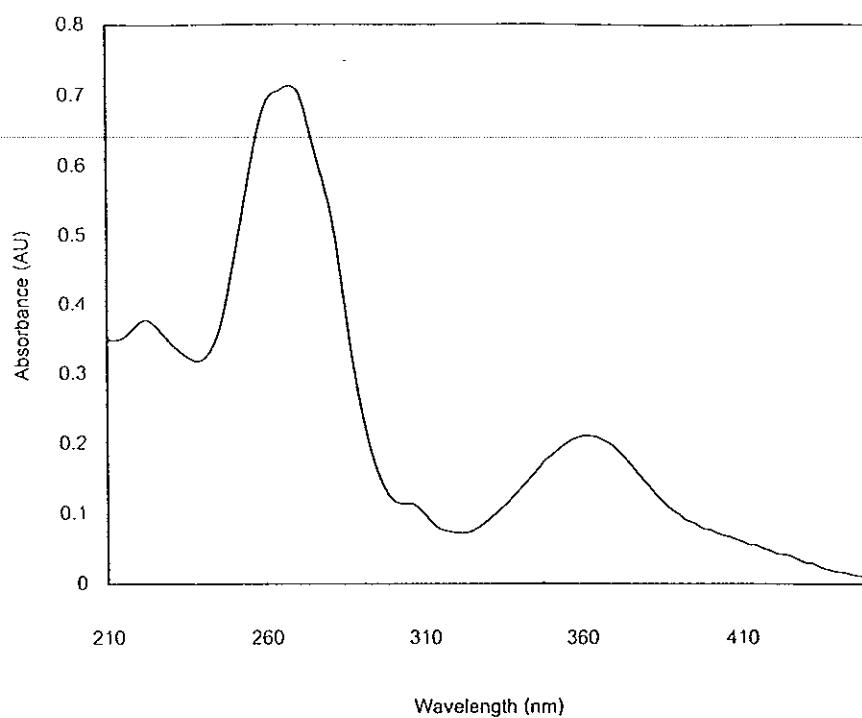


Figure 3.70 UV (MeOH) spectrum of TR18

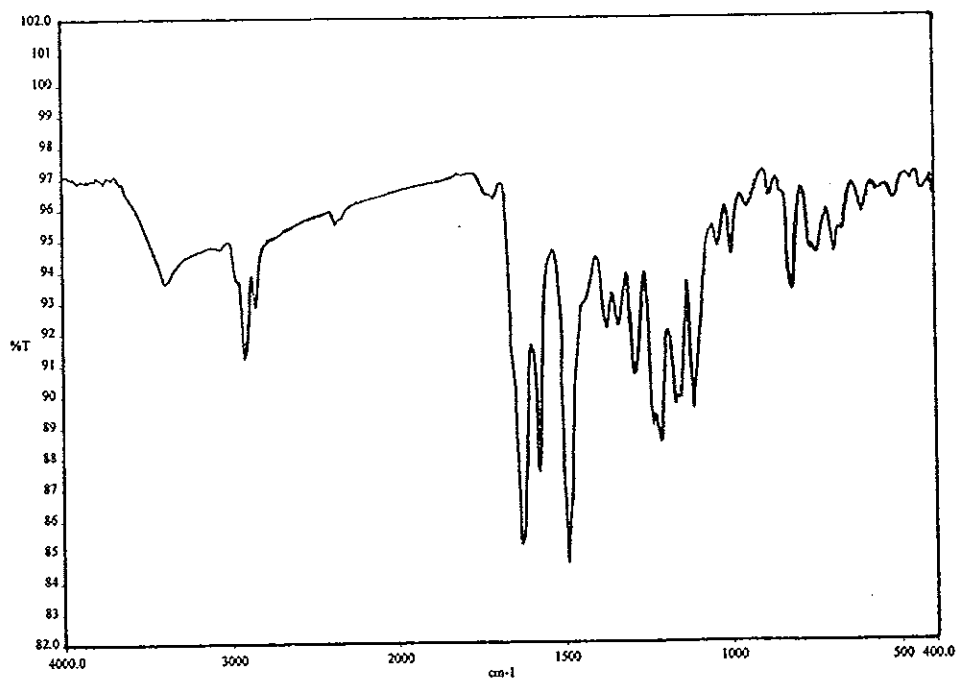


Figure 3.71 FT-IR (neat) spectrum of TR18

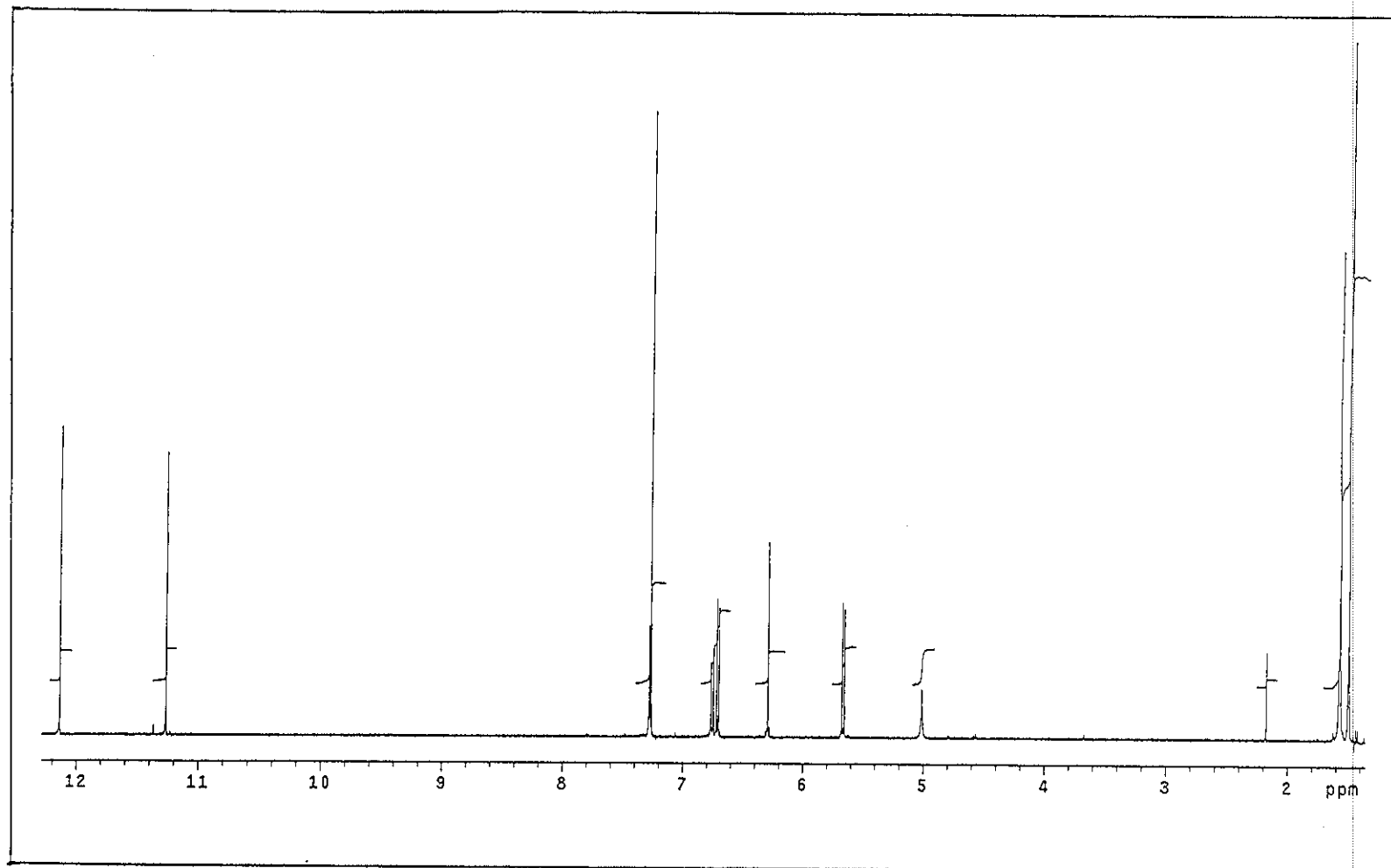


Figure 3.72 ^1H NMR (500 MHz)(CDCl_3) spectrum of TR18

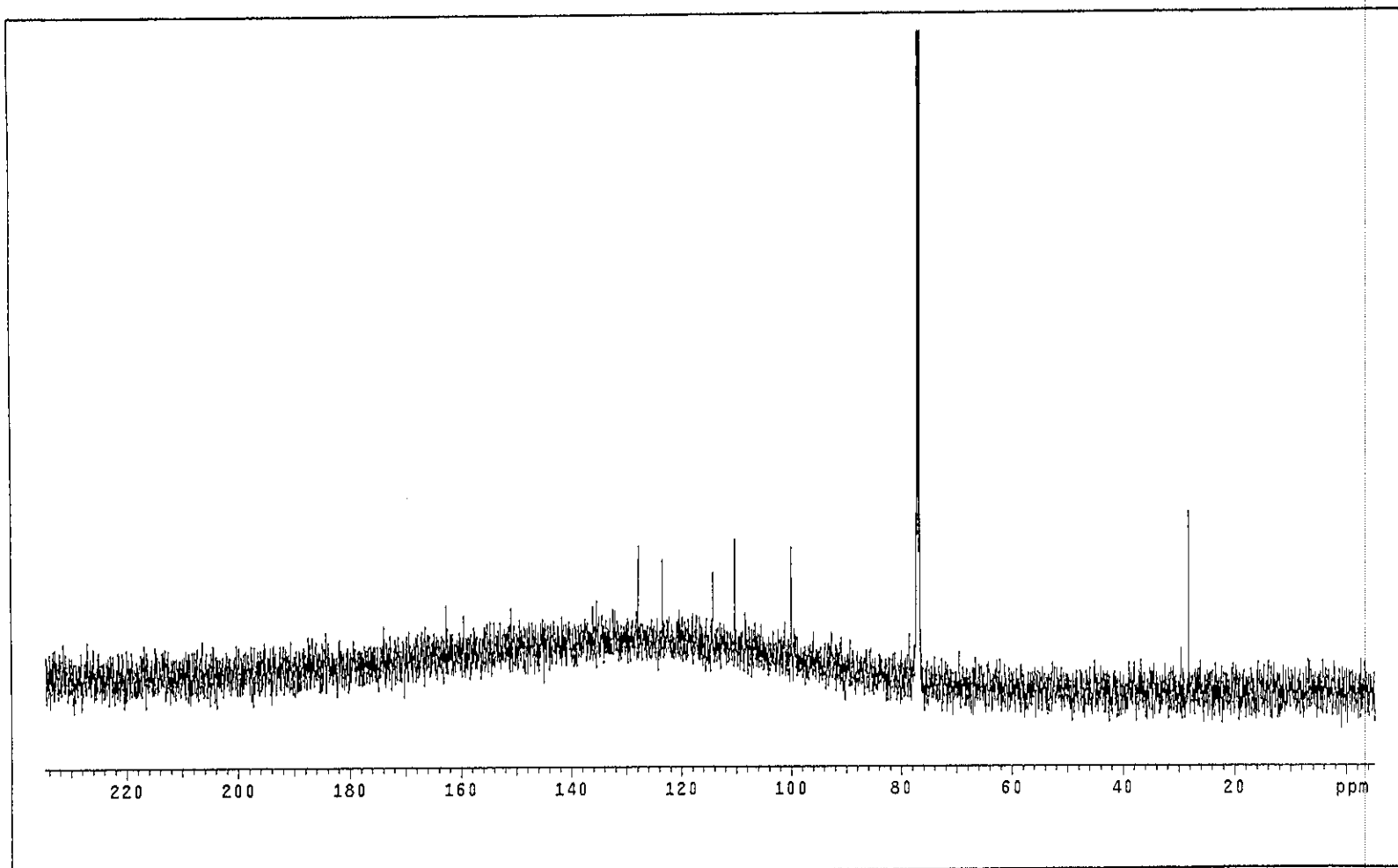


Figure 3.73 ^{13}C NMR (125 MHz)(CDCl_3) spectrum of TR18

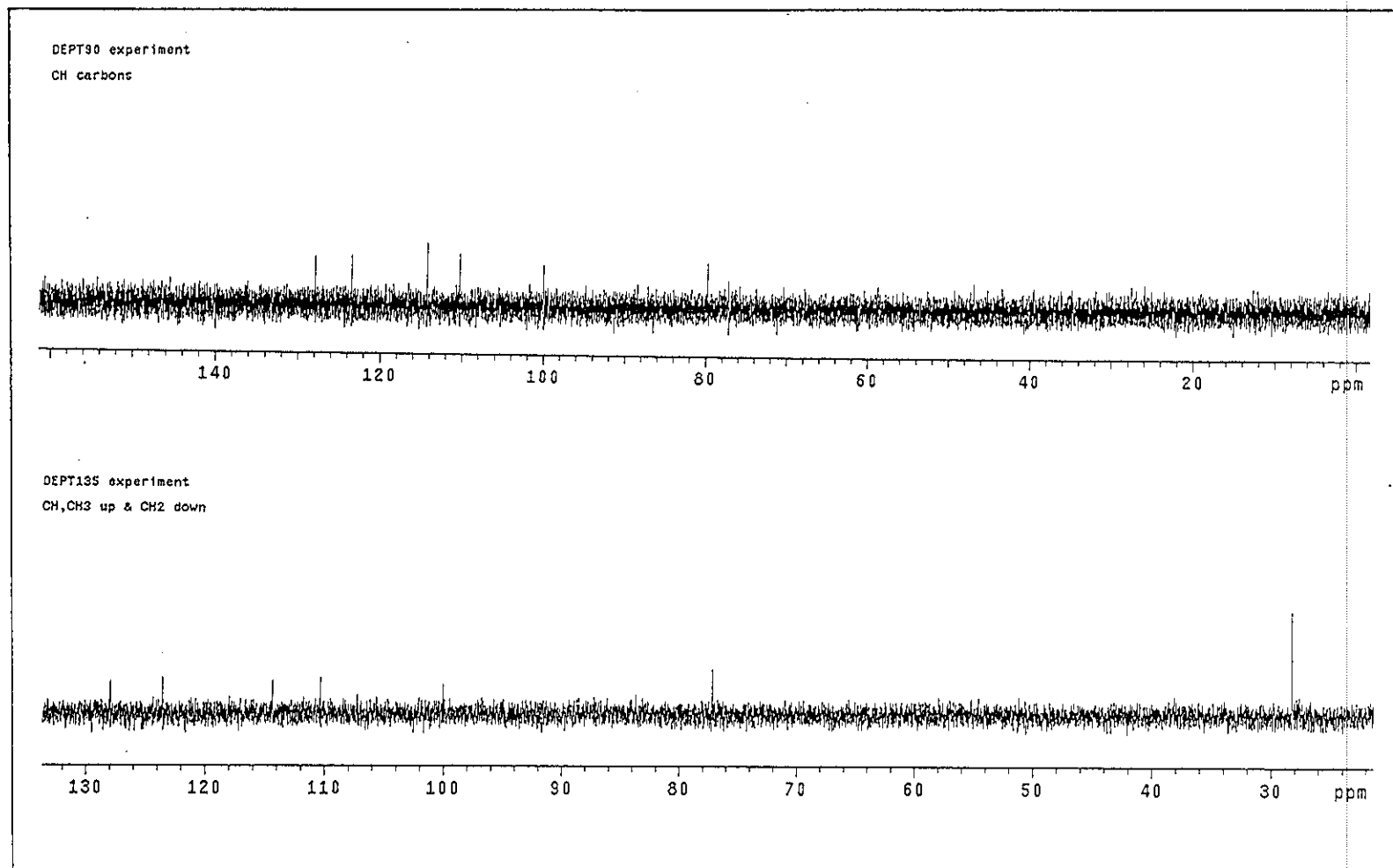


Figure 3.74 DEPT spectrum of TR18

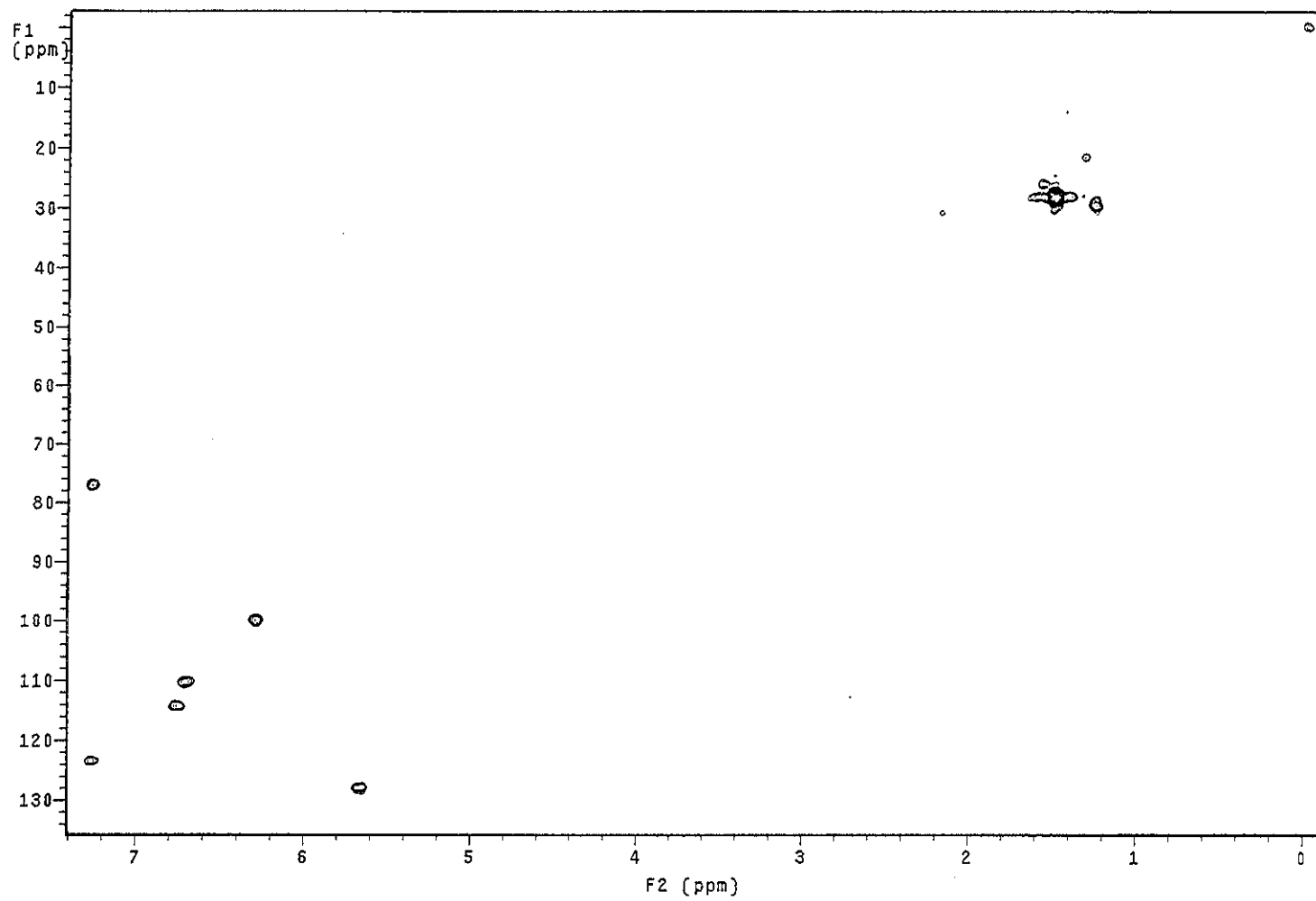


Figure 3.75 2D HMQC spectrum of TR18

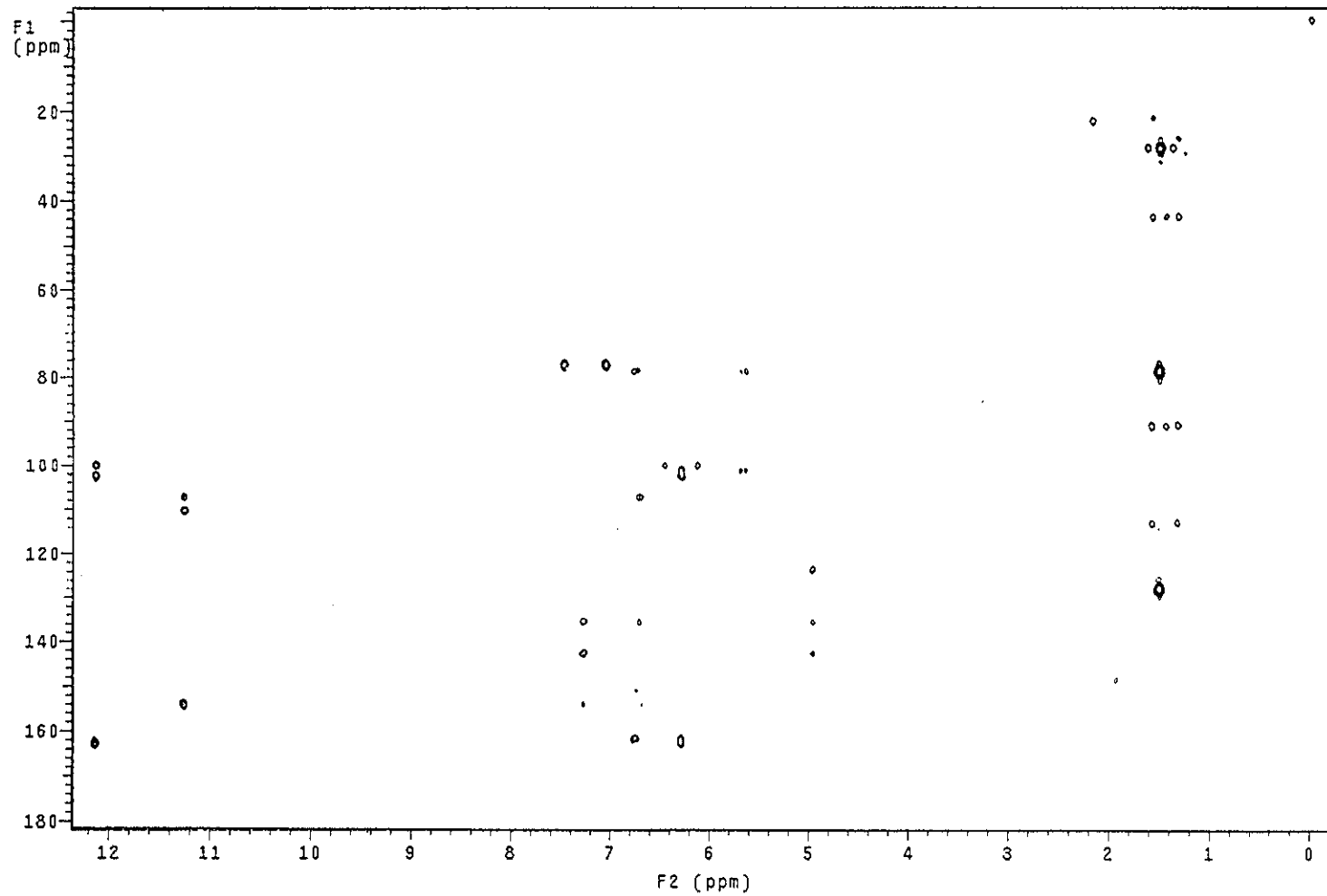


Figure 3.76 2D HMBC spectrum of TR18

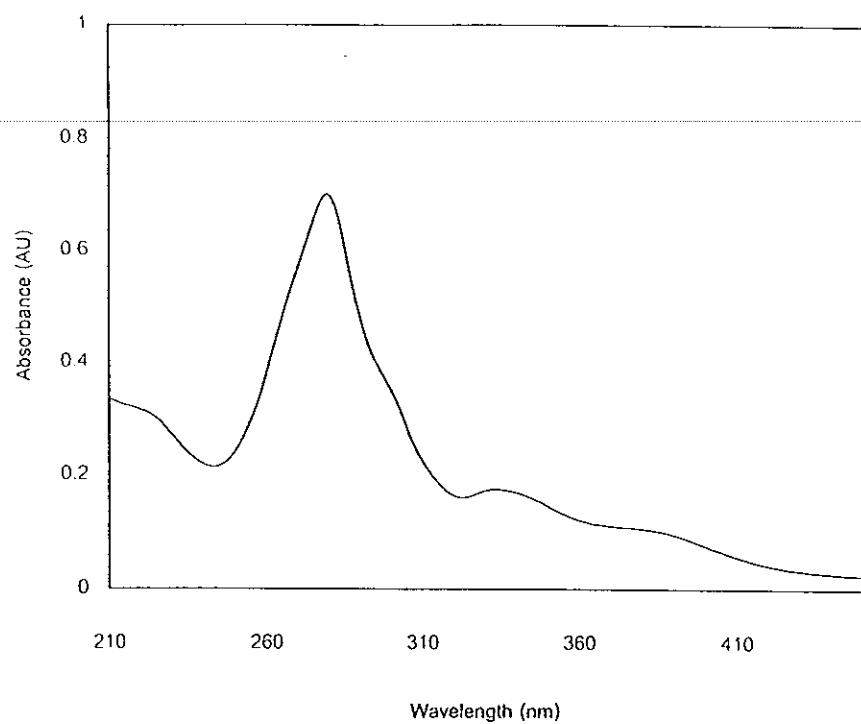


Figure 3.77 UV (MeOH) spectrum of TR17

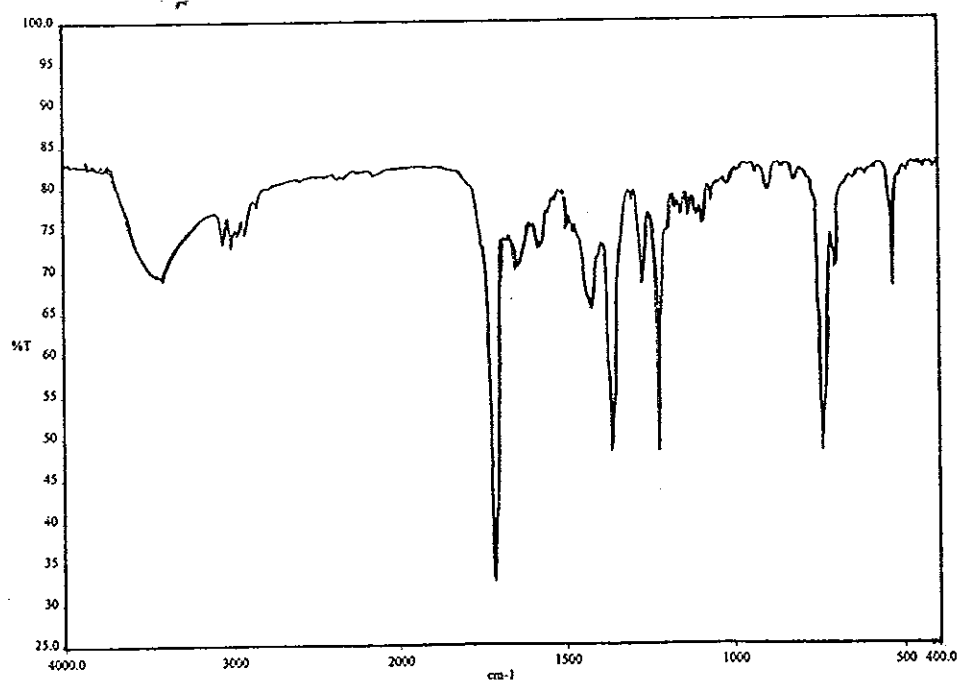


Figure 3.78 FT-IR (neat) spectrum of TR17

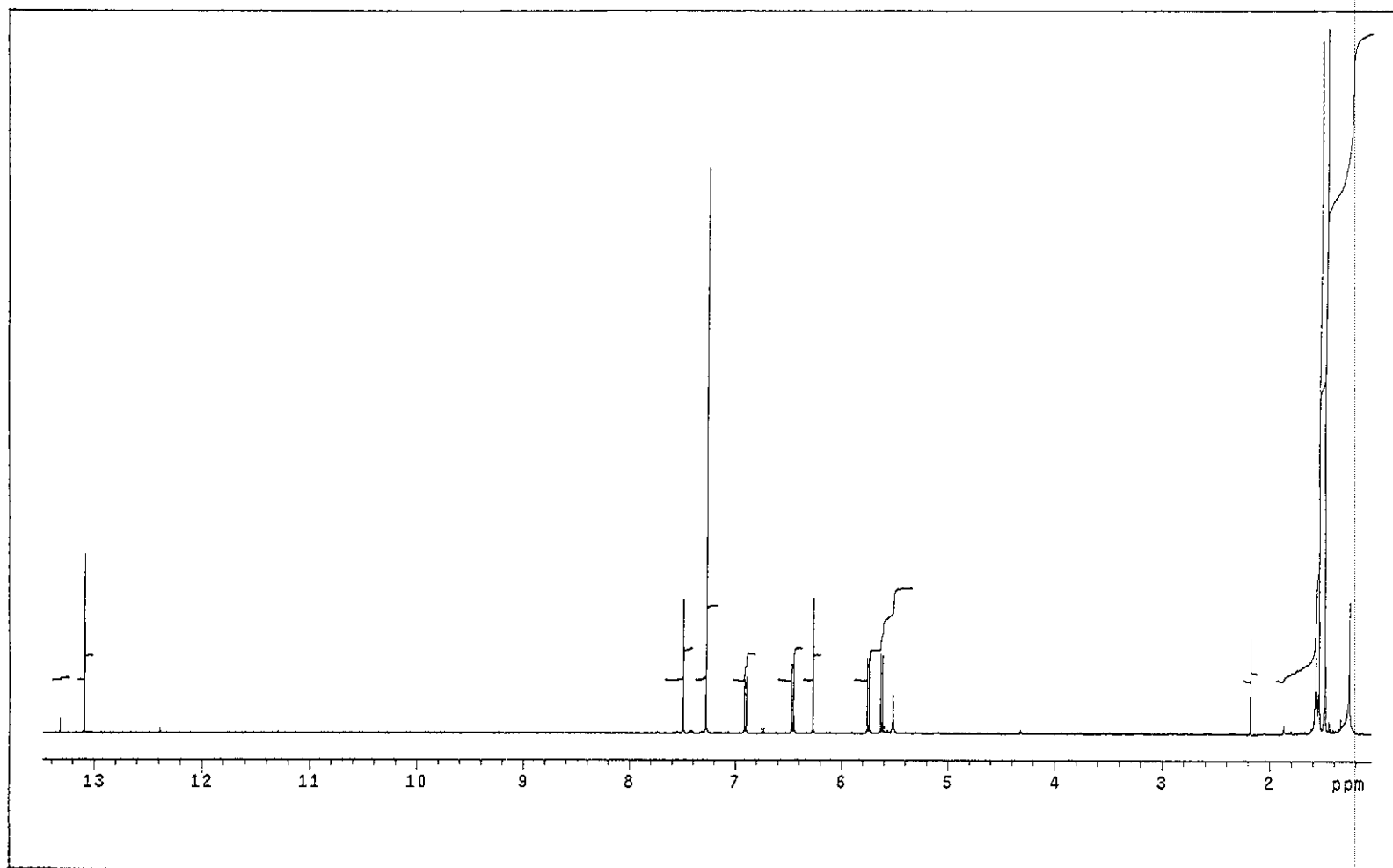


Figure 3.79 ^1H NMR (500 MHz)(CDCl_3) spectrum of TR17

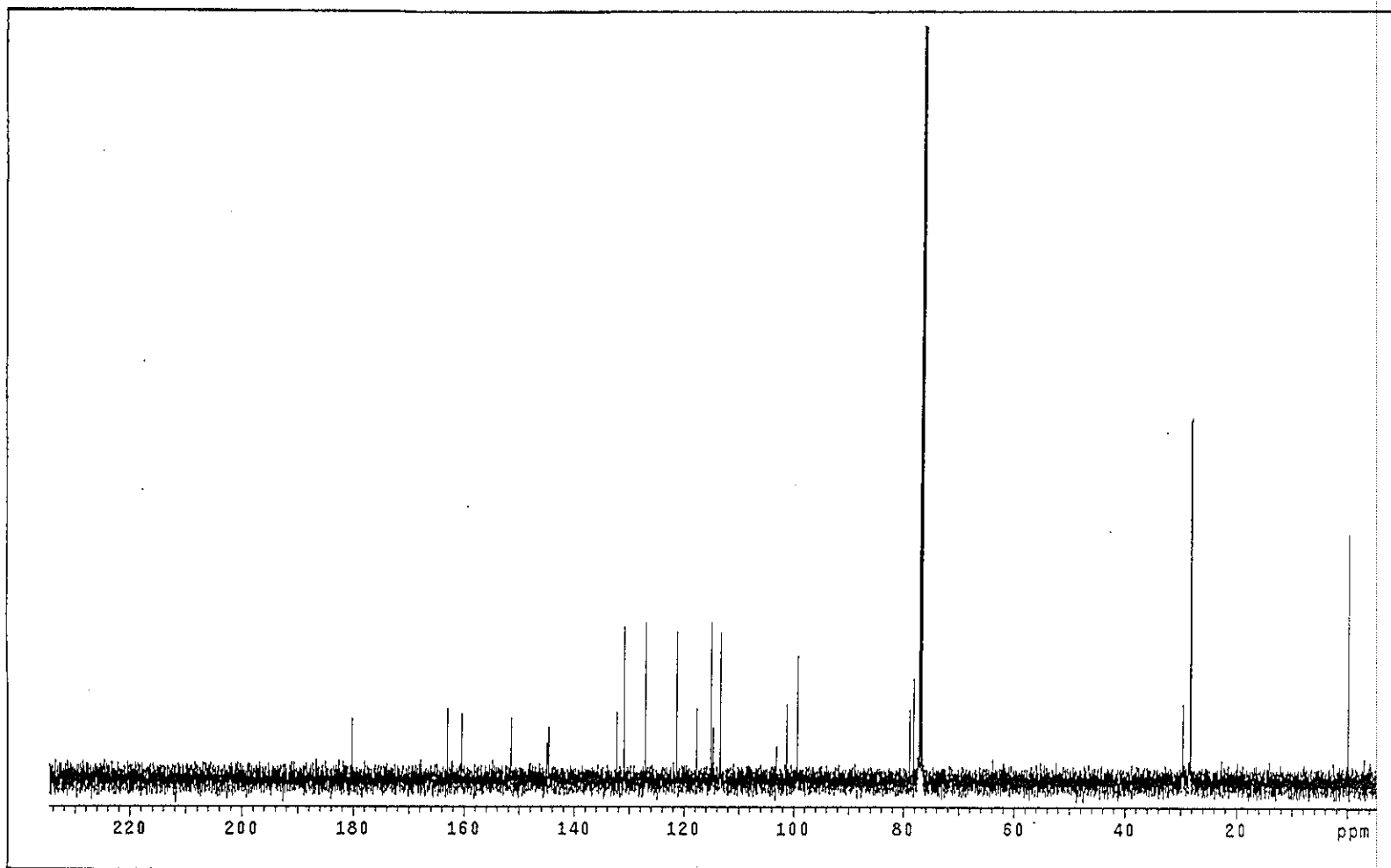


Figure 3.80 ^{13}C NMR (125 MHz)(CDCl_3) spectrum of TR17

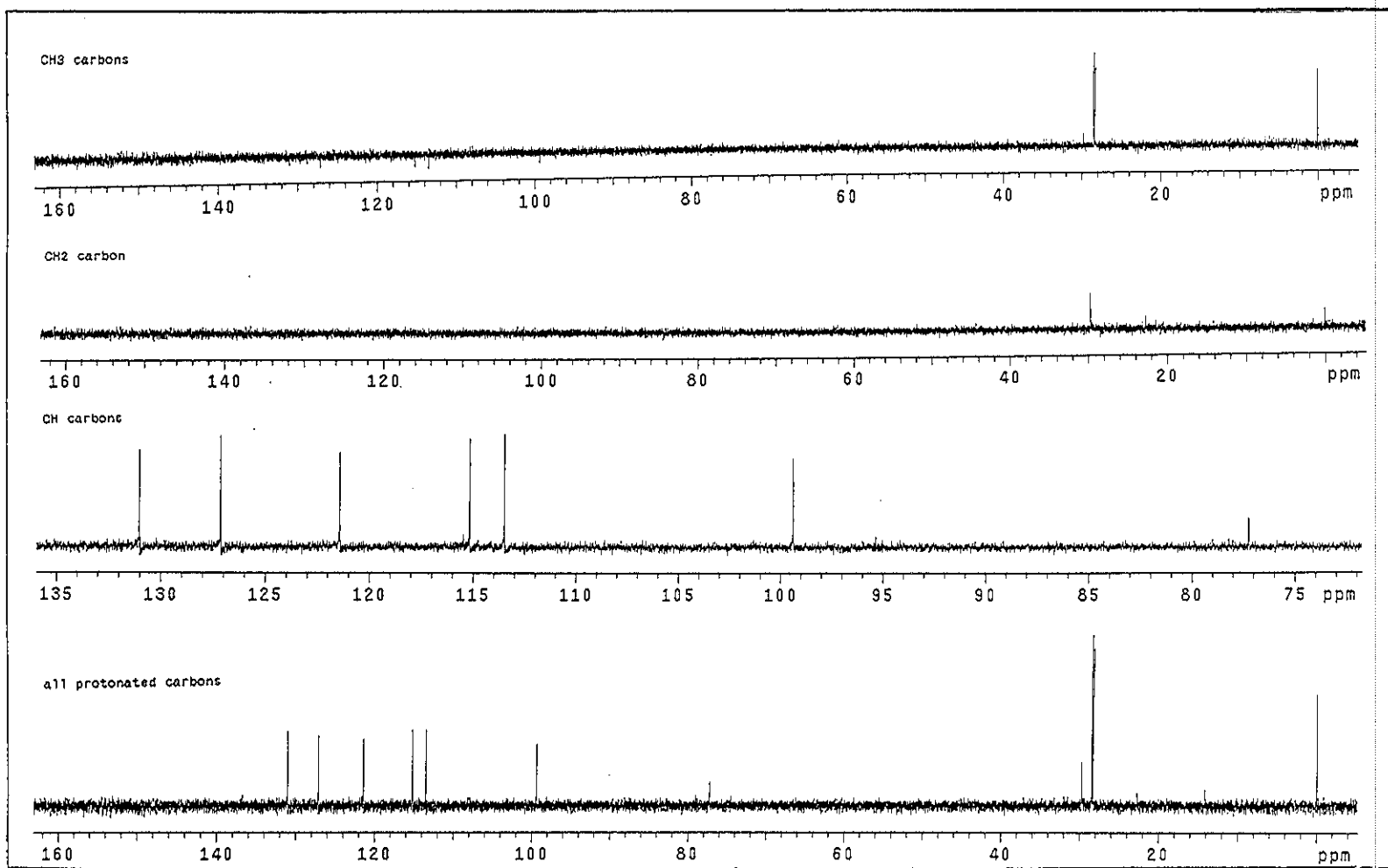


Figure 3.81 DEPT spectrum of TR17

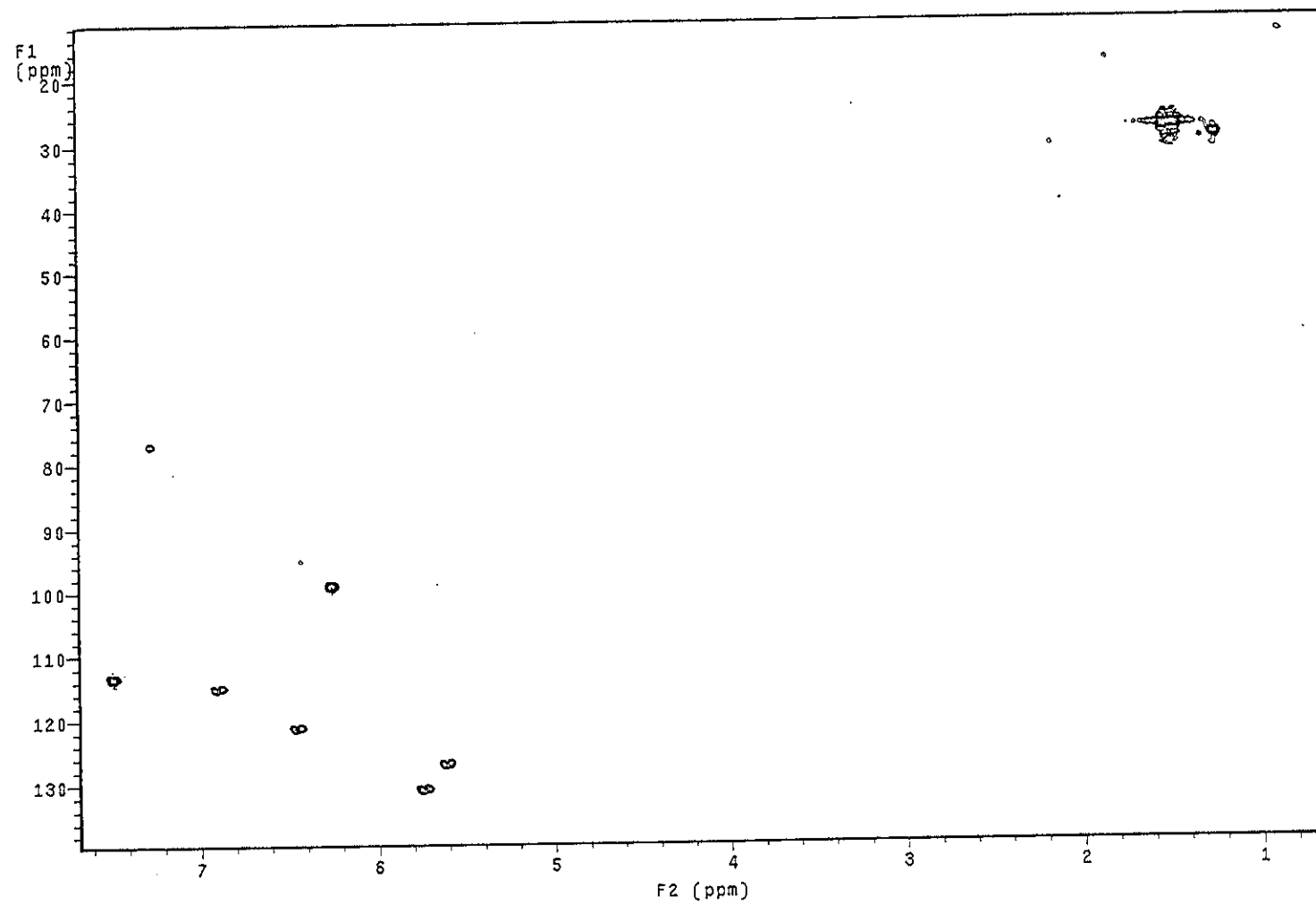


Figure 3.82 2D HMQC spectrum of TR17

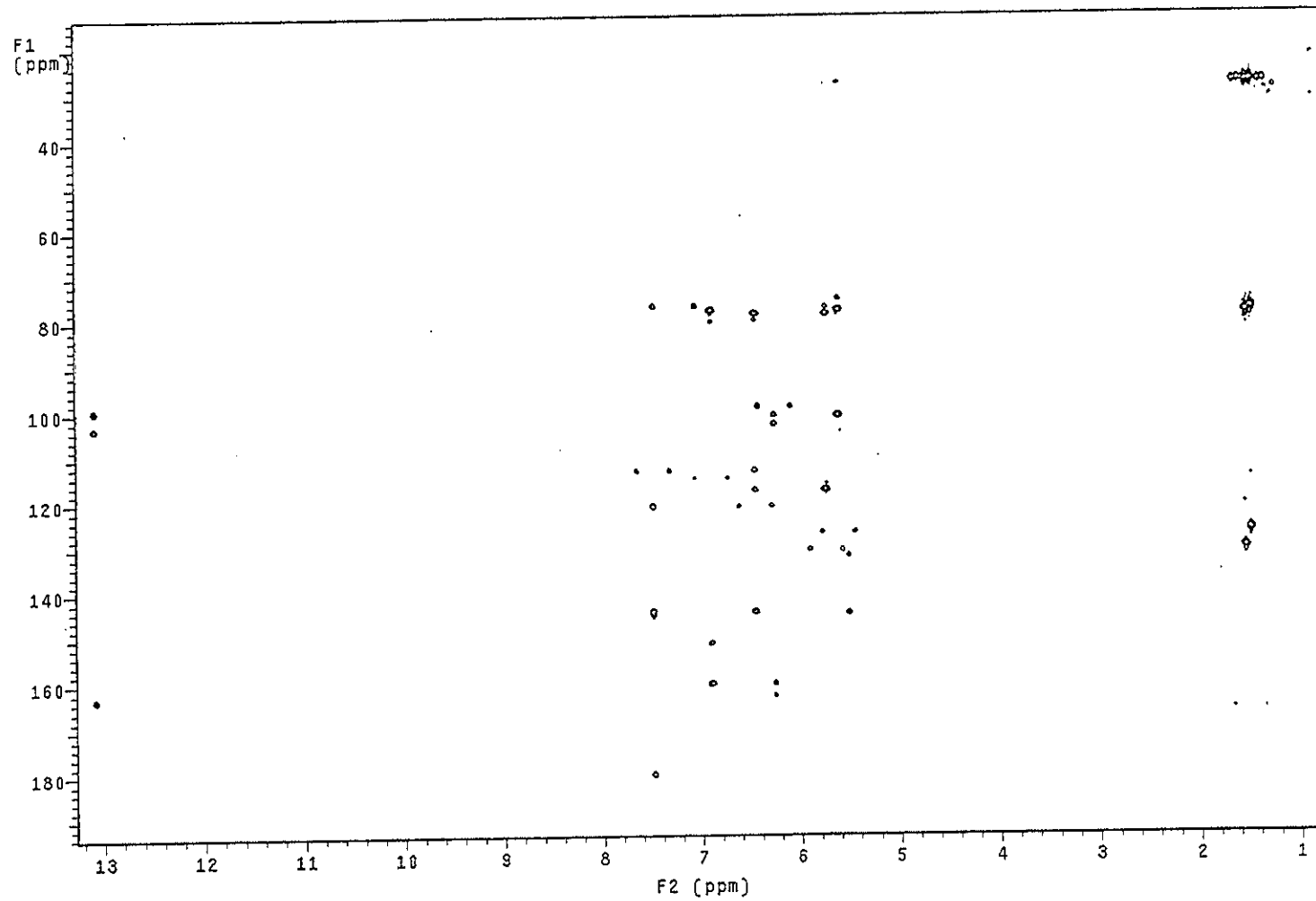


Figure 3.83 2D HMBC spectrum of TR17

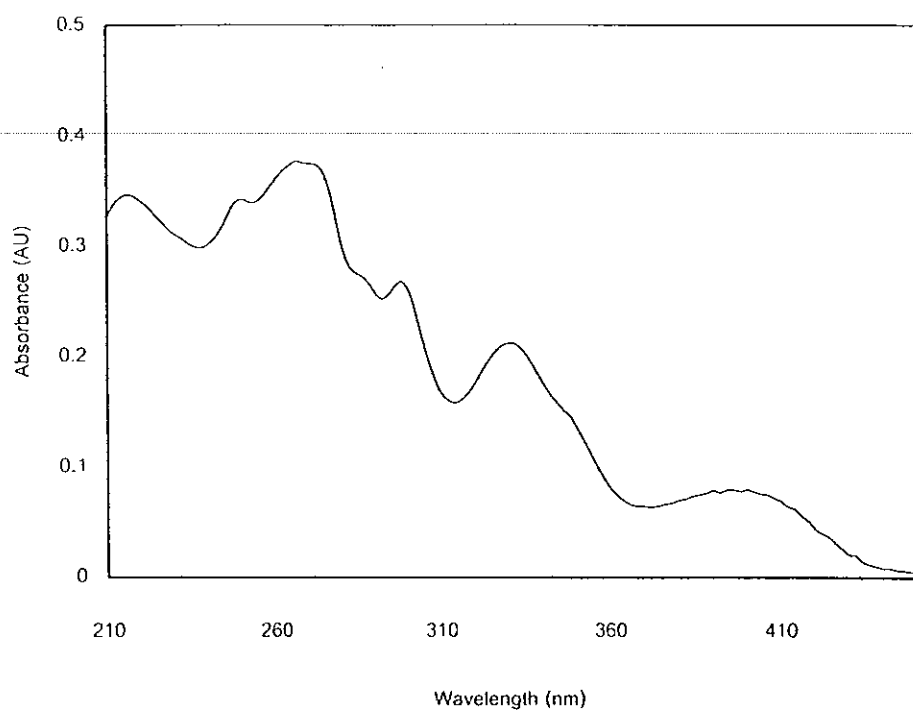


Figure 3.84 UV (MeOH) spectrum of TR16

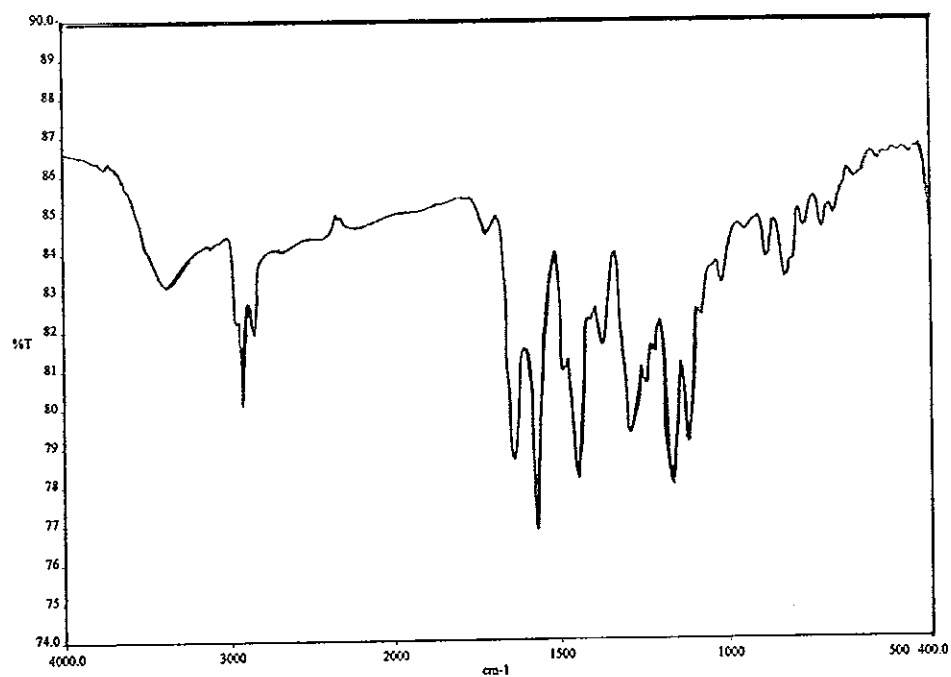


Figure 3.85 FT-IR (neat) spectrum of TR16

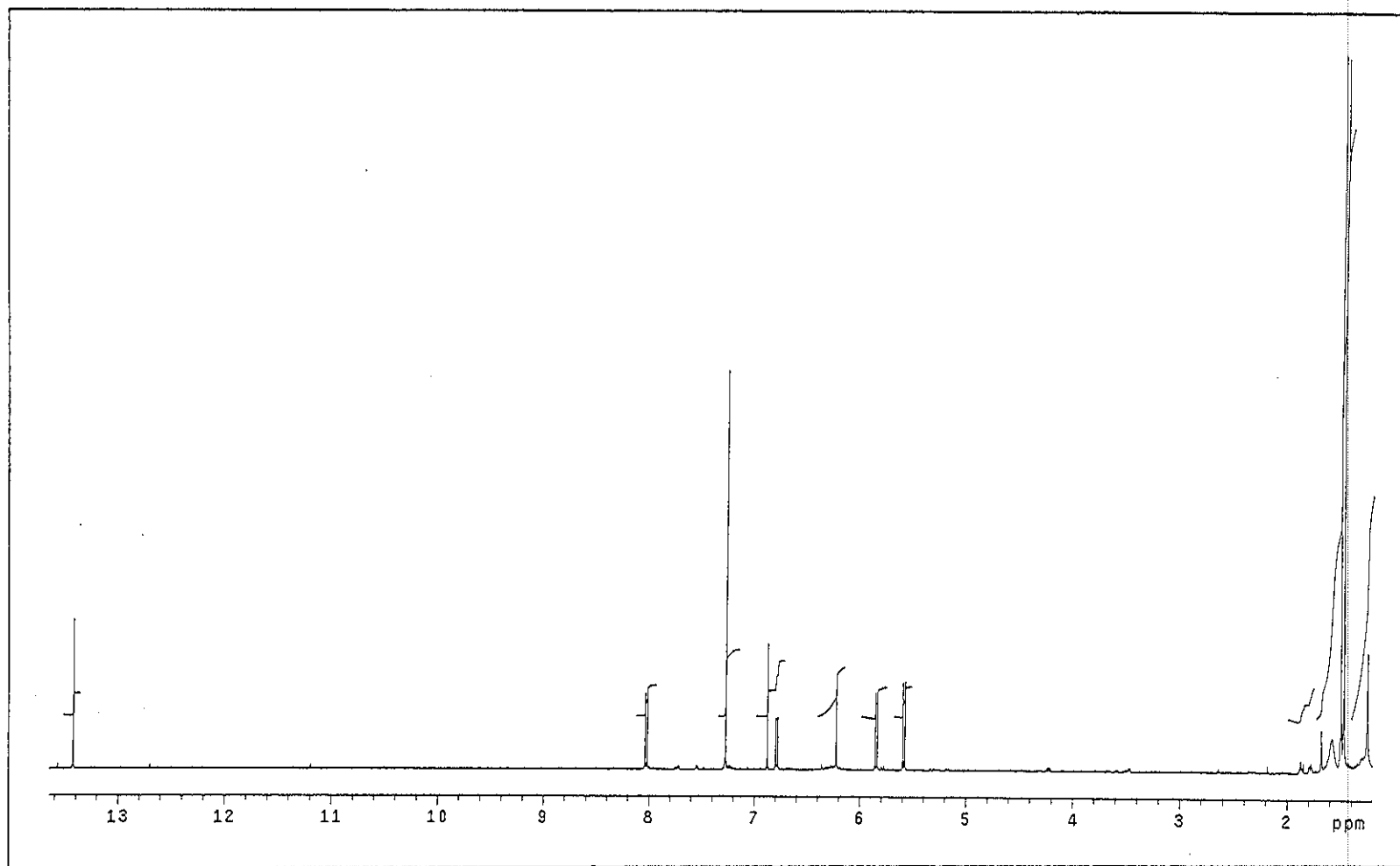


Figure 3.86 ^1H NMR (500 MHz)(CDCl_3) spectrum of TR16

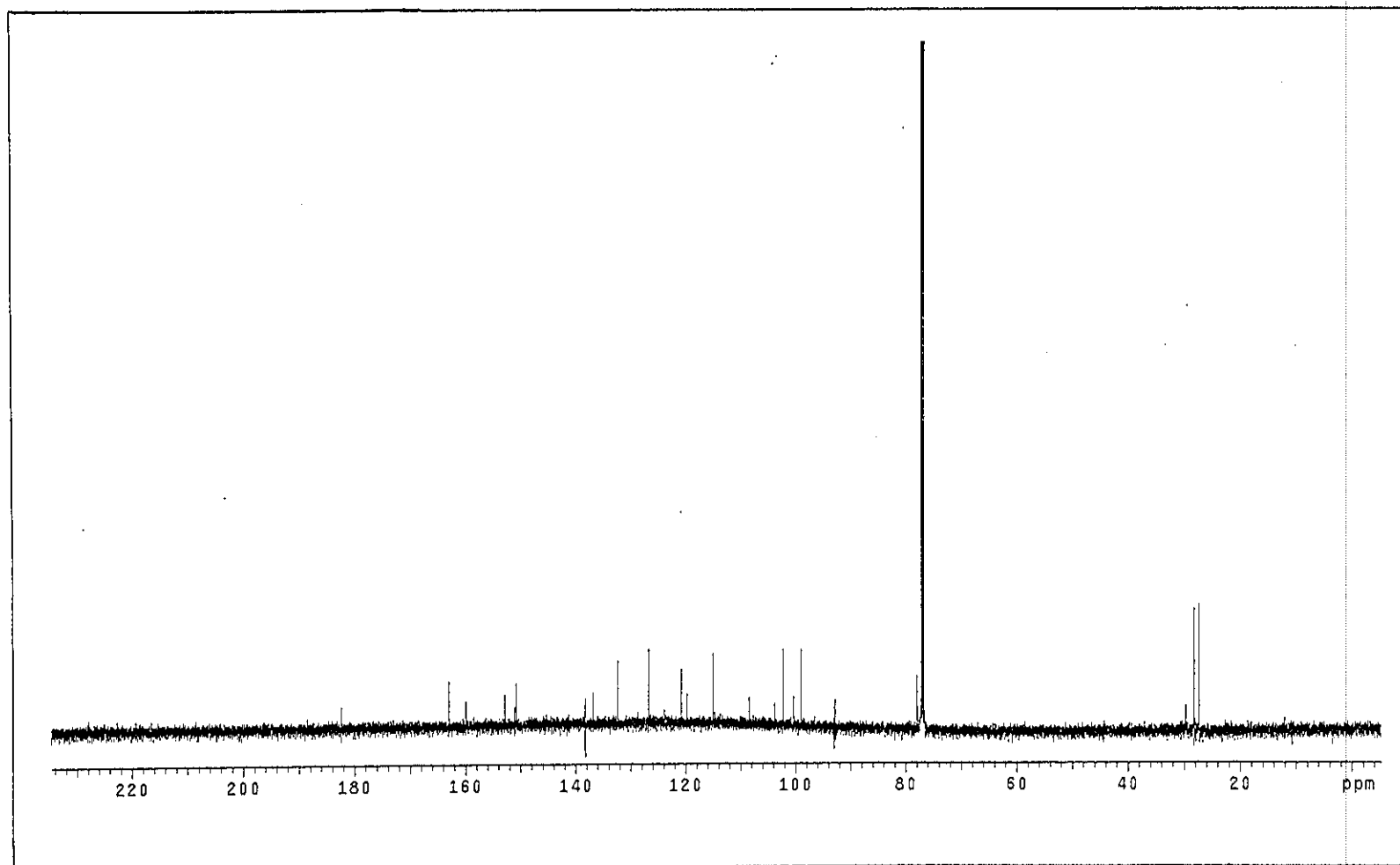


Figure 3.87 ^{13}C NMR (125 MHz)(CDCl_3) spectrum of TR16

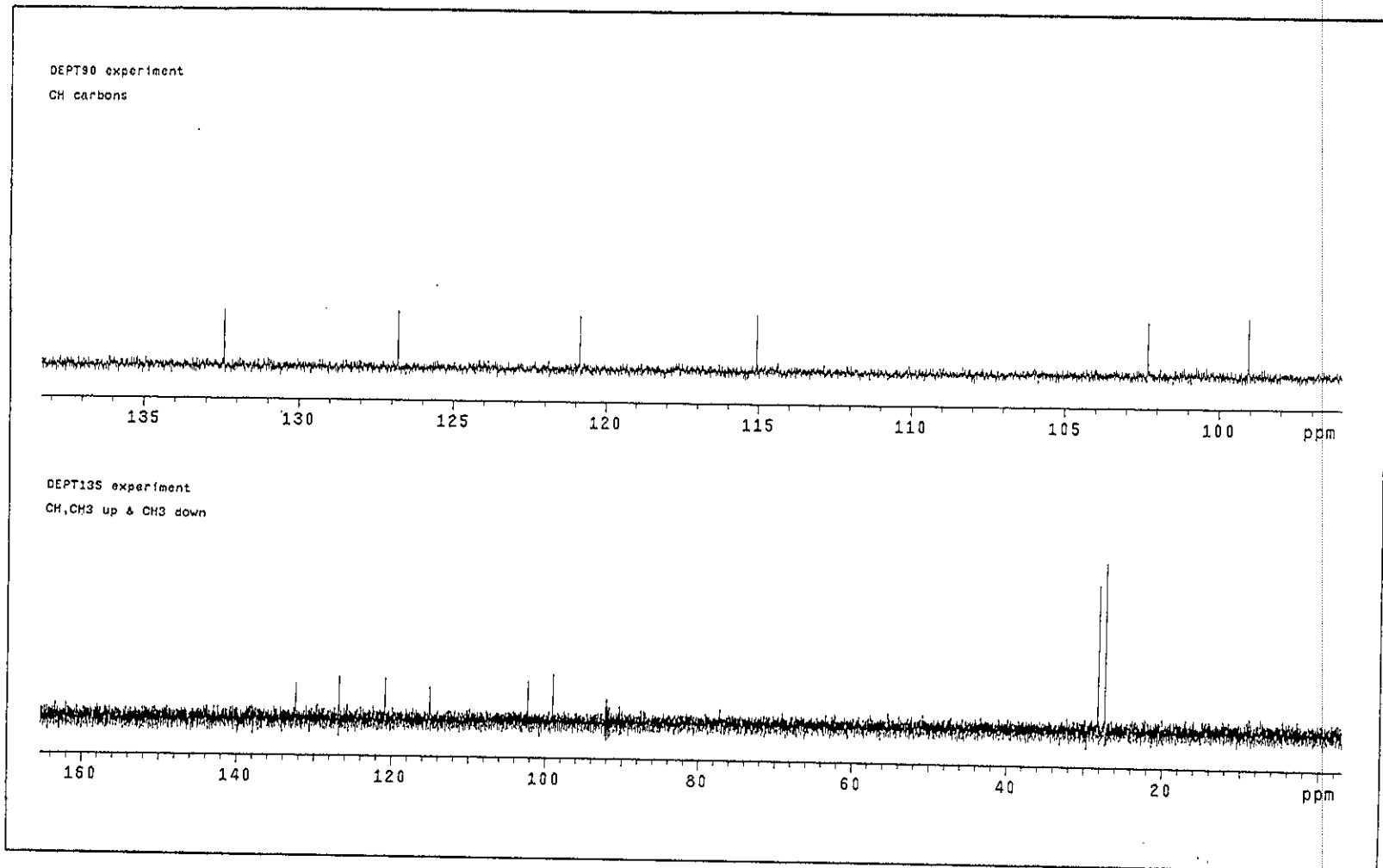


Figure 3.88 DEPT spectrum of TR16

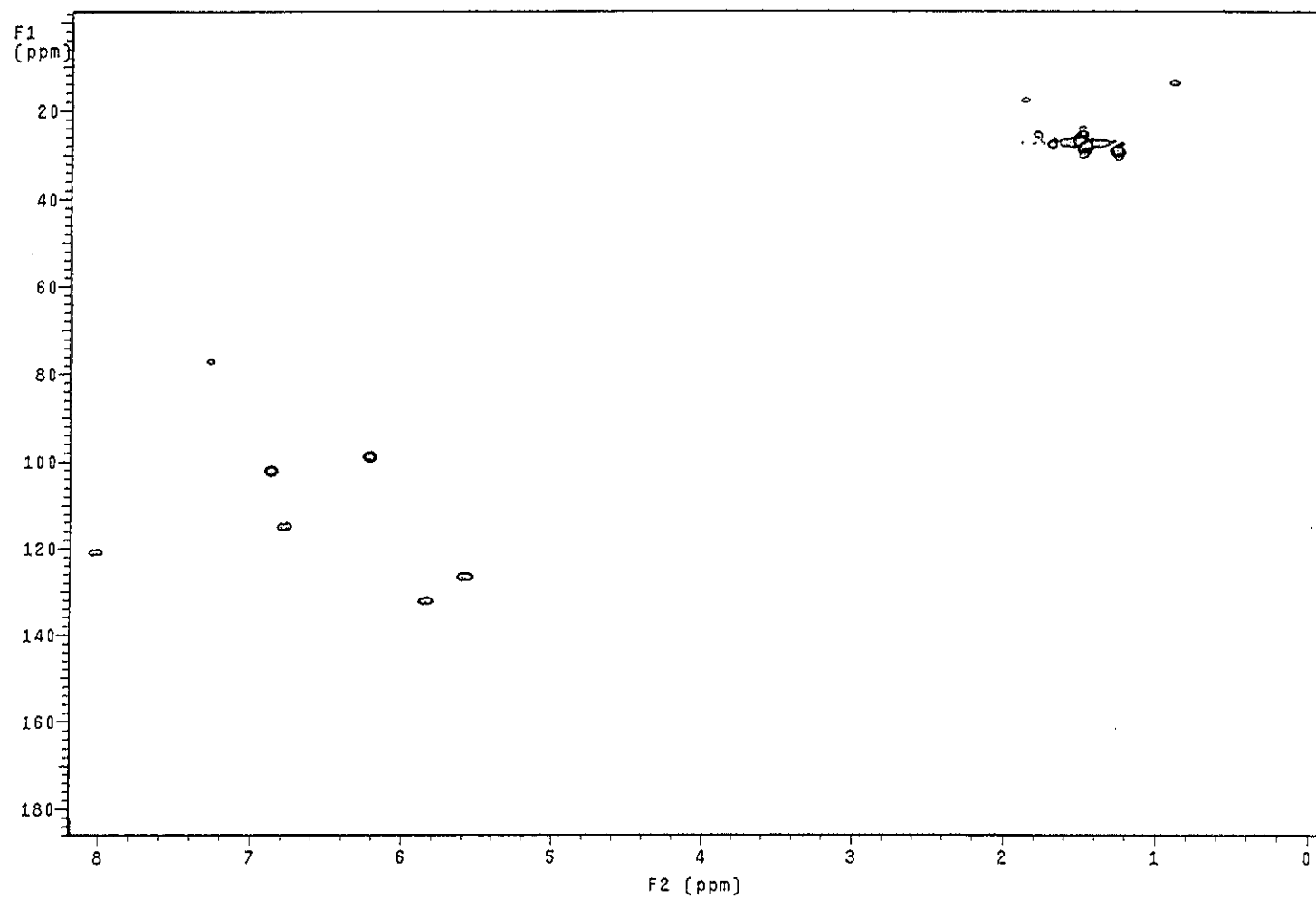


Figure 3.89 2D HMQC spectrum of TR16

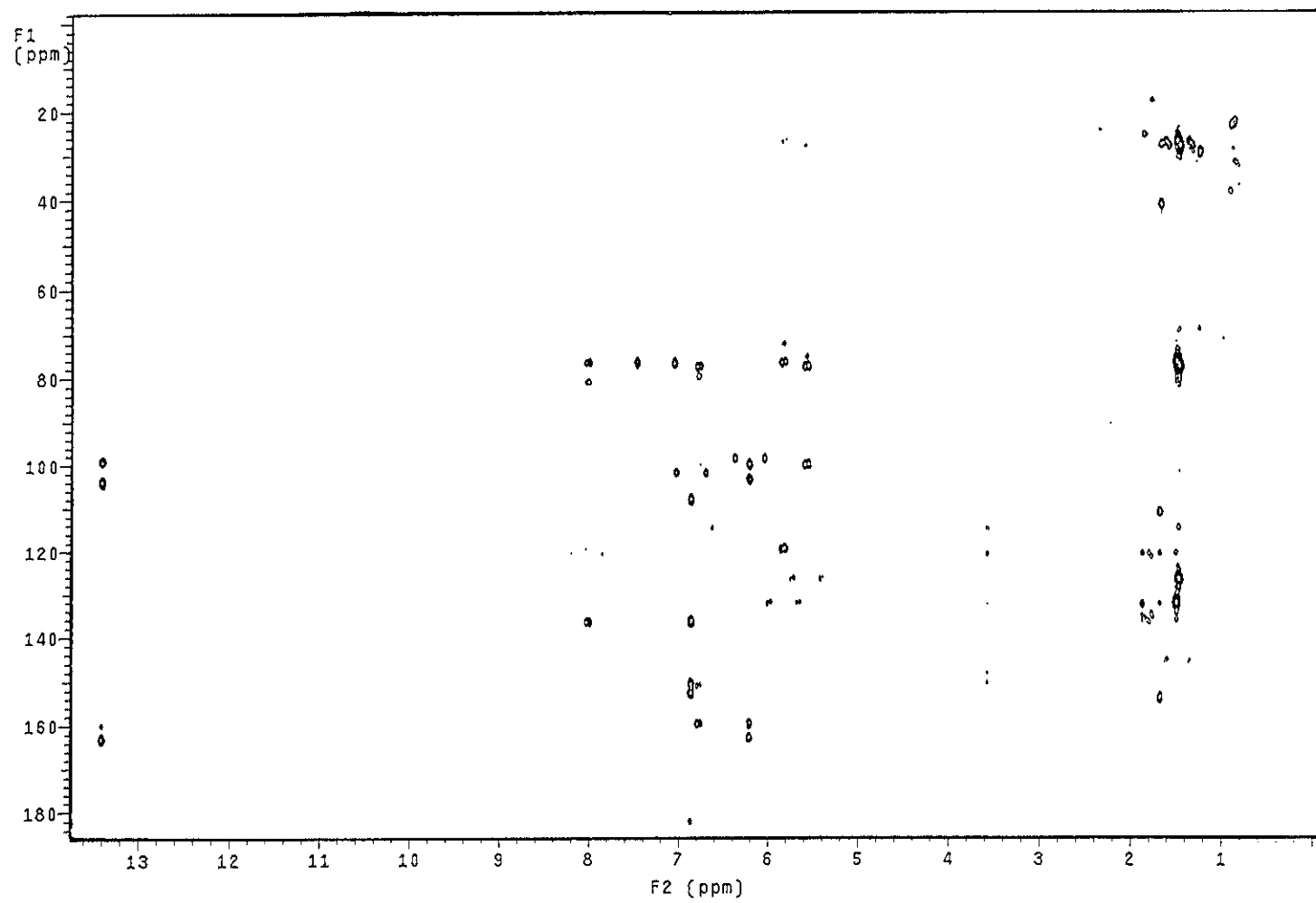


Figure 3.90 2D HMBC spectrum of TR16

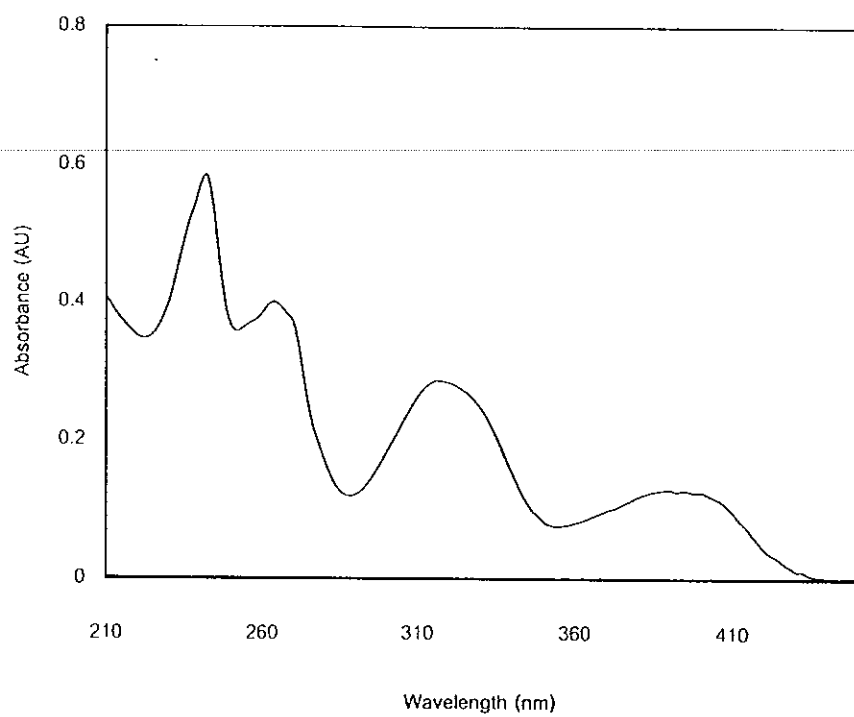


Figure 3.91 UV (MeOH) spectrum of TR12

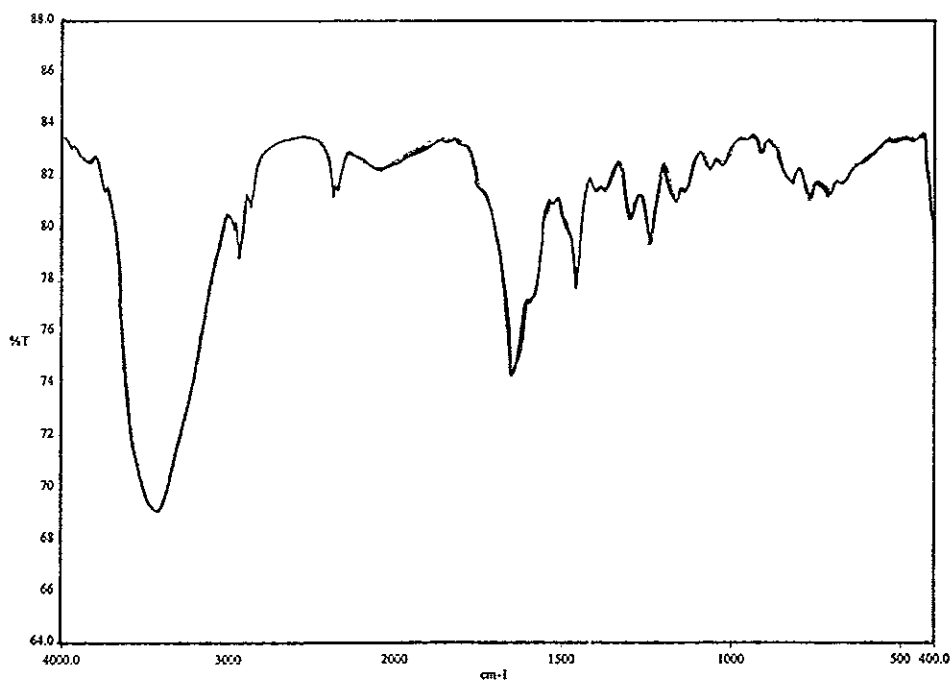


Figure 3.92 FT-IR (neat) spectrum of TR12

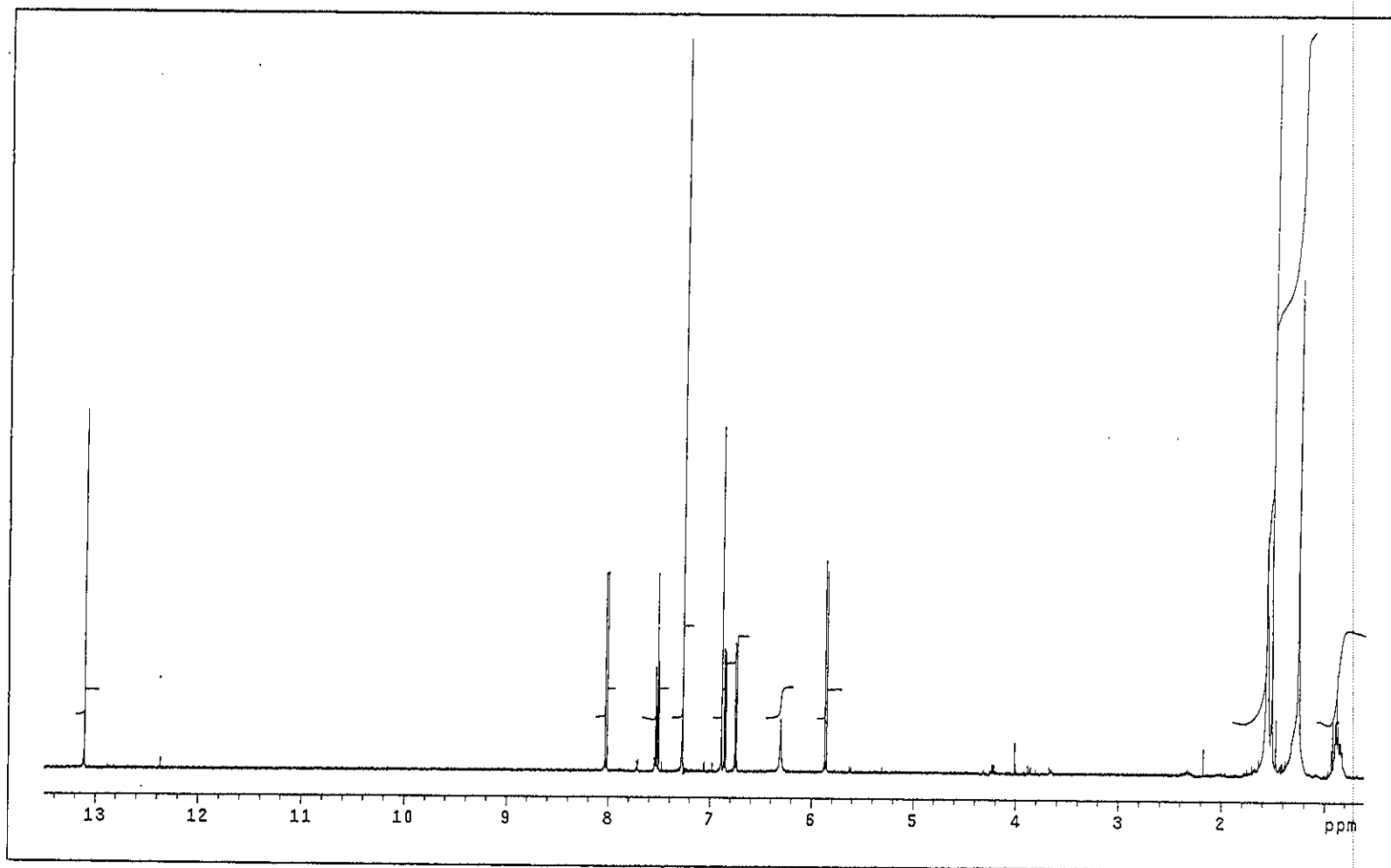


Figure 3.93 ^1H NMR (500 MHz)(CDCl_3) spectrum of TR12

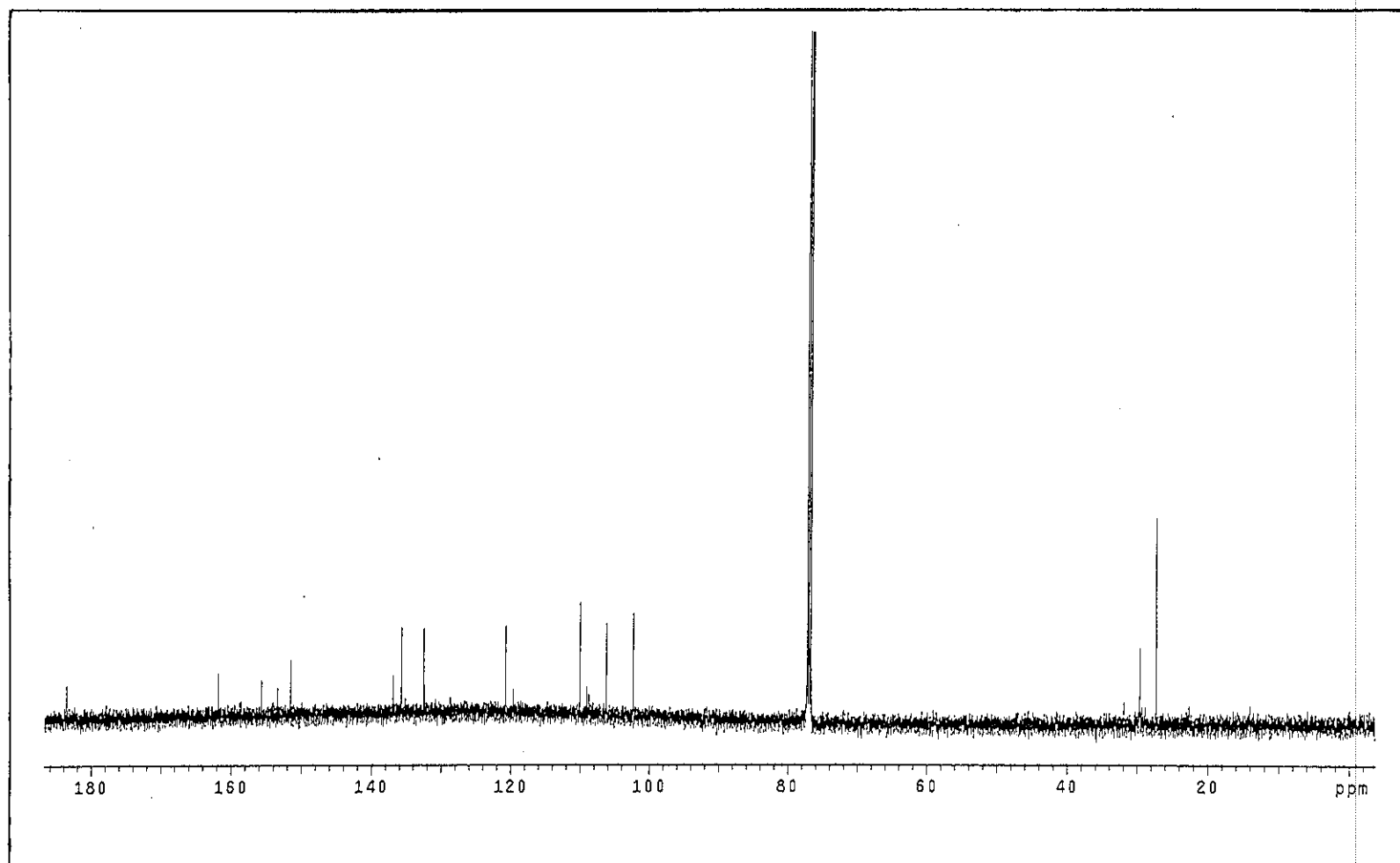


Figure 3.94 ^{13}C NMR (125 MHz)(CDCl₃) spectrum of TR12

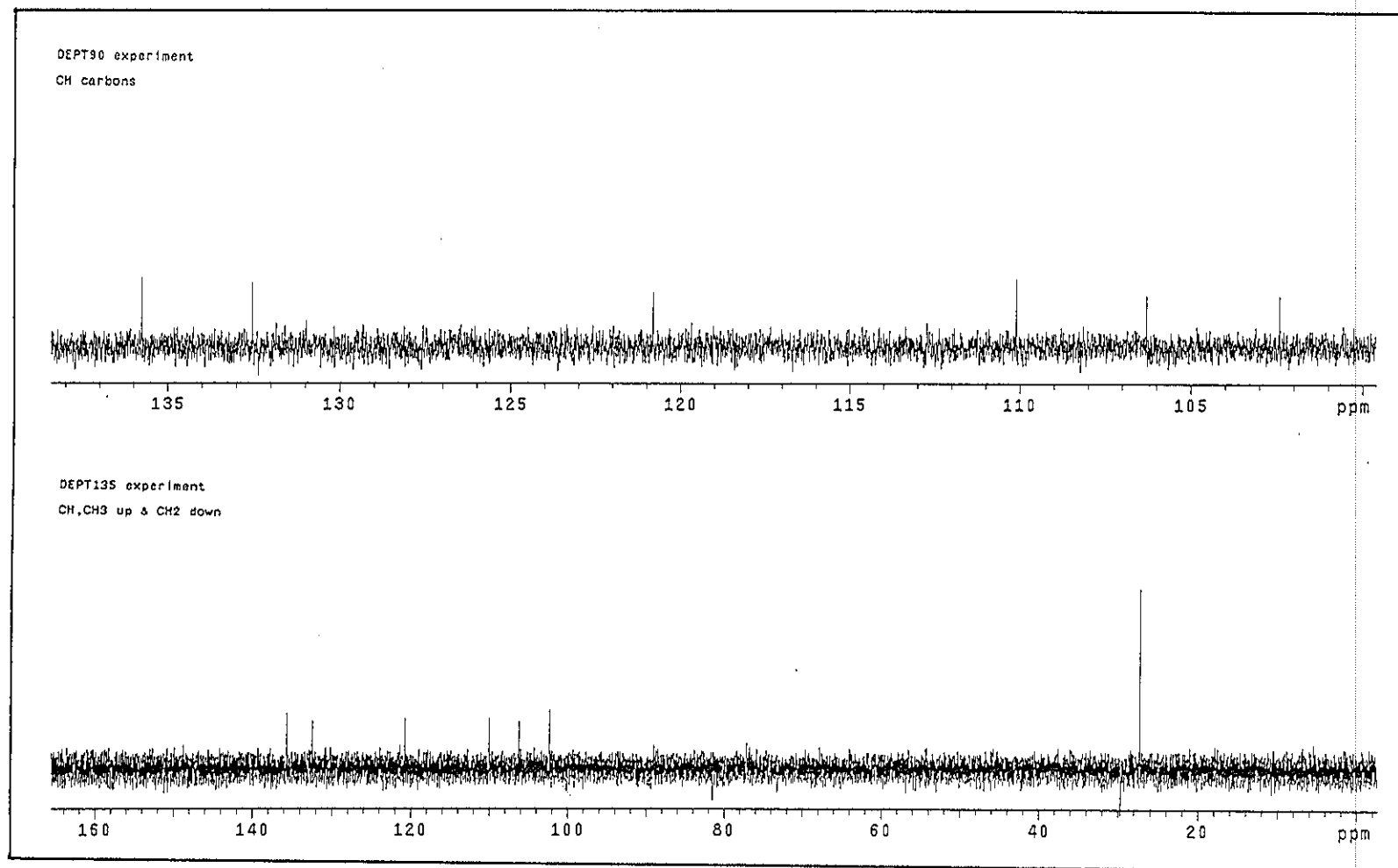


Figure 3.95 DEPT spectrum of TR12

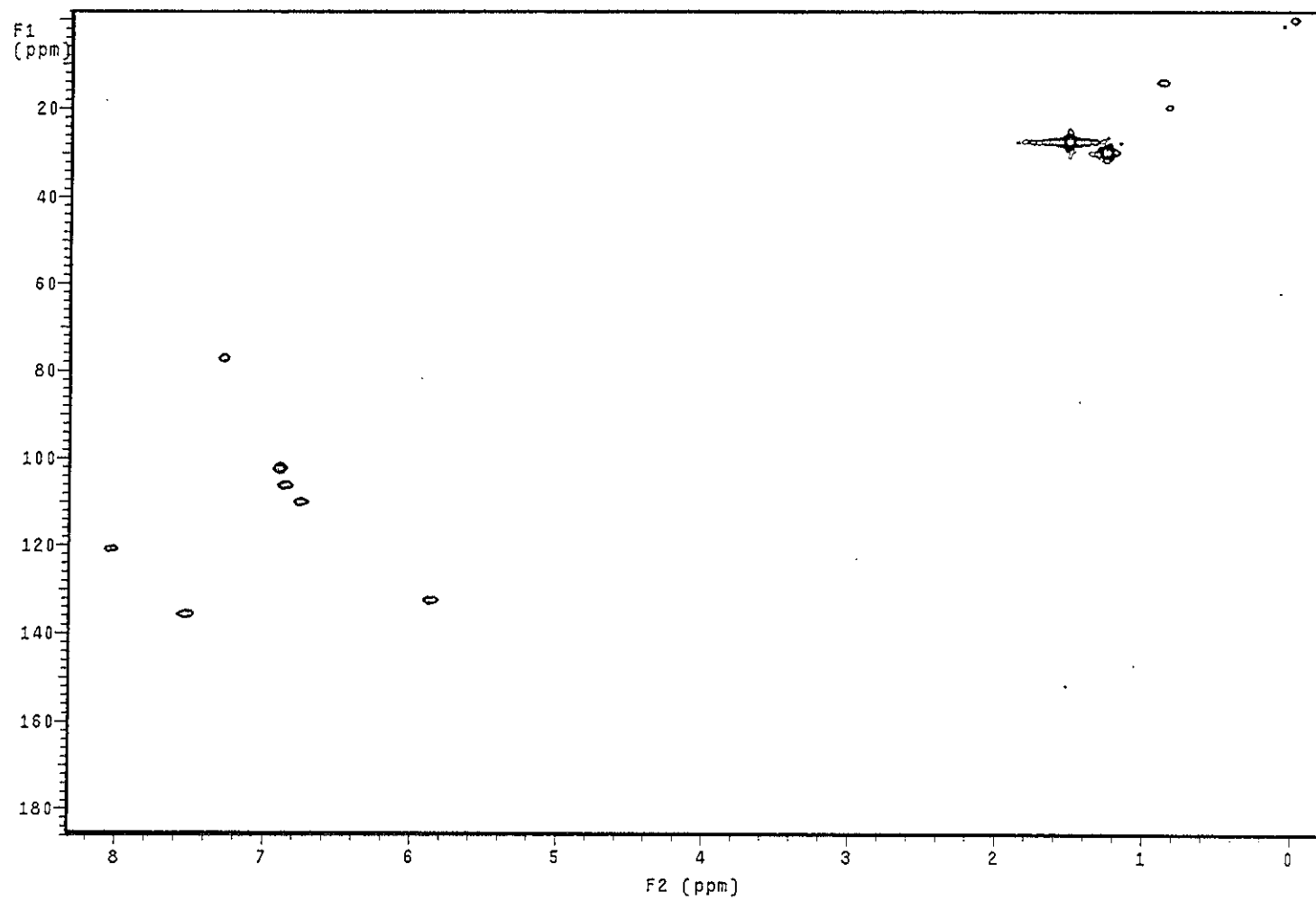


Figure 3.96 2D HMQC spectrum of TR12

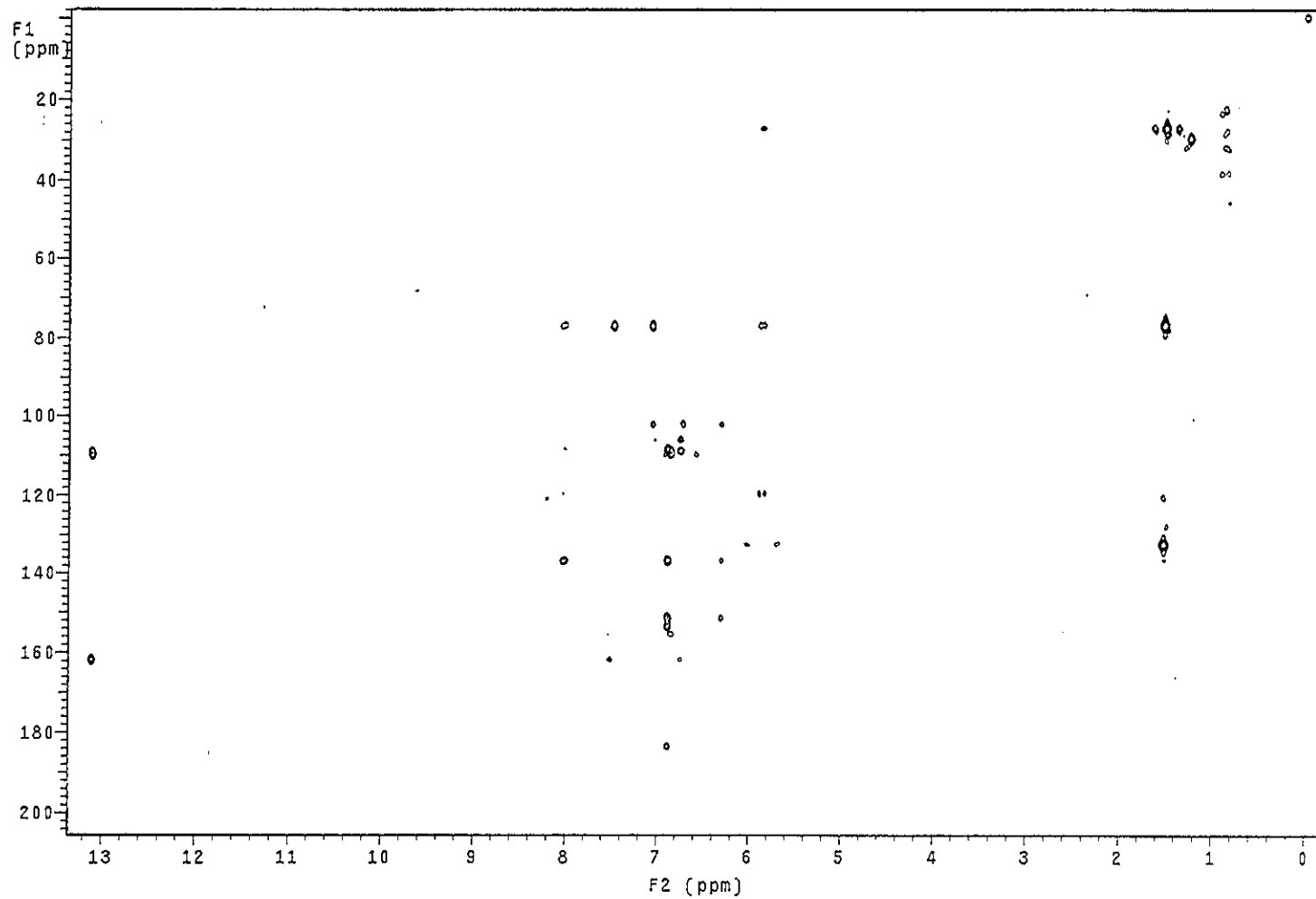


Figure 3.97 2D HMBC spectrum of TR12

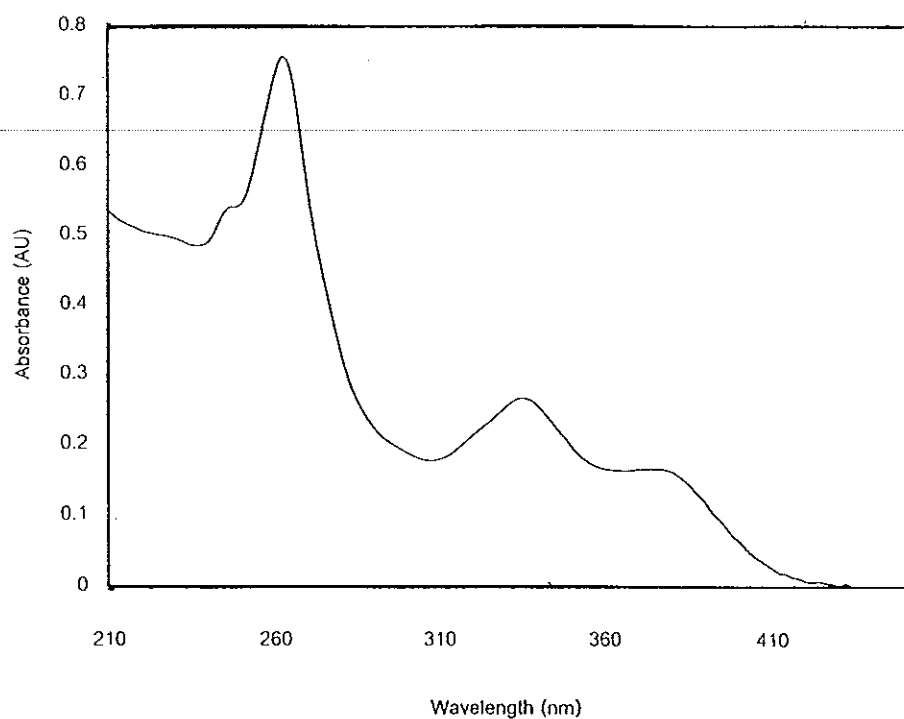


Figure 3.98 UV (MeOH) spectrum of TR7

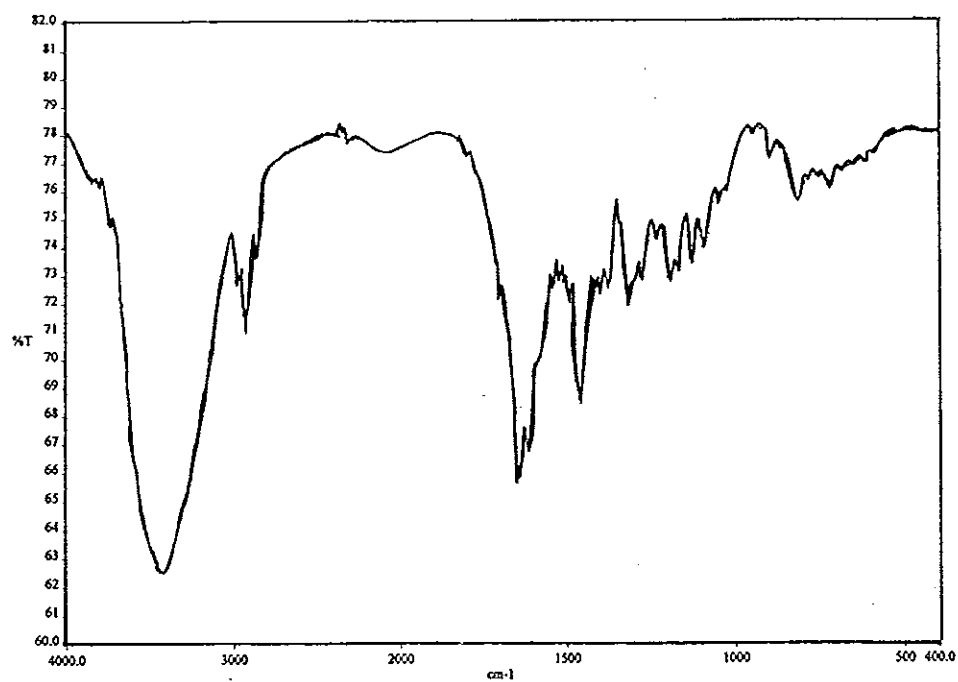


Figure 3.99 FT-IR (neat) spectrum of TR7

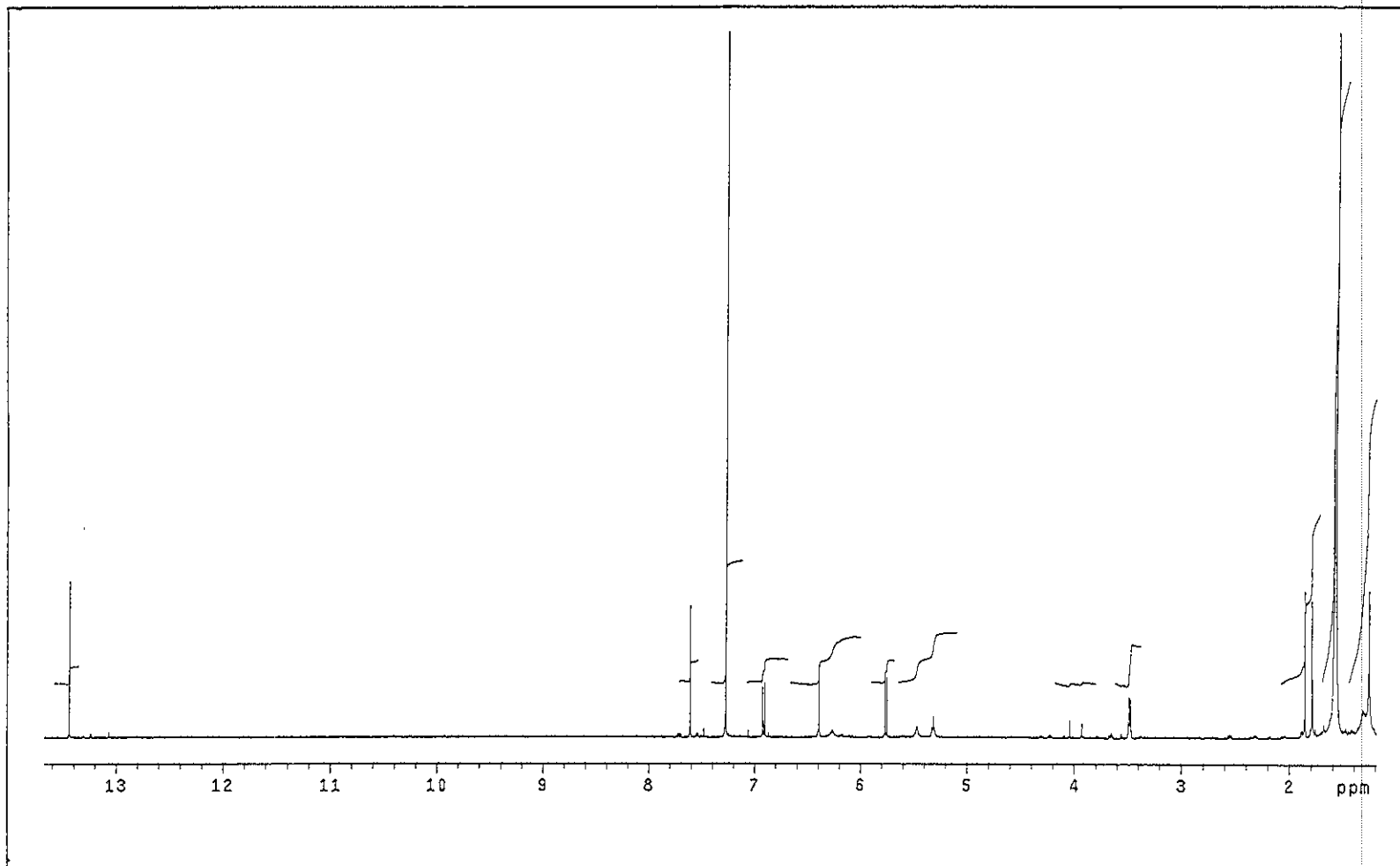


Figure 3.100 ^1H NMR (500 MHz)(CDCl_3) spectrum of TR7

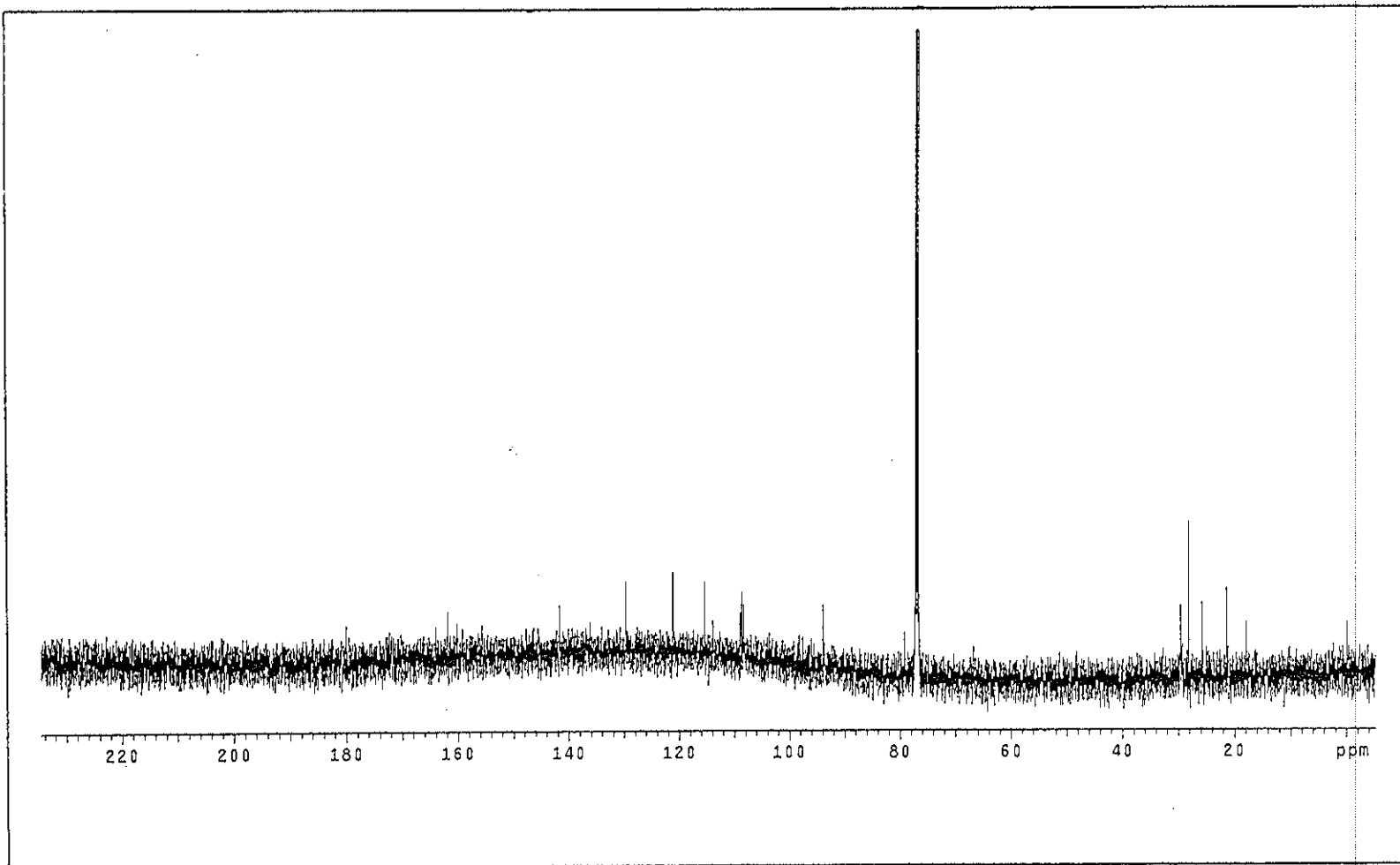


Figure 3.101 ^{13}C NMR (125 MHz)(CDCl_3) spectrum of TR7

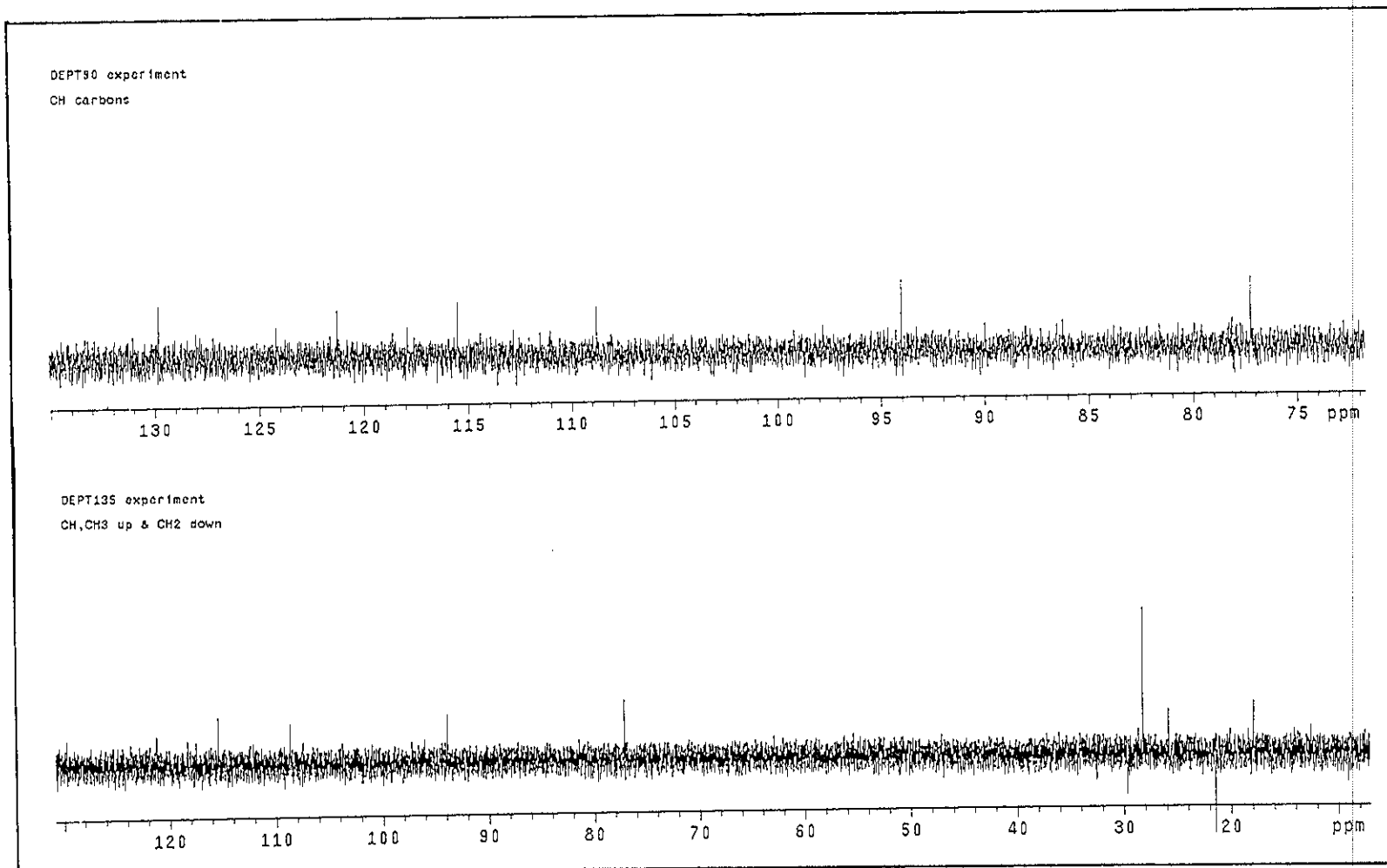


Figure 3.102 DEPT spectrum of TR7

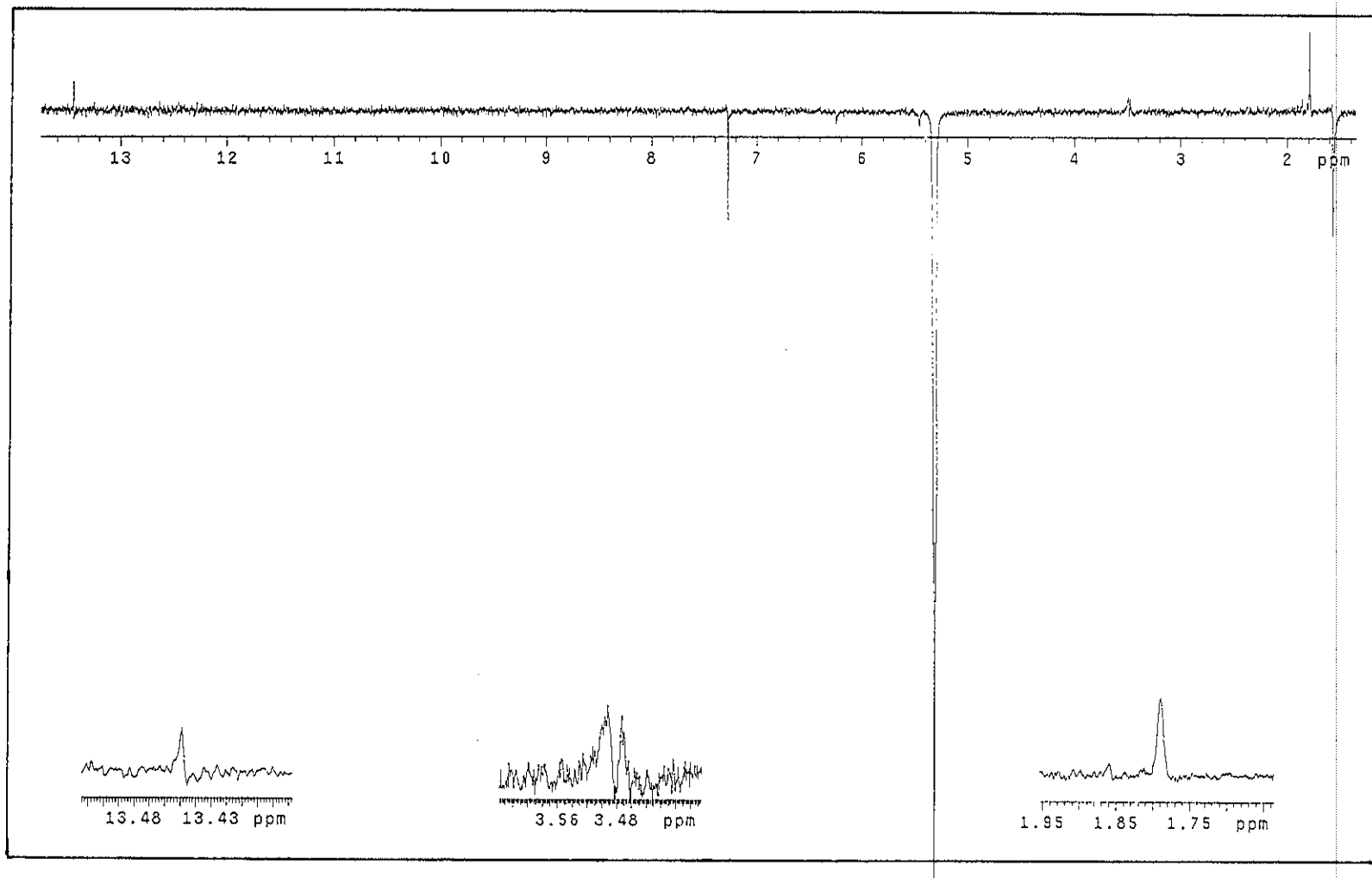


Figure 3.103 NOEDIFF spectrum of TR7 after irradiation at δ_H 5.31

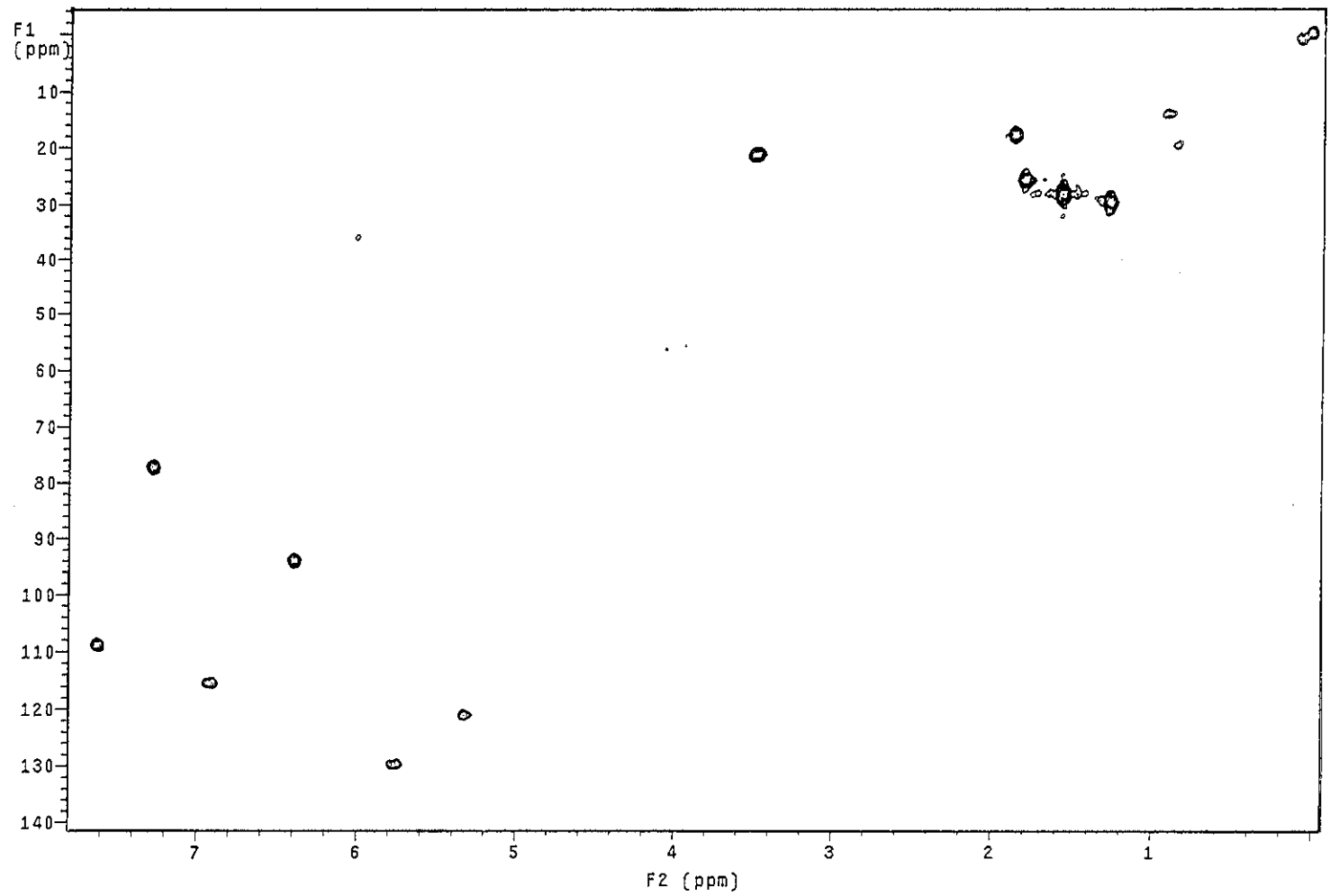


Figure 3.104 2D HMQC spectrum of TR7

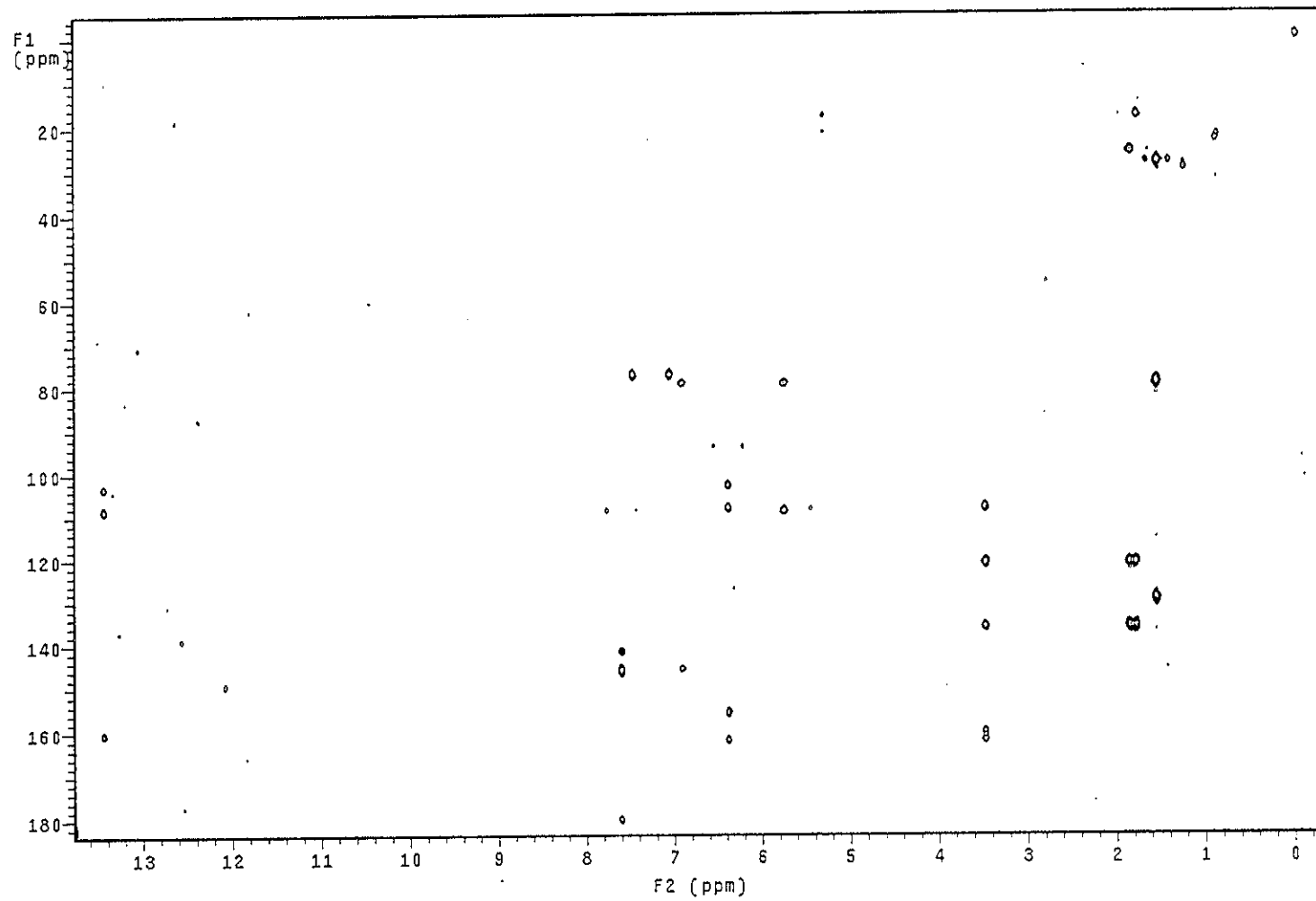


Figure 3.105 2D HMBC spectrum of TR7

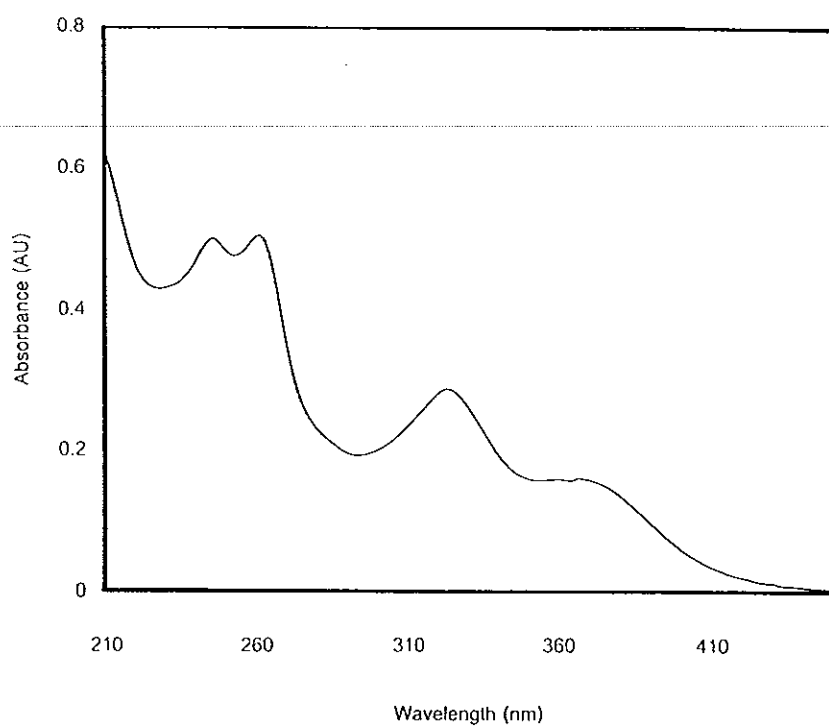


Figure 3.106 UV (MeOH) spectrum of TR11

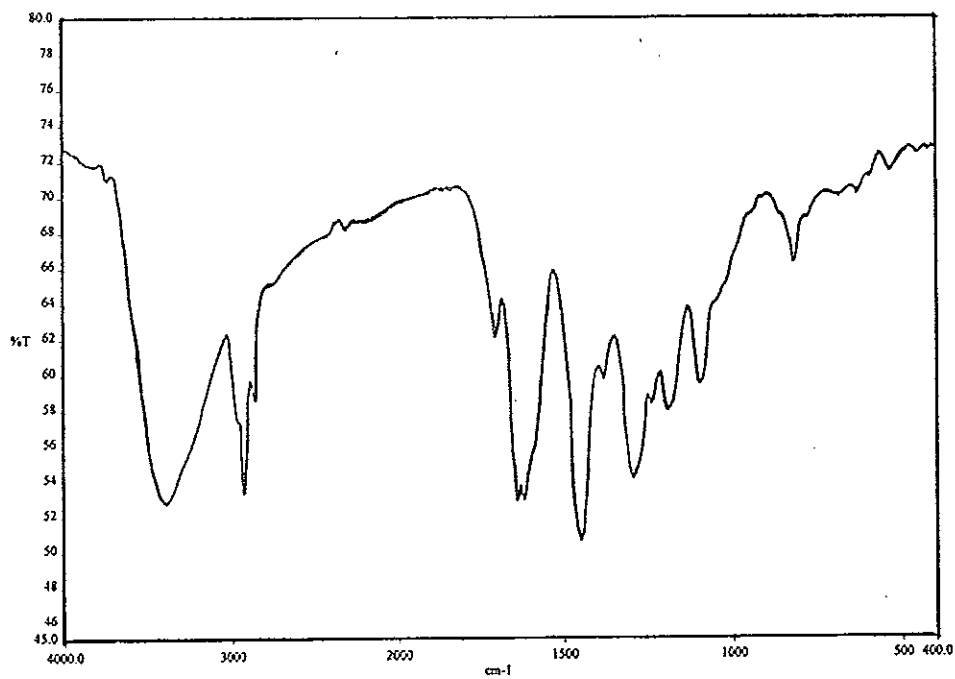


Figure 3.107 FT-IR (neat) spectrum of TR11

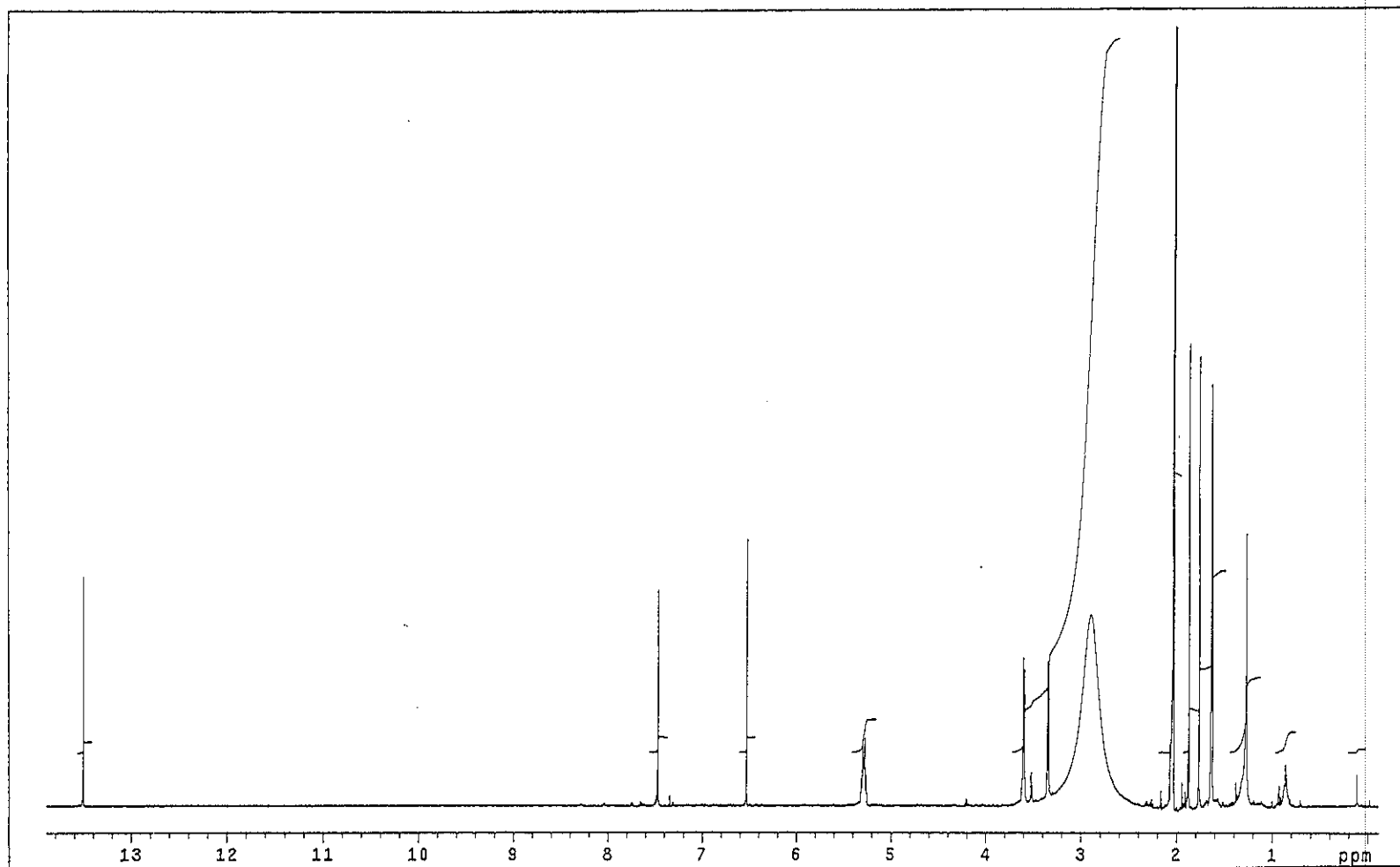


Figure 3.108 ^1H NMR (500 MHz)(Acetone- d_6) spectrum of TR11

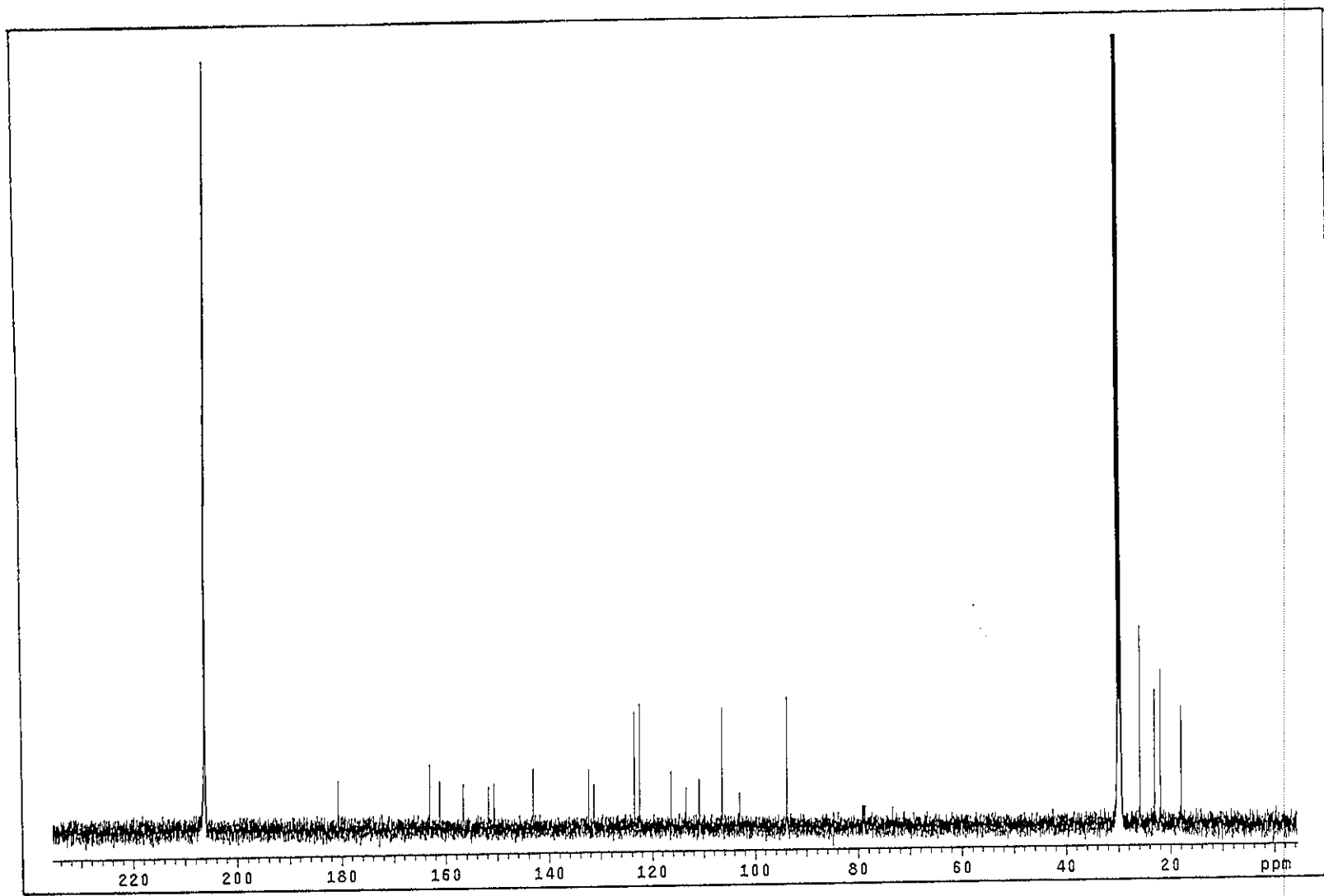


Figure 3.109 ^{13}C NMR (125 MHz)(Acetone- d_6) spectrum of TR11

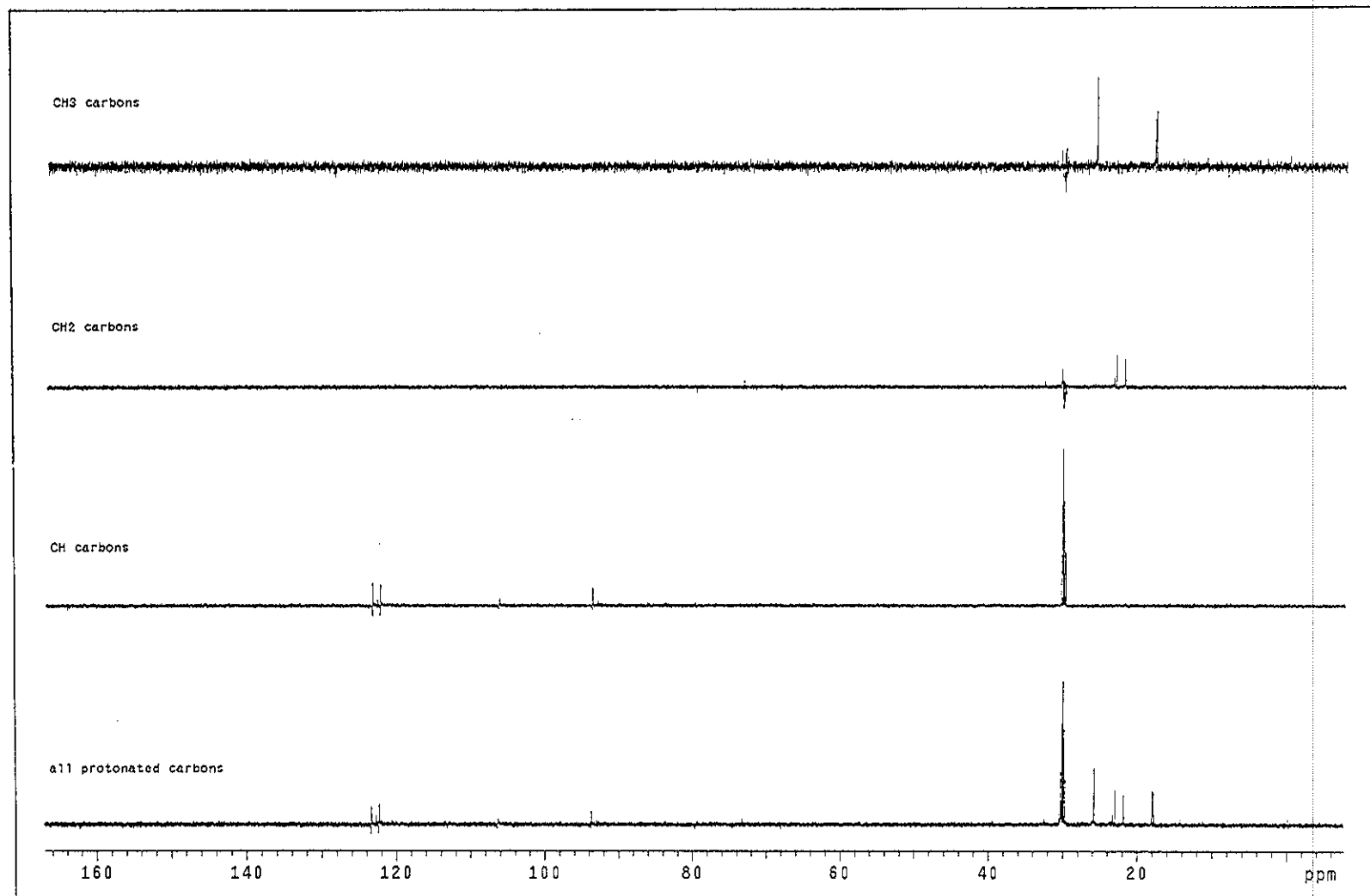


Figure 3.110 DEPT spectrum of TR11

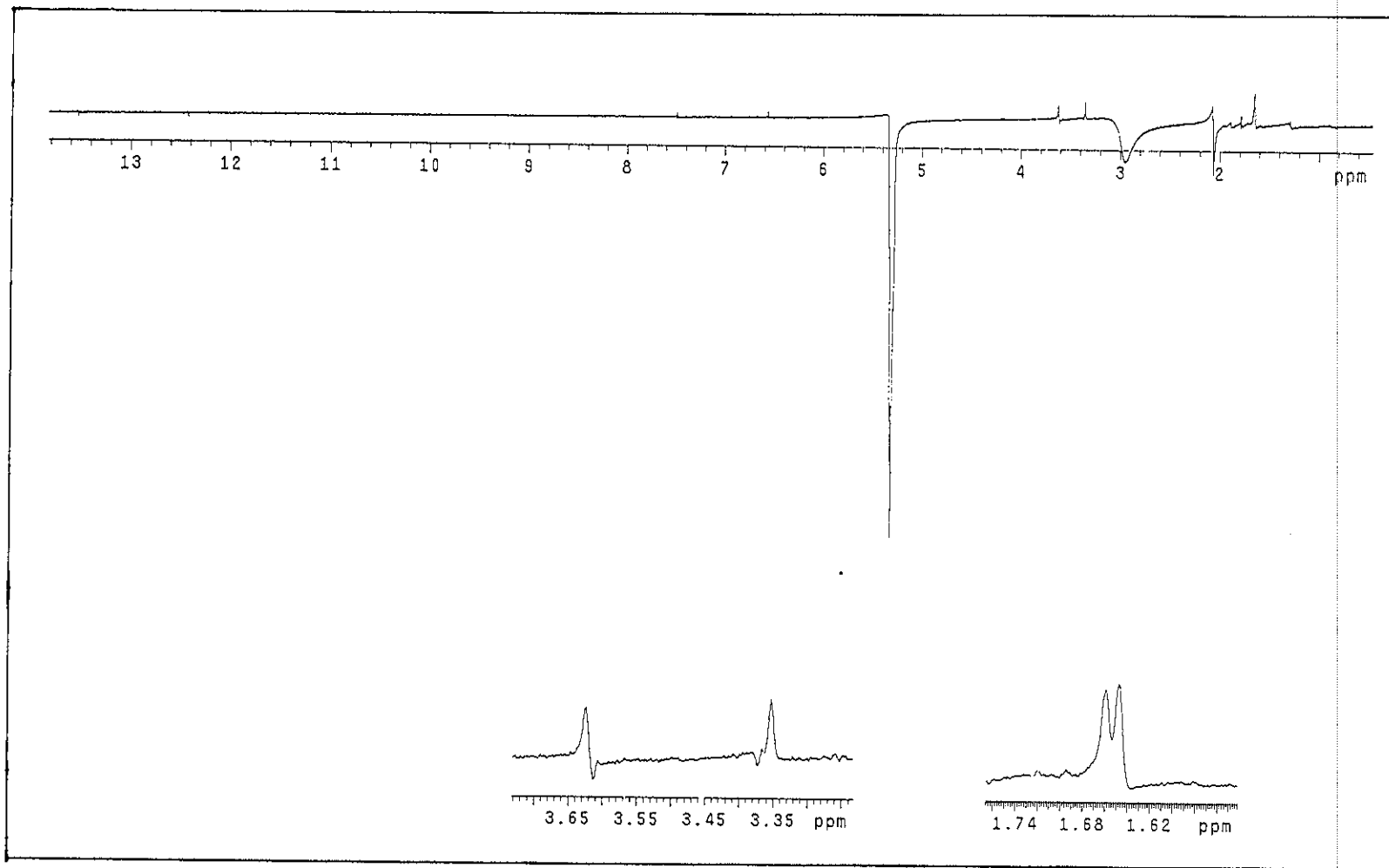


Figure 3.111 NOEDIFF spectrum of TR11 after irradiation at δ_H 5.30

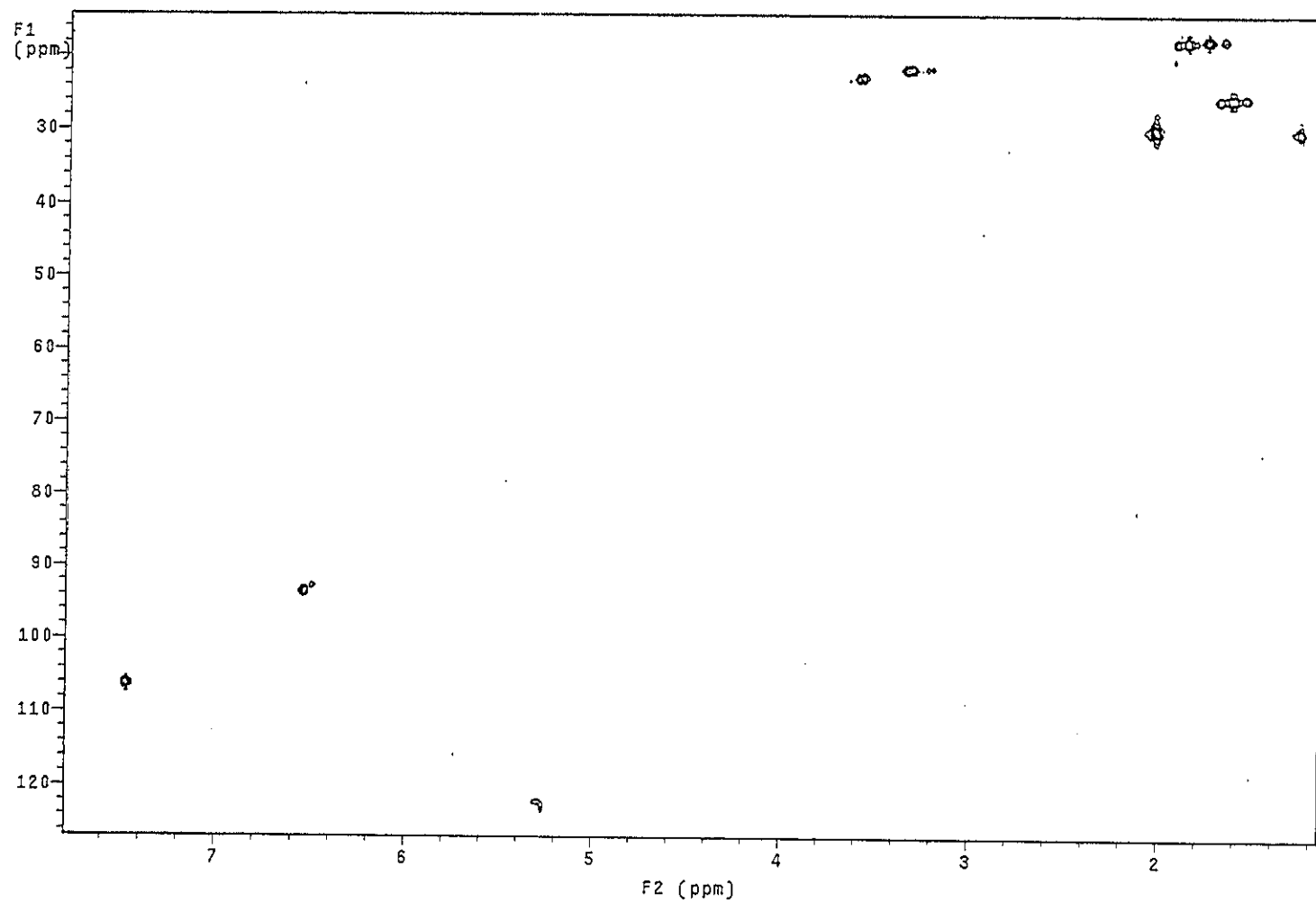


Figure 3.112 2D HMQC spectrum of TR11

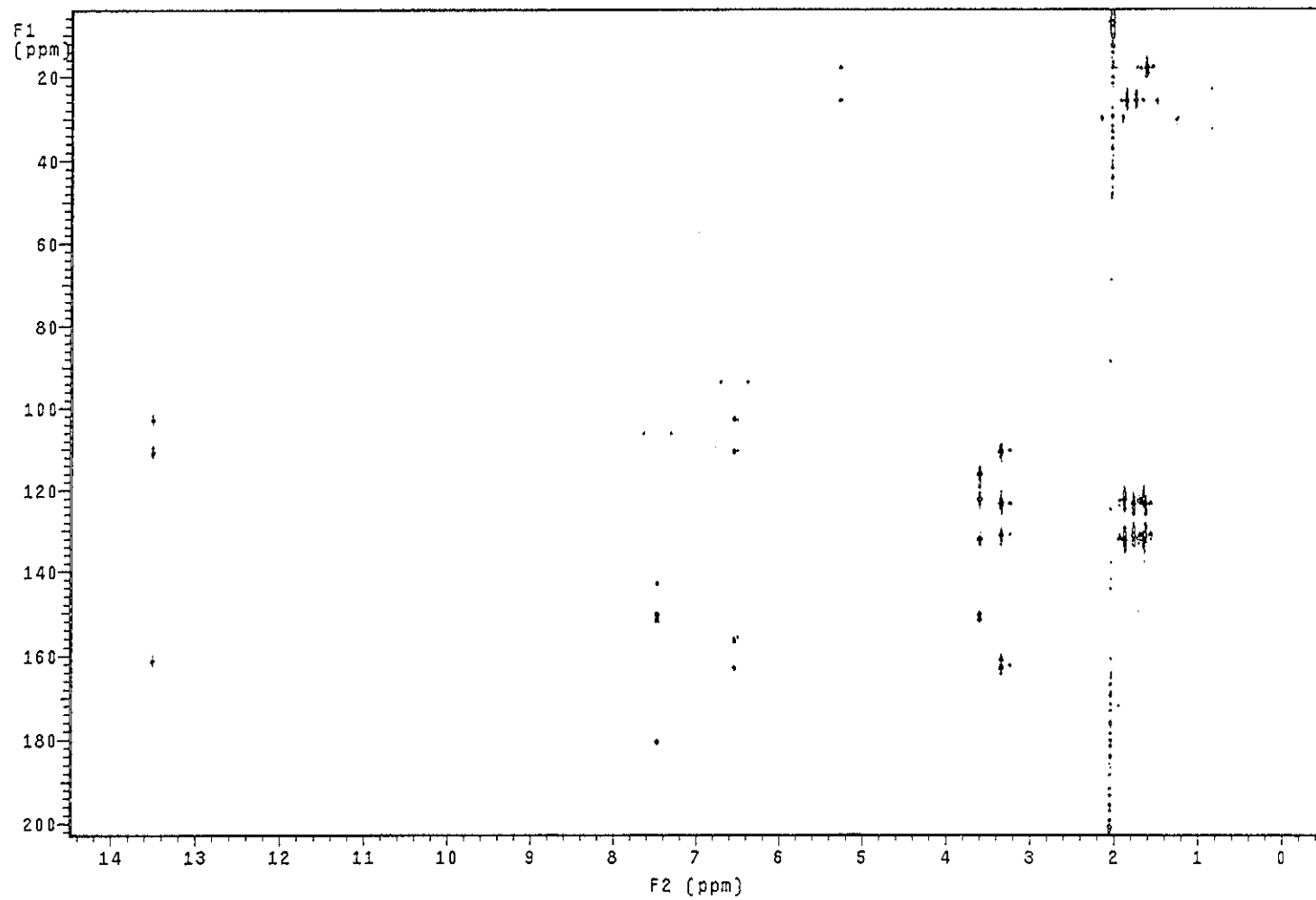


Figure 3.113 2D HMBC spectrum of TR11

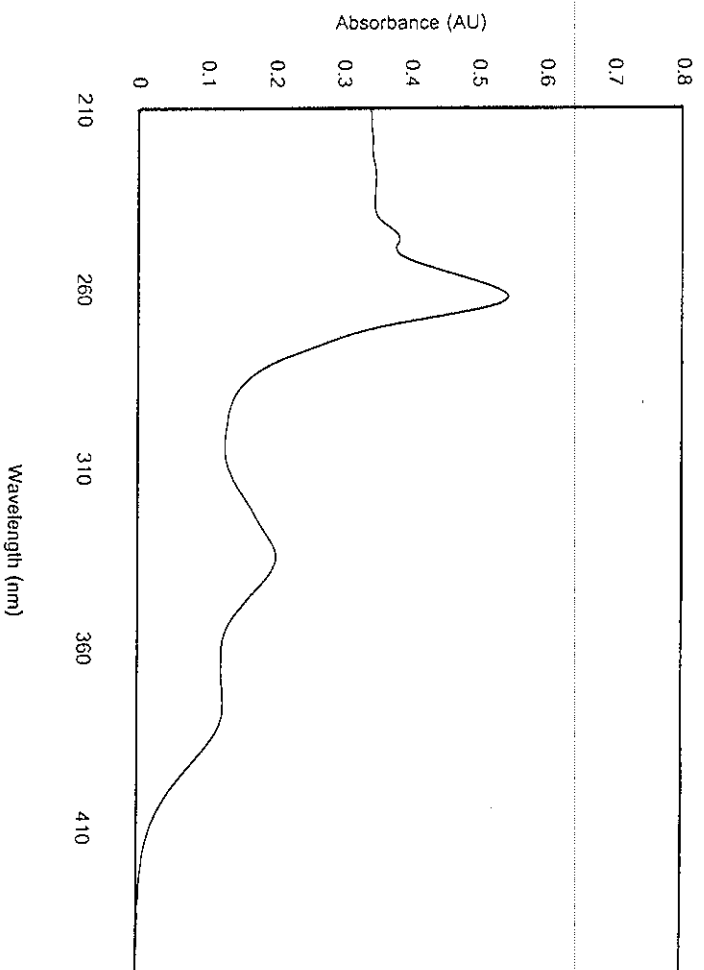


Figure 3.114 UV (MeOH) spectrum of TR3

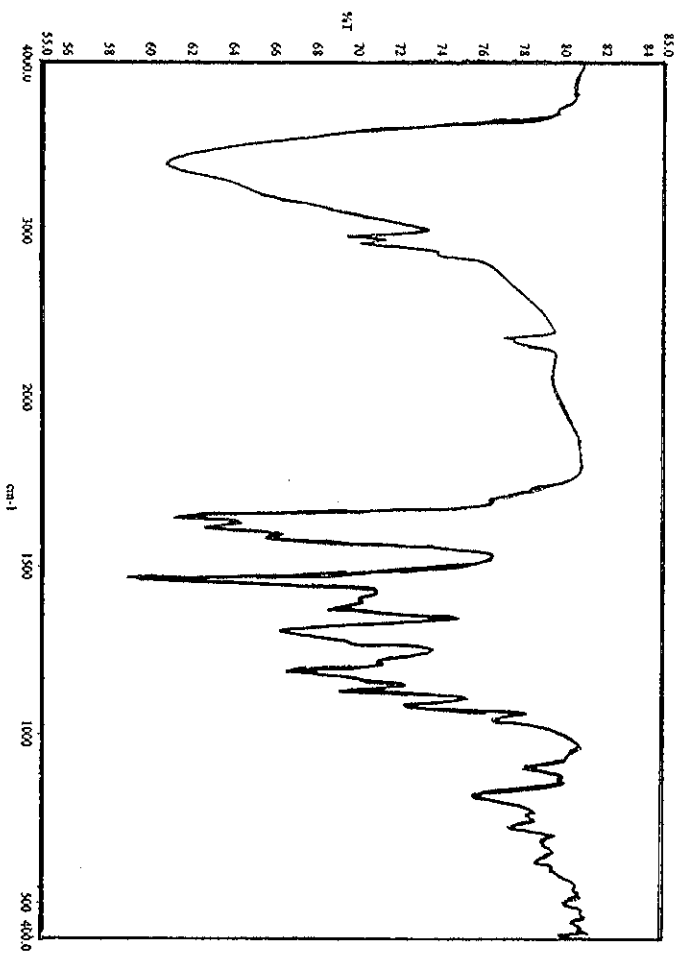


Figure 3.115 FT-IR (neat) spectrum of TR3

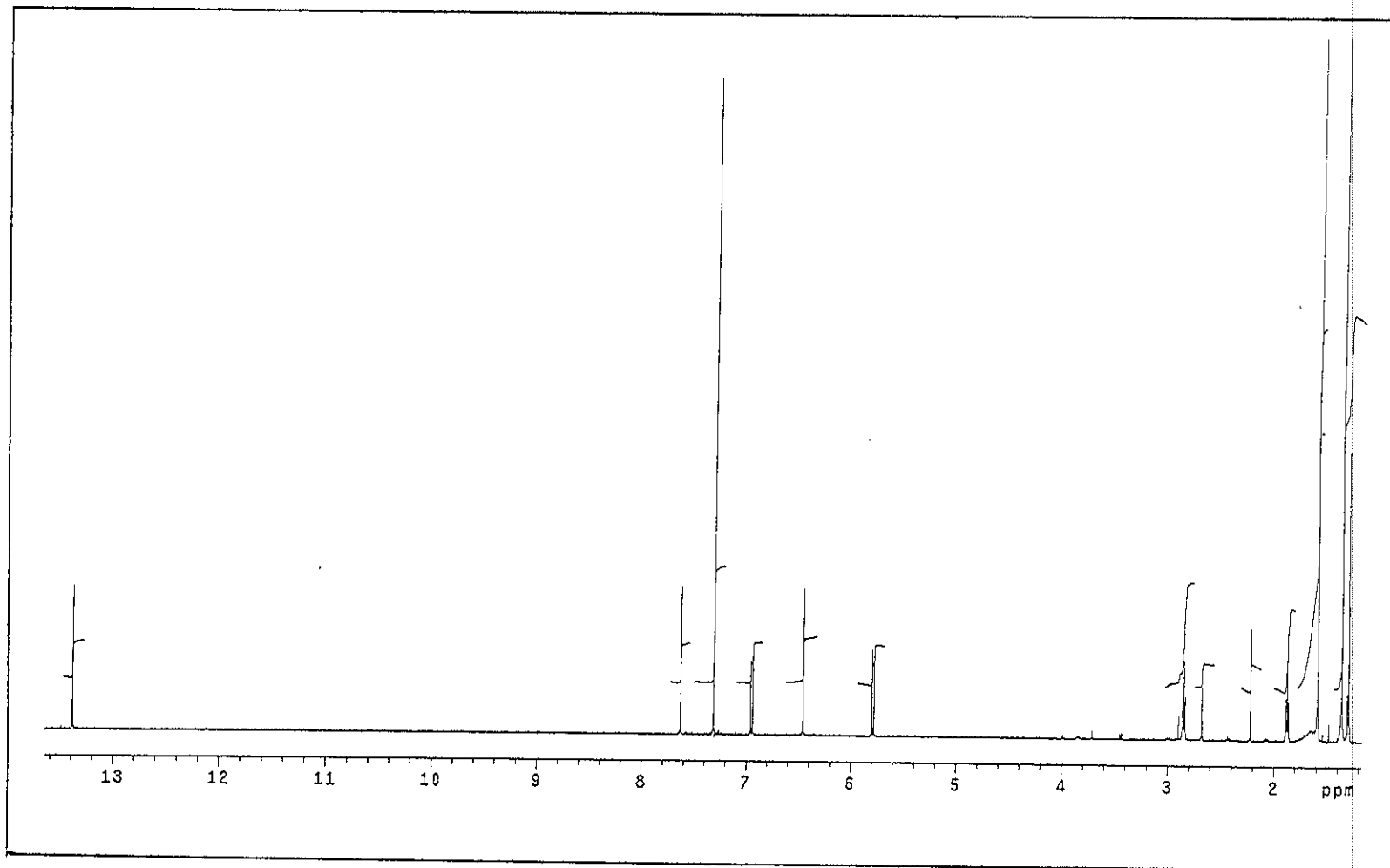


Figure 3.116 ^1H NMR (500 MHz)(CDCl_3) spectrum of TR3

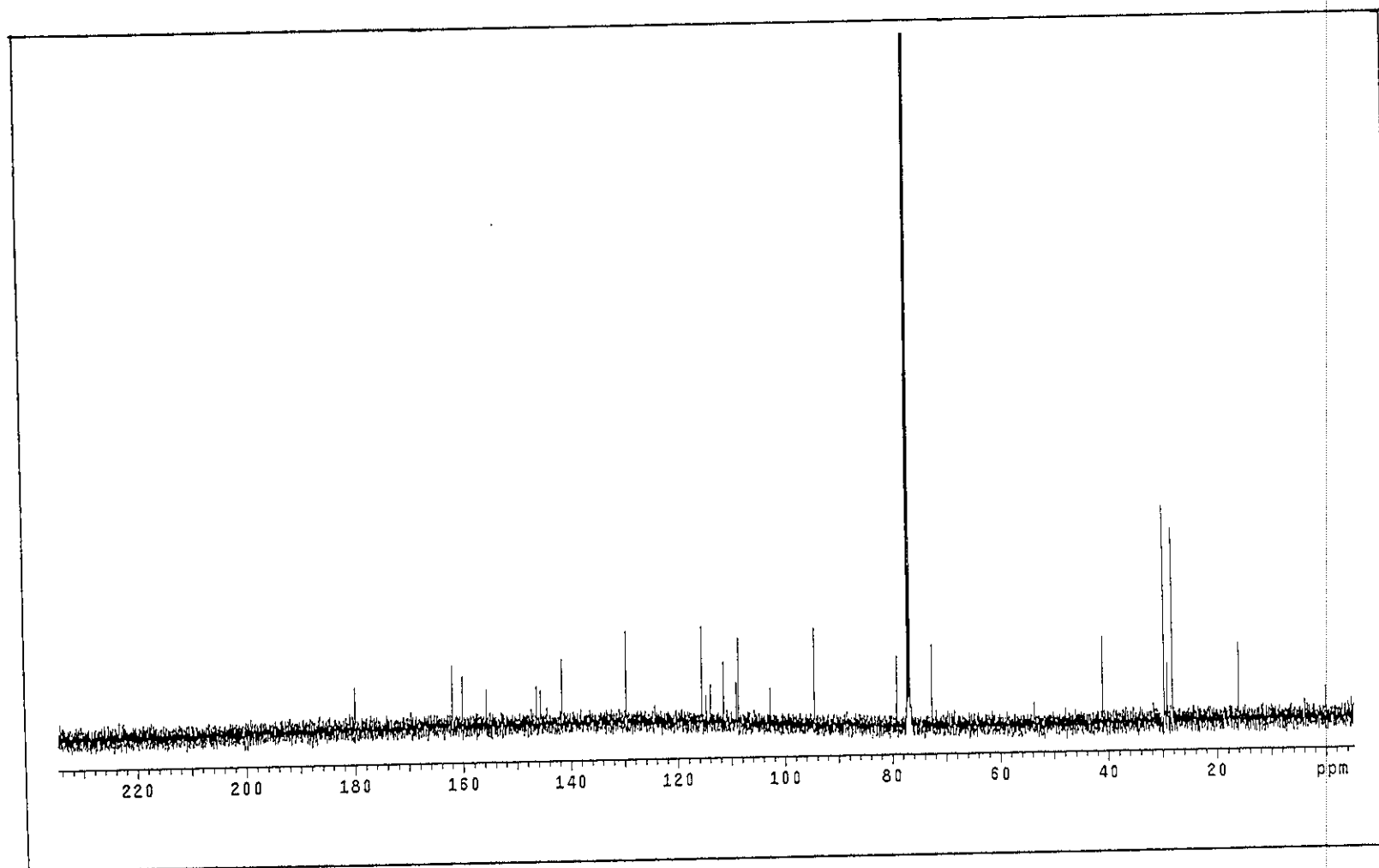


Figure 3.117 ^{13}C NMR (125 MHz)(CDCl_3) spectrum of TR3

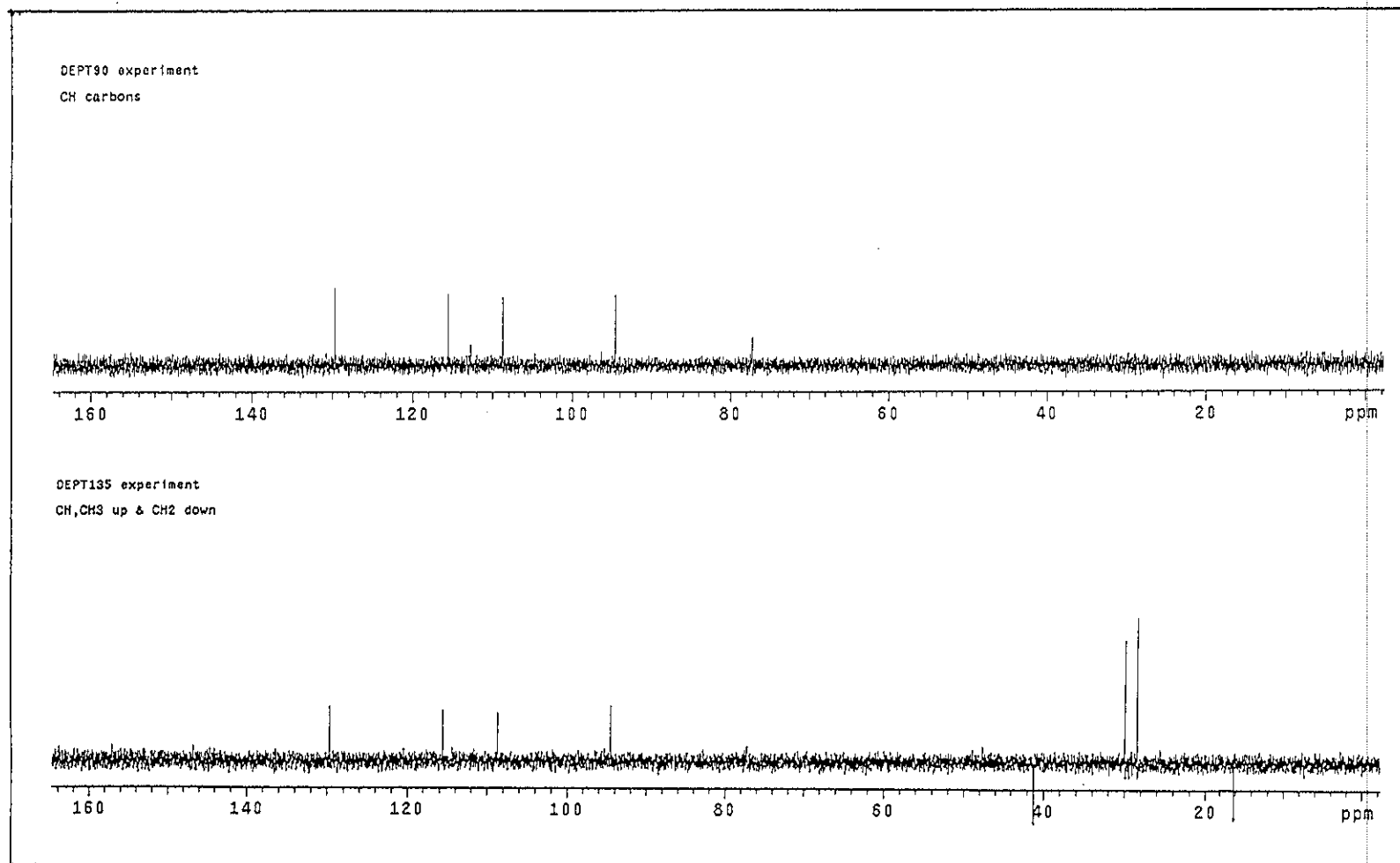


Figure 3.118 DEPT spectrum of TR3

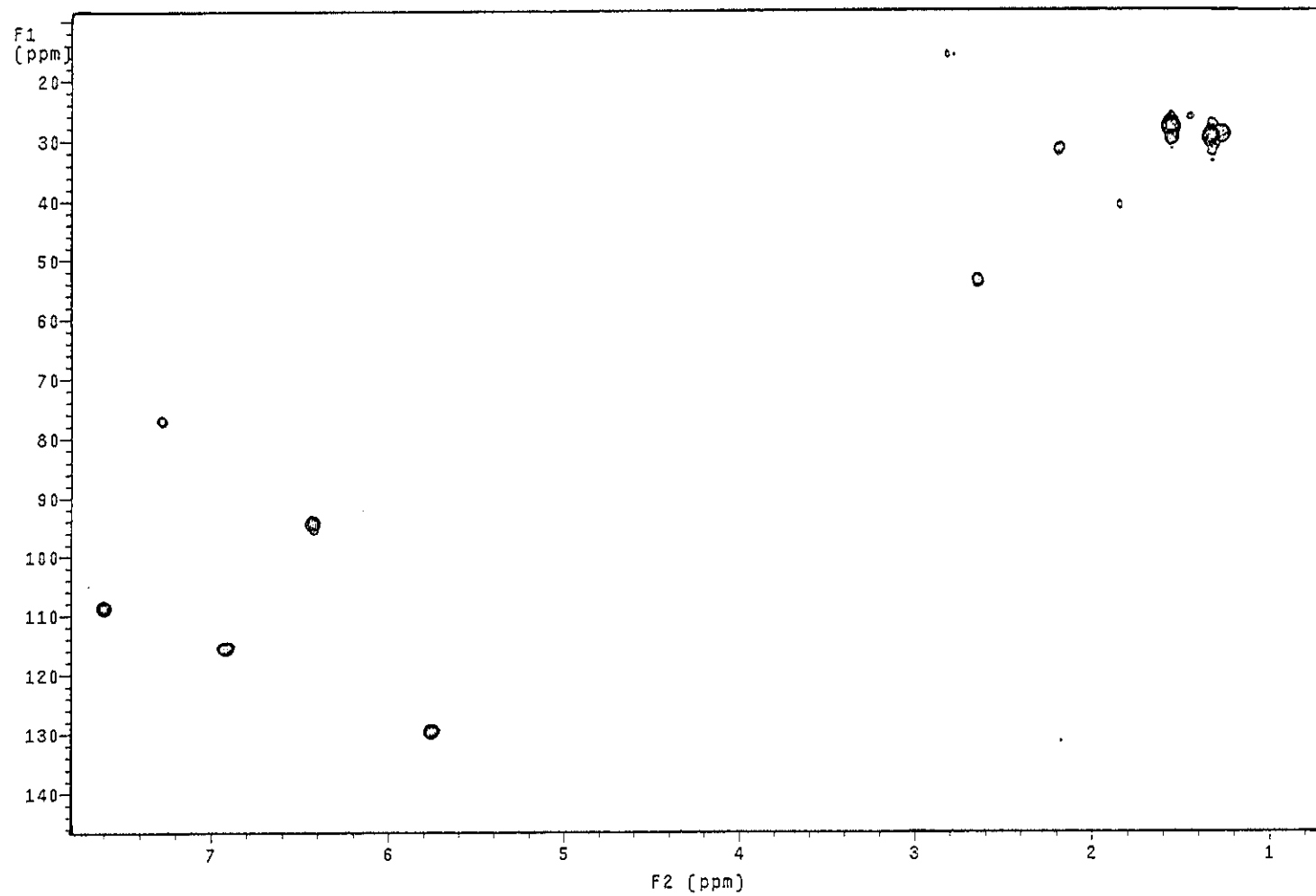


Figure 3.119 2D HMQC spectrum of TR3

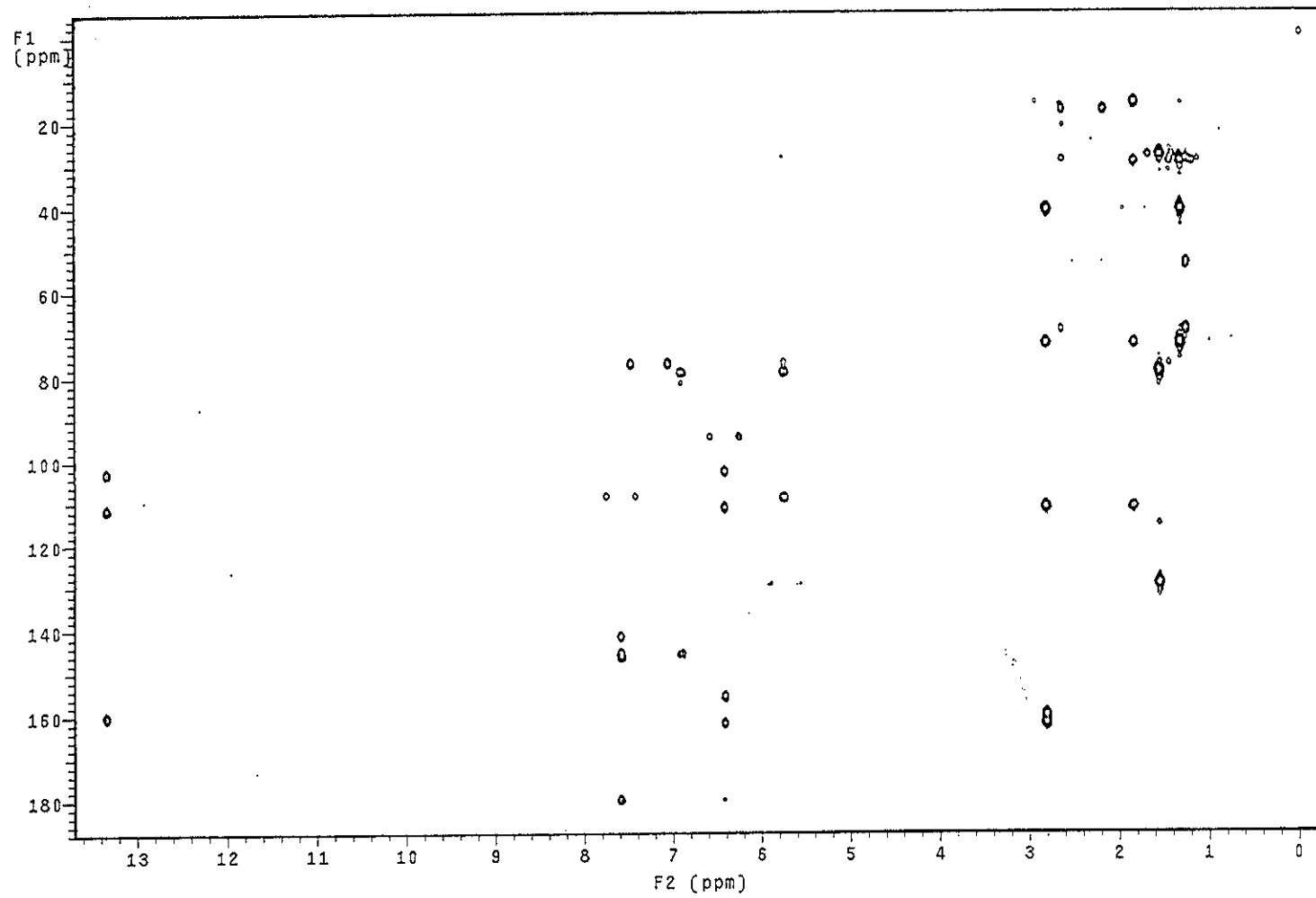


Figure 3.120 2D HMBC spectrum of TR3

Abs

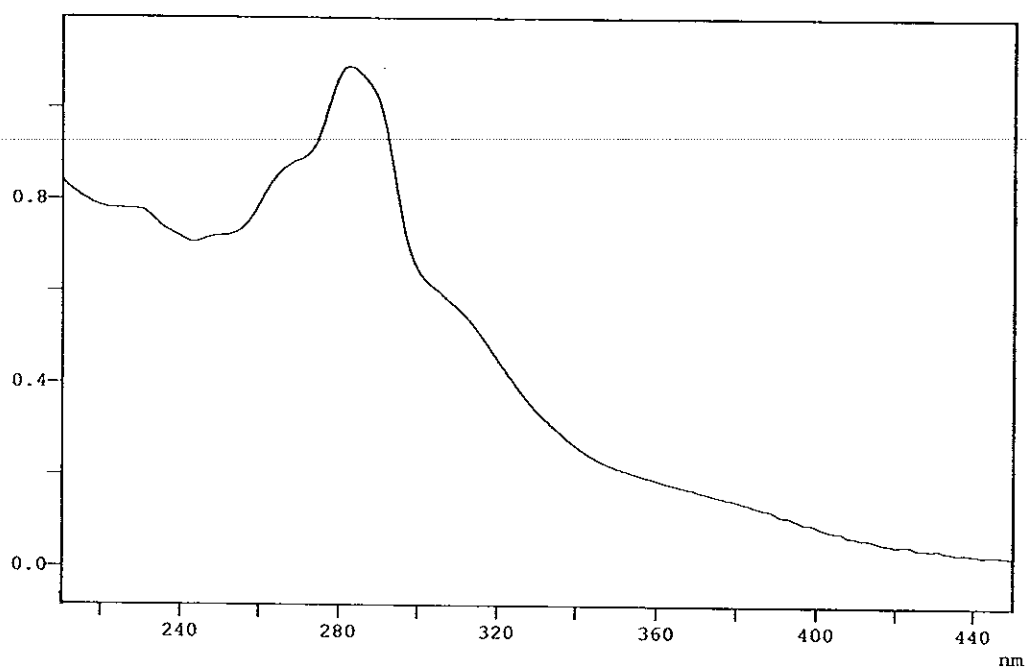


Figure 3.121 UV (MeOH) spectrum of TR9

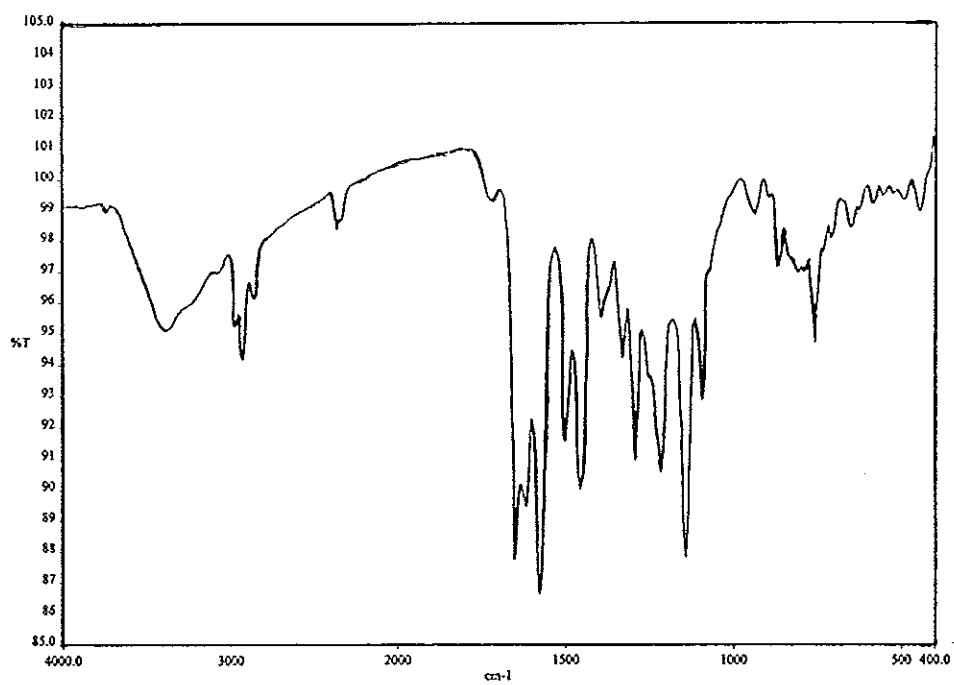


Figure 3.122 FT-IR (neat) spectrum of TR9

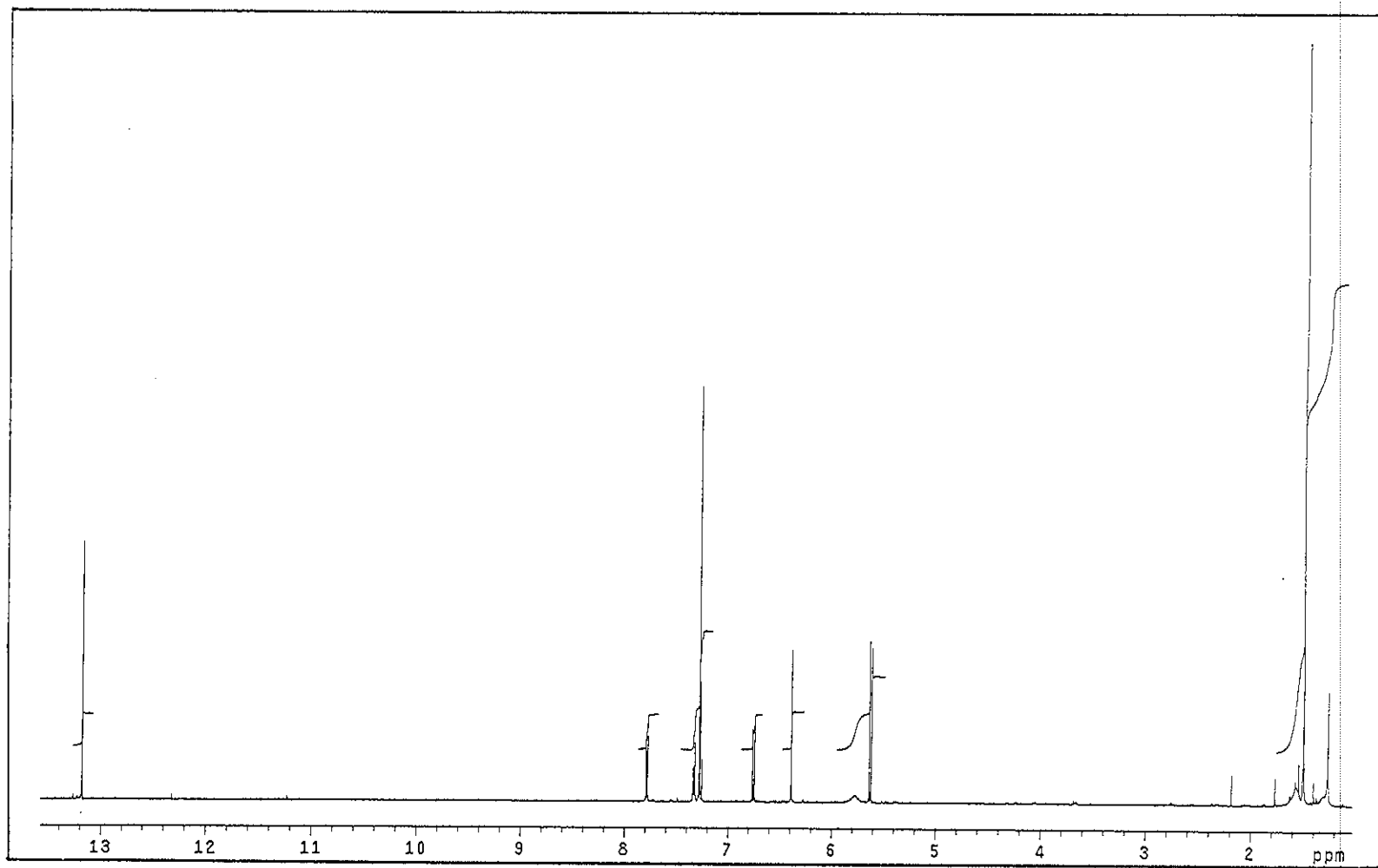


Figure 3.123 ^1H NMR (500 MHz)(CDCl_3) spectrum of TR9

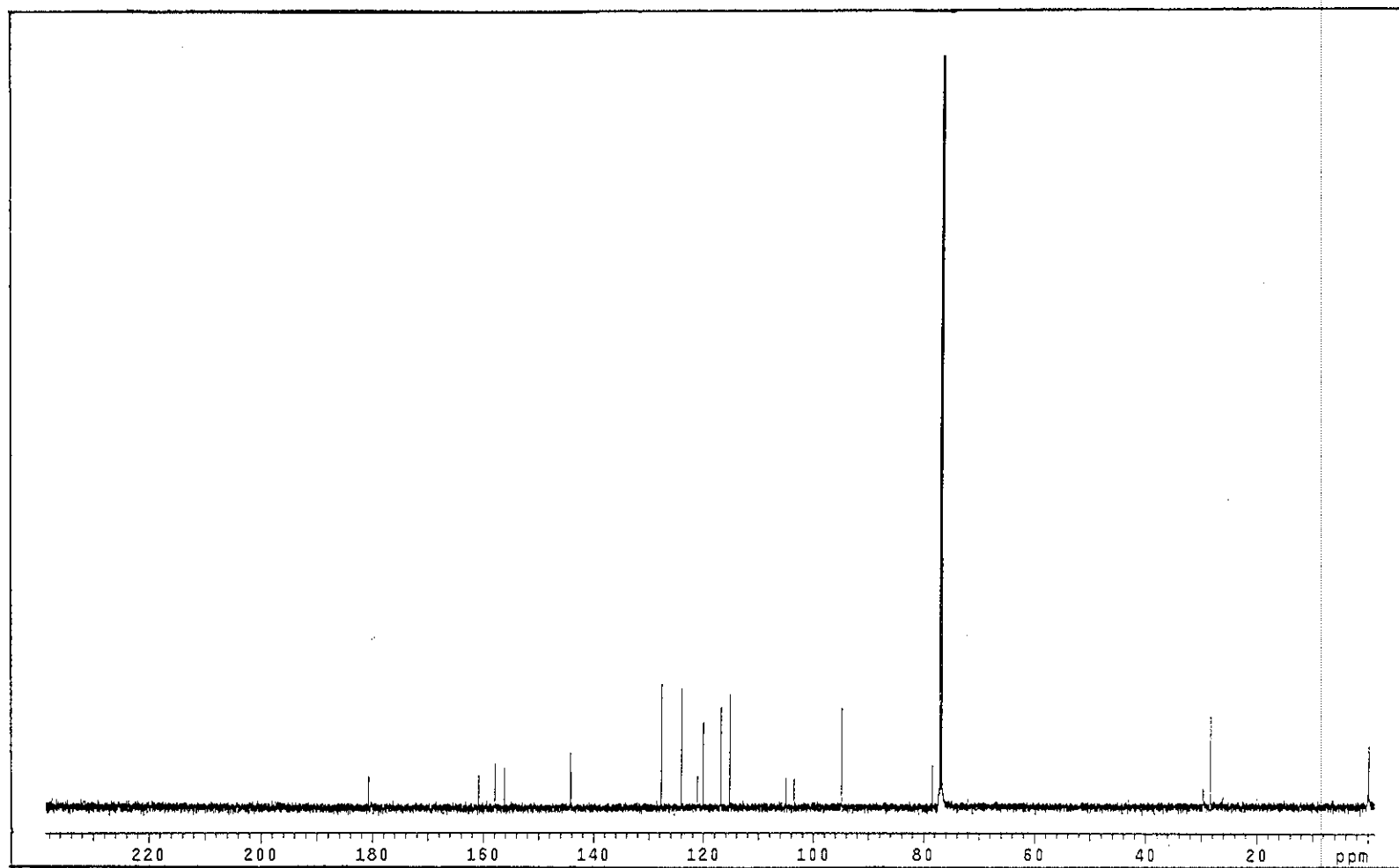


Figure 3.124 ^{13}C NMR (125 MHz)(CDCl_3) spectrum of TR9

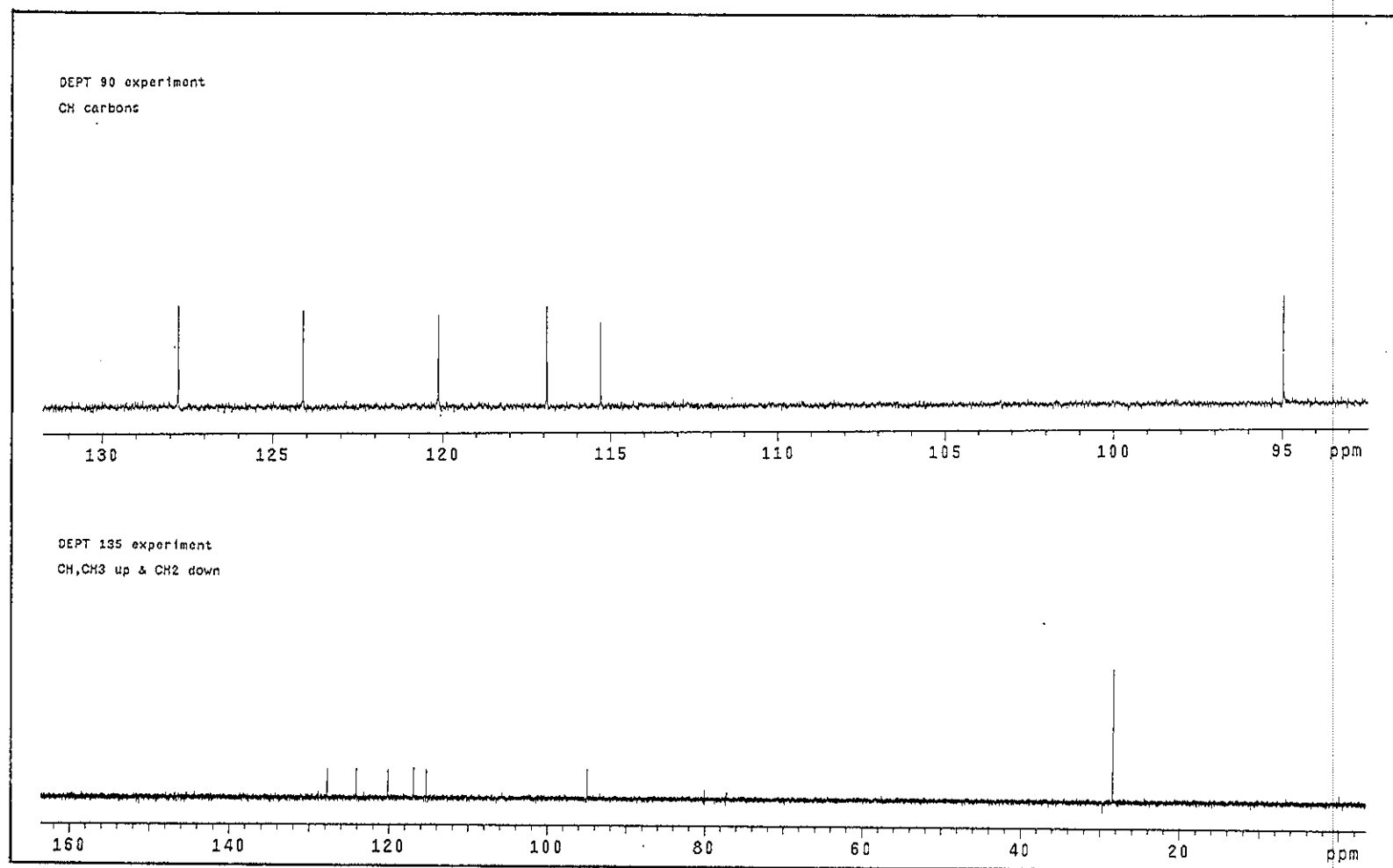


Figure 3.125 DEPT spectrum of TR9

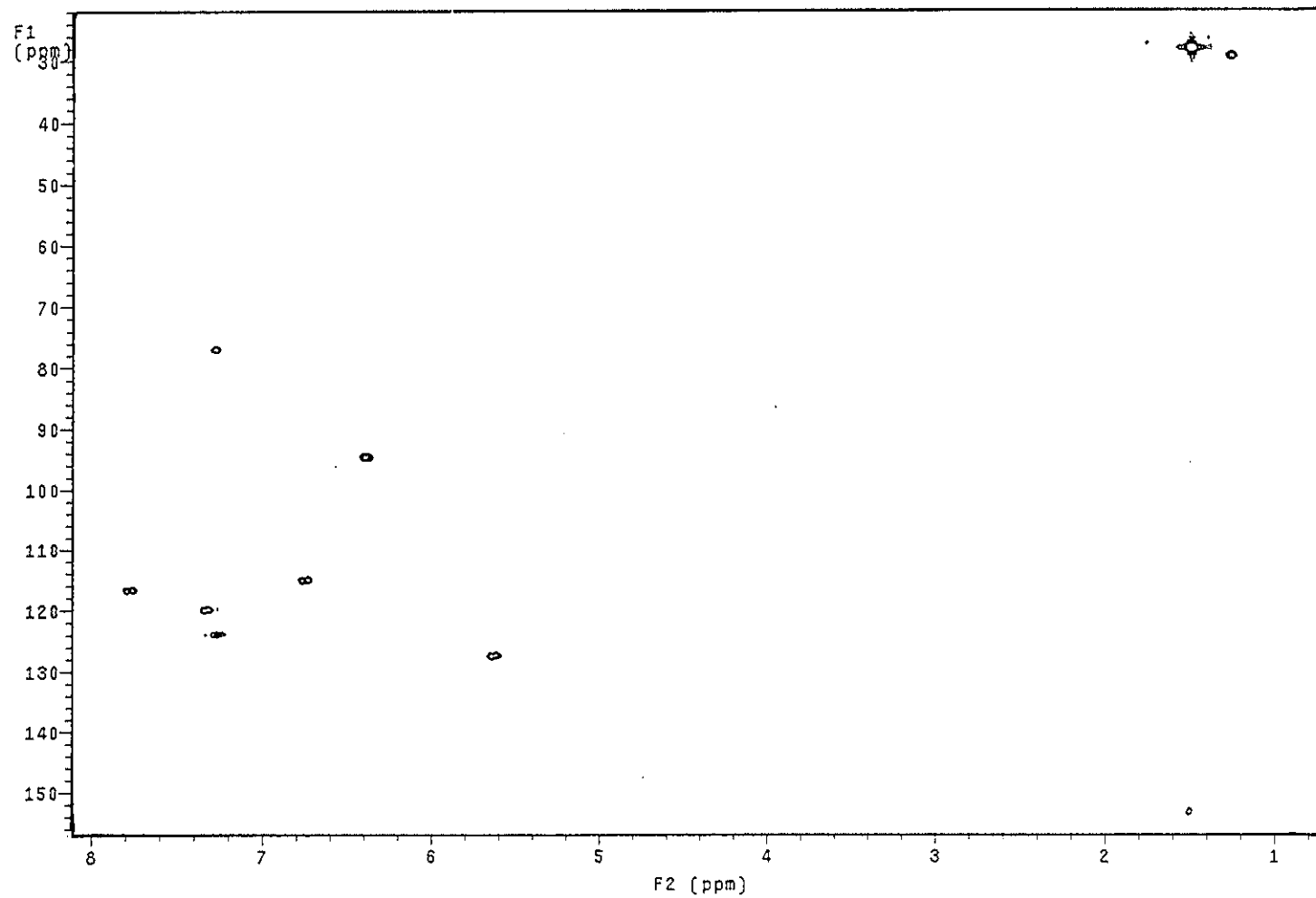


Figure 3.126 2D HMQC spectrum of TR9

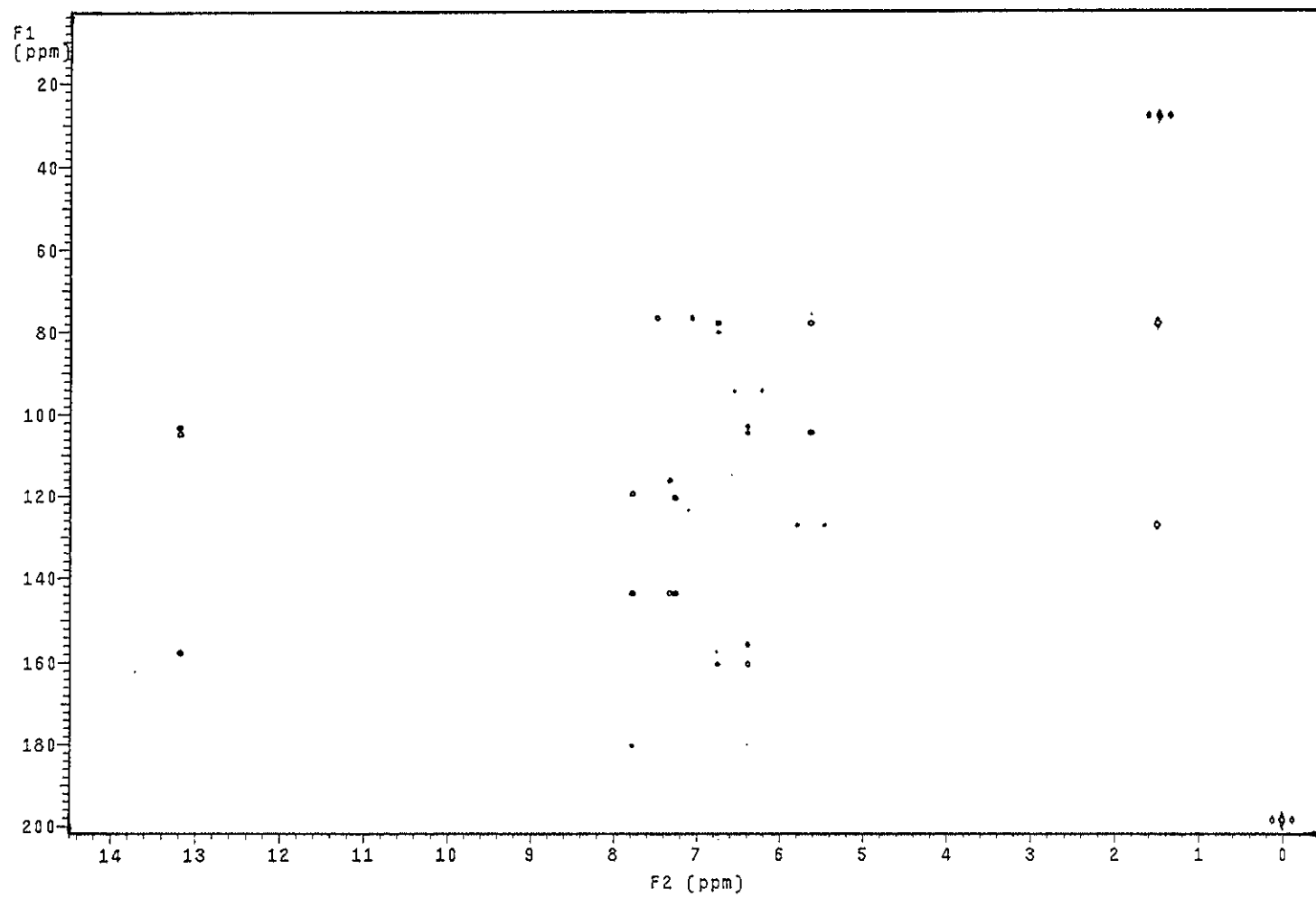


Figure 3.127 2D HMBC spectrum of TR9

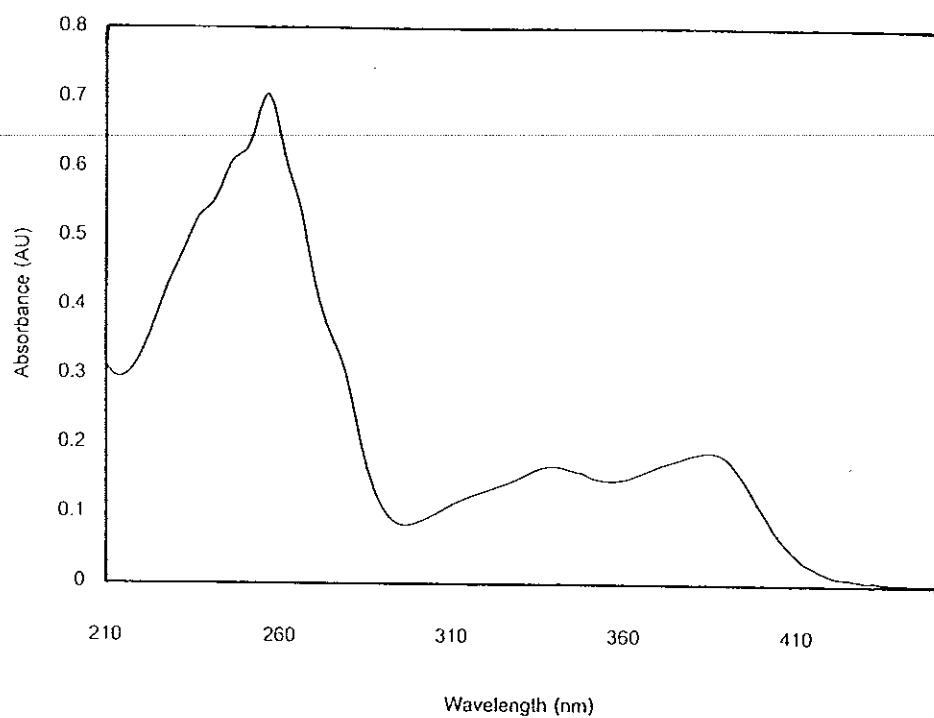


Figure 3.128 UV (MeOH) spectrum of TR5

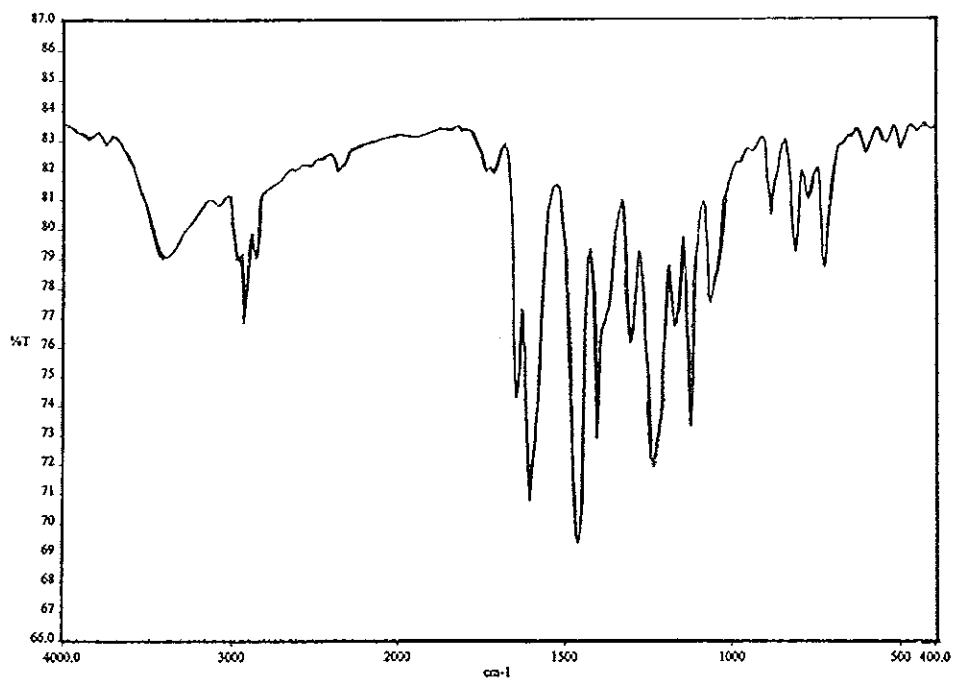


Figure 3.129 FT-IR (neat) spectrum of TR5

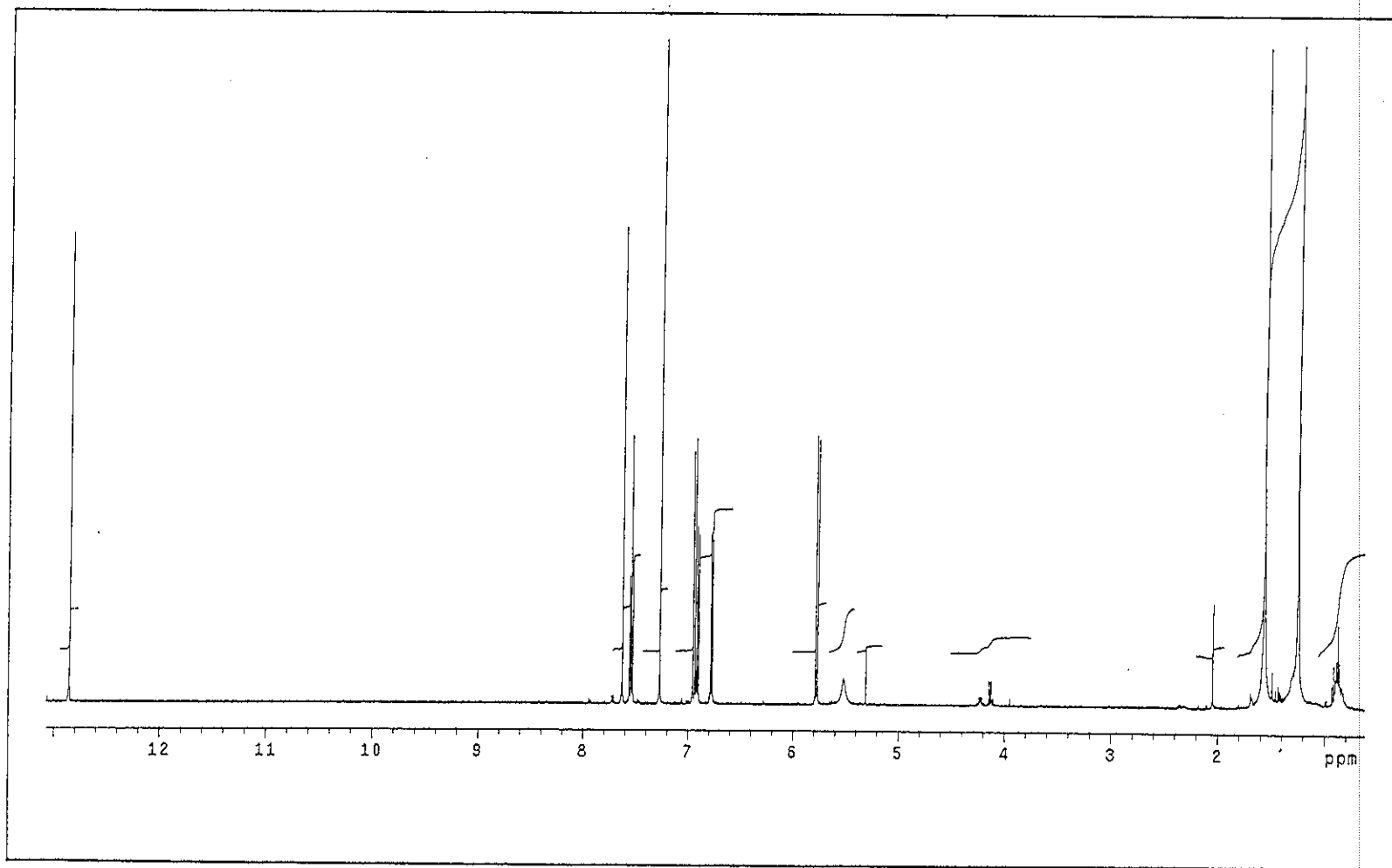


Figure 3.130 ^1H NMR (500 MHz)(CDCl_3) spectrum of TR5

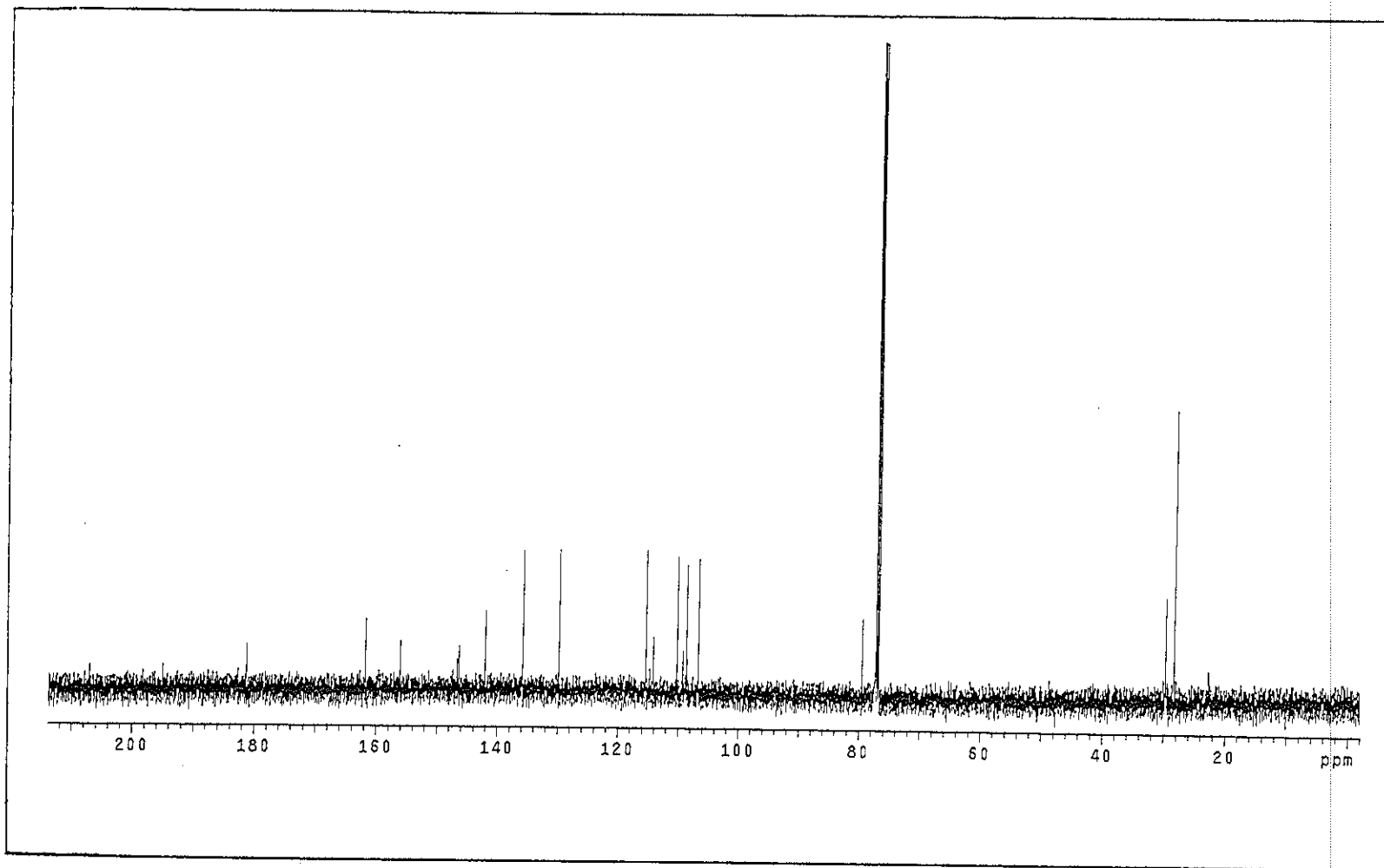


Figure 3.131 ¹³C NMR (125 MHz)(CDCl₃) spectrum of TR5

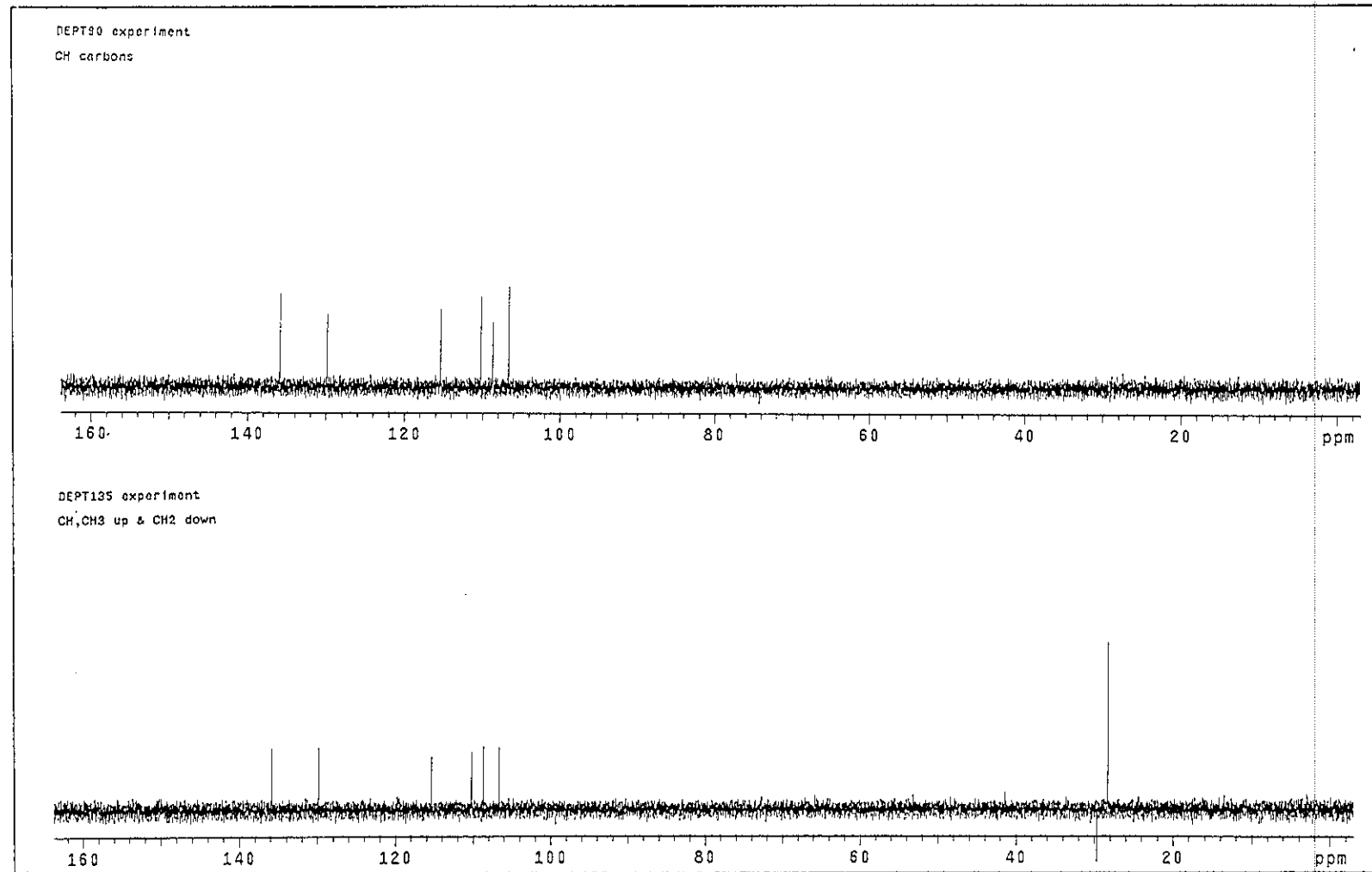


Figure 3.132 DEPT spectrum of TR5

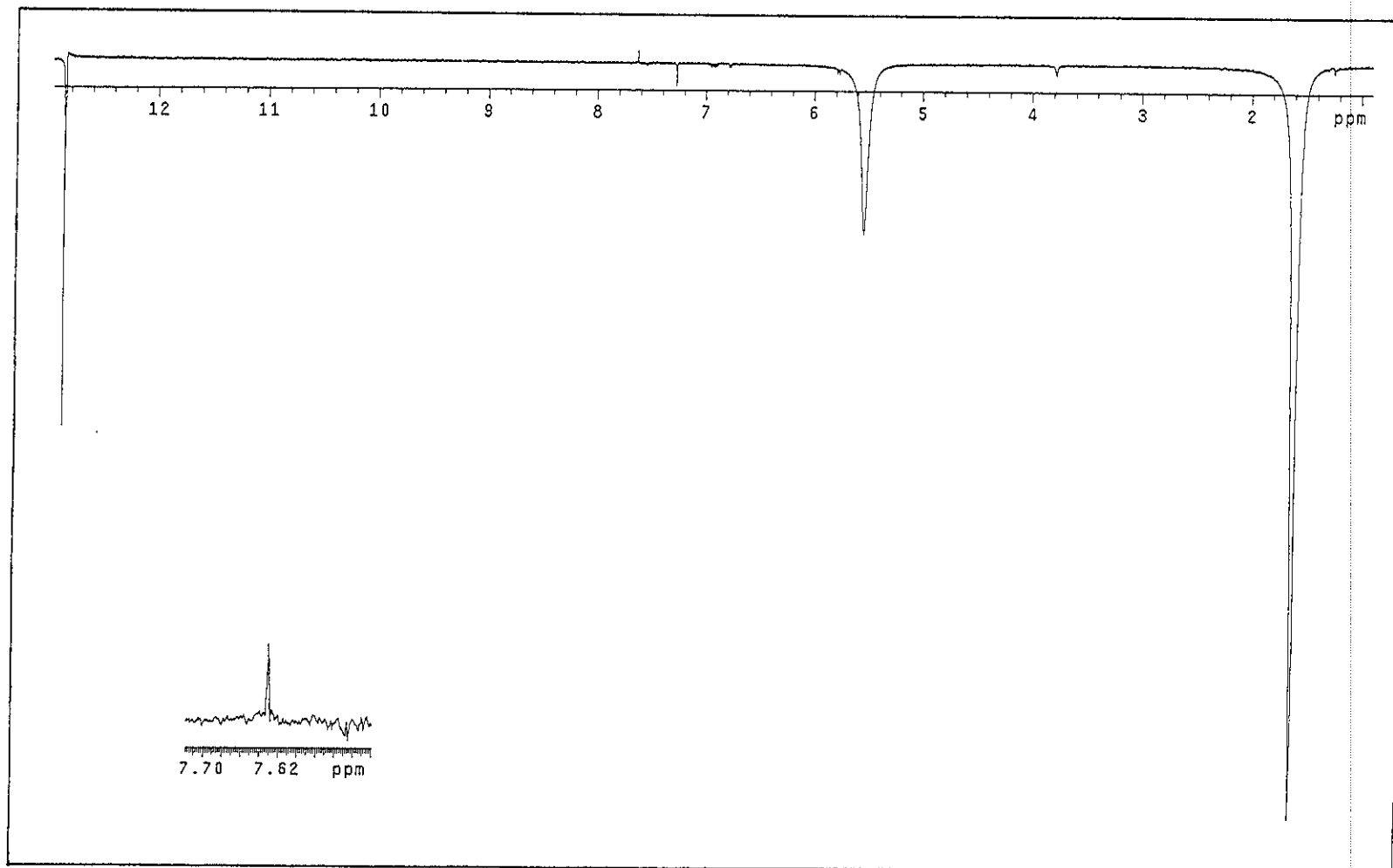


Figure 3.133 NOEDIFF spectrum of TR5 after irradiation at δ_H 5.52

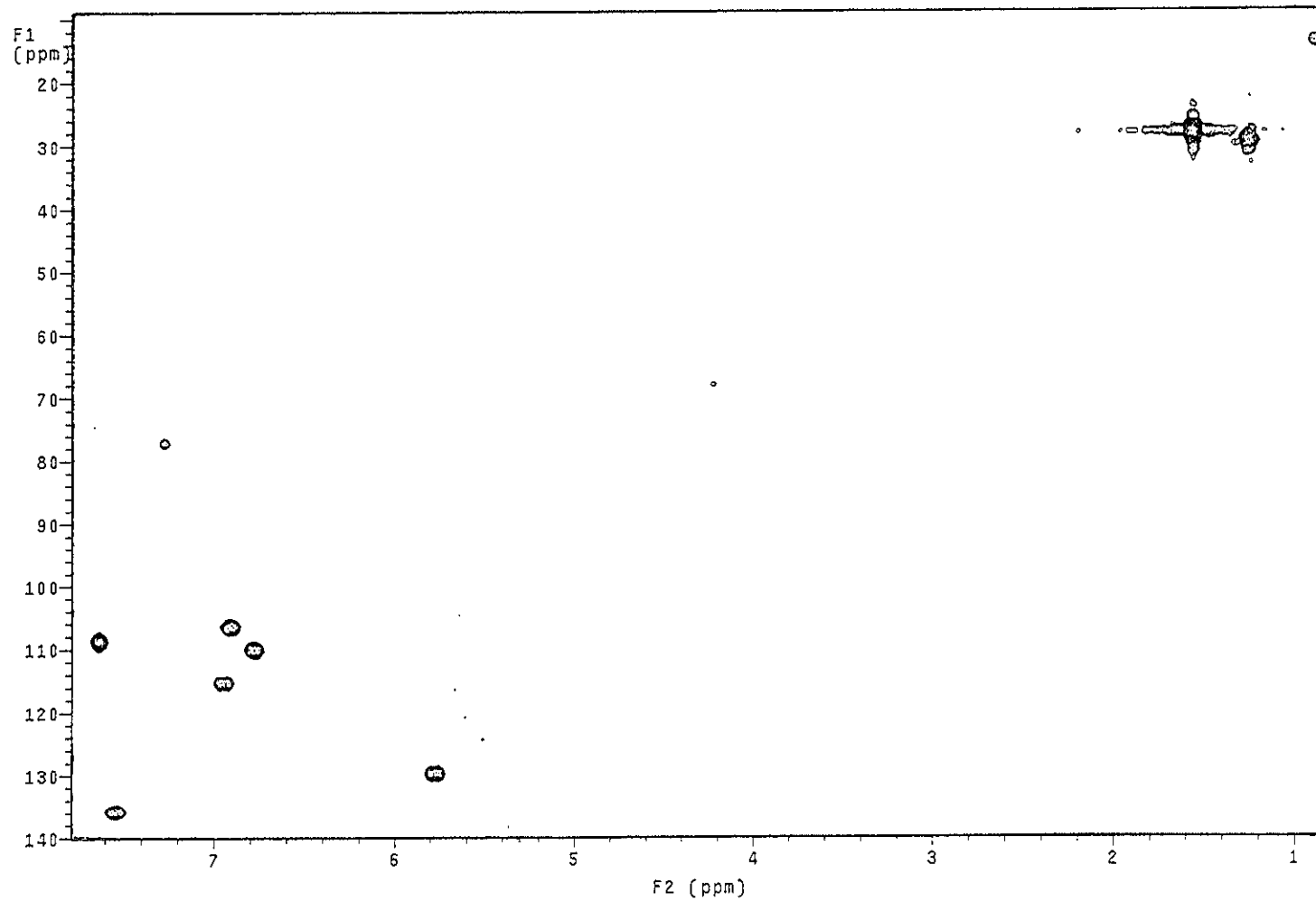


Figure 3.134 2D HMQC spectrum of TR5

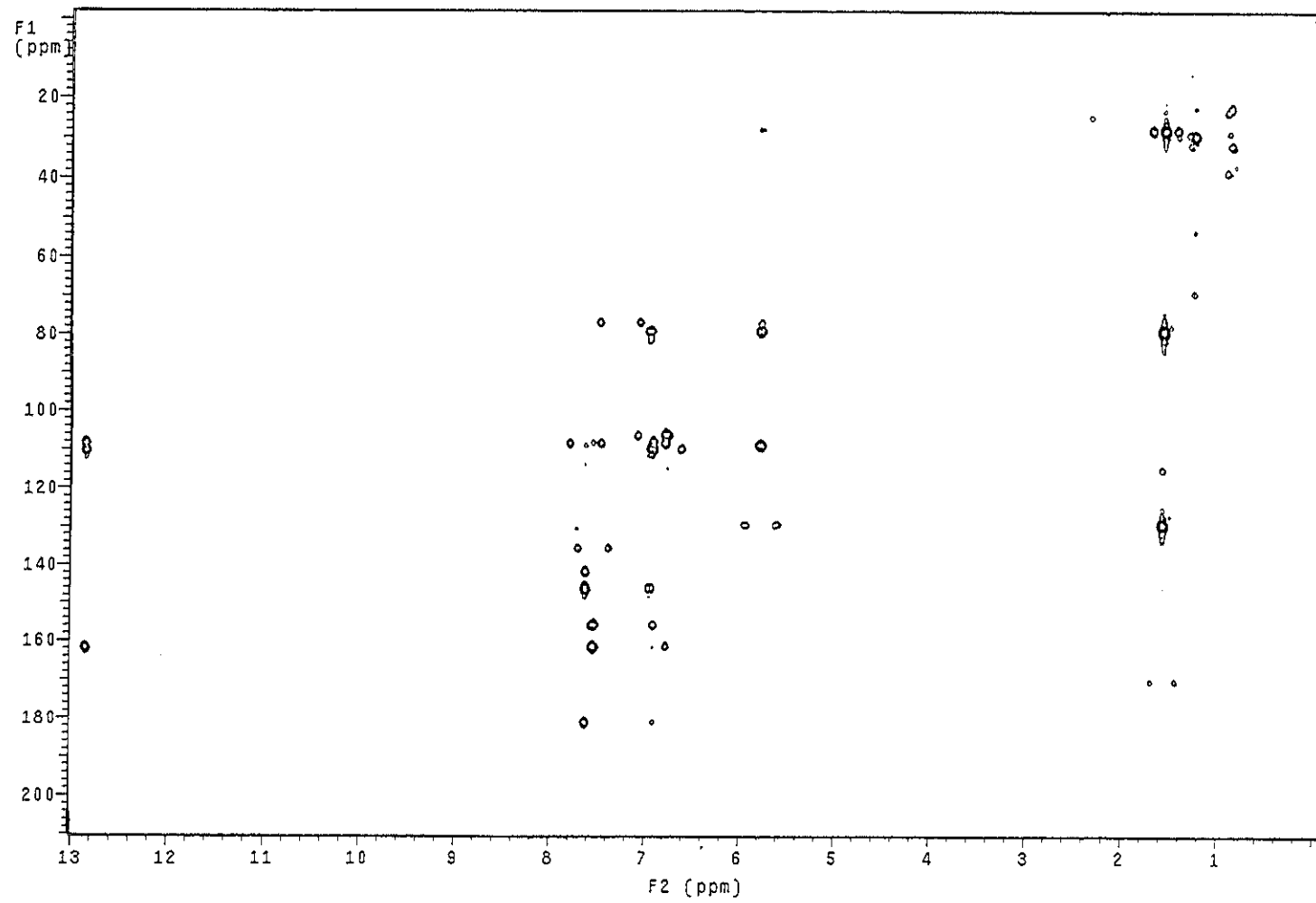


Figure 3.135 2D HMBC spectrum of TR5

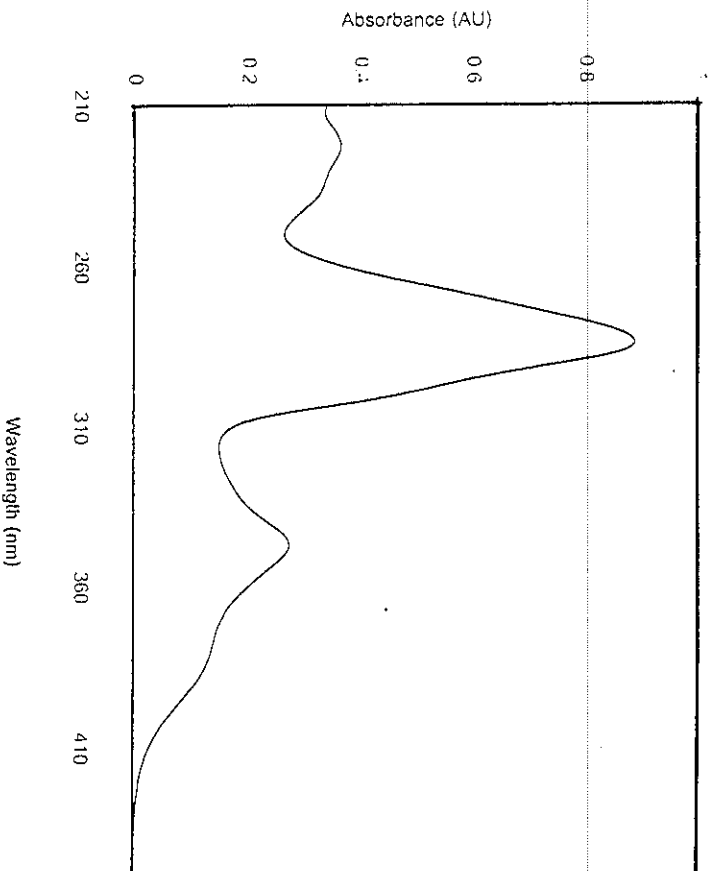


Figure 3.136 UV (MeOH) spectrum of TR13

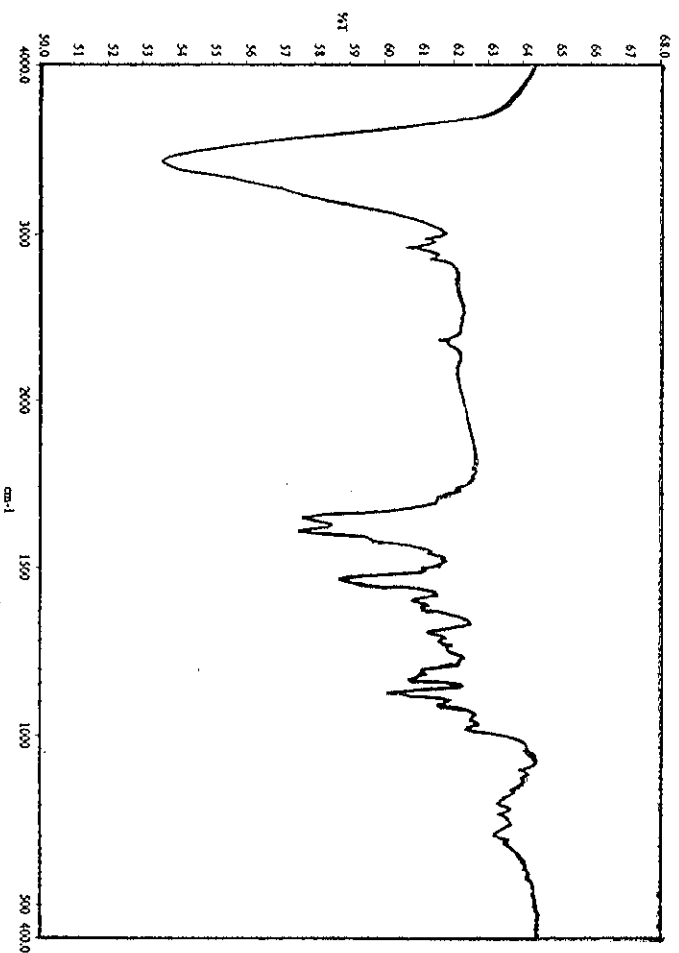


Figure 3.137 FT-IR (neat) spectrum of TR13

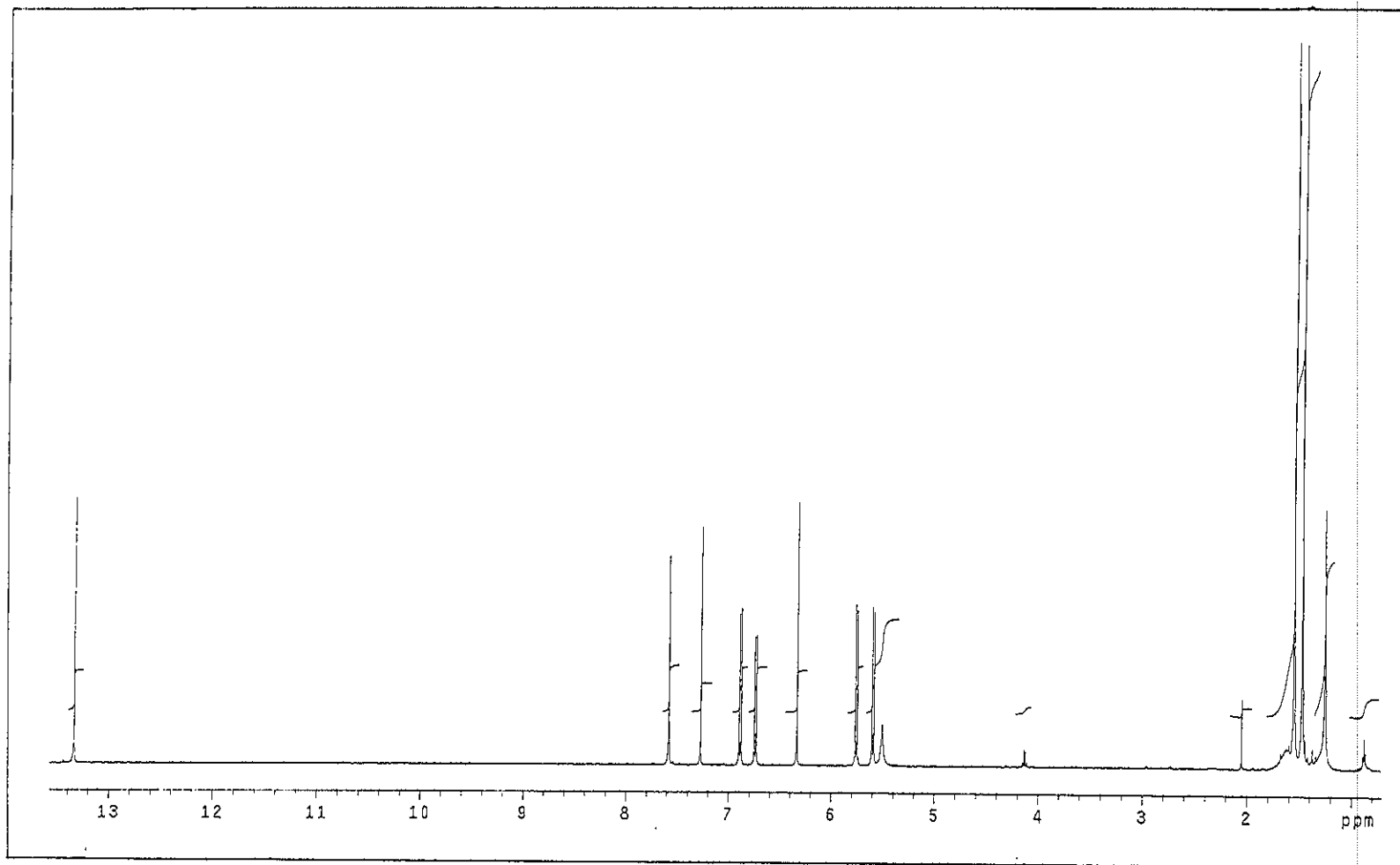


Figure 3.138 ^1H NMR (500 MHz)(CDCl_3) spectrum of TR13

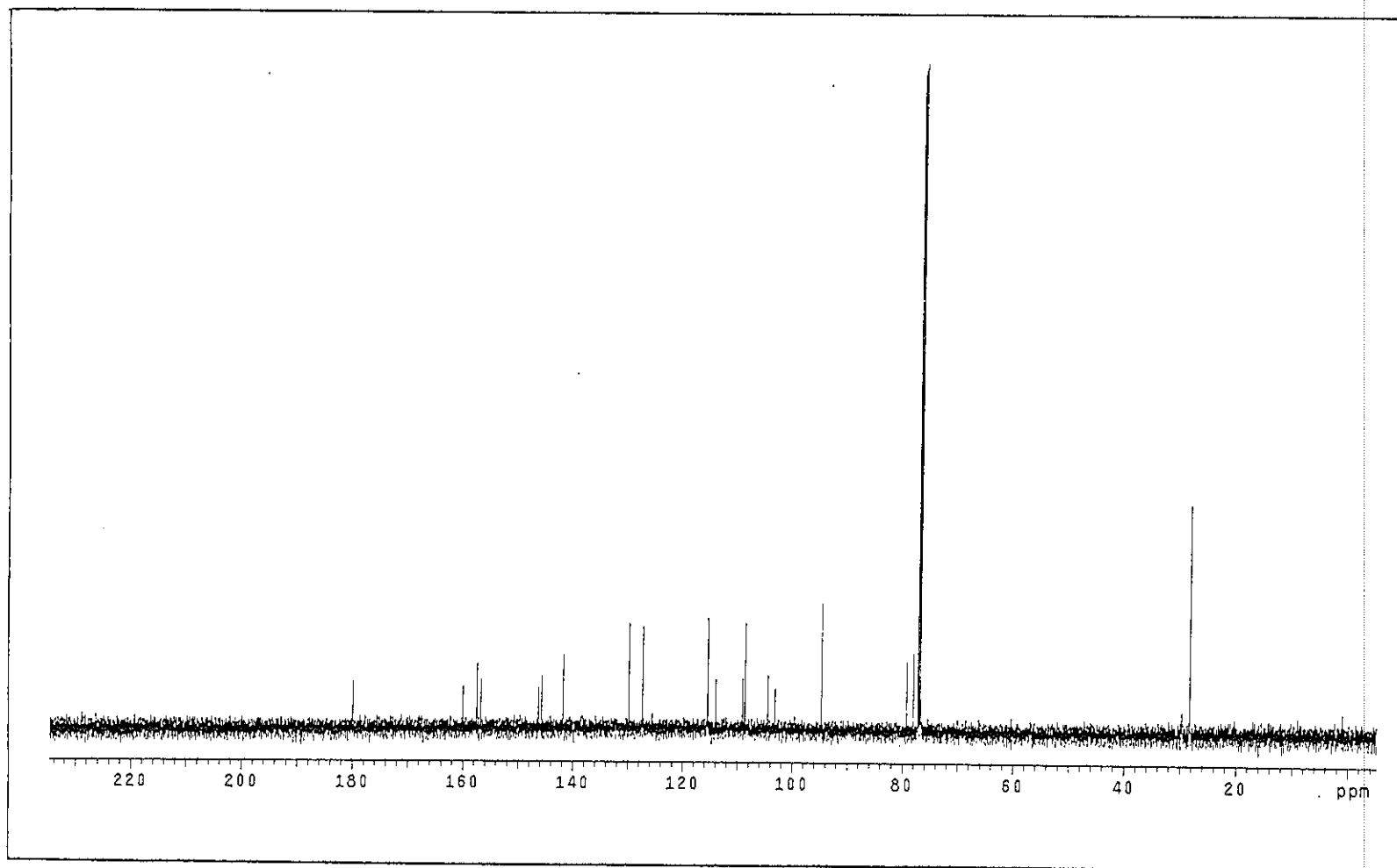


Figure 3.139 ^{13}C NMR (125 MHz)(CDCl_3) spectrum of TR13

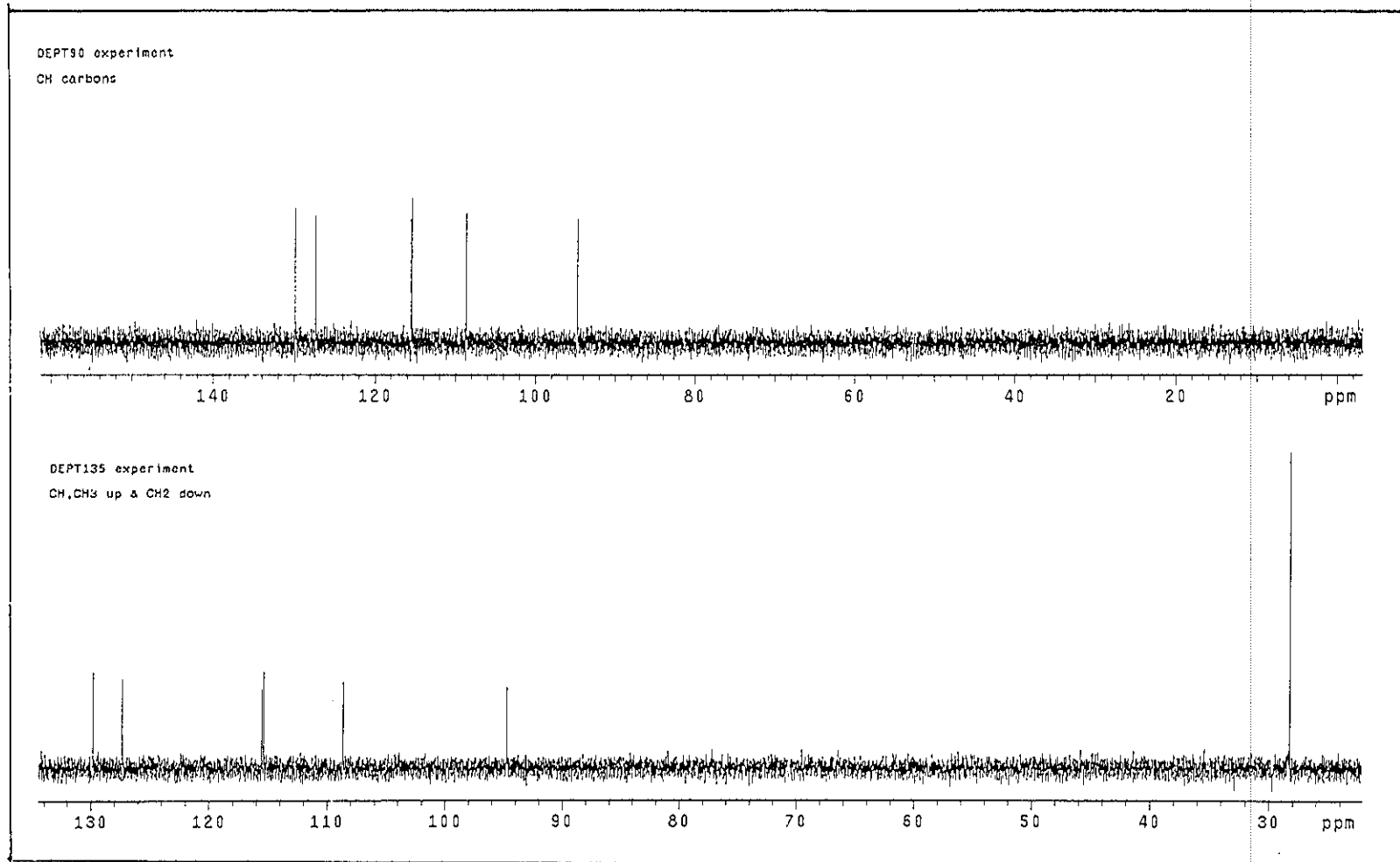


Figure 3.140 DEPT spectrum of TR13

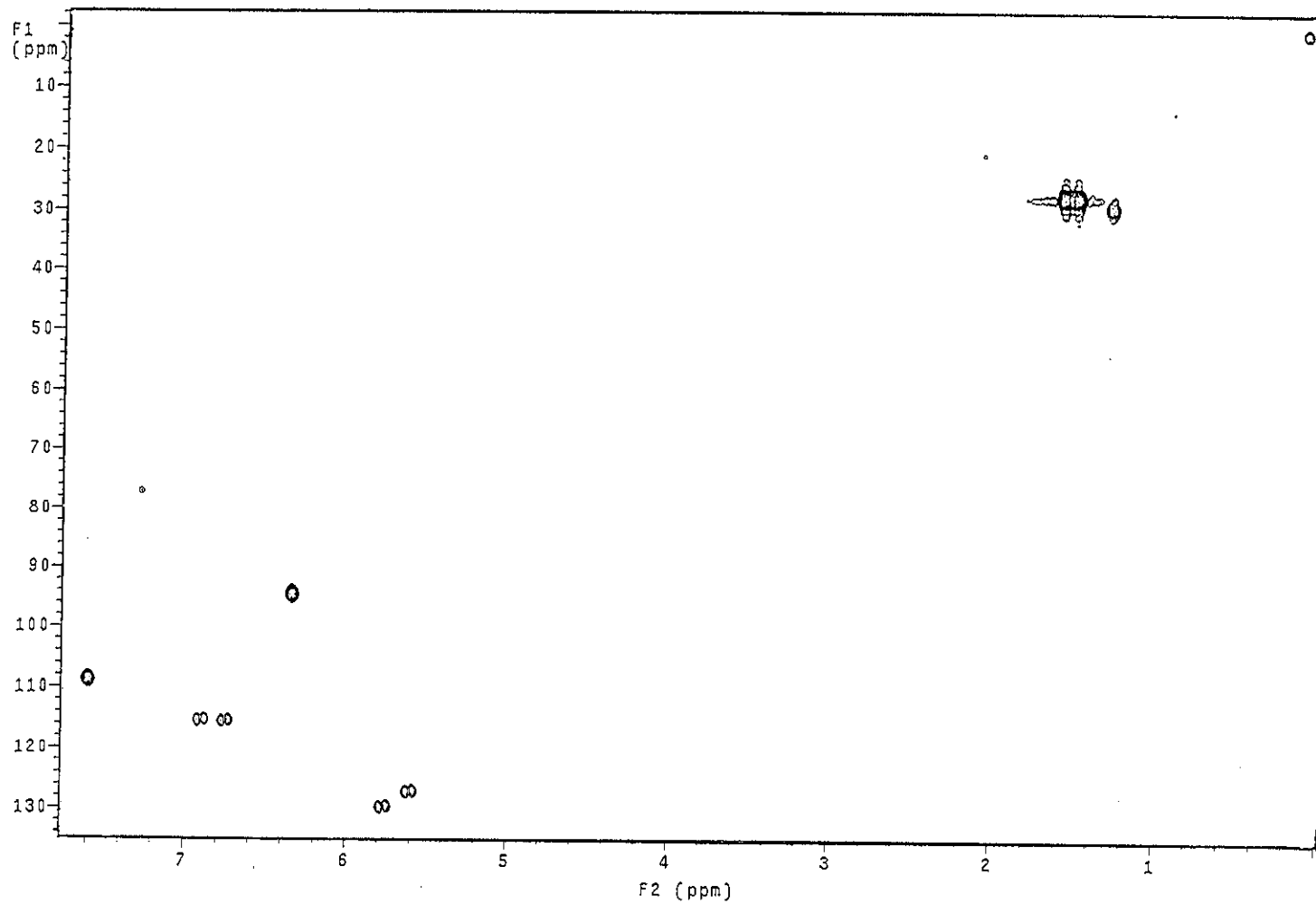


Figure 3.141 2D HMQC spectrum of TR13

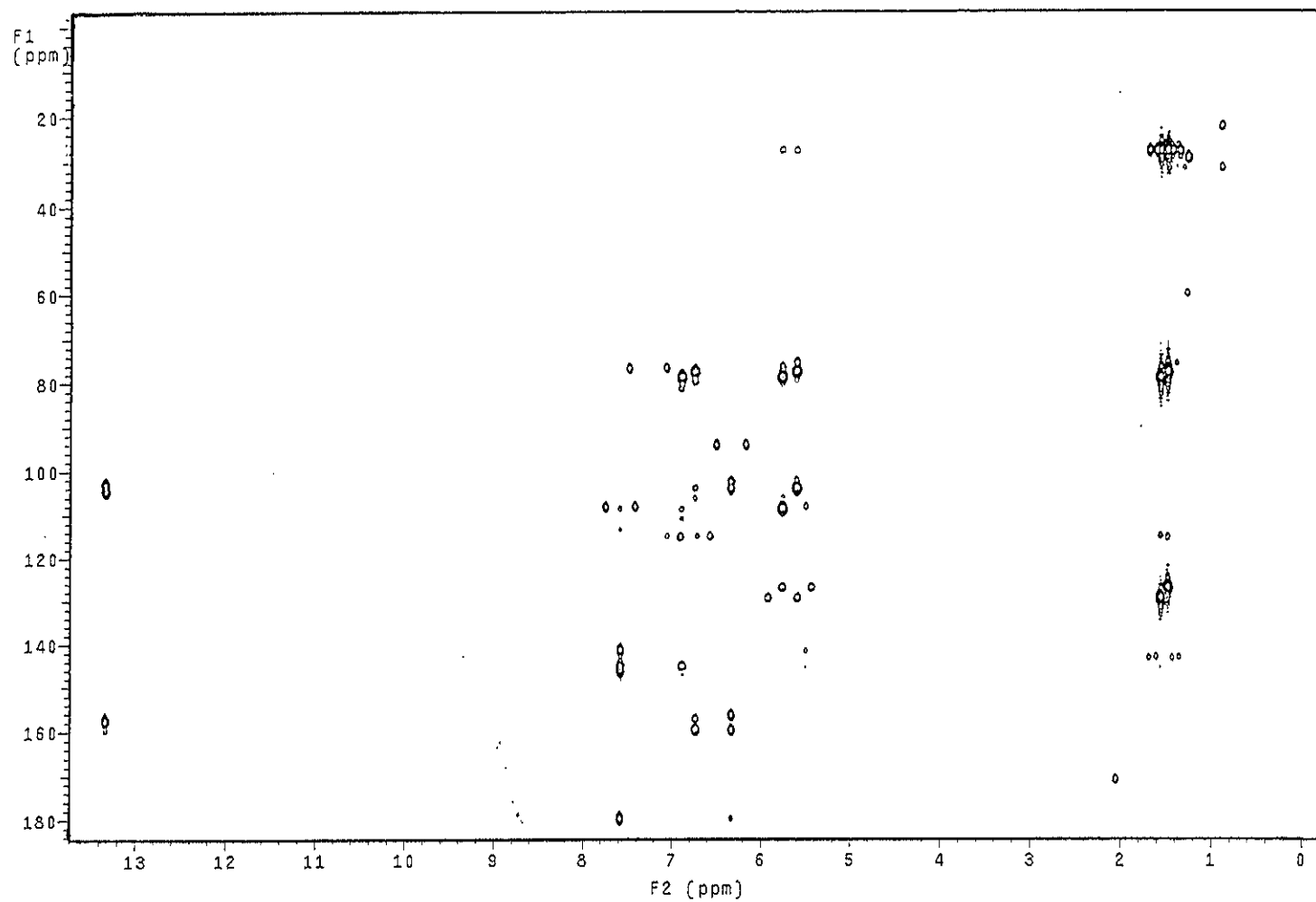


Figure 3.142 2D HMBC spectrum of TR13

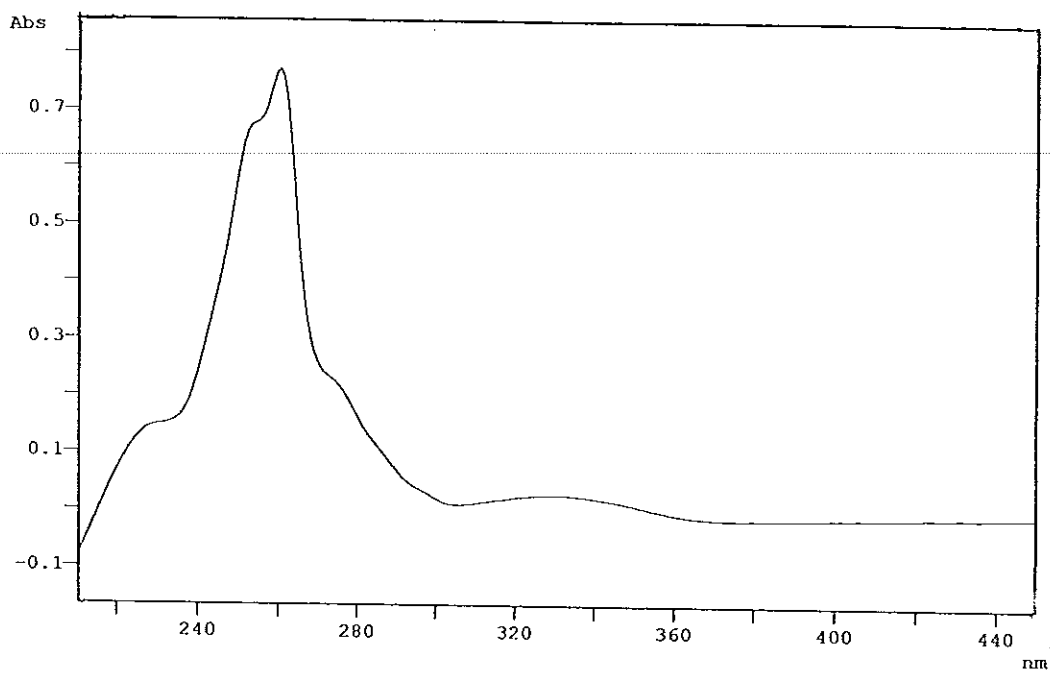


Figure 3.143 UV (MeOH) spectrum of TR20

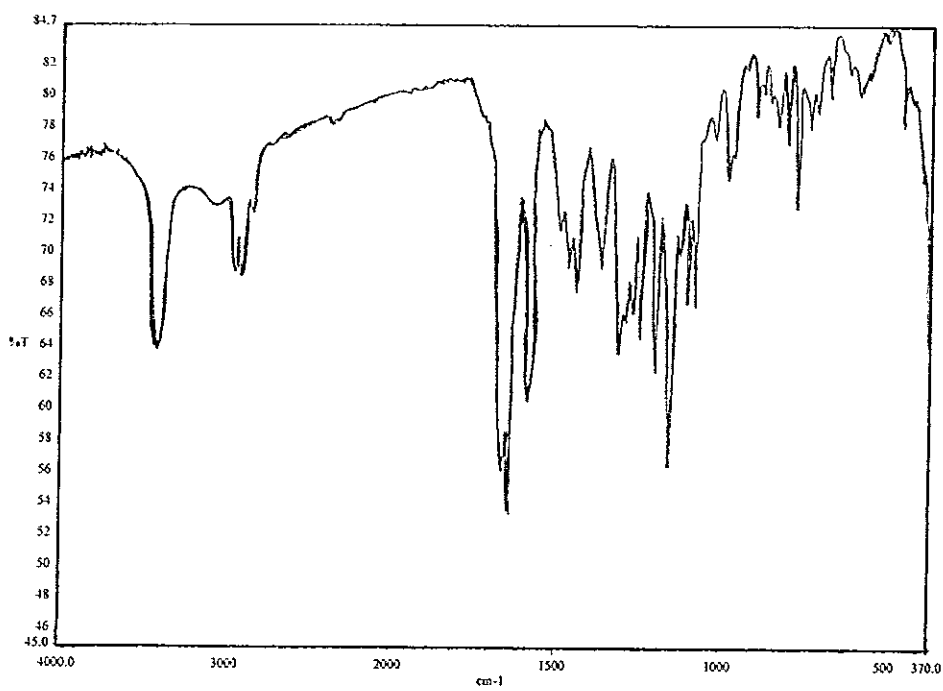


Figure 3.144 FT-IR (neat) spectrum of TR20

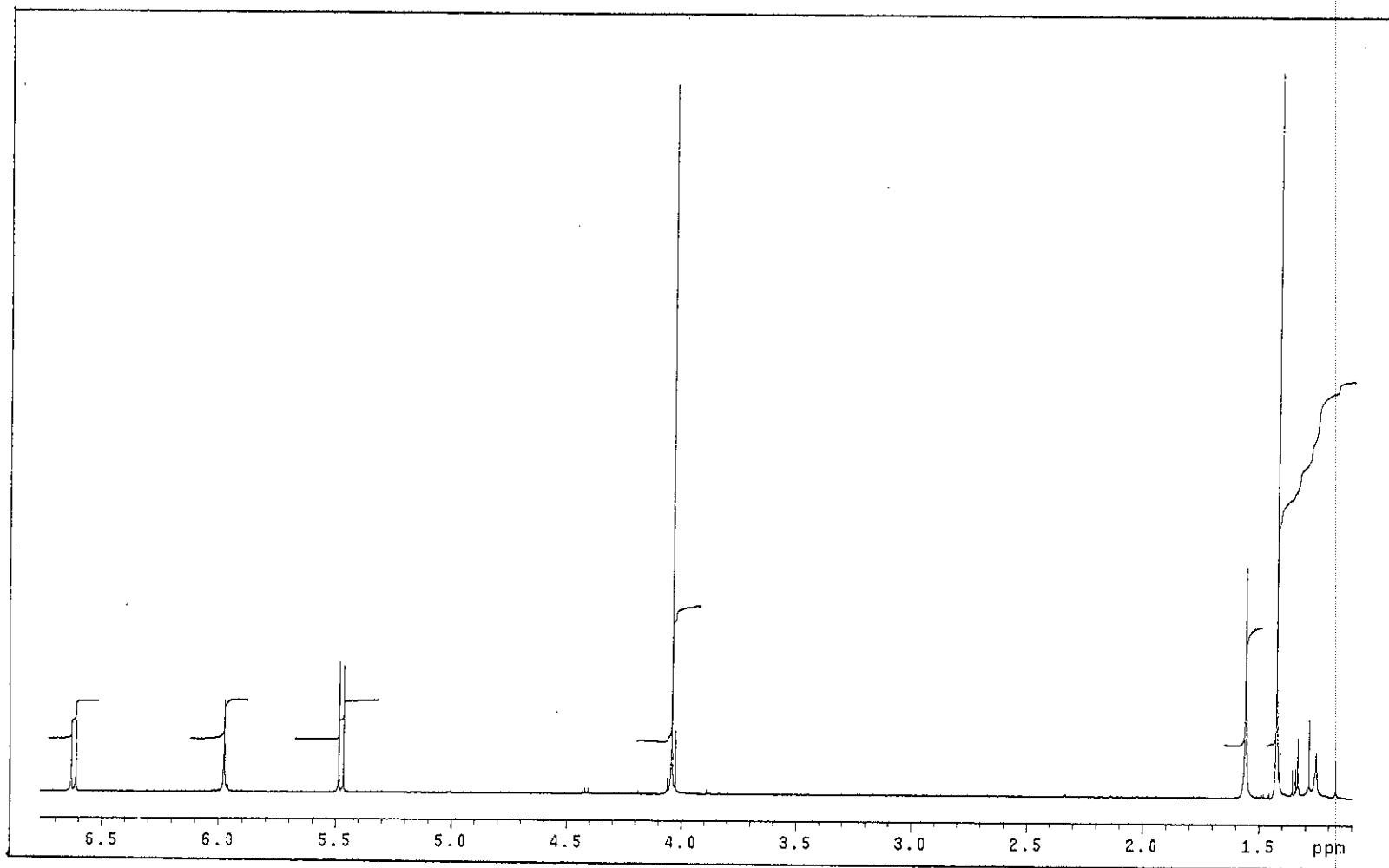


Figure 3.145 ^1H NMR (500 MHz)(CDCl_3) spectrum of TR20

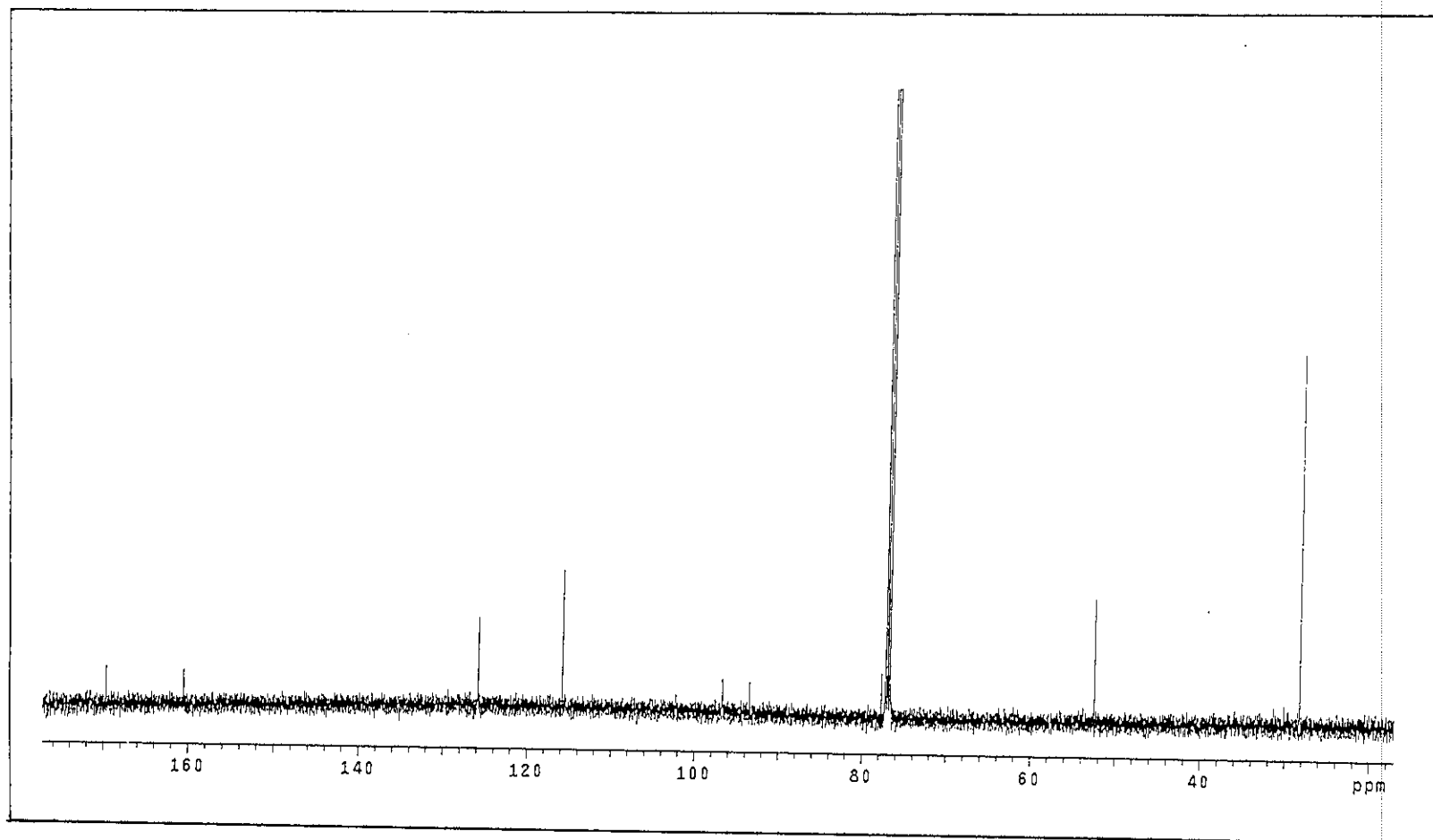


Figure 3.146 ^{13}C NMR (125 MHz)(CDCl_3) spectrum of TR20

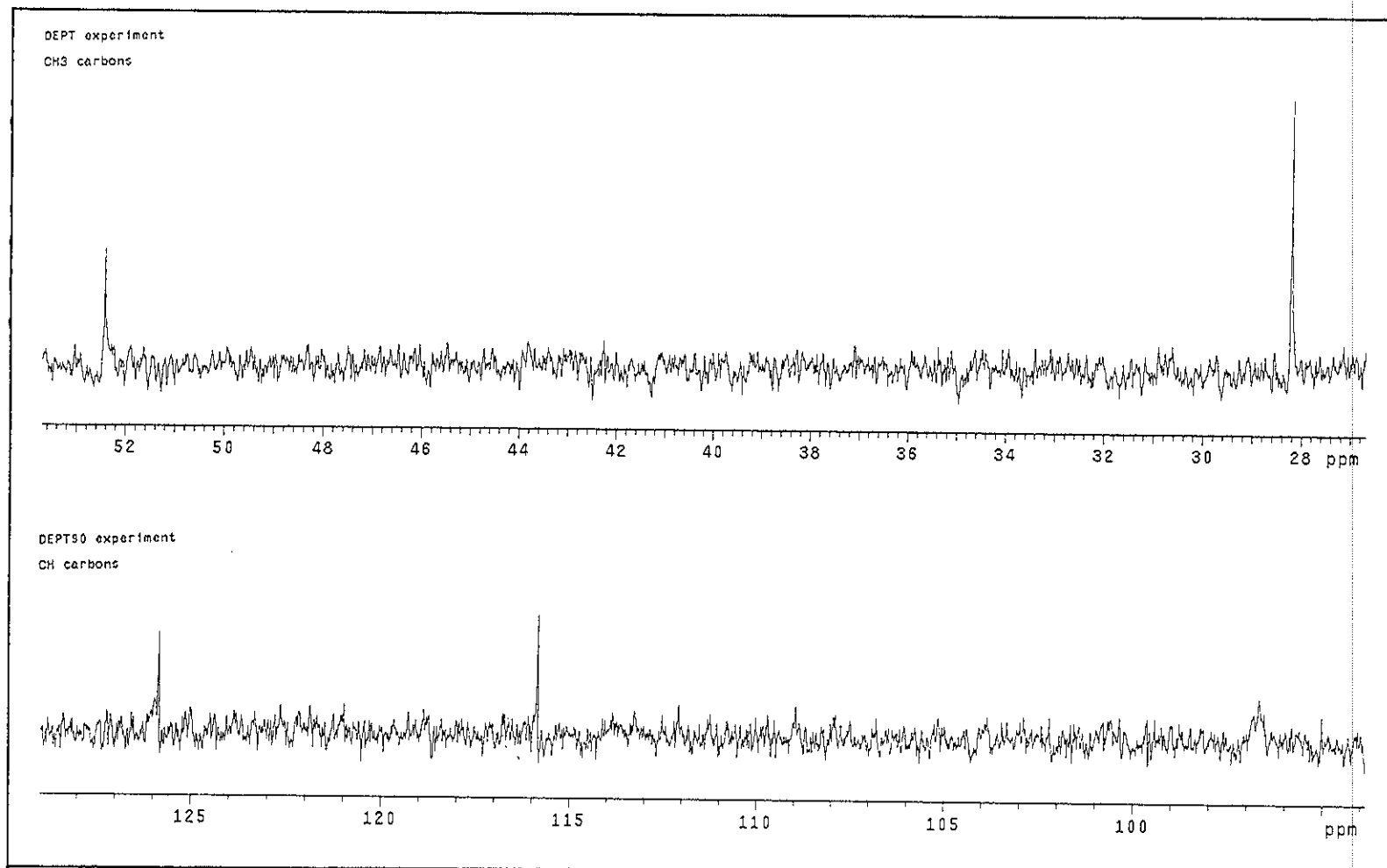


Figure 3.147 DEPT spectrum of TR20

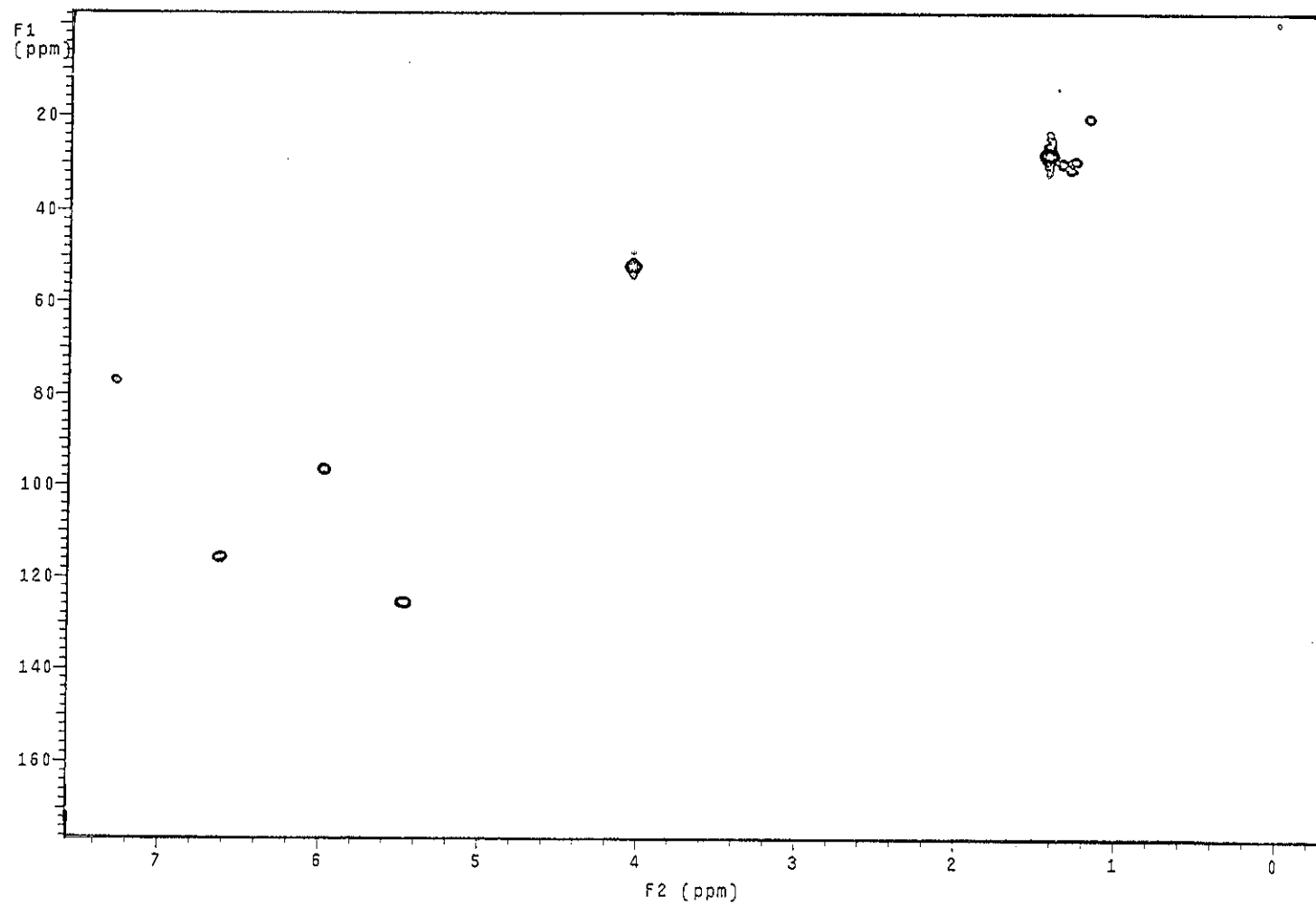


Figure 3.148 2D HMQC spectrum of TR20

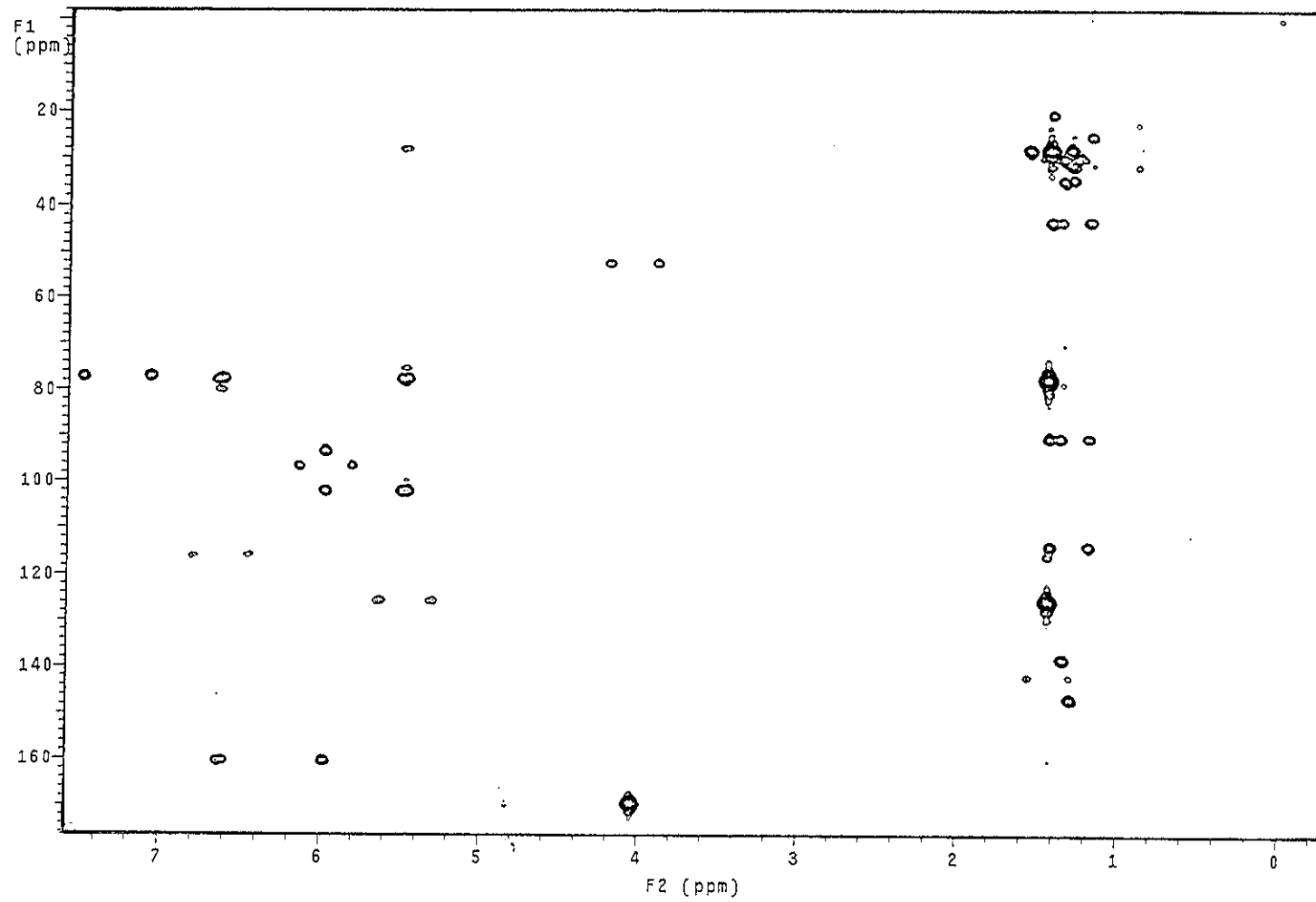


Figure 3.149 2D HMBC spectrum of TR20

BIBLIOGRAPHY

เต็ม สมิตินันท์. 2523. “ชื่อพันธุ์ไม้แห่งประเทศไทย (ชื่อพฤกษศาสตร์-ชื่อพื้นเมือง)”, กรมป่าไม้
กรุงเทพฯ : พันธุ์พลับพลึง.

Ali, S., Goundar, R., Sotheeswaran, S. and Spino, C.1999. “Phytochemicals from
Garcinia sesillis and *Garcinia vitiensis*”, *Chem. Res. Commun.* 9, 31-38.

Ali, S., Goundar, R., Sotheeswaran, S., Beaulieu, C. and Spino, C. 2000.
“Benzophenones of *Garcinia pseudoguttifera* (Clusiaceae)”, *Phytochemistry.*
53, 281-284.

Burkhardt, G., Schild, W., Becker, H. and Grubert, M. 1992. “Biphenyls and xanthonenes
from the Podostemaceae”, *Phytochemistry.* 31(2), 543-548.

Cao, S-G., Wu, X-H., Sim, K-Y., Tan, B.K.H., Pereira, J.T., Wong, W.H., Hew, N.F.
and Goh, S.H. 1998a. “Cytotoxic caged tetraprenylated xanthonoids from
Garcinia gaudichaudii (Guttiferae)”, *Tetrahedron Lett.* 39, 3353-3356.

Cao, S-G., Sng, H.L.V., Wu, X-H., Sim, K.Y., Tan, B.K.H., Pereira, J.T. and Goh, S.H.
1998b. “Novel cytotoxic polyprenylated xanthonoids from *Garcinia*
gaudichaudii (Guttiferae)”, *Tetrahedron.* 54(36), 10915-10924.

Chairungrilerd, N., Takeuchi, K., Ohizumi, Y., Nozoe, S. and Ohta, T. 1996a.
“Mangostanol, a prenyl xanthone from *Garcinia mangostana*.”, *Phytochemistry.*
43(5), 1099-1102.

- Chairungrilerd, N., Furukawa, K.I., Ohta, T., Nozoe, S. and Ohizumi, Y. 1996b. "Histaminergic and serotonergic receptor blocking substances from the medicinal plant *Garcinia mangostana*", *Planta Med.* 62, 471-472.
- Clarke, G.D., Crombie, L. and Whiting, A.D. 1974. "Conversion of phenols into chromens: regiospecificity and scope", *J.C.S. Perkin I.* 3, 1007-1015.
- Cuesta Rubio, O., Padron, A., Velez Castro, H., Pizza, C. and Rastrelli, L. 2001. "Aristophenones A and B. A new tautomeric pair of polyisoprenylated benzophenones from *Garcinia aristata*", *J. Nat. Prod.* 64(7), 973-975.
- Delle Monache, F., Botta, B., Nicoletti, M., De Barros Coelho, J.S. and Andrade Lyra, F.D. 1981. "Three new xanthone and macluraxanthone from *Rheedia benthamiana* Pl. Triana (Guttiferae)", *J.C.S. Perkin I.* 484-488.
- Delle Monache, G., Botta, B., De Mello, J.S., De Barros Coelho, J.S. and Menichini, F. 1984. "Chemical investigation of the genus *Rheedia*, VI. Three new xanthenes from *Rheedia brasiliensis*", *J. Nat. Prod.* 47(4), 620-625.
- Fukuyama, Y., Kaneshi, A., Tani, N. and Kodama, M. 1993. "Subellinone, a polyisoprenylated phloroglucinol derivative from *Garcia subelliptica*", *Phytochemistry.* 33(2), 483-485.
- Garbriel, S.J. and Gottlieb, O.R. 1972. "Tovoxanthone from *Tovomita choisyana*", *Phytochemistry.* 11, 3035-3036.

- Garcia Cortez, D.T., Young, M.C.M., Marston, A., Wolfender, J.-L. and Hostettmann, K. 1998. "Xanthones, triterpenes and biphenyl from *Kielmeyera coriacea*", *Phytochemistry*. 47(7), 1364-1374.
- Goh, S.H., Jantan, I., Gray, A.I. and Waterman, P.G. 1992. "Prenylated xanthones from *Garcinia opaca*", *Phytochemistry*. 31(4), 1383-1386.
- Gonda, R., Takeda, T. and Akiyama, T. 2000. "Studies on the constituents of *Anaxagorea luzonensis* A. GRAY", *Chem. Pharm. Bull.* 48(8), 1219-1222.
- Gopalakrishnan, G., Banumathi, B. and Suresh, G. 1997. "Evaluation of the antifungal activity of natural xanthones from *Garcinia mangostana* and their synthetic derivatives", *J. Nat. Prod.* 60(5), 519-524.
- Gopalakrishnan, G. and Balaganesan, B. 2000. "Two novel xanthones from *Garcinia mangostana*", *Fitoterapia*. 71(5), 603-605.
- Gunatilaka, A.A.L., Sriyani, H.T.B., Sotheeswaran, S. and Waight, E.S. 1983. "2,5-Dihydroxy-1,6-dimethoxyxanthone and biflavonoids of *Garcinia thwaitesii*", *Phytochemistry*. 22(1), 233-235.
- Gustafson, K.R., Blunt, J.W., Munro, M.H.G., Fuller, R.W., McKee, T.C., Cardellina II, J.H., McMahon, J.B., Cragg, M.C. and Boyd, M.R. 1992. "The guttiferones, HIV-inhibitory benzophenones from *Symphonia globulifera*, *Garcinia livingstonei*, *Garcinia ovalifolia* and *Clusia rosea*", *Tetrahedron*. 48(46), 10093-10102.

- Hano, Y., Okamoto, T., Nomura, T. and Momose, Y. 1990. "Components of the root bark of *Morus insignis* Bur. 1. Structures of four new isoprenylated xanthenes, morusignins A, B, C and D", *Heterocycles*. 31(7), 1345-1350.
- Hiranrat, A. 2001. "Chemical constituents from stem bark of *Garcinia speciosa*", M. Sc. Prince of Songkla University, Thailand.
- Hooker, J.D. 1875. "The Flora of British India", Vol.I (Ranunculaceae to Sapindaceae), L. Reeve & Co Ltd., The Oast House, Brook, NR. Ashford, Kent, England.
- Huang, Y-L., Chen, C-C., Chen, Y-J., Huang, R-L. and Shieh, B-J. 2001. "Three xanthenes and a benzophenone from *Garcinia mangostana*, *J. Nat. Prod.* 64(7), 903-906.
- Ilyas, M., Kamil, M., Parveen, M. and Khan, M.S. 1994. "Isoflavones from *Garcinia nervosa*", *Phytochemistry*. 36(3), 807-809.
- Iinuma, M., Ito, T., Tosa, H. and Tanaka, T. 1996a. "Five new xanthenes from *Garcinia dulcis*", *J. Nat. Prod.* 59, 472-475.
- Iinuma, M., Tosa, H., Ito, T., Tanaka, T. and Riswan, S. 1996b. "Three new benzophenone-xanthone dimers from the root of *Garcinia dulcis*", *Chem. Pharm. Bull.* 44(9), 1744-1747.
- Iinuma, M., Tosa, H., Ito, T., Tanaka, T. and Riswan, S. 1996c. "Garciduols A and B, new benzophenone-xanthone dimers, from *Garcinia dulcis*", *Heterocycles*. 43 (3), 535-538.

- Iinuma, M., Tosa, H., Tanaka, T. and Riswan, S. 1996d. "Three new xanthonones from the bark of *Garcinia dioica*", *Chem Pharm. Bull.* 44(1), 232-234.
- Iinuma, M., Tosa, H., Tanaka, T., Kanamaru, S., Asai, F., Kobayashi, Y., Miyauchi, K. and Shimano, R. 1996e. "Antibacterial activity of some *Garcinia* benzophenone derivatives against Methicillin-Resistant *Staphylococcus aureus*", *Bio. Pharm. Bull.* 19(2), 311-314.
- Iinuma, M., Ito, T., Miyake, R., Tosa, H., Tanaka, T. and Chellardurai, V. 1998. "A xanthone from *Garcinia cambogia*", *Phytochemistry.* 47(6), 1169-1170.
- Ito, C., Miyamoto, Y., Nakayama, M., Kawai, Y., Rao, K.S and Furukawa, H. 1997. "A novel depsidone and some new xanthonones from *Garcinia Species*", *Chem. Pharm. Bull.* 45(9), 1403-1413.
- Ito, C., Itoigawa, M., Furukawa, H., Rao, K.S., Enjo, F., Bu, P., Takayasu, J., Tokuda, H. and Nishino, H. 1998. "Xanthonones as inhibitors of Epstein-Barr virus activation", *Cancer letters.* 132, 113-117.
- Ito, C., Itoigawa, M., Mishina, Y., Tomiyasu, H., Litaudon, M., Cosson, J.P., Mukainaka, T., Tokuda, H., Nishino, H. and Furukawa, H. 2001. "Cancer chemopreventive agents. New depsidones from *Garcinia* plant", *J. Nat. Prod.* 64(2), 147-150.
- Kosela, S., Hu, L-H., Yip, S-C., Rachmatia, T., Sukri, T., Daulay, T.S., Tan, G-K., Vittial, J.J. and Sim, K-Y. 1999. "Dulxanthone E: a pyranoxanthone from leaves of *Garcinia dulcis*", *Phytochemistry.* 52, 1375-1377.

- Kosela, S., Hu, L-H., Rachmatia, T., Hanafi, M. and Sim, K-Y. 2000. "Dulxanthones F-H, three new pyranoxanthones from *Garcinia dulcis*", *J. Nat. Prod.* 63(3), 406-407.
- Kosin, J., Ruangrunsi, N., Ito, C. and Furukawa, H. 1998. "A xanthone from *Garcinia atroviridis*", *Phytochemistry.* 47(6), 1167-1168.
- Likhitwitayawuid, K., Phadungcharoen, T., Mahidol, C. and Ruchirawat, S. 1997 "7-O-methylgarcinone E from *Garcinia cowa*", *Phytochemistry.* 45(6), 1299-1301.
- Likhitwitayawuid, K., Phadungcharoen, T. and Krungkrai, J. 1998a. "Antimalarial xanthones from *Garcinia cowa*", *Planta Medica.* 64(1), 70-72.
- Likhitwitayawuid, K., Channahasathien, W., Ruangrunsi, N. and Krungkrai, J. 1998b. "Xanthones with antimalarial activity from *Garcinia dulcis*", *Planta Medica.* 64 (3), 281-282.
- Lin, Y-M., Anderson, H., Flavin, M.T., Pai, Y-H.S., Mata-Greenwood, E., Pengsuparp, T., Pezzuto, M.J., Schinazi, R.F., Hughes, S.H. and Chen, F-C. 1997. "In vitro anti-HIV activity of biflavonoids isolated from *Rhus succedanea* and *Garcinia multiflora*", *J. Nat. Prod.* 60(9), 884-888.
- Marques, V.L.L., De Oliveira, F.M., Conserva, L.M., Brito, R.G.L. and Guilhaon, G.M.S.P. 2000. "Dichromenoxanthones from *Tovomita brasiliensis*", *Phytochemistry.* 55, 815-818.

- Minami, H., Kuwayama, A., Yoshizawa, T. and Fukuyama, Y. 1996. "Novel prenylated xanthenes with antioxidant property from the wood of *Garcinia subelliptica*", *Chem. Pharm. Bull.* 44(11), 2103-2106.
- Minami, H., Hamaguchi, K., Kubo, M. and Fukuyama, Y. 1998. "A Benzophenone and a xanthone from *Garcinia subelliptica*", *Phytochemistry.* 49(6), 1783-1785.
- Nguyen, D.L.H. and Harrison, J.L. 2000. "Xanthenes and triterpenoids from the bark of *Garcinia vilersiana*", *Phytochemistry.* 53, 111-114.
- Nyemba, A-M., Mpondo, T.N., Connolly, J.D. and Rycroft, D.S. 1990. "Cycloartane derivatives from *Garcinia lucida*", *Phytochemistry.* 29(3), 994-997.
- Okudaira, C., Ikeda, Y., Kondo, S., Furuya, S., Hirabayashi, Y., Koyano, T., Saito Y. and Umezawa, K. 2000. "Inhibition of acidic sphingomyelinase by xanthone compounds isolated from *Garcinia speciosa*", *Journal of Enzyme Inhibition.* 15 (2), 129-138.
- Owen, P.J. and Scheinmann, F. 1974. "Extractives from Guttiferae. Part XXVI. Isolation and structure of six xanthenes, a biflavanoid, and triterpenes from the heartwood of *Pentaphalangium solomonse* Warb.", *J.C.S. Perkin I.* 3, 1018-1021.
- Panthong, K. 1999. "Investigations of Bioactive Compounds from *Callophyllum teysmannii* var. *inophylloide* (Guttiferae), *Ventilago harmandiana* (Rhamnaceae) and *Anogeissus acuminata* var. *lanceolata* (Combretaceae)", Ph.D. Dissertation. Mahidol University, Thailand.

- Parveen, M., Khan, N.U., Achari, B. and Dutta, P.K. 1991. "A triterpene from *Garcinia mangostana*", *Phytochemistry*. 30(1), 361-362.
-
- Peres, V. and Nagem, T.J. 1997. "Trioxxygenated naturally occurring xanthenes", *Phytochemistry*. 44(2), 191-214.
- Peres, V., Nagem, T.J. and Oliveira, F.F. 2000. "Tetraoxxygenated naturally occurring xanthenes", *Phytochemistry*. 55, 683-710.
- Permana, D., Lajis, N.H., MacKeen, M.M., Ali, A.M., Aimi, N., Kitajima, M. and Takayama, H. 2001. "Isolation and bioactives of constituents of the roots of *Garcinia atroviridis*", *J. Nat. Prod.* 64(7), 976-979.
- Rukachaisirikul, V., Kaewnok, W., Koysoomboon, S., Phongpaichit, S. and Taylor, W.C. 2000a. "Caged-tetraprenylated xanthenes from *Garcinia scortechinii*", *Tetrahedron*. 56, 8539-8543.
- Rukachaisirikul, V., Adiar, A., Dampawan, P., Taylor, W.C. and Turner, P.C. 2000b. "Lanostanes and friedolanostanes from the pericarp of *Garcinia hombroniana*", *Phytochemistry*. 55, 183-188.
- Spino, C., Lal, J., Sotheeswaran, S. and Aalbersberg, W. 1995. "Three prenylated phenolic benzophenones from *Garcinia myrtifolia*", *Phytochemistry*. 38(1), 233-236.
- Tershima, K., Kondo, Y., Mohammad, A. and Niwa, M. 1999. "A New xanthone from the stems of *Garcinia Kola*", *Nat. Prod. Lett.* 14(2), 91-97.

Thoison, O., Fahy, J., Dumontet, V., Chiaroni, A., Riche, C., Tri, M.V. and Sevenet, T. 2000. "Cytotoxic prenylxanthenes from *Garcinia bracteata*", *J. Nat. Prod.* 63(4), 441-446.

Whitmore, M.A. 1973. "*Tree Flora of Malaya*", Malasia: Forest Department Ministry of Primary Industries, Longman, 218.

Xu, Y-J., Cao, S-G., Wu, X-H., Lai, Y-H., Tan, B.H.K., Pereira, J.T., Goh, S.H., Venkatraman, G., Harrison, L.J. and Sim, K.Y. 1998. "Griffipavixanthone, a novel cytotoxic bixanthone from *Garcinia griffithii* and *G. parvifolia*", *Tetrahedron Lett.* 39, 9103-9106.

Xu, Y-J., Chiang, P-Y., Lai, Y-H., Vittal, J.J., Wu, X-H., Tan, B.K.H., Imiyabir, Z. and Goh, S-H. 2000. "Cytotoxic prenylated depsidones from *Garcinia parvifolia*", *J. Nat. Prod.* 63(10), 1361-1363.

Xu, Y-J., Lai, Y-H., Imiyabir, Z. and Goh, S-H. 2001. "Xanthenes from *Garcinia parvifolia*", *J. Nat. Prod.* 64, 1191-1195.

VITAE

Name Miss Thunwadee Ritthiwigrom
Birth Date 7 April 1977
Place of Birth Yala, Thailand

Educational Attainment

Degree	Name of Institution	Year of Graduation
Bachelor of Science (Chemistry)	Prince of Songkla University	1995-1999
Master of Science (Organic Chemistry)	Prince of Songkla University	1999-2002

Scholarship Awards during Enrolment

The partail support from Higher Education Development Project : Postgraduate Education and Research Program in Chemistry, funded by The Royal Thai Government